

Green Energy and Technology

Carlo Pellegrino
Flora Faleschini



Sustainability Improvements in the Concrete Industry

Use of Recycled Materials for Structural
Concrete Production

 Springer

Green Energy and Technology

More information about this series at <http://www.springer.com/series/8059>

Carlo Pellegrino · Flora Faleschini

Sustainability Improvements in the Concrete Industry

Use of Recycled Materials for Structural
Concrete Production

 Springer

Carlo Pellegrino
Department of Civil, Environmental
and Architectural Engineering
University of Padua
Padua
Italy

Flora Faleschini
Department of Civil, Environmental
and Architectural Engineering
University of Padua
Padua
Italy

ISSN 1865-3529

Green Energy and Technology

ISBN 978-3-319-28538-2

DOI 10.1007/978-3-319-28540-5

ISSN 1865-3537 (electronic)

ISBN 978-3-319-28540-5 (eBook)

Library of Congress Control Number: 2016950883

© Springer International Publishing Switzerland 2016

This work is subject to copyright. All rights are reserved by the Publisher, whether the whole or part of the material is concerned, specifically the rights of translation, reprinting, reuse of illustrations, recitation, broadcasting, reproduction on microfilms or in any other physical way, and transmission or information storage and retrieval, electronic adaptation, computer software, or by similar or dissimilar methodology now known or hereafter developed.

The use of general descriptive names, registered names, trademarks, service marks, etc. in this publication does not imply, even in the absence of a specific statement, that such names are exempt from the relevant protective laws and regulations and therefore free for general use.

The publisher, the authors and the editors are safe to assume that the advice and information in this book are believed to be true and accurate at the date of publication. Neither the publisher nor the authors or the editors give a warranty, express or implied, with respect to the material contained herein or for any errors or omissions that may have been made.

Printed on acid-free paper

This Springer imprint is published by Springer Nature

The registered company is Springer International Publishing AG

The registered company address is: Gewerbestrasse 11, 6330 Cham, Switzerland

Contents

1 Introduction	1
1.1 Objectives of the Book	1
2 Recycled Aggregates for Concrete Production: State-of-the-Art	5
2.1 Construction and Demolition Waste	5
2.1.1 Processing Procedures for Recycled Aggregates Production	8
2.1.2 International Codes, Guidelines and Regulations	9
2.1.3 RAC Concrete—Mixture Proportioning	15
2.1.4 RAC Concrete—Mechanical Properties	17
2.1.5 RAC Concrete—Durability	18
2.1.6 RAC Concrete—Structural Concrete	19
2.2 Metallurgical Slag	20
2.2.1 EAF Slag—Characterization	23
2.2.2 EAF Slag Concrete	25
2.3 Fly Ash	27
References	29
3 Workability and Rheology of Fresh Recycled Aggregate Concrete	35
3.1 Introduction	35
3.2 Rheology Background	37
3.2.1 Rheological Models and Flow Curve Equations	37
3.2.2 Bingham Parameters	40
3.2.3 Time-Dependent Behavior	42
3.2.4 Stability and Segregation	43
3.2.5 Relative Contributions on the Behavior of Fresh Concrete	43
3.2.6 Governing Equations	46
3.3 Test Methods for Evaluating Fresh Concrete Properties	47

3.4	Evaluation of Rheological Parameters with Coaxial Cylinders Viscometer	53
3.4.1	Reiner-Riwlin Equation	54
3.4.2	Plug Flow and Gravel Migration Influence	58
3.4.3	Rheographs	61
3.5	Mix Proportion Design of Coarse Recycled Aggregate Concrete and Its Effect on Workability.	61
3.5.1	DVR, DWR and EMV Proportioning Methods	62
3.5.2	Slump Test Results	66
3.5.3	Viscometric Results.	67
3.5.4	Slump—Yield Stress Relation.	70
3.6	Conclusions	73
	References.	74
4	Electric Arc Furnace Slag Concrete.	77
4.1	Introduction	77
4.2	EAF Slag Properties	78
4.2.1	Physical Properties	78
4.2.2	Chemical Composition	80
4.3	Ordinary Strength Concrete with EAF Aggregates	82
4.3.1	Fresh Concretes Properties	82
4.3.2	Mechanical Properties	85
4.3.3	Durability-Related Properties.	87
4.3.4	Structural Behavior of RC Beams with EAF Concrete	91
4.4	High Strength Concrete with EAF Aggregates	97
4.4.1	Fresh and Hardened Concrete Properties.	98
4.4.2	Durability-Related Concrete Properties	102
4.5	Conclusions	104
	References.	105
5	Sustainability of Recycled Concretes Through Life Cycle Assessment	107
5.1	Introduction	107
5.2	Recycled Aggregates and Potential Environmental Issues.	109
5.3	Sustainability Indicators	110
5.3.1	Life Cycle Assessment	111
5.3.2	Abiotic Depletion and Exhaustion Time Indicators.	117
5.3.3	Land Use	118
5.4	LCA of Natural and Recycled Aggregates	119
5.4.1	Natural Aggregates	119
5.4.2	Electric Arc Furnace Slag Aggregates.	124
5.5	LCA of Concretes with Recycled Aggregates.	126
5.5.1	Concrete with EAF Slag	127
5.5.2	The Influence of Cement Content on Concrete Emissions	129

- 5.5.3 The Influence of Aggregates Specific Weight
on Concrete Emissions: System Boundary Expansion. 130
- 5.5.4 The Choice of the Functional Unit 132
- 5.6 Natural Aggregates Depletion at Local Scale 133
- 5.7 Land Use Preservation 135
- 5.8 Conclusions 137
- References. 138
- 6 Experimental Database of EAF Slag Use in Concrete 141**
 - 6.1 Introduction 141
 - 6.2 Physical Properties 141
 - 6.3 Chemical Composition 143
 - 6.4 Mineralogy 143
 - 6.5 Leaching. 149
 - 6.6 Application in Concrete as Recycled Aggregate. 152
 - 6.7 Conclusion 172
 - References. 173

List of Figures

Figure 2.1	Scheme of a C&DWs treatment plant	10
Figure 2.2	Recycled concrete aggregate	16
Figure 2.3	Steel slag production in Europe [72]	20
Figure 2.4	Slag cooling	22
Figure 2.5	Light-brown FA and dark-grey FA	29
Figure 3.1	Comparison of Newtonian, shear-thickening and shear-thinning fluids	36
Figure 3.2	Newton’s equation for a viscous fluid: F is the shear force (N), A is the area of the plane parallel to the applied force (m^2), τ is the shear stress (Pa), η is the viscosity (Pa s), $\partial u/\partial z$ is the velocity gradient, equal to the shear rate $\dot{\gamma}(s^{-1})$	36
Figure 3.3	Slump test	48
Figure 3.4	Penetrating rod test methods: Kelly-ball and Vicat apparatus	49
Figure 3.5	Experimental apparatus for evaluating filling ability of fresh concretes.	50
Figure 3.6	ConTec BML Viscometer	53
Figure 3.7	Sampling profile using a ConTec BML viscometer for evaluating Bingham parameters of fresh recycled aggregate concrete with 35 % RA	54
Figure 3.8	Viscometric measurement of fresh recycled concrete with 35 % RCA and $w/c = 0.4$	58
Figure 3.9	Schematic representation of plug flow (from [46]) and its influence on a viscometric measurement performed on fresh recycled concrete with 35 % RCA and $w/c = 0.4$	59
Figure 3.10	Iterative procedure applied to extract Bingham rheology with plug state at plug flow boundary R_s (from [46])	60

Figure 3.11	The use of rheographs for highlighting the effect of adding water, water-reducing admixture (WRA), air-entrainer admixture (AEA) and silica fume (SF) on Bingham parameters (adapted from [50])	61
Figure 3.12	Recycled aggregates with high attached mortar content.	63
Figure 3.13	<i>Left</i> RAC20/0.4–1 %WRA; <i>Right</i> EMV20/0.4-1 %WRA	68
Figure 3.14	Effect of WRA content, substitution ration and aggregates proportioning method (w/c = 0.4)	69
Figure 3.15	Effect of WRA content, substitution ration and aggregates proportioning method (w/c = 0.5)	70
Figure 3.16	Scatter plot and distribution of residuals of theoretical and experimental slump value according to Murata and Kukawa relation	71
Figure 3.17	Scatter plot and distribution of residuals of theoretical and experimental slump value according to de Larrad relation	72
Figure 4.1	Electric arc furnace slag vs. siliceous aggregates.	78
Figure 4.2	SEM-BSE image of the cross section of the slag aggregate (from [4])	81
Figure 4.3	Aggregates grading curves.	84
Figure 4.4	Splitting surfaces of the concretes with EAF slag	86
Figure 4.5	SEM-BSE image of the efflorescence + EDS spectrum.	88
Figure 4.6	Disposition of steel reinforcement in the cross-section of the beams (from [12]).	92
Figure 4.7	Disposition of steel reinforcement in type A beams (from [12])	93
Figure 4.8	Load versus deflection at midspan diagrams for type A beams (from [12]).	94
Figure 4.9	Load versus crack width diagrams for type A beams (from [12])	94
Figure 4.10	Crack patterns in RC structural elements after bending failure (from [12]).	94
Figure 4.11	Bending failure: concrete cracking in A1 beams	95
Figure 4.12	Bending failure: concrete crushing in A2 beams	95
Figure 4.13	Load versus deflection at midspan diagrams for type B beams (from [12]).	96
Figure 4.14	Load versus crack width diagrams for type B beams (from [12])	96
Figure 4.15	Crack patterns in RC structural elements after shear failure (from [12]).	96
Figure 4.16	Shear failure in B2 beams	97
Figure 4.17	Cubic compressive strength of the examined concretes.	100
Figure 4.18	Tensile strength of the examined concretes.	101
Figure 4.19	Splitting failures of two HPC concretes.	101

Figure 4.20 Elastic modulus of the examined concretes (from [4]). 102

Figure 4.21 Ordinary performance concrete: conventional (a) and EAF (b); High performance concrete: conventional (c) and EAF (d). 103

Figure 5.1 Life Cycle Assessment phases. 112

Figure 5.2 Land quality evolution: transformation and occupation effects (adapted from [32]) 118

Figure 5.3 Block diagram of the activities in the analyzed quarry (from [39]) 121

Figure 5.4 Block diagram of the activities in the treatment plant of EAF aggregates (from [39]) 125

Figure 5.5 The effect of system boundaries expansion on carbon emissions for aggregates productive chains. Upper: transportation emission per unit mass; transportation per unit volume 131

Figure 5.6 The effect of system boundaries expansion on carbon emissions for concrete production. Transportation emissions are expressed per unit volume of concrete. 132

Figure 5.7 Extraction and imports rate of natural aggregate in the analyzed territory [43]. 134

Figure 5.8 Temporal evolution of *I/DMC* in the analyzed territory [43] 135

Figure 5.9 Quarry exhaustion time: *ER* stands for extraction rate, t_R is the exhaustion time 137

List of Tables

Table 2.1	CDWs European production [17].	8
Table 2.2	Acceptance criteria for RA according to German standards	11
Table 2.3	Substitution ratio (in % by volume) according to EN 206-1 [29] and DIN 1045-2 [30].	12
Table 2.4	Maximum allowable quantity of RA in concrete according to Italian normative	13
Table 2.5	Acceptance criteria for RA according to Japanese standards	14
Table 2.6	Classification of recycled aggregate according to Portuguese normative	14
Table 2.7	Physical properties of steel slag.	24
Table 2.8	Chemical composition of EAF slag.	24
Table 3.1	One-parameter test methods for the assessment of fresh concrete properties	47
Table 3.2	Main physical properties of aggregates used (from [46]).	66
Table 3.3	Mix design of the concrete analyzed (from [46]).	67
Table 3.4	Results of slump test	68
Table 4.1	Shape of EAF aggregates (from [12])	79
Table 4.2	Physical properties of EAF slag (coarse fraction)	80
Table 4.3	Physical properties of EAF slag (fine fraction) [13].	80
Table 4.4	Physical properties of aggregates (from [12])	82
Table 4.5	Mixture details (from [12])	83
Table 4.6	Physical properties of aggregates (from [13])	83
Table 4.7	Mixture details (from [13])	84
Table 4.8	Results of the slump test (from [13]).	85
Table 4.9	Mechanical properties of concretes (from [12]).	85
Table 4.10	Mechanical properties of concretes (from [13]).	86
Table 4.11	Compressive strength in specimens after accelerated ageing for 32 days (from [13])	89

Table 4.12	Compressive strength in specimens after accelerated ageing for 32 days plus weathering for 90 days (from [13]).	90
Table 4.13	Compressive strength in specimens after freezing/thawing cycles for 25 days (from [13]).	90
Table 4.14	Compressive strength in specimens wetting/drying cycles for 30 days (from [13])	91
Table 4.15	Experimental and theoretical results in terms of ultimate load P_{ult} and deflection f_{ult} . (from [12]).	93
Table 4.16	Experimental and theoretical (from [12]).	95
Table 4.17	Mix details for HPC and OPC design with EAF slag referring to 1 m ³ of concrete (from [4]).	98
Table 4.18	Mix details natural aggregates concrete referring to 1 m ³ of concrete (from [4]).	99
Table 4.19	Fresh properties of HPC and OPC concretes with EAF slag (from [4]).	99
Table 4.20	Apparent diffusion coefficients for OPC and HPC with EAF slag (from [17]).	104
Table 5.1	Environmental emissions for natural aggregates ($FU = 1$ ton)	124
Table 5.2	Environmental emissions for EAF aggregates ($FU = 1$ ton)	126
Table 5.3	Mix details of the two analyzed concretes.	127
Table 5.4	Mechanical properties of the two analyzed concretes.	128
Table 5.5	Environmental emission related to global and regional scale categories—cement ($FU = 1$ kg).	128
Table 5.6	Total environmental emission related to global and regional scale categories—NA concrete and EAF slag concrete ($FU = 1$ m ³)	128
Table 5.7	Mix details of the two analyzed concretes.	129
Table 5.8	Mechanical properties of the two analyzed concretes.	130
Table 5.9	Total environmental emission related to global and regional scale categories—NA concrete and EAF slag concrete ($FU = 1$ m ³)	130
Table 5.10	Example of inventory data for land use.	136
Table 6.1	Field of applications of the collected works.	142
Table 6.2	Physical properties of EAF slag—database	144
Table 6.3	Chemical composition of EAF slag—database	148
Table 6.4	Chemical composition of EAF slag—database	150
Table 6.5	Leaching potential of EAF slag—database	151
Table 6.6	Concrete mixtures details including EAF slag	153

Chapter 1

Introduction

1.1 Objectives of the Book

The recycling of building materials has relatively ancient origins, since when Romans used construction waste such as ceramics in the so-called opus caementicium, the roman concrete, or when they used crushed slag from the crude iron production for roads building. However, from long time ago, recycling of mineral fraction of demolition wastes and a great part of industrial waste has been not considered as a real, effective alternative of waste disposal. Additionally, for centuries, the construction industry has consumed raw materials, causing also great stream of wastes, which needed to be landfilled. An enormous amount of space was dedicated to the disposal of those materials, leading to the increase of the ecological footprint of construction market.

In the last decades however the research community was pushed to study new fields of application for the wastes coming from construction and demolition operations, driven both by the arise of an environmental consciousness in the society, and also by the realization of the possible depletion of non-renewable natural resources, at least at local scale. From many years also iron and more generally steelmaking slag have been employed as compounds of cement-based materials: for instance the use of ground granulated blast furnace slag in cement manufacture as a partial substitute of Portland cement clinker has become a very well-known practice, currently standardized in EN 197-1. The use of other kinds of slag as artificial aggregates in concrete for civil engineering applications is also commonly diffused.

Accordingly many research works have been developed in the last years, aiming to explore the possibility to substitute, at high percentages, natural aggregates or traditional binders with recycled materials, e.g. recycled aggregates coming from construction and demolition waste (C&DW), metallurgical industry, and supplementary cementing materials. Promising results have been obtained with the production of “green concretes”, which can be potentially ready-applied into the

market, as in the case of concretes including coarse recycled aggregates from C&DW. Their use for structural purposes is also accepted by the current design codes, but generally aggregates origin and the strength class of the structure where they will be placed limit their maximum content. Most of the mechanical and durability properties of recycled aggregate concrete have been widely studied, and currently we are able to properly design this material, for the intended target during structure service life. However few aspects are still not sufficiently explored: this is the case of the workability and rheology of fresh recycled concrete mixtures. Very few data are currently available to predict how this material will flow during casting conditions.

Less research works have been carried out about the use of metallurgical slag use in cement-based materials. Over recent decades the steelmaking industry in Europe has been radically transformed; electric arc furnace technology has largely replaced blast furnaces and Linz-Donawitz converters, leading to the appearance of a new by-product: Electric Arc Furnace (EAF) oxidizing slag. Promising results have been obtained when using this material for producing structural concrete, however still few data exist about its durability and long-term behavior.

Benefits obtained through the use of recycled components in construction materials should be however quantified: often the term “green-concrete” is used, but few proofs of the real embodied energy of the product are given.

The book is structured as follows: Chap. 2 provides the state-of-the-art about the current uses of recycled aggregates, coming from construction and demolition waste and from by-products, in cement-based materials; also supplementary cementing materials are covered by this review. The existing Codes and Guidelines regulating their application for structural concrete in several Countries are described.

Chapter 3 deals with a particular property of recycled aggregate concrete: its workability and rheology in the fresh state. The most diffused experimental methods for evaluating workability, consistency, flowability and passing ability are reviewed. Rheology of fresh cement-based materials, i.e. cement pastes, mortar and fresh concrete, is discussed, particularly with respect to fresh recycled concrete. Some experimental data collected from literature have been used, aiming to highlighting the influence of some design parameters on the overall behavior of the mixtures in the fresh state.

The design of concretes with recycled aggregate coming from metallurgical slag is covered by Chap. 4: some results collected from experimental campaign have been used to assess the influence of aggregates properties on the overall mechanical strength and durability of the concrete. The use of electric arc furnace slag for both replacing coarse and fine aggregates has been discussed.

Chapter 5 analyzes the environmental problems related to the use of recycled materials in concrete. Here a procedure for evaluating the environmental impacts of recycled aggregates and recycled concretes is described. Some examples about how performing a comparative estimation between two different recycled concretes are provided. Additionally some other environmental indicators, useful to capture environmental problems at local and regional scale, are described.

Lastly Chap. 6 provides a database about the available experimental results about electric arc furnace slag characterization and possible application in civil engineering applications. This original database can be used for comparing the properties of different slag, and to assess how they influence the properties of the material where they have been placed.

Chapter 2

Recycled Aggregates for Concrete Production: State-of-the-Art

2.1 Construction and Demolition Waste

All the waste materials coming from construction and demolition operations are known as C&DWs. These materials represent one of the most voluminous stream of waste generated in the world, accounting for about 25–30 % of the whole waste produced in the EU. As an indicative data, approximately 3 billion tons of waste are generated in EU 27 each year. Of this, around one third (1 billion tons) comes from construction and demolition activities [1]. C&DW typically comprises large quantities of inert mineral materials, with smaller amounts of a range of other components, depending on the source and separation techniques. The Waste Framework Directive 2008/98/EC [2] excludes from its definition the uncontaminated soil and other naturally occurring material, which are excavated during construction activities, when the material is used, and remains on site. However C&DW definition and composition may vary from state to state (e.g. with respect to the inclusion of excavated soil), and hence some caution is needed when reviewing statistics about its production in Europe and, more generally speaking, around the world. In the US total C&DW was estimated to be 170 million tons in 2003 [3]: a large fraction of this amount ends up in C&D landfills, and barriers to materials recovery still exist. Several reasons can explain the still low valorization of C&DW, including that buildings are not designed to be nor reused nor recycled, there is a lack of recovery facilities in some areas, and for some materials, the demand is too low due to the unwillingness to use recycled materials in place of virgin ones principally for some regulatory preventions. The competitiveness of C&DW recycling could be improved with several operations, i.e. raising the price of raw materials, through taxation, and setting End-of-Waste criteria for certain C&DW fractions [4].

Concerning C&DW composition, generally it is divided into five main fractions: metal, concrete and mineral, wood, miscellaneous and unsorted mixed fraction. More precisely, it may contain:

- concrete;
- bricks, tiles and ceramics;
- wood;
- glass;
- plastic;
- bituminous mixtures and tars;
- metals (ferrous and non-ferrous);
- soils and stones;
- insulation materials (including asbestos);
- gypsum-based materials (including plasterboards);
- chemicals;
- waste electronic and electrical equipment (WEEE);
- packaging materials;
- hazardous substances.

In this list several hazardous substances appear, which are generally present in building materials because they are used, together with concrete, for completing the structure and for realizing the finishes. These substances are asbestos (found in insulation, roofs and tiles and fire-resistant sealing), lead based paints (found on roofs, tiles and electrical cables), phenols (in resin-based coatings, adhesives and other materials), polychlorinated biphenyls (PCBs) (which can be found in joint sealing and flame-retardant paints/coats, as well as electrical items) and polycyclic aromatic hydrocarbons (PAHs) (frequently present in roofing felt and floorings). The composition of C&DW generally varies highly in relation to the site, because of the local typology and construction technique, climate conditions, economic activities and technologic development of an area, and hence it is difficult to define univocally a composition representative for a large region. The composition of C&DW is also changing during time, due to ageing of the existing buildings and to the low-quality structures, especially build between 1960s and 70s, which are coming to the end of their lifetimes and needing demolishing [5]. Selective demolition of existing structures can determine clear benefits in this context: it would not only reduce the amount of waste destined to landfill, but also increases the quality of the recycled aggregates, minimizing the quantity of impurities and contaminant in the C&DW [6]. However this approach is still under debate, mainly because of the slight practical value and economic benefit, even though some Countries are encouraging this practice [7]. Additionally, in the next future, waste management will be more controlled by the waste treatment BAT reference document (WT BREF) currently under preparation, including when dealing with C&DW management [8].

Concerning C&DW composition, as an indicative data, also inside a single State, it can be very different: for instance in Northern Italy, soils and stone represent the 17 % of the whole waste, but in Central Italy this datum decreases until the 4 % [9]. In average, Italian composition of C&DW is constituted by about 32 % of mixed construction and demolition waste, 27 % of a mixture of concrete, bricks, tiles and

ceramics, 14 % of iron and steel, and 11 % of bituminous mixtures. In the typical Finnish C&DW, wood and mineral materials constitute the predominant fraction (respectively about 36 and 35 %), followed by metal (nearly to 14 %) and the rest is other materials e.g. glass, plastic, gypsum and mixed waste [10]. In Germany 72.4 million tons of building waste were produced in 2007, corresponding to a recycling rate of about 68%: around 70 % is constituted by mineral debris from buildings, concrete and asphalt together represent about 25 %, and construction site waste is about 3 %, including gypsum-based waste [9]. In Greece, C&DW exceeded 3.9 million tons in 2000, representing about 656 kg per capita [11]. In Great Britain the production of recycled aggregate follows a WRAP Quality Protocol, and about 60 % of the recycled C&DW is used as aggregate, general fill or land reclamation. Around 17 % of UK aggregate needs are already met from recycled material [12]. Japan is one of the country where recycling of C&DW is more advanced: by 2000, demolished concrete was recycled up to 96 %, exceeding the target (90 %) proposed by the Japanese Ministry of Construction in the “recycled 21” program in 1992. RCA is applied almost at all as sub-base material for road carriageways [13]. Norwegian C&DW comes both from residential and non residential sources: in 2003 it was estimated that 1.256 million tons were generated, being principally constituted by concrete and bricks (about 67 %) [14]. In the US, 170 million tons of C&DW were produced in 2003: 39 % came from residential and 61 % from nonresidential sources. Cochran et al. [15] estimated that about 3.75 million tons of C&D waste were generated in 2000 in Florida, constituted mainly by concrete, representing the 56 % of all the waste. In Asia various studies have been done separately in some cities: in Shanghai C&D waste generation estimate was 13.71 million tons in 2012, and waste concrete, bricks and blocks represented more than 80 % of the whole [16].

The official data regarding the non-hazardous inert wastes’ recycling in Italy indicate that there are about 52 million tons of C&DWs produced per year [9], even though this number is poorly reliable. Between these, a relevant number of this waste is constituted by contaminated soils, which are generally also sent to inert waste treatment plants. Technology for separating and recovering C&DWs is well established, readily accessible and in general inexpensive. During the process of recycled aggregate production, the undesirable fractions are eliminated, and through grading and sorting, recycled aggregates are obtained. Also at the European level, the statistical significance of figures about C&DWs production is quite poor, and the different available sources are reporting fragmented data and several discrepancies. Currently the level of recycling and material recovery of C&DW varies greatly (between less than 10 % and over 90 %) across the Union, even though this number should increase and be homogenized in the next future, according to Article 11.2 of Waste Framework Directive [2], which states that “*Member States shall take the necessary measures designed to achieve that by 2020 a minimum of 70 % (by weight) of non-hazardous construction and demolition waste excluding naturally occurring material defined in category 17 05 04 in the List of Wastes shall be prepared for re-use, recycled or undergo other material recovery*” (including

Table 2.1 CDWs European production [17]

State	(×1000 ton)	State	(×1000 ton)
Belgium	22,239	Lithuania	357
Bulgaria	2235	Luxembourg	8867
Czech Republic	9354	Hungary	3072
Denmark	3176	Malta	988
Germany	190,990	Netherlands	78,064
Estonia	436	Austria	9010
Ireland	1610	Poland	20,818
Greece	2086	Portugal	11,071
Spain	37,497	Romania	238
France	260,226	Slovenia	1509
Croatia	8	Slovakia	1786
Italy	59,340	Finland	24,645
Cyprus	1068	Sweden	9381
Latvia	22	United Kingdom	105,560
Liechtenstein	0	Norway	1543

backfilling operations using waste to substitute other materials). According to the Eurostat [17], the C&DWs production of the European countries in 2010 is reported in Table 2.1, overall representing about 867 million tons.

C&DWs are characterized by high potential for recycling and re-use, since some of their components have high resource value, particularly with respect to a re-use market for recycled aggregates. Depending on their quality, recycled aggregates coming from C&DWs can be employed in roads, drainage and other construction projects, including structural concrete production. However this recycling potential is still under-exploited, especially in those States where the recycling rate is still low.

2.1.1 Processing Procedures for Recycled Aggregates Production

Two categories of plants are available for treating C&DWs and processing them into recycled aggregates: stationary and mobile ones. Stationary facilities are recycling plants located in an enclosed site authorized to recycle C&DW, through the use of fixed equipment and conducting no off-site operations. Mobile recycling machinery and equipment are instead sent to worksites to recycle waste at the source. The same equipment (screens, crushers, magnetic separators, etc.) is furnished by modules that allow recycling operations directly on the site.

Fixed plants may have the disadvantage of being far from the site where demolition takes place, but generally the system is more productive than the mobile

one (and therefore the burden associated to the increased transport is compensated by the better quality of the product and the higher capacity of the plant). Stationary plants generally process also natural aggregates and have higher capacity than mobile ones, allowing to limit the processing cost of the recycled aggregate (economies of scale). In Spain for instance there is a predominance of stationary facilities (48 stationary, vs. 1 mobile), even though in the last years some of them (4.1 %) temporarily engaged in mobile equipment rentals for off-site operations [18]. On the contrary, in Piemonte region (Italy) mobile plants account for 83% of the total and stationary facilities for only 4.4 % [19].

Plants can accept different types of C&DW, depending essentially on the basis of how clean it is and the materials it contains. The standard classification of the input material is clean, mixed and dirty. Preliminary cleaning can be performed through separation (typically in dry conditions), to eliminate impurity e.g. wood, plastic and paper. Magnetic separation is also useful to remove steel and iron from the input material.

The same processes take place in both the plants, aiming to separate the contaminants from the bulk stony material, and to obtain a useful grading:

- separation;
- crushing;
- separation of ferrous elements;
- screening;
- decontamination and removal of impurity (i.e. wood, paper, plastics,...).

The first operation to be done aims to reduce the debris dimensions, which have to be used to feed easily the crusher. Then, several operations, mainly mechanical actions, are conducted to reduce again the size of the material, being grinding, squeezing and impacting. Primary and secondary crushing could be performed, with milling operations, to achieve the required grading. At the end of the productive chain, washing could also be done, even though this procedure is not very common due to the difficulties in the produced mud disposal (both in terms of costs and administrative procedures).

A simplified scheme of a C&DWs treatment plant is represented in Fig. 2.1.

2.1.2 International Codes, Guidelines and Regulations

Recycled aggregates (RA) coming from C&DWs are valuable materials, for which a re-use market already exists, and it consists mainly in earthworks, road base, pavements and other construction applications. From an economical point of view, they are particularly attractive in densely populated areas, i.e. where demand and supply are close together. In those cases, low transportation costs and limited availability of natural aggregates are key factors that make recycled aggregate

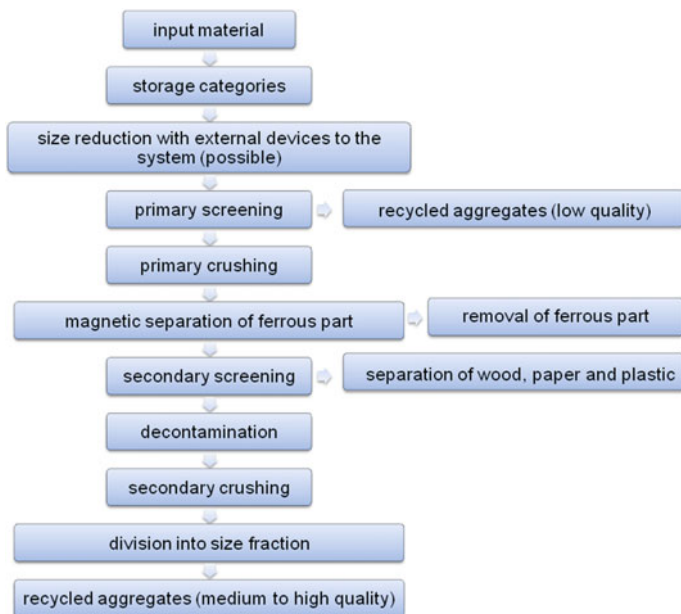


Fig. 2.1 Scheme of a C&DWs treatment plant

competitive with their natural counterparts, without any necessity of specific policy instruments (e.g. taxation of raw natural materials).

Their use in structural concrete production has been widely explored in literature, principally at the lab-scale level, often reporting good results when the replacement ratio of natural aggregates is limited, and high quality RA are used. However, the international codes, guidelines and recommendations vary greatly from country to country, with respect to the maximum allowable quantity and quality allowed in structural concrete mixtures. In this section a brief outline of the current situation about the existing codes and normative regulating the use of recycled aggregates is given, paying a particular attention on their application for concrete production.

Belgium In Belgium, the set of standards which regulates the use of recycled aggregates is made up by the existing European ones:

- EN 13242:2008—Aggregates for unbound and hydraulically bound materials for use in civil engineering work and road construction [20];
- EN 13043:2002—Aggregates for bituminous mixtures and surface treatments for roads, airfields and other trafficked areas [21];
- EN 13285:2010—Unbound mixtures—Specifications [22];
- EN 14227 serie—Hydraulically bound mixtures [23].

Recycled aggregates characterization is performed using the existing standards for natural aggregates, and additionally, with:

- EN 933-11:2009—Tests for geometrical properties of aggregates—Part 11: Classification test for the constituents of coarse recycled aggregate [24];
- EN 1744-6:2006—Tests for chemical properties of aggregates—Part 6: Determination of the influence of recycled aggregate extract on the initial setting time of cement [25].

A national standard, PTV 406 Technical Prescription “Recycled aggregates from construction and demolition waste” [26] also exists, and it regulates the composition of the recycled aggregate that could be used in concrete production. Three RA classes are defined: recycled concrete aggregate (RCA), recycled masonry aggregate (RMA), and mixed aggregate, being a mixture of both concrete and masonry aggregates.

The use of recycled aggregates for concrete production is regulated through the European existing standards, and it is limited to the coarse recycled concrete aggregate fraction (CRCA). It can be used in the exposure class X0 and XC1, and Belgian environmental classes E0 and E1. Concretes produced with these aggregates should have a maximum strength class limited to C25/30; when higher strength classes and different exposure conditions are used, the technical validity should be experimentally demonstrated. The maximum allowed substitution ratio is 20 % in volume of the total coarse aggregates in the mixture.

Germany In Germany, the set of standards which regulates the use of recycled aggregates for concrete production is given by the European existing ones, and additionally by the standard DIN 4226-100 [27]. In the latter, some specifications about the aggregates requirements in relation to the field of application are defined. Four types of RA are allowed (Type 1–4), depending on the content of concrete, natural aggregates, clinker, non-pored bricks, sand-lime bricks, asphalt, other materials such as pored bricks, lightweight concrete, no-fines concrete, plaster, mortar, porous slag, pumice, stone, and foreign substances, e.g. glass, non ferrous metal slag, gypsum, plastic, wood, paper, etc. For each class of RA, two acceptance criteria are defined: oven-dry density and absorption ratio of aggregate. The limits are reported in Table 2.2.

Table 2.2 Acceptance criteria for RA according to German standards

	Oven-dry density criterion (kg/m ³)	Absorption ratio of aggregate criterion (%)
Type 1: concrete chippings/concrete crusher sand	≥ 2000	≤ 10
Type 2: construction chippings/construction crusher sand	≥ 2000	≤ 15
Type 3: masonry chippings/masonry crusher sand	≥ 1800	≤ 20
Type 4: mixed chippings/mixed crusher sand	≥ 1500	No requirement

Only the chipping of concrete according to type 1 and type 2 (as defined in the above standard) can be used for concrete production. Type 1 RA can be associated to a RCA: it contains at least 90 % of concrete and natural aggregates, not more than 10 % of clinker, non-pored bricks, sand-lime bricks, less than 2 % of other mineral materials and less than 1 % of asphalt. Foreign substances such as glass, metal slag, etc. should be less than 0.2 %. Type 2 RA contains instead at least 70 % of concrete and natural aggregates, not more than 30 % of clinker, non-pored bricks, sand-lime bricks, less than 3 % of other mineral materials and less than 1 % of asphalt. Other substances can be present in a quantity not greater than 0.5 %.

The other type of aggregates, i.e. masonry chippings and mixed chippings are excluded from the reuse as aggregate in structural concrete. Additionally also crusher sand is excluded from the reuse as recycled aggregate: the minimum RCA diameter allowed is 2 mm. Further limits are reported in the German Committee for Reinforced Concrete (DAFSTB) Code [28]: Concrete with Recycled Aggregate, where a limitation on the strength class (C30/37) and on the substitution ratios are given in relation with the exposure class and application (Table 2.3).

Great Britain In Great Britain the normative distinguishes two types of recycled aggregates, RCA and RA, the former coming just from concrete-based material, characterized by a limitation of about 5 % in masonry content (in weight), and the second from a mixed waste. The complementary UK Standard to EN 206-1, BS 8500-2 2015 [31], limited the use of RA to the production of road surfaces or underpinning works [9]. The use of recycled aggregates is limited until C16/20 strength class, and only in the mildest structure exposure conditions. This choice is governed by the absence of a specific regulation about recycled aggregates use, which is reflected in a great variability of their properties, composition and origin. Concerning the RCA, they are admitted to partially substitute natural aggregates, until 20 % in weight, up to concrete strength class C40/50, and within prescribed exposure classes: X0, XC1, XC2, XC3, XC4, XF1, DC-1. Exposure to salt (XS, XD) and severe freeze-thaw (XF2–XF4) are excluded. Higher replacement ratio are allowed only with documented experimental results, hence if the prescriber takes his own responsibility for the results.

Italy In Italy, the existing set of European standards are applied to characterize recycled aggregates. The approach is very similar to the other European countries. The Italian Code for constructions regulates the maximum allowable quantities of RA in concrete, with respect to concrete strength class and exposure conditions [32], as reported in Table 2.4.

Table 2.3 Substitution ratio (in % by volume) according to EN 206-1 [29] and DIN 1045-2 [30]

Field of application		Type 1	Type 2
Dry	Exposure class XC 1	≤ 45	≤ 35
Humid	Exposure class X 0	≤ 45	≤ 35
	Exposure class XC 1 to XC 4	≤ 45	≤ 35
	Exposure class XF 1 and XF 3	≤ 35	≤ 25
	Exposure class XA 1	≤ 25	≤ 35

Table 2.4 Maximum allowable quantity of RA in concrete according to Italian normative

Origin of recycled aggregate	Concrete class	Rate of use
Demolition of building (debris)	=C8/10	Up to 100 %
Demolition of concrete or reinforced concrete	≤ C30/37	Up to 30 %
	≤ C20/25	Up to 60 %
Reuse in certified precast concrete industries—any class of concrete	≤ C45/55	Up to 15 %
Reuse in certified precast concrete industry—class of concrete > C45/55	Same class of original concrete	Up to 5 %

The Code however does not provide any information about the values of mechanical or physical properties that the recycled aggregates should comply with; these limits are present in the EN standards, specifically in the EN 12620 “Aggregates for Concrete” [33]. This standard defines the properties needed by the aggregates to comply with the requirements stated in the EN 206-1 [29]. The Italian standards UNI 8520-1 [34] and UNI 8520-2 [35] provide some complementary instructions necessary to apply the above standard. Lastly, UNI EN 13242 “Aggregates for unbound and hydraulically bound materials for use in civil engineering work and road construction” [20] provides the possible applications of recycled aggregates in specific fields, i.e. civil engineering work and road construction.

Japan In Japan, three types of recycled aggregates are currently considered, depending on their quality in terms of composition and physical properties: high-quality recycled aggregates (type H), medium-quality (type M) and low-quality (type L). One of the first regulation in the field of recycled aggregate use was JIS A 5021 [36], which established standards for high-quality recycled aggregate use in concrete since 2005. This standard has been recently substituted with the novel JIS A 5021:2011 [37]. Recycled aggregates type H is produced through advanced processing, including crushing, grinding and classifying, of concrete masses generated in the demolition of structures. Class H recycled aggregates should comply with stricter limits about composition, contaminants content and physical properties with respect to medium-quality M [38] and low-quality recycled aggregates L [39].

Type H aggregates, characterized by not more than 3 % of other non concrete and non virgin aggregates material, can be used, without restrictions, in structures with nominal strength lower than 45 MPa. Type M aggregates can be used in members that are not subjected to frost action, such as piles, underground beams, and concrete filled in steel tubes. Lastly, type L could be used in backfilling, filling and leveling concrete applications. The latter type of aggregates can be used only with type B blended cements, as a measure against alkali-aggregates reactivity. The acceptance criteria for RA (type H, M and L), in terms of minimum OD (oven-dry) density and maximum absorption ratio, are specified in Table 2.5.

Table 2.5 Acceptance criteria for RA according to Japanese standards

	Oven-dry density criterion (kg/m ³)	Absorption ratio of aggregate criterion (%)
Type H coarse	≥ 2500	≤ 3
Type H fine	≥ 2500	≤ 3.5
Type M coarse	≥ 2300	≤ 5.0
Type M fine	≥ 2200	≤ 7.0
Type L coarse	No requirement	≤ 7.0
Type L fine	No requirement	≤ 13.0

Netherlands In the Netherlands, the set of standards which regulates the use of recycled aggregates for concrete production is given by the European existing ones, and additionally by the standard NEN 5905 [40], where the requirements that RA should satisfy are reported. Two types of recycled aggregates are defined, depending on their composition. The current normative allows the use of RCA, characterized by at least 95 % of concrete-originated material, for concrete manufacturing for pre-stressed and reinforced structures, but it is limited to the coarse fraction (CRCA). RCA should not contain more than 5 % of masonry, 0.1 % of organic materials, and 1 % of impurities (asphalt is not included in this definition). It should satisfy three minimum requirements in terms of minimum OD density, maximum chloride and sulfate content, being respectively 2000 kg/m³, 0.05 and 1 %. CRCA can be applied in structures with a maximum strength class equal to C40/50, and in non-aggressive environments. For non-structural concrete (i.e. strength class lower than C16/20), also mixed RA can be used: this type of aggregate should satisfy the same physical and chemical requirements of RCA, but its composition can be made by until 65 % of masonry and 1 % of organic material.

Portugal In Portugal the use of recycled aggregates for structural purposes is regulated by the LNEC E 471 standard [41]: this specification classifies coarse recycled aggregates and defines minimum requirements for their use in concrete. Various other standards exist about the use of RA for several applications: LNEC E 472 [42] focuses on hot mix asphalt applications, LNEC E 473 [43] is about unbound pavement layers, and LNEC E 474 [44] is about embankment and capping layer of transport infrastructures.

Three types of recycled aggregates are defined with respect to their composition, e.g. concrete, masonry, asphalt, floating matter and other materials content, according to the classification reported in Table 2.6. Only classes ARB1 and

Table 2.6 Classification of recycled aggregate according to Portuguese normative

Classes	Concrete (%)	Masonry (%)	Bituminous (%)	Contaminant (%)	Floating (%)
ARB1	≥ 90	≤ 10	≤ 5	≤ 0.5	≤ 0.2
ARB2	≥ 70	≤ 30	≤ 5	≤ 1	≤ 0.5
ARC	≥ 90	–	≤ 10	≤ 2	≤ 1

ARB2, which are made principally by concrete-origin aggregates, are allowed to be applied into structural concrete. Class ARC is excluded from structural applications: coarse ARC aggregate can be only used for non-structural applications, i.e. leveling and filling concrete, in non-aggressive exposure classes. It is worth noting that, for these applications, no limits about the maximum replacement level exist for ARB1 and ARB2 types.

The replacement ratio for structural application is defined in accordance with the exposure and strength class of the structures where they will be placed: ARB1 aggregates can be used in structures with a maximum strength class of C40/50, up to 25 % replacement of natural aggregates. ARB2 aggregates can instead be used in structures with maximum strength class of C35/45, up to 20 % replacement of natural aggregates. In both the cases, the exposure classes of the structure where they will be placed is limited in certain ranges, and it should fall within the followings: X0, XC1, XC2, XC3, XC4, XS1 and XA1. The use of fine recycled aggregates for concrete production is not allowed. In addition, concrete produced with recycled aggregate could not be used in structures in contact with water for human consumption.

Spain In Spain the use of recycled aggregates for structural concrete application is regulated by the Structural Concrete Instruction EHE-08 [45]. RA should comply with some compositional requirements, i.e. ceramic materials must not exceed 5 % of the total weight sample, light particles, asphalt and other impurities such as glass, plastic, etc, should not exceed 1 %. The Code fixes the limit of maximum substitution ratio for structural concrete applications equal to 20 % in volume of the whole coarse aggregates. The maximum characteristic compressive strength of the structures where RA could be placed should be 30 MPa. For non-structural concrete applications, in the Annex 18 of the previous Code, the maximum allowable content of RA could arise up to 100 % of the whole coarse aggregates.

US In the United States there is no regulatory barrier to the use of recycled concrete aggregate in structural concrete: since 1982, ASTM C33 [46] has included crushed hydraulic cement concrete in its definition of coarse aggregate, while ASTM 125 [47] allowed crushed hydraulic-cement concrete as manufactured sand. However the use of recycled concrete aggregate still remains limited for structural purposes.

2.1.3 RAC Concrete—Mixture Proportioning

For satisfactorily high quality concrete, recycled aggregate must comply with some minimum requirements, mainly concerning chemical stability and physical–mechanical characteristics. International codes and standards establish different requirements, in relation to the specific necessity of each Country, the composition of the input C&DW, the available construction techniques and climate conditions. In general terms, high quality RA are mainly constituted by low quantity of masonry aggregates (less than 5 % in weight of the sample), low content of

impurities, OD density should be comparable to the natural aggregates one, and water absorption should be limited.

Mix proportions also greatly influence the final performance of concrete. In particular, the design of recycled aggregate concrete (RAC) is usually carried out by simply replacing the Natural Aggregate (NA) of a Natural Aggregate Concrete (NAC) with recycled material. Differences in physical properties among aggregates, such as surface texture and water absorption, are just taken into account as a parameter which the aggregates should comply with. When replacement ratio is limited (not greater than 20 %), ordinary performances concrete made with RCA (mostly composed by concrete-material) are not affected by the substitution. However, when the substitution ratio increases, or when specific performances are required, e.g. durability in severe exposure conditions, high strength, etc., the use of RCA may determine a loss of performances, both in mechanical and durability terms.

Typically, when designing RAC, RA is taken as NA, through two possible methods: Direct Volume Replacement (DVR), and Direct Weight Replacement (DWR), substituting NA with an equivalent amount of RCA in volume or weight percentage respectively. This is the main cause of the poor mechanical performance often reported in the literature when different kinds of RAC mixes were tested [48–50], principally in the test conditions above reported (high replacement ratio, high strength target, severe exposure conditions). A novel method, recently introduced by Fathifazl et al. [51], called Equivalent Mortar Volume (EMV), has been used to prevent the strength losses often reported in literature. The method basically considers RCA as a two-phase material, composed of NA and the mortar attached to it (here denoted as RM, residual mortar), which must be quantified and counted in the proportion of the mix (Fig. 2.2). Since the physical properties of RCA are affected by the RM quantity and characteristics, this method can directly account for any deficiencies in low-quality aggregate, balancing the mix without affecting the mechanical and durability-related performance of the final concrete. This allows the RAC mix to be prepared with a similar internal structure to that of NAC [52, 53].

Fig. 2.2 Recycled concrete aggregate



As regards possible workability problems, replacement of NA by RA generally confers greater stiffness to concrete, as confirmed by the lower slump values often reported in the literature when testing the fresh properties of recycled concretes. Several authors have confirmed this problem [54, 55], arguing that the reasons for this behavior are closely related to the physical properties of the RA: higher water absorption, higher angularity and rough surface texture. The lower quality of the recycled aggregates, the higher slump losses have been indeed experimentally observed. This problem can be overcome following two approaches: the first is through the use of water-reducing admixtures (WRA) in the mix, acting directly on concrete mix design. Alternatively, certain mixing procedures for RACs can be also applied. The commonly named Mixing Water Compensation Method [56] for elaborating concrete, based on added water which recycled aggregate absorbs to the total needed by the mix, allows acceptable workability to be achieved. In the case of EMV methodology, the parameters controlling workability should be carefully taken into account, due to the reduced amount of fresh mortar in the mix in favor of increased coarse aggregate volume.

Other techniques to improve RCA quality, and therefore limiting possible deficiencies in RAC properties, are currently available, such as the Autogenous Cleaning. This method, at least when implemented at the laboratory scale, led to positive results in terms of enhancement of properties of crushed concrete particles, especially in terms of reduction of RM content and, consequently, on their water absorption [57].

2.1.4 RAC Concrete—Mechanical Properties

Concrete strength is the key mechanical property of structural concrete. Particularly uniaxial strength in compression is accepted as the representative index of compressive strength, which is also related to strength under other stress states, i.e. tensile and flexural strength, elastic modulus, etc. Several factors affect concrete strength, starting from the water/cement ratio, which is particularly important because it directly affects concrete porosity and the quality of the interfacial transition zone (ITZ). In addition, aggregate size, mineralogy and type (natural–limestone or siliceous aggregates, recycled, artificial, etc) are also particularly relevant in influencing concrete strength. Recycled aggregate quality can highly affect RAC concrete properties too, and its composition is one of the most important acceptance criteria which should be verified. Referring to RCA, the quantity of the adhered mortar attached to the virgin aggregates, is also a very important parameter to be analyzed when designing RAC.

Concerning the quality of the microstructure of ITZ in RAC, as reported in [58], SEM observations revealed that the aggregate-cement matrix interfacial zone is very porous with respect to the same ITZ in a conventional concrete, which is denser. Increasing substitution ratio generally decreases mechanical strength, as obtained in numerous research works [48–50]. A linear relation between RAC

density (depending directly on RCA substitution ratio, which has typically lower density than NA) and compressive strength was also obtained in [59]. The quality of recycled aggregate, in terms of RM mechanical properties, affects the strength of recycled aggregate concrete when the water-binder ratio is low; on the contrary, this not happens when the water-binder ratio is high, being the strength principally affected by the water content in the mix. Admixture types and content, and the rate of loading also influences RAC quality and strength.

Typically, the full replacement of NA with RCA through both DVR and DWR concrete design methods leads to a reduction of 20–25 % in 28-days compressive strength, with respect to conventional mixtures. An increase of cement content may be useful to achieve the same strength of the control concretes, but it is considered nor cost- nor environmental-effective. Additionally, the reduction in the elastic modulus can reach 45 % when the RCA replacement is 100 % [60].

A full replacement of NA with RCA has been used successfully in concretes with low-medium compressive strength, i.e. until 20–40 MPa [61]. Some studies have been carried out also to assess the feasibility of using RCA in HPC [62], obtaining in most cases that high replacement ratios (more than 30 %) significantly affect concrete strength and density. With the increase of the RCA content, water absorption, shrinkage and creep strains increase *ceteris paribus*. However, it should be recalled that the source of RCA is very important with respect to RAC properties [63], and the more restrictive the acceptance criteria, the lower differences would be expected between recycled and conventional concretes.

2.1.5 RAC Concrete—Durability

Durability of RAC can be evaluated through several experimental methods, depending on the deterioration process which should be represented at laboratory scale. Generally the lower properties of recycled aggregates, i.e. the lower density and mechanical strength, within the higher absorption and porosity, determine RAC to be less durable in terms of carbonation, chloride penetration, permeation, and freezing/thawing resistance [64]. Another internal source of deterioration arises from the possible contamination of recycled aggregates by gypsum or admixtures and binders, which lead to an increased content of sulfates inside the mix [65]. The same may occur if recycled aggregate is contaminated by chlorides, which can lead to an internal source of chlorides inside the mix. In both the cases the addition of mineral admixtures, such as fly ash, can reduce the chloride penetration depth, in particular at low water/cement ratio (a factor which also, per se, improves RAC durability).

It has to be recalled that also the mixture proportioning method may affect concrete durability: recent research works demonstrated that, for instance, when the EMV proportioning method is used, durability-related properties in chlorides-exposed environment are improved with respect to RAC proportioned with DWR method [53].

2.1.6 RAC Concrete—Structural Concrete

A number of experiments on structural elements have been performed in literature, with the aim of analyzing structural properties of real-scale elements. One of the most important property that was analyzed is related to the flexural behavior of reinforced recycled concrete beams: a typical load scheme which can be found in many papers involves simply supported beams subjected to four point bending tests. In this test, the specimens are loaded at two points, symmetrically with respect to the mid-span of the element. Generally, flexural behavior is discussed with reference to control virgin concrete beams, in which the reinforcement ratio, curing conditions, and concrete mix design (except for the aggregates substitution effect) are maintained constant. The parameters which are often analyzed are load, deflection at the mid-span, and when it is possible, the stresses in the reinforcement.

Flexibility of RAC beams is generally greater than in NA concrete, under the conditions of same bending moment, w/c ratio, steel reinforcement ratio. In addition, RAC beams experienced often wider cracks and smaller crack spacing, with a lower flexural strength compared to the companion control members. Those results may discourage the use of RAC in structural concrete elements, because it creates further uncertainty with respect to the serviceability and long-term performances of RCA concrete structure [66, 67]. However when high quality RAC are used, or when EMV proportioning method is applied, also structural properties highly improve, reducing significantly the dispersion of the results: at both the service and ultimate states, the flexural performance of reinforced RCA-concrete can be comparable or even superior to that of concrete made entirely with natural aggregates. The flexural theory based on equilibrium equations and the current code provisions for flexural design of conventional RC beams seem to be satisfying also for RAC beams design [68].

Unlike in RC beams subjected to flexure, where longitudinal reinforcement has a prior role in the structural response of the element, concrete plays a more significant role in beams subjected to shear loading. In fact, shear behavior is governed by the shear capacity of the reinforcement, as well as the concrete shear capacity. Also in this case a number of works have tried to assess the influence of RAC in the response of RC beams subjected to shear, both when transversal reinforcement (i.e. stirrups) was present and when no.

In general terms, shear strength of RAC beams is lower than in NAC beams with the same reinforcement ratio and shear span-to-depth ratio [69, 70]. The current codes and existing model underestimate shear capacity of RC members, both made with NAC and RAC, hence, the use of RCA does not determine uncertainty which could not be accounted by the models. The same consideration given for the flexural behavior can be given if high-quality RA are used.

Lastly, Corinaldesi et al. [71] investigated also the behavior of reinforced beam-column joints under cyclic loading, to assess the seismic performance of RC frame joints. The parameters observed were the failure modes, the hysteresis loops, the ductility and the variation of strength and stiffness under the seismic loads.

The joint made of RAC showed adequate structural behavior, however, to achieve safe structural performance, the actual RAC shear strength and stiffness should be considered during the design.

2.2 Metallurgical Slag

Several kinds of slag could be used in concrete production, as cement or aggregate replacement. Among the materials that are currently used, or at lab-scale or already covered by specific regulations and standards, Granulated Blast Furnace slag (GBS) and Air-cooled Blast Furnace slag (ABS) are generally used as supplementary cementing material (SCM). In addition, Electric Arc Furnace slag—from carbon (EAF-C) or stainless/high alloy steel production (EAF-S)—can be potentially used as natural aggregate replacement. Lastly, Basic Oxygen Furnace slag (BOF) has been experimentally used for both the applications.

Between these materials, a particular interest emerges about steel by-products, because of the great amount of slag deriving during its production. In fact, the total amount of steel slag generated in 2006 was about 16.9 million tones. Euroslag, an international organization dealing with iron and steel slag matters, divides this amount in: 57.7 % basic oxygen furnace slag, 25.9 % are electric arc furnace slags from carbon steel production, 5.9 % are electric arc furnace slag from high alloy steel production and 11.1 % come from secondary metallurgical slag (Fig. 2.3).

Steel slag is produced during the separation of molten steel from impurities in steel furnaces. The slag appears as a molten liquid and is a complex solution of silicates and oxides that solidifies upon cooling. As previously stated, there are several types of steel slag produced during the steel-making process: among these, basic oxygen furnace steel slag (BOF slag), electric arc furnace slag (EAF-slag) and



Fig. 2.3 Steel slag production in Europe [72]

ladle furnace slag (LDF-slag) or refining slag are particularly important, at least in terms of amount produced.

Steel can be produced in electric arc furnaces by melting recycled steel scrap, using heat generated by an arc, created by a large electric current. The slag is formed through the addition of lime, which removes impurities from within the steel. Slag has a lower density than steel and therefore floats on top of the molten bath of steel.

Basic oxygen furnaces are characterized by a different industrial process: hot liquid blast furnace metal, scrap and fluxes, which consist of lime (CaO) and dolomitic lime (CaO-MgO), are initially charged into the furnace. Then, the oxygen, which is injected into the furnace, reacts and removes the impurities in the charge. Those impurities are mainly constituted by carbon as gaseous carbon monoxide, and silicon, manganese, phosphorus and some iron as liquid oxides, which combine with lime and dolomitic lime to form the BOF steel slag.

After being tapped from the furnace, molten steel is transferred in a ladle for further refining to remove additional impurities still contained into the steel. During this operation, known also as ladle refining, additional steel slag are generated by adding again fluxes to the ladle to melt.

Steel mill scale is produced during processing of iron in steel mills. During the processing of steel in steel mill, iron oxides are formed on the surface of the metal during the continuous casting, reheating and hot rolling operations. The iron oxides, also known as steel mill scale, are then removed by water sprays.

According to the physico-chemical properties of each kind of slag, a specific use for each type of material can be found: for example, steel slag are suitable as amour stone and for air quality control; steel slag and ABS are both suitable for gabions manufacture, railway ballast, roofing and for the treatment of waste water; steel slag and GBS are both suitable as sealants; and finally GBS can be applied as sand blasting. In general, both steel slag and blast furnace slag are used for unbound mixtures and hydraulically bound mixtures, for bituminous mixtures, in concrete, in mortar and in embankments. The steel mill scale is similar to steel slag and therefore, like steel slag, it can be used in concrete production.

The use of slag aggregates from iron and steel production in construction has old origins, since when the Romans used crushed slag from the crude iron production for roads building. Nowadays, slag is still used to build roads. Currently it is not only used for road surfaces constructions but also as aggregates for concrete production. Slag must be treated through sieving, crushing and wetting process. The processing techniques are fundamental to obtain high-performances slag. Attention should be paid to allow an adequate particle grading for the intended use, to fit the properties in accordance with product standards or specifications.

A great interest is currently focused in Electric Arc Furnace slag (EAF), because of the great numbers related to its production, which involves approximately 10 million tons every year of material, and it is destined to grow because of the increase in the use of this technology.

EAF slag is the main by-product of steel production in electric arc furnace plant. It could be classified into two types: black basic slag, with a lime content less than 40 %, resulting from the cold loading of scrap; and white basic slag, with a lime content higher than 40 %, generated during grinding, when more lime is added to remove sulfur and phosphorus from the produced steel [73]. An electric arc furnace is a furnace that heats scrap metal or recycled stainless steel by means of an electric arc and it produces steel. The fusion is possible due to an electric arc which is constituted by three cylindrical electrodes made of graphite, which enter inside the crucible of the furnace from the vault. The components of this type of furnace are three: the first is the hearth, the second is the shell and lastly there is a roof. The hearth is a metal structure lined with refractory material and which is able to oscillate so the inclination of the kiln can be changed (this facilitates the operations of slagging and tapping). The shell is a metal cage which allows to contain the material and then pours it into the oven. The roof can be moved to allow the opening during loading of the material, and it is also envisaged of three holes for the passage of the electrodes. Limestone and slag correction agents, e.g. bauxites, can be used as additives, i.e. slag formers. The operations required to produce steel (and EAF slag) are:

- furnace charging;
- melting;
- refining;
- de-slagging;
- tapping;
- furnace turn-around.

During the steel production, slag is also formed: slag has a lower density than steel and therefore floats on top of the molten bath of steel. Then slag is cooled, generally with water, at least for 24 h (see Fig. 2.4), it is aged for about two months



Fig. 2.4 Slag cooling

or more under atmospheric conditions, and then it is ready to be treated again for its processing as aggregate. Typical treatments to be performed on the EAF slag are:

- Pre-screening;
- Screening;
- Crushing;
- Secondary screening;
- Secondary crushing;
- Magnetic separation;
- Tertiary screening—particle size separation;
- Storage;
- Washing and stabilization.

2.2.1 EAF Slag—Characterization

EAF slag is a crushed product, which generally has very good mechanical properties, constituted by particles with a hard, dense and angular shape. It has generally high abrasion resistance, low aggregate crushing value (ACV) and excellent resistance to fragmentation. However, the productive process and the chemical composition of the metal scraps molted in the furnace significantly influence its characteristics.

Several research works were performed in literature aiming to characterize EAF slag, trying to establish a suitable application for this material. One of the first research work was published in 1997 by Al-Negheimish et al. [74], who investigated its potential use in cement-based materials, by means of tests on the main mechanical properties, such as compressive and tensile strength. No studies about the long term concrete properties were done. The slag used was relatively non-porous, with a low absorption rate and with an angular shape that helped in developing very strong interlocking properties. The same characteristics in terms of shape and texture of the slag were derived by the further works of Anastasiou and Papayianni [75, 76], Manso et al. [77], Xue et al. [78], Ahmedzade and Sengoz [79], Pellegrino and Gaddo [80], Pellegrino et al. [81]. EAF slag was appearing as a black color stone, with a rough surface texture, characterized by a higher bulk density than natural aggregates, and in general, a higher porosity. This was also confirmed by SEM images taken in [74]. Some physical properties, experimentally evaluated in some research works reported in literature, were collected and are reported in Table 2.7.

A very discussed problem relates to possible expansion phenomena that may occur in steel slag aggregates. This is due to the presence of some expansive compounds, which may hydrate and increase their molecular volume, affecting the dimensional stability of the aggregate. Accordingly, it is very important to define the content of those components, i.e. free lime (CaO) and free periclase (MgO),

Table 2.7 Physical properties of steel slag

Property	EAF slag	Reference
Specific gravity (t/m ³)	3.5	Manso et al. [77]
	3.51	Maslehuddin et al. [83]
	3.33	Papayianni et al. [76]
	3.64–3.97	Pellegrino and Gaddo [80]
Los Angeles (%)	15–20	Manso et al. [77]
	11.6	Maslehuddin et al. [83]
	<20	Pellegrino and Gaddo [80]
Compressive strength (MPa)	>130 MPa	Manso et al. [77]
Percentage of voids (%)	55.5	Papayianni et al. [76]
Water absorption (%)	0.3–0.9	Manso et al. [77]
	0.85	Maslehuddin et al. [83]
	2.50	Papayianni et al. [76]
	0.18–0.45	Pellegrino and Gaddo [80]

which presence may hinder the potential use of slag in construction industry. Free lime and periclase are often detected in BOF slag, whereas their presence has been not frequently experimentally observed in EAF slag. Pretreatment operations are recommended to lower the potential expansion of those materials. Ageing and weathering of slag are often applied, as also steam or autoclave curing. Several works in literature have demonstrated the effectiveness of pretreatment operations in reducing the content of potential expansive compounds [77, 80, 82].

Table 2.8 lists the chemical composition of some EAF slag used in literature. Typically the most abundant oxides corresponded to Fe₂O₃, CaO, SiO₂ and Al₂O₃. EAF slag is generally basic, i.e. the sum of the basic oxides over the sum of the acid oxides is greater than 1. Several indexes are available to classify slag basicity, between which the most common is the ratio B_2 , between CaO and SiO₂. However, several works recommend to use the B_4 index, reported in Eq. (2.1):

$$B_4 = (\text{CaO} + \text{MgO})/(\text{SiO}_2 + \text{Al}_2\text{O}_3) > 1 \quad (2.1)$$

Table 2.8 Chemical composition of EAF slag

	Manso et al. [82]	Pellegrino and Gaddo [80]	Tossavainen [84]
	Spain	Italy	Sweden
SiO ₂ (%)	15.30	10.1	32.2
Al ₂ O ₃ (%)	7.40	5.70	3.70
CaO (%)	23.90	24.20	45.50
MnO (%)	4.50	5.10	2.0
MgO (%)	5.10	1.90	5.20
Fe _x O _y (%)	42.50	37.20	27.41

According to Daugherty et al. [85], as the acidity of the slag increases, glassy phases are more likely to be produced; on the contrary, basic slags are mainly crystalline. Generally EAF slag are less basic than LDF and BOF slag: Engström et al. [86] obtained for BOF slag a B_4 index equal to 3.9, whereas for EAF slag this value decreases until 1.4. It should be noted that the reactivity of CaO increases with the slag basicity [87], and hence problems of expansion linked to EAF slag seem to be very limited. This result is also confirmed by the mineralogical composition of the slag often reported in literature, which is mainly constituted by the following mineral forms: wustite, hematite, magnetite, merwinite, etc.

Another environmental obstacle limiting the use of some slags in construction is represented by the potential leaching of hazardous substances. Particularly some EAF-slags from stainless steelmaking can have insufficient properties to be used as construction material, and may sometimes not meet the environmental requirements due to high leaching rates of chrome. The leaching from steel slags is generally characterized as a surface reaction, followed by a solid-solid diffusion process, in order to retain equilibrium in the materials. A minimization of the surface area of the slag is therefore likely to reduce leachability. Pre-treatment operations are often effective not only in reducing potential expansion phenomena, but also to reduce the concentrations of harmful substances or the high leaching levels of these elements.

2.2.2 EAF Slag Concrete

Since a long time the use of steel slag has been proposed for designing blended cement, in cement clinker, as aggregate or hydraulic binder in road construction. However, not much is reported as aggregate for cement mortar and concrete manufacture. In the few available literature studies, mainly EAF slag has been used. The analyzed concrete properties were limited to some mechanical characterization, or simple fresh concrete workability measurement.

The first complete chemical analysis on EAF slag was conducted in 1999 in Spain [73], even though the first works were approached in Germany in 1994 and subsequently in France in 1998. The studies were carried out using optical microscopy, inductively coupled plasma spectroscopy (ICP) for the chemical part, X-Ray diffraction (XRD) and infrared (IR) absorption spectroscopy for the mineralogical characterization. Also scanning electron microscopy (SEM) was used to obtain images of the material media. Since the first results, EAF slag appeared as a material with high porosity, dense and compact, with a surface characterized by high iron content. Particle density was very high, whereas water absorption was limited, according to the standard DIN 40 301 "Ferrous and non-ferrous blast furnace slags for building uses" which was active at that time. Also dimensional stability was investigated, because of the increasing necessity to establish if slag could meet the standards as a building material.

After a couple of years, several studies arose as an emerging research topic, regarding slag application in asphalt mixtures. In Arabian areas, where the availability of good-quality aggregate is generally scarce, the research on slag-concrete was significant: several studies aimed to compare mechanical properties of EAF concretes with crushed limestone aggregate concrete. Maslehuddin et al. [83] produced concrete mixes where they substituted all the coarse aggregates with EAF slag, maintaining the dune sand content constant in both recycled and traditional specimens. Results highlighted that, as the substitution ratio increased, compressive strength increased *ceteris paribus*, maintaining the same aggregates grading curve. At the same time, also flexural strength increased, whereas the absorption, volume of permeable voids and pulse velocity decreased, revealing a denser concrete. Furthermore, results of durability tests were positive, because of the high impermeability of slag concrete.

One of the most important works about EAF slag appeared in 2005 in Spain [82], with the aim of analyzing the durability of slag concrete, and in particular it focused about the possible expansion of EAF concrete, due to the presence of some internal compounds, potentially not volumetrically stable when hydrated (periclase and free lime). Accelerated ageing tests were performed to study the effects of this expansion on mechanical strength. In addition, slag pre-treating processes were analyzed: reduction to standard aggregate sizes following an appropriate crushing, and the successive exposure to weathering over several weeks were demonstrated to be two necessary phases to obtain a stabilized product. A correctly performed treatment requires a permanent wetting, homogenization through a periodic turning of the heaps and a minimum weathering period of 90 days, and it provides a significant improvement in stabilizing the slag, both dimensionally and chemically. Another suggestion extracted from this study relates to the use of an air-entrainer agent for slag concrete, because of the high slag porosity, which could lead to severe deterioration of structures exposed to freezing and thawing cycles. A number of specimens were casted, using different substitution ratios for slag and limestone aggregates: in all the cases, the mechanical resistance was comparable to traditional concrete strength. An exception was obtained for the mix made just by slag (100 % EAF aggregates), which collapsed and could not be practicable. Accelerated ageing tests were performed according to American ASTM standards: one was performed in autoclave, one in a moist room, one providing freezing and thawing cycles, one with wetting and drying conditions and the latter was a leaching simulation.

Another research topic focused on the possibility of using slag as a raw material for Portland cement clinker production, in some percentages. Starting from the knowledge that cement with slag may be weaker than Portland cement, some tests were performed in Greece [88], following the experience of BOF slag—cements. EAF slag has a chemical composition similar to that of cement, like most of metallurgical slags. The main difference is the high iron oxide content, which exists in both di- and trivalent states; another difference was evidenced by previous researches, which stated that pozzolanic activity is low if slag is not pre-treated. So, no mechanical differences would be expected during hydration, and only the possible expansion of slag must be evaluated. Specimens with a substitution ratio

of about 10 % on the total were casted, to allow the slag not to affect the hydraulic behavior of the cement produced. XRD analyses were performed, to detect hydration products, and mechanical tests were conducted on small specimens. Results were promising: expansion was under EN 197-3 limit, compressive strength was as good as traditional Portland cement (no significant differences), and the reduction of material costs was remarkable.

Some other works were performed in order to assess the potential use of slag as fine aggregate in concrete [89]. The results have shown a potential use of this material, but an increase of cement content is necessary to do not affect the mechanical strength of EAF concretes.

Also in Italy a research work was conducted to assess the potential use of EAF slag, produced from a local plant, in structural concrete. The research activity, which lasts since more than 6 years, is focused on the application of EAF-C type slag (coming from carbon steel production) for structural concrete production. The first experimental campaign aimed to explore slag use as full replacement of coarse aggregates in concrete, through the analysis of the most common mechanical and durability-related properties, i.e. resistance against wetting/drying and freezing/thawing cycles, and accelerated ageing [81]. Results were excellent in concrete exposed to ordinary environmental conditions. Further experimental campaigns were devoted to assess the potential use of EAF slag fine particles: also in this case promising results were obtained. Contextually to these activities, the first experimental tests on structural reinforced elements casted with EAF slag were done [90]. High performances concrete was also produced including EAF slag as full replacement of coarse natural aggregates [91].

2.3 Fly Ash

The use of alternative binders is very common in the concrete industry. Particularly, fly ash (FA) is widely employed as partial replacement of ordinary Portland cement in concrete, and nowadays around 15–25 % of cement is generally replaced by FA in normal structural concrete mixes. Coal fly ash has been successfully used in concrete industry since more than 50 years, primarily as mineral admixture in Portland cement concrete and also as a component of blended cement [92]. Concerning its first use, fly ash can either partially substitute Portland cement or be applied as an addition into ready-mix concrete at the batch plant [93]. It is generally accepted that the use of those Supplementary Cementing Materials (SCMs) promotes sustainability of concrete industry. Usual structural and durability-related properties were widely analyzed in literature [94–96]. In addition, several authors have attempted to relate some properties of SCM-concretes with parameters such as fly ash fineness [97], glass phase content soluble [98] and reactive silica content [99], water to powder ratio [100] and curing conditions [101].

High quantities of FA can be used in concrete, also as partially replacement of fine sand fraction, and as filler. This use is allowed also for low quality fly ash, characterized by low pozzolanic properties.

Fly ash represents the most important coal combustion by-product: approximately 6 million tons are actually used in the EU 15 member states as concrete additions. FA production is about 1Mt/y in Italy and 40 Mt/y in Europe. FA is a product of burning finely ground coal in a boiler to produce electricity: it is removed from the plant of exhaust gases primarily by electrostatic precipitators or baghouses, and secondarily by scrubber systems. Within a power station, coal is fed to a series of mills that pulverize the combustible matter to a very fine powder. This powder is then fed into a boiler which combusts the coal to produce heat, which is used to produce steam required for power generation. During the coal combustion process, minerals present in the coal fuse to form glassy aluminosilicate spheres. These spheres remain in suspension within the flue gas from the boiler and they are collected downstream by either electrostatic or mechanical precipitation.

American Society for Testing and Materials (ASTM) C618-08 [102] classifies fly ash into two big categories, according to their chemical composition and other physical properties. This classification distinguishes FA also from the coal type burned in the coal-fired power plants, being FA quality highly dependent on the burned material. Those classes are Class F (low calcium) and Class C (high calcium) fly ash. Combustion of bituminous or anthracite coal normally produces Class F (low calcium) fly ash and combustion of lignite or sub-bituminous coal normally produces Class C (high calcium) fly ash. High calcium fly ash contains large amounts of free lime and sulfite than that of low calcium fly ash. In Europe, the EN 450-1 standard of 2012 defines the specifics for a correct use of FA in concrete [103].

The mineralogical composition of FA is very complex. FAs are a heterogeneous mixtures of mineral phases and amorphous glassy phases with small amount of unburned carbon. The glassy phase of low calcium fly ash is aluminosilicate type whereas that of high calcium fly ash is a mixture of calcium aluminate and ferrous aluminosilicate. High calcium fly ash contains large amounts of calcium-bearing minerals like lime, anhydrite, gypsum, tricalcium aluminate, alite, gehlenite, akermanite, portlandite and larnite. Some other minerals like quartz, hematite and magnetite are also present in high calcium fly ash. On the other hand, low calcium fly ash mainly contains quartz, mullite, hematite, magnetite and small amounts of calcite [104].

Concerning the physical properties of FAs, also in this case a huge variability was reported in literature. The specific gravity of fly ash may vary from 1.3 to 4.8 t/m³, and the shape is generally roundish (which depends by the spherical glassy phase shape). However, large sized or irregular shaped particles can also be formed from the fusion of smaller fragments and incomplete melting. In addition, there could be also hollow spheres (cenospheres) and microsphere-filled spheres (plerospheres): these lasts are cenosphere, which encapsulate a mass of microspheres with 1 μm or less in diameter. The formation of such spheres is due to many physical and chemical reactions that occur during coal combustion: initially



Fig. 2.5 Light-brown FA and dark-grey FA

lignite is heated up to about 950–1000 °C and thereafter reactions may occur for some seconds, as the FA is swept towards the stack inlet. The smallest particles are then adhering to the larger ones, thus forming clumps or agglomerate of small particles. Particle size distribution can be very different, and it depends upon the initial grinding of the coal and the efficiency of the thermal power plant and even fluctuations in power generation. Also the color of coal ash can be an index of chemical and mineral constituents. High lime containing FA is normally tan and light in color. Iron containing FA is brownish in color. The dark grey to black color of FA indicates the presence of a high amount of unburned carbon. Figure 2.5 shows two fly ashes: on the left, a light-brown FA from coal-combustion; on the right, a dark-grey FA, rich in unburned carbon content, coming from a co-combustion process where coal is burned together with refuse derived fuel (RDF).

References

1. JRC-IES, European Commission Joint Research Centre, Institute for Environment and Sustainability (2011) Supporting environmentally sound decisions for construction and demolition (C&D) waste management. Publications Office of the European Union, Luxembourg
2. European Parliament, Council of the European Union (2008) Directive 2008/98/EC of the European Parliament and of the Council of 19 November 2008 on waste and repealing certain directives. Official Journal of the European Union
3. United States Environmental Protection Agency (2009) Estimating 2003 building-related construction and demolition materials amounts. Office of Resource Conservation and Recovery, EPA, US
4. Monier V, Hestin M, Trarieux M, Mimid S, Domrose L, van Acoleyen M, Hjerp P, Mudgal S (2011) Study on the management of construction and demolition waste in the EU. Contract 07.0307/2009/540863/SER/G2. Final report for the European Commission DG Environment
5. Kojo R, Lilja R (2011) Talonrakentamisen materiaalitehokkuuden edistäminen (Removing the barriers to material efficiency in house construction). Ympäristöministeriö, Finland
6. Silva R, de Brito J, Dhir R (2014) Properties and composition of recycled aggregates from construction and demolition waste suitable for concrete production. *Constr Build Mater* 65:201–217

7. Regione del Veneto (2014) Modalità operative per la gestione e l'utilizzo nel settore delle costruzioni di prodotti ottenuti dal recupero e di rifiuti. D.lgs. n. 152/2006 e s.m.i., Parte IV, Titolo I. BUR 69 del 15/09/2014, Venezia, Italy
8. Dahlbo H, Bachér J, Lähtinen K, Jouttijärvi T, Suoheimo P, Mattila T, Sironen S, Myllymaa T, Saramäki K (2015) Construction and demolition waste management—a holistic evaluation of environmental performance. *J Clean Prod.* doi:[10.1016/j.jclepro.2015.02.073](https://doi.org/10.1016/j.jclepro.2015.02.073)
9. Vázquez E (ed) (2013) Progress of recycling in the built environment, Final Report of the RILEM Technical Committee 217-PRE. Springer, Berlin
10. Meinander M, Mroueh UM, Bacher J, Laine-Ylijoki J, Wahlström M, Jermakka J, Teirasvuo N, Törn M, Laaksonen J, Heiskanen J, Kaila J, Vanhanen H, Dahlbo H, Saramäki K, Jouttijärvi T, Mattila T, Retkin R, Suoheimo P, Lähtinen K, Sironen S, Sorvari J, Myllymaa T, Havukainen J, Horttanainen M, Luoranen M (2012) Future development directions of waste recycling. Final report of NeReMa project. <http://www.vtt.fi/inf/pdf/technology/2012/T60.pdf>. Accessed 30 Aug 2015
11. Fatta D, Papadopoulos A, Avramikos E, Sgourou E, Moustakas K, Kourmoussis F, Mentzis A, Loizidou M (2003) Generation and management of construction and demolition waste in Greece—an existing challenge. *Resour Conserv Recy* 40:81–91
12. Mineral Product Association MPA (2013) Cement fact sheet 6: use of recycled aggregates in concrete. London
13. Gary Ong KC, Akbarnezhad A (2015) Microwave-assisted concrete technology. CRC Press, Boca Raton
14. Bergsdal H, Bohne RA, Brattebø H (2008) Projection of construction and demolition waste in Norway. *J Ind Ecol* 11:27–39
15. Cochran K, Townsend T, Reinhart D, Heck H (2007) Estimation of regional building-related C&D debris generation and composition: case study of Florida, US. *Waste Manage* 27:921–931
16. Ding T, Xiao J (2014) Estimation of building-related construction and demolition waste in Shanghai. *Waste Manage* 34:2327–2334
17. Eurostat (2010) Waste generation by economic activity and households
18. Rodríguez G, Medina C, Alegre FJ, Asensio E, Sánchez de Rojas MI (2015) Assessment of construction and demolition waste plant management in Spain: in pursuit of sustainability and eco-efficiency. *J Clean Prod* 90:16–24
19. Blengini GA, Garbarino E (2010) Resources and waste management in Turin (Italy): the role of recycled aggregates in the sustainable supply mix. *J Clean Prod* 18:1021–1030
20. Comité Européen de Normalisation (2008a) EN 13242:2008 aggregates for unbound and hydraulically bound materials for use in civil engineering work and road construction. Brussels, Belgium
21. Comité Européen de Normalisation (2002) EN 13043:2002—Aggregates for bituminous mixtures and surface treatments for roads, airfields and other trafficked areas. Brussels, Belgium
22. Comité Européen de Normalisation (2010) EN 13285:2010—unbound mixtures—specifications. Brussels, Belgium
23. Comité Européen de Normalisation (2013a) EN 14227 serie—hydraulically bound mixture. Brussels, Belgium
24. Comité Européen de Normalisation (2009) EN 933-11:2009—tests for geometrical properties of aggregates—part 11: classification test for the constituents of coarse recycled aggregate. Brussels, Belgium
25. Comité Européen de Normalisation (2006) EN 1744-6:2006—tests for chemical properties of aggregates—part 6: determination of the influence of recycled aggregate extract on the initial setting time of cement. Brussels, Belgium
26. Organisme impartial de Contrôle de Produits pour la Construction COPRO (2012) PTV 406 technical prescription recycled aggregates from construction and demolition waste. Zellik, Belgium

27. Deutschen Instituts für Normung (2002) DIN 4226-100:2002-02. Aggregates for concrete and mortar—part 100: recycled aggregates, Germany
28. Deutscher ausschuss für elsenbeton DAfStb (1998) Code: concrete with recycled aggregates, Germany
29. Comité Européen de Normalisation (2013b) EN 206-1:2013. Concrete—specification, performance, production and conformity. Bruxells, Belgium
30. Deutschen Instituts für Normung (2008) DIN 1045-2:2008-08. Concrete, reinforced and prestressed concrete structures—part 2: Concrete—specification, properties, production and conformity—application rules for DIN EN 206-1. Germany
31. British Standards Institution BSI (2015) BS 8500-2:2015. Concrete. Complementary British Standard to BS EN 206. Specification for constituent materials and concrete, UK
32. Italian Ministry of Infrastructures (2008) DM 14/01/2008 Norme Tecniche per le Costruzioni (Technical Standards for Construction), NTC 2008, Italy
33. Comité Européen de Normalisation (2008b) EN 12620:2008. Aggregates for concrete. Bruxells, Belgium
34. Ente Italiano di Normazione UNI (2005) UNI 8520-1. Aggregati per calcestruzzo—Istruzioni complementari per l'applicazione della EN 12620—Parte 1: Designazione e criteri di conformità. Italy
35. Ente Italiano di Normazione UNI (2005) UNI 8520-2. Aggregati per calcestruzzo—Istruzioni complementari per l'applicazione della EN 12620—Parte 2: Requisiti, Italy (in Italian)
36. Japanese Industrial Standard JIS (2005) JIS A 5021:2005. Recycled aggregate for concrete-class H, Japan
37. Japanese Industrial Standard JIS (2011) JIS A 5021:2011. Recycled aggregate for concrete-class H, Japan
38. Japanese Industrial Standard JIS (2012a) JIS A 5022:2012. Recycled concrete using recycled aggregate Class M, Japan
39. Japanese Industrial Standard JIS (2012b) JIS A 5023:2012. Recycled concrete using recycled aggregate Class L, Japan
40. Nederlands Normalisatie-instituut (2010) NEN 5905: 2010. Dutch supplement to NEN-EN 12620+A1 Aggregates for concrete. Delft, Nederlands
41. Laboratório Nacional de Engenharia Civil LNEC (2009a) LNEC E 471: 2009. Guide for the use of recycled aggregates in concrete. Lisboa, Portugal
42. Laboratório Nacional de Engenharia Civil LNEC (2009b) LNEC E 472: 2009. Guide for the production of recycled hot mix asphalt. Lisboa, Portugal
43. Laboratório Nacional de Engenharia Civil LNEC (2009c) LNEC E 473: 2009. Guide for the use of recycled aggregates in unbound pavement layers. Lisboa, Portugal
44. Laboratório Nacional de Engenharia Civil LNEC (2009c) LNEC E 474: 2009. Guide for the use of recycled materials coming from construction and demolition waste in embankment and capping layer of transport infrastructures. Lisboa, Portugal
45. Ministerio de Fomento (2011) EHE-08: 2011. Comisión Permanente Del Hormigón: Instrucción de Hormigón Estructural, Madrid, Spain (in Spanish)
46. ASTM International (2013) ASTM C33/C33 M. Standard specification for concrete aggregates. West Conshohocken, PA, US
47. ASTM International (2014) ASTM C125-14. Standard terminology relating to concrete and concrete aggregates. West Conshohocken, PA, US
48. Kou S, Poon CS, Etxeberria M (2011) Influence of recycled aggregates on long term mechanical properties and pore size distribution of concrete. *Cem Concr Comp* 33:286–291
49. Kou S, Poon CS, Agrela F (2011) Comparisons of natural and recycled aggregate concretes prepared with the addition of different mineral admixtures. *Cem Concr Comp* 33:788–795
50. Schubert S, Hoffmann C, Leemann A, Moser K, Motavalli M (2012) Recycled aggregate concrete: experimental shear resistance of slabs without shear reinforcement. *Eng Struct* 41:490–497

51. Fathifazl G, Abbas A, Razaqpur AG, Isgor OB, Fournier B, Foo S (2009) New mixture proportioning method for concrete made with coarse recycled concrete aggregate. *J Mater Civ Eng*: 601–611
52. Abbas A, Fathifazl G, Isgor OB, Razaqpur AG, Fournier B, Foo S (2009) Durability of recycled aggregate concrete designed with equivalent mortar volume method. *Cem Concr Comp* 31:555–563
53. Vázquez E, Barra M, Aponte D, Jiménez C, Valls S (2013) Improvement of the durability of concrete with recycled aggregates in chloride exposed environment. *Constr Build Mater* 67:61–67
54. Lima C, Caggiano A, Faella C, Martinelli E, Pepe M, Realfonzo R (2013) Physical properties and mechanical behaviour of concrete made with recycled aggregates and fly ash. *Constr Build Mater* 47:547–559
55. Barbudo A, de Brito J, Evangelista L, Bravo M, Agrela F (2013) Influence of water reducing admixtures on the mechanical performance of recycled concrete. *J Clean Prod* 59:93–98
56. Ferreira L, de Brito J, Barra M (2012) Influence of the pre-saturation of recycled coarse concrete aggregates on concrete properties. *Mag Concr Res* 63:617–627
57. Pepe M, Toledo Filho RD, Koenders EAB, Martinelli E (2014) Alternative processing procedures for recycled aggregates in structural concrete. *Constr Build Mater* 69:124–132
58. Poon CS, Shui Z, Lam L (2004) Effect of microstructure of ITZ on compressive strength of concrete prepared with recycled aggregates. *Constr Build Mater* 18:461–468
59. Li WX, Zhang X, Liu X (2009) Mechanical properties of recycled aggregate concrete. Study of the impact of factors. *Chin Concr J* 10:60–63
60. Xiao J, Li J, Zhang C (2005) Mechanical properties of recycled aggregate concrete under uniaxial loading. *Cem Concr Res* 35:1187–1194
61. Etxeberria M, Vázquez E, Marí A, Barra M (2007) Influence of amount of recycled coarse aggregates and production process on properties of recycled aggregate concrete. *Cem Concr Res* 37:735–742
62. Limbachiya MC, Leelawat T, Dhir RK (2000) Use of recycled concrete aggregate in high-strength concrete. *Mater Struct* 33:574–580
63. Ajdukiewicz A, Kliszczewicz A (2002) Influence of recycled aggregates on mechanical properties of HS/HPC. *Cem Concr Compos* 24:269–279
64. Otsuki N, Miyazato SI, Yodsudjai W (2003) Influence of recycled aggregate on interfacial transition zone, strength, chloride penetration and carbonation of concrete. *J Mater Civ Eng* 15:443–451
65. Tovar-Rodríguez G, Barra M, Pialarissi S, Aponte D, Vázquez E (2013) Expansion of mortars with gypsum contaminated fine recycled aggregates. *Constr Build Mater* 38:1211–1220
66. Sato R, Maruyama I, Sogabe T, Sogo M (2007) Flexural behavior of reinforced recycled concrete beams. *J Adv Concr Technol* 5:43–61
67. Ajdukiewicz A, Kliszczewicz A (2007) Comparative tests of beams and columns made of recycled aggregate concrete and natural aggregate concrete. *J Adv Concr Technol* 5:259–273
68. Fathifazl G, Razaqpur AG, Isgor OB, Abbas A, Fournier B, Foo S (2009) Flexural performance of steel-reinforced recycled concrete beams. *ACI Struct J* 106:858–867
69. Choi HB, Yi CK, Cho HH, Kang KI (2010) Experimental study on the shear strength of recycled aggregate concrete beams. *Mag Concr Res* 62:103–114
70. Fathifazl G, Razaqpur AG, Isgor OB, Abbas A, Fournier B, Foo S (2009) Shear strength of reinforced recycled concrete beams without stirrups. *Mag Concr Res* 61:477–490
71. Corinaldesi V, Letelier V, Moriconi G (2011) Behaviour of beam–column joints made of recycled-aggregate concrete under cyclic loading. *Constr Build Mater* 25:1877–1882
72. European Slag Association, European Steel Association (2012) Euroslag and Eurofer. Position Paper on the Status of Ferrous Slag. Duisburg, Germany
73. Luxàn MP, Sotolongo R, Dorrego F, Herrero E (2000) Characteristics of the slags produced in the fusion of scrap steel by electric arc furnace. *Cem Concr Res* 30:517–519

74. Al-Negheimish AI, Al-Sugair FH, Al-Zaid RZ (1997) Utilization of local steel making slag in concrete. *J King Saud Univ Eng Sci* 9:39–55
75. Anastasiou F, Papayianni I (2006) Criteria for the use of steel slag aggregates in concrete. In: Konsta-Gdoutos MS (ed) *Measuring, monitoring and modeling concrete properties*. Springer, The Netherlands, pp 419–426
76. Papayianni I, Anastasiou E (2010) Production of high-strength concrete using high volume of industrial by-products. *Constr Build Mater* 24:1412–1417
77. Manso JM, Gonzalez JJ, Polanco JA (2004) Electric arc furnace slag in concrete. *J Mater Civ Eng* 16:639–645
78. Xue Y, Wu S, Hou H, Zha J (2006) Experimental investigation of basic oxygen furnace slag used as aggregate in asphalt mixture. *J Hazard Mater* 138:261–268
79. Ahmedzade P, Sengoz B (2009) Evaluation of steel slag coarse aggregate in hot mix asphalt concrete. *J Hazard Mater* 166:300–305
80. Pellegrino C, Gaddo V (2009) Mechanical and durability characteristics of concrete containing EAF slag as aggregate. *Cem Concr Comp* 31:663–671
81. Pellegrino C, Cavagnis P, Faleschini F, Brunelli K (2013) Properties of concretes with black/oxidizing electric arc furnace slag aggregate. *Cem Concr Comp* 37:232–240
82. Manso JM, Polanco JA, Losanez M, Gonzalez JJ (2006) Durability of concrete made with EAF slag as aggregate. *Cem Concr Comp* 28:528–534
83. Maslehuddin M, Sharif AM, Shameem M, Ibrahim M, Barry MS (2003) Comparison of properties of steel slag and crushed limestone aggregate concretes. *Constr Build Mater* 17:105–112
84. Tossavainen M, Engstrom F, Yang Q, Menad N, Larsson ML, Bjorkman B (2007) Characteristics of steel slag under different cooling conditions. *Waste Manage* 27(7):1335–1344
85. Daugherty KE, Saad B, Weirich C, Eberendu A (1983) The glass content of slag and hydraulic activity. *Silic Ind* 4:107–110
86. Engström F, Björkman B, Samuelsson C (2009) Mineralogical influence of different cooling conditions on leaching behaviour of steelmaking slags. Paper presented at the 1st International Slag Valorisation Symposium, Leuven, 6-7/4/2009
87. Shi C, Qian J (2000) High performance cementing materials from industrial slag—a review. *Resour Conserv Recy* 29:195–207
88. Tsakiridis PE, Papadimitriou GD, Tsvivilis S, Koroneos C (2008) Utilization of steel slag for Portland cement clinker production. *J Hazard Mater* 152:805–811
89. Qasrawi H, Shalabi F, Asi I (2009) Use of low CaO unprocessed steel slag in concrete as fine aggregate. *Constr Build Mater* 9:1118–1125
90. Pellegrino C, Faleschini F (2013) Experimental behavior of reinforced concrete beams with electric arc furnace slag as recycled aggregate. *ACI Mater J* 110:197–206
91. Faleschini F, Fernández-Ruiz MA, Zanini MA, Brunelli K, Pellegrino C, Hernández-Montes E (2015) High performance concrete with electric arc furnace slag as aggregate: mechanical and durability properties. *Constr Build Mater* 101:113–121
92. Bouzoubaâ N, Zhang MH, Malhotra VM, Golden DM (1996) Blended fly ash cements—a review. *ACI Mater J* 96:641–650
93. Siddique R, Khatib JM (2010) Abrasion resistance and mechanical properties of high-volume fly ash concrete. *Mater Struct* 42:709–718
94. Papadakis VG, Tsimas S (2002) Supplementary cementing materials in concrete. Part I: efficiency and design. *Cem Concr Res* 32:1525–1532
95. Papadakis VG, Antiohos S, Tsimas S (2002) Supplementary cementing materials in concrete. Part II: a fundamental estimation of the efficiency factor. *Cem Concr Res* 32:1533–1538
96. Aponte DF, Barra M, Vázquez E (2012) Durability and cementing efficiency of fly ash in concrete. *Constr Build Mater* 30:537–546
97. Bentz DP, Garboczi EJ (1991) Simulation studies of the effects of mineral admixtures on the cement paste-aggregate interfacial zone. *ACI Mater J* 88:518–529

98. Aughenbaugh KL, Chancey RT, Stutzman P, Juenger MC, Fowler DW (2013) An examination of the reactivity of fly ash in cementitious pore solutions. *Mater Struct* 46:869–880
99. Ranganath RV, Bhattacharjee B, Krishnsmoorthy S (1998) Influence of size fraction of ponded ash on its pozzolanic activity. *Cem Concr Res* 28:749–761
100. Siddique R, Aggarwal P, Aggarwal Y (2012) Influence of water/powder ratio on strength properties of self-compacting concrete containing coal fly ash and bottom ash. *Constr Build Mater* 29:73–81
101. Eren O (2002) Strength development of concretes with ordinary Portland cement, slag or fly ash cured at different temperatures. *Mater Struct* 235:536–540
102. ASTM International (2008) ASTM C618-08a. Standard specification for coal fly ash and raw or calcined natural pozzolan for use in concrete. West Conshohocken, PA, US
103. Comité Européen de Normalisation (2012) EN 450-1: 2012. Fly ash for concrete—part 1: definition, specifications and conformity criteria. Brussels, Belgium
104. de Brito J, Saikia N (2013) Recycled aggregate in concrete. Green energy and technology. Springer-Verlag, London

Chapter 3

Workability and Rheology of Fresh Recycled Aggregate Concrete

3.1 Introduction

Workability is the property that is usually referred to those freshly mixed concrete, or mortars, which can be easily mixed, placed into formwork, consolidated and finished. Terms like consistency, flowability, mobility, placeability and pumpability have been often associated to fresh concrete properties too, to describe its rheological behavior, at a macroscopic scale of observation.

At this scale of observation, cementitious materials, which are in reality composite materials (e.g. concrete is a concentrated suspension of solid particles—aggregates—in a viscous liquid-cement paste; mortars can be thought as concretes where the aggregates have smaller size; cement paste is made by cement grains in water, as suspension liquid), flow as a liquid. Those materials can exhibit very different behavior in the fresh state, depending principally by the mix proportions and casting conditions (temperature, relative humidity, etc.).

In a steady state flow, they can display both Newtonian, shear-thickening and shear-thinning behavior: Fig. 3.1 shows this three flow curves, where in the x -axis shear rate is plotted, and in the y -axis there is the shear stress. In the first case, the apparent viscosity, which is the proportionality factor between the shear stress applied to a liquid and the velocity gradient induced by the shear force itself, is constant (Fig. 3.2). Otherwise, the apparent viscosity depends on the applied shear rate, which can be increasing (shear-thickening) or decreasing (shear-thinning).

Additionally, most of the cement-based materials are characterized by a yield stress, which must be exceeded by a fluid in rest before flow can occur. Alternatively, for a fluid in motion, this stress indicates the limit below which the flow stops.

Concrete in its fresh state can be thought of as a fluid [1], under some hypotheses, such as that a certain degree of flow can be reached and that the material is mostly homogeneous. These constraints cannot be reached in all the cases, such as for

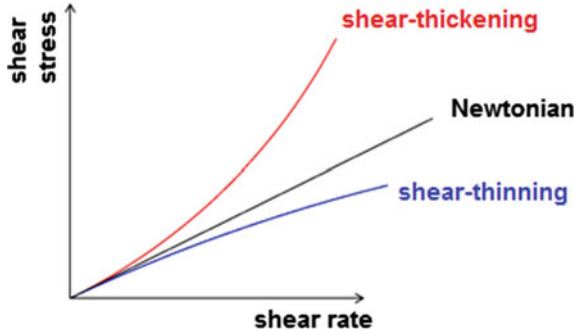


Fig. 3.1 Comparison of Newtonian, shear-thickening and shear-thinning fluids

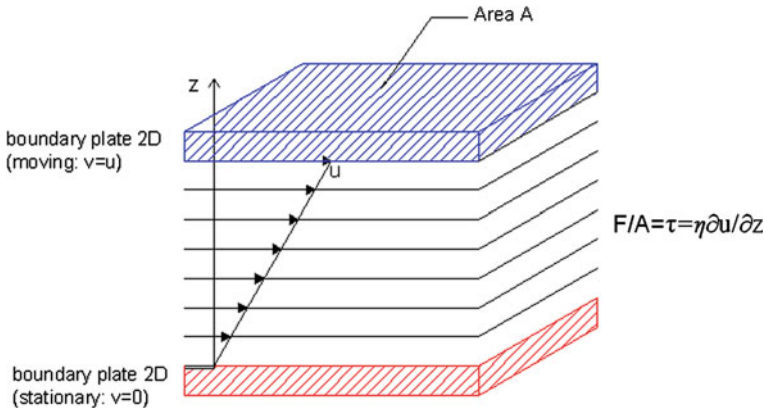


Fig. 3.2 Newton’s equation for a viscous fluid: F is the shear force (N), A is the area of the plane parallel to the applied force (m^2), τ is the shear stress (Pa), η is the viscosity (Pa s), $\partial u/\partial z$ is the velocity gradient, equal to the shear rate $\dot{\gamma}(s^{-1})$

rolled-compacted concrete, but generally at least 8–10 cm of slump are required. There are several models used to describe the flow-curve of concretes: the most well-known is the Bingham one.

Generally fresh concretes do not have any structural breakdown at the shear rate ranges used at lab-scale. However, some concretes do not follow the linear trend of this curve, and other models have been derived. Particularly, self-compacting concrete (SCC) does not follow the linear function described by the Bingham model: the admixtures used for reaching SCC properties, used to prevent segregation and increase flowability, have implications on the rheological properties, being the experimentally evaluated flow curves not linear. If Bingham model would be applied for describing the flow of SCC, a negative value of the yield stress may be computed, thus being physically non-sense [2].

Mortars can be thought as concretes where no coarse aggregates are present, hence its study has significant importance when dealing with a separation of the contributes of each component in concrete, at smaller scale of observation. They may undergo structural breakdown, and the measured data are sensitive to the previous shear story. The equilibrium flow curve typically follows the Bingham curve [3].

Cement paste are instead the most discussed materials, which showed disagreeing behaviors, following different flow curves, as obtained during various experimental campaigns by several authors. Even though a great heterogeneity has been observed in the results reported in literature (probably associated to different experimental methods and techniques adopted by the authors, differences in the materials, undetected plug phenomena which may occur and slippage at the smooth surface of the viscometers), there are some common aspects that have frequently observed and can describe, at least qualitatively, the behavior of fresh cement paste. First, the material breaks down during the test; then, hysteresis loops are observed; the shape of the sample changes during the test, probably due to the chemical reactions occurring or due to competition between coagulation and deflocculation processes. Additionally, the yield stress decreases in time, in line with reduction in the apparent viscosity.

It is recalled that the terminology used along this chapter is based on the NIST Special Publication 946 [4].

3.2 Rheology Background

3.2.1 *Rheological Models and Flow Curve Equations*

Several models have been derived to describe the rheological behavior of fresh cement-based materials under steady state flow conditions. Between the non-Newtonian models, the most used one for concrete is the above cited Bingham model; other relations are useful instead to describe some particular types of concretes, e.g. SCC, and cement pastes. Here a brief description of those models is given.

The Newtonian model (Eq. 3.1) is the simplest formulation for describing a viscous fluid: the viscosity μ (Pa s) is constant and does not depend on the shear rate $\dot{\gamma}$ (s^{-1}). Accordingly a linearly proportional relation exists between the shear stress and the shear rate. Typically this relation well represents the rheological behavior of low molecular weight fluids at low shear rate.

$$\tau = \mu\dot{\gamma} \quad (3.1)$$

However, in most cases, the viscosity may be dependent on the shear rate: the general expression for describing the so-called viscous fluids is given in Eq. 3.2:

$$\tau = \mu(\dot{\gamma}) \cdot \dot{\gamma} \quad (3.2)$$

A large number of models have been developed using the previous Eq. 3.2 as a basis, where the viscosity is expressed through Eq. 3.3. Power laws can be indeed described through Eq. 3.4, where the value of the flow index n (-) can be >1 (shear-thickening), <1 (shear-thinning), or $=1$ (Newtonian). The parameter A represents the consistency coefficient (Pa s^n). The main disadvantage of using power law models is that they fail in describing the Newtonian regimes occurring in some cases, e.g. at low or high shear rates. However most non-Newtonian fluids show shear-thinning behavior and can be well described by power laws; furthermore some suspensions can exhibit shear thickening behavior (e.g. SCC).

$$\mu(\dot{\gamma}) = A \cdot \dot{\gamma}^{n-1} \quad (3.3)$$

$$\tau = A\dot{\gamma}^n \quad (3.4)$$

As stated in the previous section, cement-based materials often display a yield stress which should be exceeded before flow can start: accordingly they can be thought as viscoplastic fluids, being Hookean solids up to a certain shear stress, and then they flow as viscous fluids. The general expression for describing visco-plastic fluids is given in Eq. 3.5, where the no-motion condition ($\dot{\gamma} = 0$) can be used instead the Hook law ($\tau = G \cdot \gamma$):

$$\begin{cases} \tau = \tau_0 + \mu(\dot{\gamma}) \cdot \dot{\gamma} & \tau > \tau_0 \\ \dot{\gamma} = 0 & \tau \leq \tau_0 \end{cases} \quad (3.5)$$

Viscoplastic behavior is typically associated to suspension fluids, e.g. cement-based materials. The plastic viscosity μ of a viscoplastic fluid is defined as the viscosity of the isolated viscous flow after exceeding the yield stress, whereas the apparent viscosity of the fluid can be evaluated through Eq. 3.6:

$$\mu_{app} = \tau/\dot{\gamma} = \tau_0/\dot{\gamma} + \mu(\dot{\gamma}) \quad (3.6)$$

The Bingham model (Eq. 3.7) is a two-parameters model used for describing viscoplastic fluids exhibiting a yield response [5]; at low shear stress values, a material obeying to this law behaves as an elastic solid, whereas when the yield stress τ_0 (Pa) is exceeded, the material acts as a Newtonian fluid. This means that a linearly proportional relationship between shear stress and shear rate exists in the viscoplastic state, hence the plastic viscosity μ (Pa s) is constant and does not depends on the shear rate.

$$\begin{cases} \tau = \tau_0 + \mu\dot{\gamma} & \tau > \tau_0 \\ \dot{\gamma} = 0 & \tau \leq \tau_0 \end{cases} \quad (3.7)$$

The Herschel-Bulkley model (Eq. 3.8) is a three-parameters model used typically for SCC [6]. It describes viscoplastic materials exhibiting a yield response with a power-law relationship between shear stress and shear rate above the yield stress. It is worth to be noted that the Herschel-Bulkley relation reduces into Bingham equation when $n = 1$, where n is the flow index ($-$), and K is the consistency factor (Pa s^n).

$$\begin{cases} \tau = \tau_0 + K\dot{\gamma}^n & \tau > \tau_0 \\ \dot{\gamma} = 0 & \tau \leq \tau_0 \end{cases} \quad (3.8)$$

Similarly to Herschel-Bulkley (Eq. 3.8), the so-called Modified-Bingham relation is a three-parameters law, which can be usefully applied when dealing with SCC [7]. The model adopts the well-known Bingham parameters (yield stress τ_0 and plastic viscosity μ), and a further parameter c , which is the second order parameter (Pa s^2).

$$\begin{cases} \tau = \tau_0 + \mu\dot{\gamma} + c\dot{\gamma}^2 & \tau > \tau_0 \\ \dot{\gamma} = 0 & \tau \leq \tau_0 \end{cases} \quad (3.9)$$

Other models have been derived when dealing with cement paste flows, and are listed in the following: Eyring (Eq. 3.10), Vom Berg and Ostwald-deWaele (Eq. 3.11), Robertson-Stiff (Eq. 3.12), Atzeni et al. (Eq. 3.13), Casson (Eq. 3.14), De Kee (Eq. 3.15), Yahia and Khayat (Eq. 3.16), Sisko (Eq. 3.17). Eyring model [8] is a two-parameters rheological model (a , B and C can be summarized in two relevant parameters), whose parameters do not have any corresponding physical equivalents, but they represent fit variables. As opposed to other relations, it does not take into consideration the yield stress τ_0 . The model has been successfully applied for describing cement pastes flow in the range of high shear rates. Vom Berg [9] and Ostwald-deWaele [10] is a modified version of the Eyring model, which takes into account the yield stress as a further relevant parameter. Robertson-Stiff [11] is a generalized three-parameters model, where a represents the consistency index, b is a flow behavior index and C is a shear rate correction factor. This model can be reduced to the Ostwald-De Waele formulation for $C = 0$, Bingham model for $b = 1$ and to the Newton model in the case when $b = 1$ and $C = 0$. Also the Atzeni model [12] is a modification of the Eyring one, to be applied in concentrated suspension as cement pastes. Casson model [3] is a two-parameters model, which provides a shear-thinning gradual transition from the Newtonian to the yield region, and it has been often used to describe the rheological properties of cement pastes. De Kee [3] is three-parameters model, which takes into account also a time-dependent parameter α (s), as well as Yahia and Khayat model [13]. The Sisko model is a three parameters model, useful for combining Newtonian and non-Newtonian behavior.

$$\tau = a\dot{\gamma} + B \sin h^{-1}(\dot{\gamma}/C) \quad (3.10)$$

$$\tau = \tau_0 + B \sin h^{-1}(\dot{\gamma}/C) \quad (3.11)$$

$$\tau = a(\dot{\gamma} + C)^b \quad (3.12)$$

$$\dot{\gamma} = \alpha\tau^2 + \beta\tau + \delta \quad (3.13)$$

$$\begin{cases} \sqrt{\tau} = \sqrt{\tau_0} + \sqrt{\mu\dot{\gamma}} & \tau > \tau_0 \\ \dot{\gamma} = 0 & \tau \leq \tau_0 \end{cases} \quad (3.14)$$

$$\tau = \tau_0 + \mu\dot{\gamma} \exp(-\alpha\dot{\gamma}) \quad (3.15)$$

$$\tau = \tau_0 + 2\sqrt{\tau_0\mu}\sqrt{\dot{\gamma}\exp(-\alpha\dot{\gamma})} \quad (3.16)$$

$$\tau = a\dot{\gamma} + b\dot{\gamma}^n \quad (3.17)$$

3.2.2 Bingham Parameters

Most of cement-based materials, and particularly concrete, are characterized by the so-called yield stress τ_0 , which is one of the two fundamental Bingham parameters. It describes a motion-triggering stress, i.e. the limit stress over which flow starts, and below which it stops. This parameter represents the most important difference between cement-based fluids and purely viscous ones. If water (Newtonian fluid) or another purely viscous fluid is used in the place of fresh concrete during slump test, it will flow until the upper surface (which was horizontal), becomes horizontal again. This means that the shear rate induced by the gravity pressure gradient forces the material to flow, until the pressure gradient becomes null. This will not of course occur when concrete is tested, and the flow stops when the shear stress in the material goes below the yield stress [14].

At the origin of the yield stress, it has to be recalled that the van der Waal attractive forces play a key-role: these forces let the cement particles, which are diffusing through the liquid due to the Brownian motion, to agglomerate and form networks of solid materials. Those agglomerations will affect the proper flow of the material: the water reducing admixtures (WRA) act properly trying to reduce the effect of these surface forces, being their molecules absorbed at cement particles surface, with the aim of increasing the inter-grains distance.

Concerning plastic viscosity μ , in case of Bingham fluids this parameter is constant, and it does not depend on the shear rate. As already seen, other flow curves provide plastic viscosity formulations depending on the shear rate, decreasing (shear-thinning) or increasing (shear-thickening) with it. Coming back to the previous example of slump test, it is worth noting that the apparent viscosity

plays a role in the definition of the time of the material flow, necessary to obtain again an upper horizontal surface.

The origin of the apparent viscosity of a fluid (Eq. 3.6) is highly dependent on the viscous dissipation in the interstitial fluid; hence it is a function of the viscosity of the suspending fluid and of the particles packing fraction. Various models can describe this dependence, and they can be more or less simplified, according to the situations they want to represent. The simplest analytical relation that can be used is the Einstein relation (Eq. 3.18):

$$\mu = \mu_0(1 + 2.5\phi) \quad (3.18)$$

where μ is the apparent viscosity of the suspension, μ_0 is the viscosity of the suspending fluid and ϕ is the suspended particle volume fraction [1]. This relation can be used for volume fractions lower than 5 %: it cannot represent any practical application in cases of cement pastes, being the w/c ratio necessary to reach this value at least equal to 6. Another relation which can be applied is the Krieger Dougherty equation (Eq. 3.19), an empirical formulation depending also on the dense packing fraction ϕ_m , also known as close packing fraction, which is a geometric property of packing of non-interacting rigid particles [15]. This parameter represents the maximum volume fraction that allows the suspension to flow, which is about 0.55–0.64 respectively for random loose and random close packing of monodispersed spheres.

$$\mu = \mu_0 \left(1 - \frac{\phi}{\phi_m}\right)^{-[\eta]\phi_m} \quad (3.19)$$

This relation can be applied also for larger values of ϕ (higher than 10 %): however it should be recalled that in those cases, as the value assumed by ϕ approaches to ϕ_m , the viscosity will be a result of both hydrodynamics effects inside the interstitial fluid and also contacts between particles. $[\eta]$ is the intrinsic viscosity, and it depends on particle shapes: for rigid uncharged spherical particles, it can be assumed equal to 2.5.

Other relations can be used (Eqs. 3.20 and 3.21), trying to relate the suspension concentration to the viscosity or the shear stress to the shear rate, thus assuming that there is only one value for the viscosity of the whole system. However, those formulations cannot be easily applicable to concrete mixtures, due to the complexity of the suspension. Roscoe model (Eq. 3.20) takes into account particle interaction [1], and uses a constant k ; Mooney (Eq. 3.21) considers the maximum packing factor ϕ_m [1].

$$\mu = \mu_0(1 - 1.35\phi)^{-k} \quad (3.20)$$

$$\mu = \mu_0 \exp\left(\frac{[\eta]\phi}{1 - \phi/\phi_m}\right) \quad (3.21)$$

3.2.3 Time-Dependent Behavior

When dealing with real fluids, the simplest ideal constitutive equation represented by the Newton's law of viscosity should be extended, taking into account, as previously seen, various conditions. First, shear rate may be dependent on the shear rate (non-Newtonian fluid); then viscoelastic behavior may occur (fluids with yield response); lastly, flow may be time-dependent. Fresh cement-based materials properties may be indeed dependent on the flow history of the material. This latter extension may be caused by both physical and chemical phenomena: in case of cement-based materials, thixotropy, structural breakdown and workability losses are the most important time effects which may occur. For those materials, typically described with non-Newtonian models, the apparent viscosity becomes both dependent on the shear rate and on time (Eq. 3.22):

$$\eta_{app} = \eta(\dot{\gamma}, t) \quad (3.22)$$

Often, talking about fresh concrete rheology, we refer to “thixotropic behavior”: it is defined as “*the decrease of viscosity under constant shear stress followed by a gradual recovery of structure when the stress is removed*” [16, 17]. This term describes the reversible changes that may occur in short observation times on the fresh concrete properties [18, 19]. A typical example is related to the loss of workability, and increase of yield stress, experienced by concrete left resting for a certain time. However, referring to thixotropy, these changes should have a transient effect, i.e. they should be reversible: when concrete is sheared again at high rates, the system should go back to its previous state.

“Structural breakdown” is associated to the process of breaking of chemical connections between cement particles, which causes a decrease in the yield stress and viscosity, similarly to the thixotropic breakdown effect, but with the difference that this process typically involves cement particles with greater size than in the former case (respectively $>40 \mu\text{m}$ for structural breakdown, and $<40 \mu\text{m}$ for thixotropy). In this case the build-up observed due to the thixotropic behavior is not displayed by the material when re-sheared: accordingly, this process is considered non-reversible.

With longer resting time, we refer to “workability loss” when the experimentally measured yield stress exponentially increases with time, and viscosity increases linearly, until the material cannot flow anymore. This process determines non-reversible changes, mainly related to hydration phenomena of the cement paste, and hence they will refer to the long-term behavior of the material (concrete hardening).

3.2.4 *Stability and Segregation*

Another critical aspect relates to the proportioning of concretes with lightweight or heavyweight aggregates, which can lead to stability problems of the mixtures: concrete components density can be indeed very different, varying from 1000 (water) to 3200 kg/m³ (cement grains). In the former case, if aggregates are characterized by a lower specific weight than water, they may float over the suspended liquid; in the latter case, segregation and bleeding may occur, depending on the phase which is migrating, respectively coarse aggregates and water. In both the cases, the expected performances of the produced concretes can be significantly lowered, both for local increases of w/c ratio and depletion of the aggregates skeleton.

Particularly, when referring to segregation of one phase with respect to another (multi-phase problem), two possible phenomena can be present: a static and a dynamic one. Static segregation occurs when the coarse aggregates, characterized by higher specific density than the suspending fluid, are deposited on the bottom of the formwork, due to gravity. This phenomenon is highly related to the yield stress of the suspending fluid. On the contrary, when concrete is placed, other reasons may enhance this process: this is the case of the so-called dynamic segregation. Particularly, the aggregates migrate from the high shear rate zones to the lower shear rate ones, and this behavior can be more significant if some elements which perturb the flow are present. This is the case of aggregates blocking phenomena, which is able to block the flow due to the formation of string and stable granular arches.

The above cited aspects both refer to some properties of concretes, and particularly of SCC, in their fresh state: filling ability, passing ability, and resistance to segregation. The first property is the ability of the fresh concrete to flow easily when unconfined by formwork and reinforcement. Passing ability is associated to ease of flowing through tight openings, without segregating or blocking. The last property is the concrete ability of remaining homogeneous.

3.2.5 *Relative Contributions on the Behavior of Fresh Concrete*

The Deborah number (Eq. 3.23) is useful for identifying whether a fluid behaves as a solid-like, i.e. with an elastic behavior, or liquid-like, i.e. with a viscous behavior. This dimension-less number is defined as:

$$D_e = \frac{t_R}{t_0} \quad (3.23)$$

where t_R is the relaxation time and t_0 is the characteristic time of the observation. When this number takes very low values ($t_0 \gg t_R$), the material behaves as a fluid; on the contrary, when ($t_0 \ll t_R$), the material behaves as a solid. When the Deborah number takes values around the unit, the material is said to be visco-elastic, being both the viscous and the elastic components equivalent. This behavior typically occurs when solids are dispersed in water: the interparticles forces which arise from surface charges and the electric double layer determine the relaxation time to be in the range between 10^{-4} and 10^4 s, in the range of laboratory equipment measurements. About this specific time, it should be recalled that generally measurements, for cement-based materials, are taken within short time-scale, before setting occurs.

Fluid-like behavior is very important during cement-based materials mixing, placing, moldings and all the other operations that should be done before hardening. Solid-like behavior is also important, particularly when dealing with the well-known property to stand unsupported without flowing under gravity action, or during setting with the development of strength and stiffness. One important example of this behavior refers to the slump test for concrete: after a certain time, concrete stops flowing; this would not occur if water is used in the place of concrete for carrying out the test. The difference between these two materials stands in the solid like-behavior which concrete has below a certain rate of shear. The Bingham model is the most simple formulation which involves the solid-like behavior (Eq. 3.7): the materials following this law are characterized by a solid-like behavior until shear stress is lower than the yield stress τ_0 ; when this triggering stress is reached, the material starts flowing as a Newtonian fluid, depending on the plastic viscosity μ and the shear rate $\dot{\gamma}$.

It may be useful to individuate also, with a good level of approximation, which is the contribution of yield stress τ_0 over the plastic viscosity μ_p . One common way to quantify their influence is through the computation of the Bingham number (Eq. 3.24). This dimension-less number is the ratio between the inertia over the viscous contributions:

$$B_n = \frac{\tau_0}{\mu_p \dot{\gamma}} \cong \frac{\tau_0 D}{\mu_p v} \quad (3.24)$$

where τ_0 is the yield stress, μ_p is the plastic viscosity, D is the typical dimension of the observation and v is the flowing velocity. The yield stress becomes relevant at slow velocity, when the flow starts or is going to finish; on the contrary, at high shear rate (and high velocity), the plastic viscosity contribution increases.

Another important dimension-less number is the Reynolds number (Eq. 3.25), which is the ratio of the kinetic energy over the viscous energy:

$$R_e = \frac{\rho v D}{\mu} \quad (3.25)$$

where ρ is the density of the tested material, v is the flowing velocity, D is the typical dimension of the observation, and μ is the viscosity. In case of fluids exhibiting a yield stress, e.g. concrete and other cement-based materials, typically the viscosity is assumed to be the apparent viscosity (Eq. 3.6). Then, through the flow curve, Eq. 3.6 becomes for a Bingham material:

$$\mu_{app} = \frac{\tau_0}{\dot{\gamma}} + \mu_p \quad (3.26)$$

where τ_0 is the yield stress, $\dot{\gamma}$ is the shear rate, and μ_p is the plastic viscosity. Hence, the Reynolds number can be computed:

$$R_e = \frac{\rho v D}{\mu} = \frac{\rho v D}{\frac{\tau_0}{\dot{\gamma}} + \mu_p} = \frac{\rho v^2 D}{D \tau_0 + \mu_p v} \quad (3.27)$$

When the kinetic energy is very high, the flow exhibits some turbulent effects (range of R_e values over 2), whereas if viscous energy dominates, this indicates that the flow is largely laminar.

It has been recalled that cement-based materials can also display shear thickening behavior, and several models have been derived to describe it. In this case another number can be used to quantify its influence: the Peclet number. The total apparent relative viscosity can be indeed divided in two contributions, one linked to Brownian effect and one related to hydrodynamic forces. Shear thickening is associated to this last contribution, i.e. to the formation of clusters of purely hydrodynamic effects. It is caused by high hydrodynamic (lubrication) forces between the spherical and monodispersed particles, overcoming the repulsion force between the particles, which induce the formation of clusters of grains. This phenomenon has a transient nature, because particles can leave and join the cluster, being a fully reversible behavior. Peclet number is:

$$P_e = \frac{\mu_s v a^3}{kT} \quad (3.28)$$

where μ_s is the apparent viscosity of the suspending medium, v is the velocity, a is the particle radius, k is the Boltzmann constant, and T is the temperature. Low P_e number values indicate that Brownian viscosity dominates; conversely for high P_e number the hydrodynamic effect increases. It should be recalled that, even in this last case, Brownian effects is sufficient to allow particles to leave the cluster and maintaining the transient nature of the phenomenon. In case of shear thickening, also the Reynolds number of particles (Eq. 3.25) assumes a certain importance, because it can also be due to the transfer of momentum between the suspended particles, and hence associated to grain inertia [20].

3.2.6 Governing Equations

Fluid flow problems, such as the solving of the velocity fluid during a test (e.g. inside a rheometer, during a slump test, etc.) or casting processes, can be solved using computation flow dynamics (CFD) approach.

The equation of motion is the first law to be used, and it is based on the Newton's 2nd law applied on a large set of solid particles. For Newtonian fluid it is the well-known Navier-Stokes equation (for incompressible fluids):

$$\rho \left(\frac{\partial \mathbf{v}}{\partial t} + \mathbf{v} \cdot \nabla \mathbf{v} \right) = -\nabla p + \mu \nabla^2 \mathbf{v} + \mathbf{f} \quad (3.29)$$

where \mathbf{v} is the flow velocity, ρ is the fluid density, p is the pressure, μ is the fluid viscosity, \mathbf{f} are the body forces (per unit of volume) acting on the fluid and t is the time. This equation derives from the general form, valid also for Non-Newtonian fluids, known as Cauchy equation of motion, which is more complex:

$$\rho \left(\frac{\partial \mathbf{v}}{\partial t} + \mathbf{v} \cdot \nabla \mathbf{v} \right) = -\nabla \cdot \boldsymbol{\sigma} + \mathbf{f} \quad (3.30)$$

where \mathbf{v} is the flow velocity, ρ is the fluid density, $\boldsymbol{\sigma}$ is the total stress tensor, \mathbf{f} are the body forces (per unit of volume) acting on the fluid and t is the time. The body forces can be written as:

$$\mathbf{f} = \rho \mathbf{g} \quad (3.31)$$

The total stress tensor can be written as:

$$\boldsymbol{\sigma} = -p\mathbf{I} + \mathbf{T} \quad (3.32)$$

hence the total stress tensor can be decomposed in an isotropic pressure term p and a deviatoric component of the stress tensor \mathbf{T} . \mathbf{I} is the unit dyadic. The continuity equation is also used, using the incompressibility constraint:

$$\frac{\partial p}{\partial t} = -(\nabla \cdot \rho \mathbf{v}) \quad (3.33)$$

$$\nabla \cdot \mathbf{v} = 0 \quad (3.34)$$

The constitutive equation is represented by Eq. 3.32; the definition of the deviatoric component of the stress tensor represents one important issue, objective of a relevant rheology branch. The tensor \mathbf{T} used here can be written as:

$$\mathbf{T}(\mathbf{x}, t) = 2\eta(\mathbf{x}, t)\dot{\boldsymbol{\epsilon}}(\mathbf{x}, t) \quad (3.35)$$

where η is the shear viscosity (also known as apparent viscosity) and $\dot{\boldsymbol{\varepsilon}}(\mathbf{x}, t)$ is the strain rate tensor, which can be expressed as:

$$\dot{\boldsymbol{\varepsilon}}(\mathbf{x}, t) = \frac{1}{2}(\nabla \mathbf{v} + (\nabla \mathbf{v})^T) \quad (3.36)$$

The apparent viscosity function (Eq. 3.6) depends on the flow-curve used: it can be constant if a Newtonian model is used, or can follow a Non-Newtonian model (i.e. Bingham or Herschel-Bulkley models). For instance, with a Bingham model it becomes Eq. 3.26, where the term $\dot{\gamma}$ represents the shear rate, and is function of the strain rate tensor $\dot{\boldsymbol{\varepsilon}}$:

$$\dot{\gamma} = \sqrt{2\dot{\boldsymbol{\varepsilon}} : \dot{\boldsymbol{\varepsilon}}} \quad (3.37)$$

3.3 Test Methods for Evaluating Fresh Concrete Properties

At the first stages of cement-based materials flow, casting and molding, and in all the other practical cases occurring before hardening, the liquid-like behavior of these materials can be studied, and their fundamental characteristics can be measured through various methods. The typically used experimental methods for evaluating fresh concrete properties are divided in two main groups: one-parameter and two-parameters measuring.

In the first category, tests like slump cone, penetrating rod, Ve-Be time are used to assess either yield stress or viscosity, due to an internal (gravity) or external (vibration, external pressure) stress application. Table 3.1 summarizes these test methods: it should be recalled that yield stress measurements are relatively easier to be done, whereas to evaluate plastic viscosity, the yield stress should be exceeded, and hence the applied stress should have a greater magnitude.

Table 3.1 One-parameter test methods for the assessment of fresh concrete properties

Name of the test	Parameters analyzed	Stress applied
Slump	About yield stress	Gravity
Flow (table) test	About viscosity	Gravity
Penetrating rod	About yield stress	Applied stress
K-slump test	About segregation	Gravity
Turning tube viscometer	About viscosity	Gravity
Ve-Be time or remolding test	About yield stress	Vibration
Filling ability	About flowing between rebars	Applied pressure or gravity
V-funnel	About filling ability	Gravity
Orimet apparatus	About flowing through openings	Gravity

Concrete slump test is a very simple procedure, very popular especially at the field level, because it is used as a quality control to help detecting changes in the concrete delivered at site. The test is carried out using the Abrams cone (Fig. 3.3), which is placed on a hard non-absorbent surface; then the cone is filled with the fresh concrete in three successive stages, each time tamped, for the single layer depth, for 25 times. When the mold is lifted up (quickly), the slump is then measured. This method can be employed for concretes with a maximum aggregate diameter equal to 38 mm, and slump between 5 and 260 mm. More details can be found in the international standard EN 12350-2 [21] and ASTM C143 [22].

Flow table test (or flow test) can be alternatively used for highly workable concrete, in accordance to EN 12350-5: the test is carried out using a cone, similar to the Abram's one but truncated, and a 700 mm square table, hinged to a rigid base, which is furnished with a stop that allows the far end to be raised by 40 mm. The cone is filled with the fresh concrete, in two successive stages: each layer should be tamped for 10 times with a wooden bar, and then the upper surface is finished as done in the classical concrete slump test. The cone is removed, and then, after a little flow of the material on the table, this last is raised of the cited 40 mm and allowed to drop for 15 times. The average diameter between the experimentally evaluated ones in the two principal directions (or more) is calculated. This version of the slump test is not related with the yield stress, however it aims to evaluate the



Fig. 3.3 Slump test

flow of concrete when the applied stress exceeds the yield one. If the concrete does not flow (no spread can be evaluated), this means that the yield stress has not been exceeded, and hence this test method is not useful.

Another modified version of the slump test has been recently introduced, aiming to estimate both the yield stress and the viscosity of fresh concrete: as it is a two-parameters test, it will be described in detail in the next section.

Penetrating rod tests are based on the principle that the depth of penetration of an object in the tested material depends on its yield stress. They are typically used at the job site, however their diffusion is not widespread. Between the penetrometers, Kelly Ball test method (ASTM C360 [23]) is used to evaluate the penetration of a hemispherical metal weight into the fresh concrete: the test is carried out using a cylinder with one hand having a hemispherical shape, and the other fit with a graduated handle (Fig. 3.4). The weight (approximately 15 kg) is lowered through a frame into the fresh concrete sample, and the penetration is measured. It should be recalled that, due to its lack of use, ASTM C360 standard has been withdrawn in 1999. Vicat apparatus (EN 196-3 [24]; ASTM C191 [25]) consists instead of a metal stand with a sliding rod, an adjustable indicator which is moving on a graduated scale, and a needle, attached to the bottom end of the rod (Fig. 3.4). The test weight is approximately 300 g, thus making this test method useful for cement paste.

K-Slump test consists in inserting a tester into the fresh concrete placed in the formworks up to the level of the disc, and after 60 s, a measuring rod is lowered onto the surface of concrete and the K-slump value can be read directly on the scale. This method was widely diffused in the past, however since 2014, the ASTM C1362-09 standard [26], which covered its regulation, was withdrawn. K-slump test was typically applied to evaluate the ability of concrete to segregate.

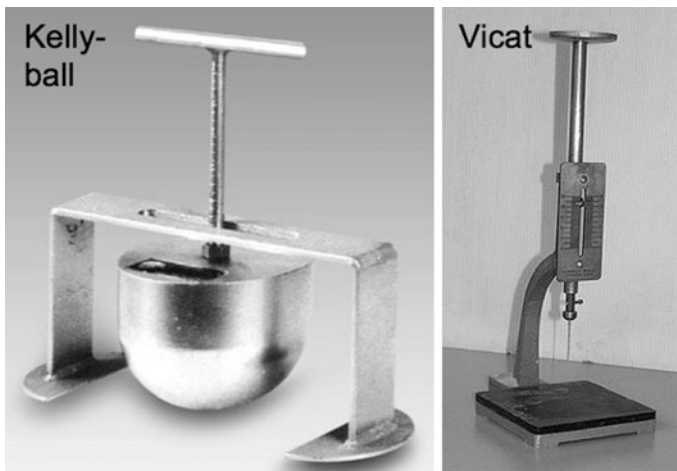


Fig. 3.4 Penetrating rod test methods: Kelly-ball and Vicat apparatus

The turning tube viscometer test has been introduced by Hopkins [27] for evaluating cement pastes' viscosity: it consists of a tube, with 60 mm diameter and 800 mm length, that should be filled by the tested material. The velocity of a ball, dropped into the fluid, between two points placed at 370 mm one from another, is then measured, and used to evaluate the viscosity through the Stokes equation.

Vebe test is described in EN 12350-3 [28]: it is a method for determining the consistency of fresh concrete, and it can be applied for mixtures with aggregates size not greater than 63 mm. Concrete is placed in an open-truncated cone; then the time necessary to re-mold it into a cylinder, after the cone is lifted away, under vibration, is measured. This method could be related to the yield stress of the material, even though not directly, because concrete starts flowing after exceeding the yield stress, due to the induced vibrations. The range of applicability of this test lies between 5 and 30 s of Vebe time.

Filling ability, passing ability, and segregation resistance of fresh concretes (mainly of SCC) can be measured through various test methods, including filling vessel test, U-box, L-box and J ring tests. Filling vessel test aims to reproduce a small scale structure with high reinforcement content, for analyzing the ability of passing through the bars and the self-leveling ability of concretes. Several geometries are available, also aiming to assess a quantification of this property in terms of filling height. U-box (also called U-shape) test is used to evaluate the narrow-opening passability of high-flowable fresh concretes (typically SCC), under a head pressure. A similar geometry has been used in the Box-shape test. Both these apparatus consist of two compartments (Fig. 3.5): the first is filled by fresh concrete, which is prevented to flow in the second room from a partition gate. When the first compartment is completely full, the obstacle is removed and the mixture is let free to flow into the second room: when the flow stops, the height of fresh concrete (filling height) in the second compartment is measured. Also the time of flow can be measured, and it can be used to evaluate fresh concrete viscosity. L-box test [29] has a similar principle of U-box and Box-shape tests: it consists of two compartments, which are not completely separated by a gate, but the obstacles between them is made by reinforcing bars, to make narrow openings on flowing path of fresh concrete (Fig. 3.5). This test does not only evaluate the filling ability of high flowable fresh concretes, but it can also be related to the slump test. Concerning to

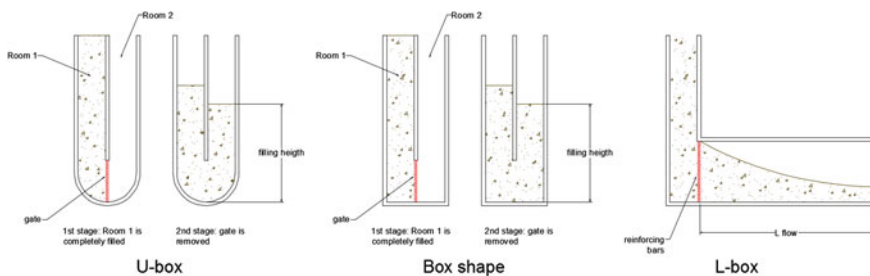


Fig. 3.5 Experimental apparatus for evaluating filling ability of fresh concretes

the former property, the difference in height before and after the flow, indicates the so-called blocking ratio, i.e. the ability to pass between the reinforcement. Concerning the latter property, L-box test provides the descent of concrete sample, which has a similar physical meaning to the slump value, being able to evaluate the 1D flowability under the constrained direction of flow. Additionally, the time of flowing is useful to evaluate the deforming velocity. J ring test [30, 31] is commonly used to evaluate fresh concrete passing ability. It consists of a steel crown with 300 mm diameter, characterized by vertical holes drilled in the ring itself, where reinforcing steel bars can be inserted. Generally this test is conducted at the same time with the slump test: the cone is placed in the center of the ring, it is lifted, and the mixture is allowed to flow through the gaps between the reinforcements. Alternatively to the slump cone, the V-funnel or the Orimet apparatus can be placed in the center of the ring. The diameter of the horizontal spread of concrete is evaluated; also the difference in height between two points (inside and outside the rebars) can be used to assess the passing ability.

V-funnel test [32] consists of a V-shaped box, characterized by a small opening in the bottom (65×75 mm). Fresh concrete is placed in the box and let to rest for about 1 min; when it is completely filled, the bottom is opened and the sample is let to flow: the time of discharging (funnel flow time) is then measured. This information can be considered as an index (indirect) about concrete viscosity. In case of mixtures containing large diameter aggregates, this test can also be used to assess the narrow opening passing ability of the concrete.

The Orimet apparatus principle is very similar to the V-funnel test: it consists of a tube (600 mm length), with an opening at the bottom. The time necessary to flow through the tube length, when the bottom is opened, is recorded, and it gives an assessment of the flowability of the mixture.

Two-parameters tests provide two measured values, which are not necessarily related to a direct evaluation of physically-based fundamental parameters, i.e. viscosity and yield stress. It is worth noting that several phenomena can hinder a correct evaluation of rheological parameters, e.g. segregation, particle migration, etc. The simplest method to derive an estimate of both the yield stress and viscosity is the modified slump cone, recently developed by Ferraris and de Larrard [33]. This test consists in measuring both the slump value, related to the yield stress, and the so-called “speed of slumping”, related to the viscosity of the mixture. Fresh concrete is placed in the Abrams cone, and then the time it takes to slump the first 100 mm is taken; the final slump measure is also collected. From these two simple measures, it is possible to estimate the Bingham parameter using an empirical conversion equation.

Speed-controlled viscometers can also be used for estimating rheological parameters of fresh cement-based materials. They can be rotating or tubular: in both the cases, existing formulations can provide correlations between the measured parameters and the investigated parameters. For instance, for a rotating viscometer, shear stress and torque can be easily correlated, as well as the shear stress and the speed of rotation. For the tubular-shape viscometers, pressure drop can be correlated to the flow rate in the tube.

When dealing with the design of a proper instrument for evaluating fresh concrete properties, at least the two parameters of the Bingham model should be assessed. Additionally, during the design, the geometrical proportions of the instrumentation are very important, also referred to the tested material property. In case of concrete testing, the maximum size of the aggregates (D_{max}) affects the dimension of the gap where the material should flow: the gap must be at least 3 times the D_{max} , in order to avoid particle interlocking (and hence increased localized stresses), and being sufficiently representative of the material volume. However, to fulfill these geometrical requirements, most of instrumentations does not allow to derive both the required Bingham parameters, but express the results in non-standard units.

In case of rheometers, those apparatus can be designed in order to evaluate the parameters necessary to build a flow curve describing the relation between shear stress and rate. The most common rheometers have a coaxial cylinder geometry or a parallel plate one. In the former case, the rheometer is made by two coaxial cylinders, one stationary, and one rotating at a given speed. Typically the inner measures also the stresses generated by the fluid. The gap between the two cylinder should comply with the above-cited geometrical limitation, and also it should be as reduced as possible, specifically with respect to the diameter of the cylinders, in order to be able to compute the shear stress and shear rates, and then the yield stress and the plastic viscosity, according to the Bingham model. It is well-accepted to use a ratio equal to 1.1 between the external and internal cylinder diameters, and a gap ranging between 3 and 5 times D_{max} .

Several types of coaxial cylinder geometry rheometers have been developed during the last decades, starting from 1970: one of the firsts is the one we referred to “two-point test”, developed by Tattersal [10], which consisted in a shaft with blades, necessary to avoid slippage, that rotated in a bucket filled with concrete, at a controlled speed. The torque generated by the fluid was measured on the shaft, but it was not possible to convert neither the rotation speed neither the torque to calculate the fundamental Bingham parameters.

This rheometer was then modified by Wallevik in the late 1980s [34], who also produced a commercial version of this apparatus, modifying the blades and attaching them radially on the shaft. The bottom part of the inner cylinder was excluded from measuring the torque, to avoid that the stresses generated by the plate of the bucket, which contains the fresh concrete, would affect the measures. Through this equipment, fundamental Bingham parameters can be evaluated, when no plug or aggregates migration problem occur. The apparatus has been modified during the following years, until obtaining the current version ConTec BML-Viscometer (Fig. 3.6), which is useful for testing coarse particles suspension with 80 mm slump or higher.

Another type of geometry found in rheometers is the parallel plate one, which is used by the BTRHEOM developed by de Larrard et al. [35]. Here, two plates are present: an upper one, rotating at a given speed, and a stationary bottom one. The torque due to the resistance of the material is measured in the upper plate. In this type of instrumentation, the shear rate is not constant, but it depends by the radial

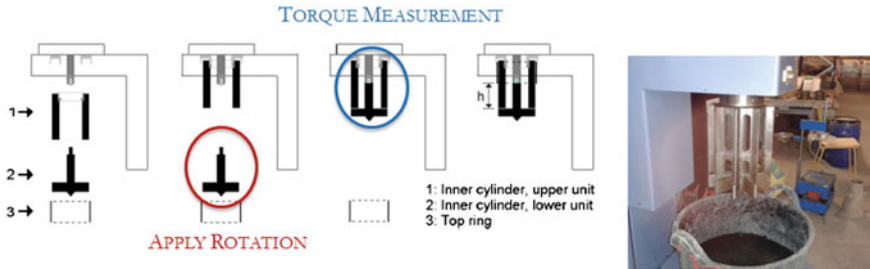


Fig. 3.6 ConTec BML Viscometer

coordinate of the point: the shear rate is null in the center of the plate, and it is maximum at the edge of the plate. This difference in the shear rate along the position makes necessary an analytical calculation for all Non-Newtonian fluids, where viscosity depends on the shear rate.

3.4 Evaluation of Rheological Parameters with Coaxial Cylinders Viscometer

Several test methods are currently available to estimate how various kinds of fresh concrete behave rheologically. Between them, viscometers can be used to obtain physical quantities for better estimating the rheological parameters; one of these, coaxial cylinder geometry for fresh concrete, has been used with good results since its first use in 1941 by Power and Wiler [36, 37], followed by Tattersall and Banfill [38] and Wallevik [34, 39], and can extract the Bingham model parameters, i.e., plastic viscosity μ and yield stress τ_0 .

The commercially available ConTec BML Viscometer 3 (Fig. 3.6) consists of an outer cylinder ($R_o = 145$ mm) rotating at an angular velocity of $\Omega = 2\pi f$ (rad/s); an inner cylinder unit ($R_i = 100$ mm), to measure the applied torque, T (Nm); and a special bottom unit, which eliminates shearing from the bottom to the outer walls. This viscometer was designed to avoid slippage between cylinders and test material, due to protruding vanes in both upper and lower units [40]. For evaluating fresh concrete properties, about 17 L of fresh material are tested, measuring 7 values of torque, with decreasing rotation speeds of the outer cylinder. For each velocity, a certain number of measures (depending on the sampling frequency) can be taken during a time interval (steady-state conditions); between each rotational velocity, there is a transient state in which no sampling occurs. After recording of the 7th point, a further increase in rotational velocity can be given to check segregation, at $f_{seg} = 2/3 f_{max}$. To reduce the aggregates interlocking effect, Wallevik recommended to choose the 10 lowest values per each sampling velocity, and average them to obtain a single value \hat{T} [39]. Figure 3.7 shows a typical sampling profile: it

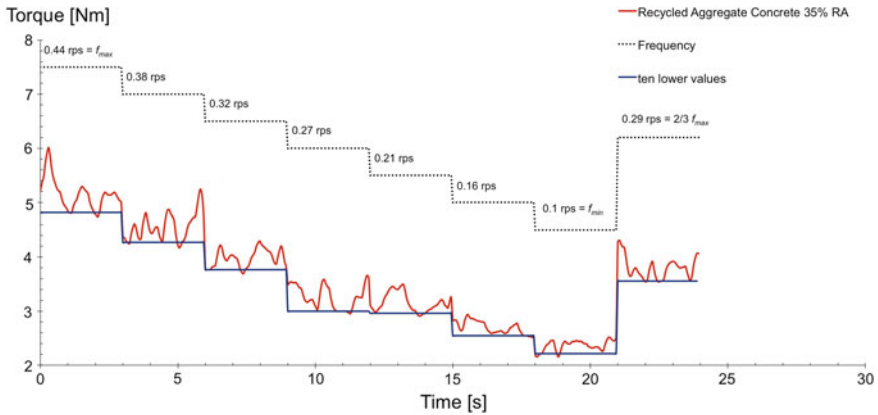


Fig. 3.7 Sampling profile using a ConTec BML viscometer for evaluating Bingham parameters of fresh recycled aggregate concrete with 35 % RA

is recalled that the same mixing conditions (temperature, humidity, mixing process) should be guaranteed to allow a suitable comparison of rheological measurements of two or more concretes.

Once collected the torque values for each applied velocity $T(N)$, the physical rheological parameters of fresh concrete batches should be evaluated solving the so-called “inverse Couette problem” and hence obtaining the flow curve $\tau(\dot{\gamma})$. Three methods can be used: the first is the integration method, where the functional form of constitutive equation is specified in advance, and integrated to obtain the relation $T(N)$, which is fitted to the experimental data. Tikhonov regularization method can be also used [41], as well as the wavelet-vaguelette decomposition method [42]. Following the first method, for a Bingham fluid the analytical solution can be obtained through the Reiner-Riwlin equation [43–45], when dealing with a wide-gap coaxial cylinder viscometer. For other functional forms of the flow curves, an analytical solution not always is possible; in case of Herschel-Bulkley and Ostwald-de Waele fluids the solutions can be found in [44]. Here, a brief description of the Reiner-Riwlin equation is provided, being the Bingham model the most used flow curve for describing fresh ordinary concrete, and recently satisfactorily applied to represent fresh recycled concrete flow [46].

3.4.1 Reiner-Riwlin Equation

Reiner-Riwlin equation is obtained by solving the velocity field (Eq. 3.38), under the following hypotheses:

low Reynolds number Re (i.e., low rotational velocity and high apparent viscosity of fluid), allowing fluid stability and symmetry along the z -axis;

no bottom effects, i.e. z -independence of cylinder height;
 with circular flow, θ -independence occurs in both the velocity field and distribution of pressure p ;
 time t -independence at each angular velocity step.

Hence the general velocity profile:

$$\mathbf{v} = v_r(r, \theta, z, t)\mathbf{i}_r + v_\theta(r, \theta, z, t)\mathbf{i}_\theta + v_z(r, \theta, z, t)\mathbf{i}_z \quad (3.38)$$

can be simplified into the following:

$$\mathbf{v} = v_\theta(r)\mathbf{i}_\theta \quad (3.39)$$

From this equation, the velocity gradient tensor $\nabla\mathbf{v}$ can be evaluated, in order to obtain the strain rate tensor:

$$\dot{\boldsymbol{\epsilon}} = \frac{1}{2} \left(\frac{dv_\theta(r)}{dr} - \frac{v_\theta(r)}{r} \right) (\mathbf{i}_r\mathbf{i}_\theta + \mathbf{i}_\theta\mathbf{i}_r) \quad (3.40)$$

Using this result into Eq. 3.37, the shear rate that applied inside the fresh concrete sample can be evaluated:

$$\dot{\gamma} = \left| \frac{dv_\theta(r)}{dr} - \frac{v_\theta(r)}{r} \right| \quad (3.41)$$

Now, using the constitutive equation of the viscoplastic state (Eq. 3.35) and Eq. 3.40, the deviatoric stress tensor can be written as:

$$\mathbf{T} = \eta(\dot{\gamma}) \left(\frac{dv_\theta(r)}{dr} - \frac{v_\theta(r)}{r} \right) (\mathbf{i}_r\mathbf{i}_\theta + \mathbf{i}_\theta\mathbf{i}_r) \quad (3.42)$$

Hence the component $T_{r\theta}$ is extracted from Eq. 3.42:

$$T_{r\theta} = \eta(\dot{\gamma}) \left(\frac{dv_\theta(r)}{dr} - \frac{v_\theta(r)}{r} \right) \quad \forall r \in [R_i, R_s] \quad (3.43)$$

which is valid in the viscoplastic zone, i.e. between the inner radius R_i and the plug radius R_s , beyond which a solid state occurs. The solid state can be described through the Hook law: for more details about plug phenomenon, look at Sect. 3.4.2. If no plug occurs, R_s is equal to R_o , the outer radius.

Now, consider the fresh concrete sample to be divided into cylindrical shells of δR thickness. The equation of rotational motion for each shell is:

$$I_R \frac{d\omega(r,t)}{dt} = \widehat{\mathbf{T}} = \widehat{\mathbf{T}}(r + \delta R/2, t) \mathbf{i}_z - \widehat{\mathbf{T}}(r - \delta R/2, t) \mathbf{i}_z \quad (3.44)$$

where I_R is the inertia moment of each shell, $\widehat{\mathbf{T}}$ is the sum of the torques applied to the shell, and ω is the angular velocity:

$$\boldsymbol{\omega} = \mathbf{i}_r \times \frac{v_\theta(r,t) \mathbf{i}_\theta}{r} = \frac{v_\theta(r,t)}{r} \mathbf{i}_z \quad (3.45)$$

At the steady state $\frac{d\omega}{dt} = 0$, hence Eq. 3.44 becomes:

$$\widehat{\mathbf{T}} \left(r + \frac{\delta R}{2} \right) = \widehat{\mathbf{T}} \left(r - \frac{\delta R}{2} \right) \quad (3.46)$$

which means that, during each measurement at a fixed rotational velocity, where steady state is assumed to occur, the torque is constant inside the concrete sample, for each radius $r \in [R_i, R_o]$. This result applies independently from the plug occurrence.

The torque applied on a cylindrical shell can be calculated according to Cauchy's stress principle:

$$\widehat{\mathbf{T}} = \widehat{\mathbf{T}} \mathbf{i}_z = \int_0^h \int_0^{2\pi} r \mathbf{i}_r \times (\mathbf{i}_r \cdot \boldsymbol{\sigma}(r) r d\theta dz) = 2\pi r^2 h T_{r\theta}(r) \mathbf{i}_z \quad (3.47)$$

where h is the height of the shell. From this equation one can derive the torque applied to the inner cylinder of the rheometer apparatus:

$$\widehat{\mathbf{T}} = 2\pi R_i^2 h T_{r\theta}(R_i) \quad (3.48)$$

Combining Eq. 3.47 with Eq. 3.43 it is possible to obtain the following:

$$\eta(\dot{\gamma}) \left(\frac{dv_\theta(r)}{dr} - \frac{v_\theta}{r} \right) = T_{r\theta}(r) = \frac{\widehat{\mathbf{T}}}{2\pi r^2 h} \quad \forall r \in [R_i, R_s] \quad (3.49)$$

With the hypothesis that the outer cylinder rotates counterclockwise, giving $v_\theta(r) > 0$, then $\widehat{\mathbf{T}}$ in Eq. 3.48 should be positive. This determines $T_{r\theta} \geq 0 \forall r \in [R_i, R_s]$; accordingly it is possible to rewrite Eq. 3.41 without the absolute sign. Now, with the Bingham model (Eq. 3.26) used for defining the apparent viscosity, Eq. 3.49 becomes:

$$\frac{dv_\theta(r)}{dr} - \frac{v_\theta}{r} + \frac{\tau_0}{\mu} = \frac{\widehat{\mathbf{T}}}{2\pi \mu r^2 h} \quad \forall r \in [R_i, R_s] \quad (3.50)$$

The shear rate can be obtained as follows:

$$\dot{\gamma} = \frac{dv_{\theta}(r)}{dr} - \frac{v_{\theta}(r)}{r} = \frac{\hat{T}}{2\pi\mu r^2 h} - \frac{\tau_0}{\mu} \quad \forall r \in [R_i, R_s] \quad (3.51)$$

Lastly, the Reiner-Riwlin equation can be obtained using the no-slip condition at the boundary between solid and viscoplastic state, and the Dirichlet boundary conditions $v_{\theta}(R_i) = 0$ and $v_{\theta}(R_s) = R_s\omega_0$. Dividing Eq. 3.50 by r , it is possible to obtain the following:

$$\frac{1}{r} \frac{dv_{\theta}(r)}{dr} - \frac{v_{\theta}}{r^2} + \frac{\tau_0}{\mu r} = \frac{\hat{T}}{2\pi\mu r^3 h} \quad (3.52)$$

which is:

$$\frac{d(v_{\theta}/r)}{dr} = \frac{\hat{T}}{2\pi\mu r^3 h} - \frac{\tau_0}{\mu r} \quad (3.53)$$

If Eq. 3.53 is integrated, it is possible to obtain:

$$\frac{v_{\theta}}{r} = -\frac{\hat{T}}{4\pi\mu r^2 h} - \frac{\tau_0}{\mu} \ln(r) + C \quad (3.54)$$

where C is the integration constant. Using the boundary condition to obtain C , it is possible to write:

$$v_{\theta}(r) = \frac{\hat{T}r}{4\pi\mu h} \left(\frac{1}{R_i^2} - \frac{1}{r^2} \right) - \frac{\tau_0 r}{\mu} \ln\left(\frac{r}{R_i}\right) \quad \forall r \in [R_i, R_s] \quad (3.55)$$

Then with the other boundary condition, and solving for the torque:

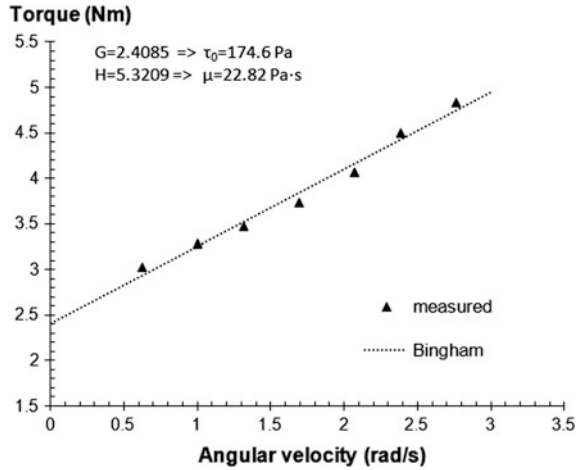
$$\hat{T} = \frac{4\pi\mu h}{1/R_i^2 - 1/R_s^2} \omega_0 + \frac{4\pi\tau_0 h}{1/R_i^2 - 1/R_s^2} \ln\left(\frac{R_s}{R_i}\right) \quad (3.56)$$

If plug does not occur, R_s can be substituted with R_o (a constant value), and Eq. 3.56 can be re-arranged into the following:

$$\hat{T} = \frac{4\pi\mu h}{1/R_i^2 - 1/R_o^2} \omega_0 + \frac{4\pi\tau_0 h}{1/R_i^2 - 1/R_o^2} \ln\left(\frac{R_o}{R_i}\right) = H\omega_0 + G \quad (3.57)$$

Plotting the measured torque \hat{T} as a function of the angular velocity ω_0 , it is possible to obtain the values of H and G shown in Eq. 3.57, which now can be related to the plastic viscosity and the yield stress through the following formulas, obtained from Eq. 3.57:

Fig. 3.8 Viscometric measurement of fresh recycled concrete with 35 % RCA and $w/c = 0.4$



$$\mu = \frac{H(1/R_i^2 - 1/R_o^2)}{4\pi h} \quad (3.58)$$

$$\tau_0 = \frac{G(1/R_i^2 - 1/R_o^2)}{4\pi h \ln\left(\frac{R_o}{R_i}\right)} \quad (3.59)$$

Figure 3.8 shows an example of calculation of H, G values through linear interpolation of $\hat{T}(\omega_0)$ measurement obtained testing a fresh recycled concrete.

Lastly, if we combine Eq. 3.51 with Eq. 3.56, the shear rate equation can be derived:

$$\dot{\gamma} = \frac{2}{r^2} \left(\frac{1}{R_i^2} - \frac{1}{R_s^2} \right)^{-1} \left[\omega_0 + \frac{\tau_0}{\mu} \ln\left(\frac{R_s}{R_i}\right) \right] - \frac{\tau_0}{\mu} \quad \forall r \in [R_i, R_s] \quad (3.60)$$

from which the shear rate gradient, useful in the analysis of gravel migration problems, can be calculated:

$$\frac{d\dot{\gamma}}{dr} = -\frac{4}{r^3} \left(\frac{1}{R_i^2} - \frac{1}{R_s^2} \right)^{-1} \left[\omega_0 + \frac{\tau_0}{\mu} \ln\left(\frac{R_s}{R_i}\right) \right] \quad \forall r \in [R_i, R_s] \quad (3.61)$$

3.4.2 Plug Flow and Gravel Migration Influence

At high τ_0/μ ratios, a solid state may occur in the fresh concrete flow inside coaxial cylinder geometry viscometers. This phenomenon, called plug flow, starts from the outer cylinder and propagates towards the inner one, creating a layer which behaves

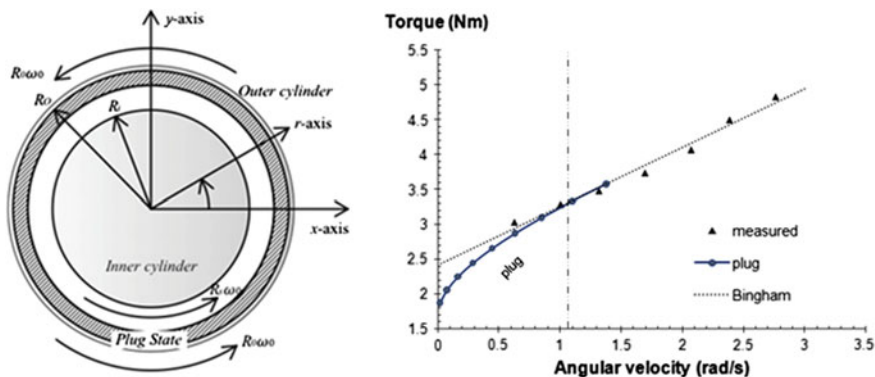


Fig. 3.9 Schematic representation of plug flow (from [46]) and its influence on a viscometric measurement performed on fresh recycled concrete with 35 % RCA and $w/c = 0.4$

as a rigid body. If not taken into consideration, plug flow leads to over-estimation of plastic viscosity μ and under-estimation of yield stress τ_0 . Figure 3.9 schematically represents how plug state occurs in a coaxial cylinders viscometer.

When a solid layer occurs, the Reiner-Riwlin equation cannot be applied directly, because the outer boundary condition changes with plug radius $v_\theta(R_s) = R_s\Omega$. The first way of solving this problem is simply to remove the data included in the plug flow range by manually deleting (\hat{T}_i, N_i) for every $N_i < N_s$ [47]. N_s is the speed below which plug flow occurs [38] and it can be evaluated through:

$$N_s = \frac{\tau_0}{\mu} \left[\frac{1}{2} \left(\frac{R_o^2}{R_i^2} - 1 \right) - \ln \left(\frac{R_o}{R_i} \right) \right] \cdot \frac{1}{2\pi} \quad (3.62)$$

Alternatively, the Bingham parameters can be estimated more accurately. An iterative procedure to calculate rheology parameters μ and τ_0 , practically estimating plug radius and then deriving the above-mentioned quantities, has been used in [46, 48]. The procedure is shown in Fig. 3.10, referring to the following equations:

$$\omega_0 = \tau_0/\mu \left[\frac{1}{2} \left(\frac{R_s^2}{R_i^2} - 1 \right) - \ln \left(\frac{R_s}{R_i} \right) \right] \quad (3.63)$$

$$\hat{T} = \frac{4\pi\mu h}{\left(\frac{1}{R_i^2} - \frac{1}{R_s^2} \right)} \Omega + \frac{4\pi\tau_0 h}{\left(\frac{1}{R_i^2} - \frac{1}{R_s^2} \right)} \ln \left(\frac{R_s}{R_i} \right) \quad (3.64)$$

$$\begin{cases} R_s : f(R_s) = \tau_0/\mu \left[\frac{1}{2} \left(\frac{R_s^2}{R_i^2} - 1 \right) - \ln \left(\frac{R_s}{R_i} \right) \right] - \omega_0 = 0 \\ \text{Given an initial } R_{s,0}, \text{ do until convergence} \\ R_{s,k+1} = R_{s,k} - \frac{f(R_{s,k})}{f'(R_{s,k})} \quad \text{with } k \geq 0 \end{cases} \quad (3.65)$$

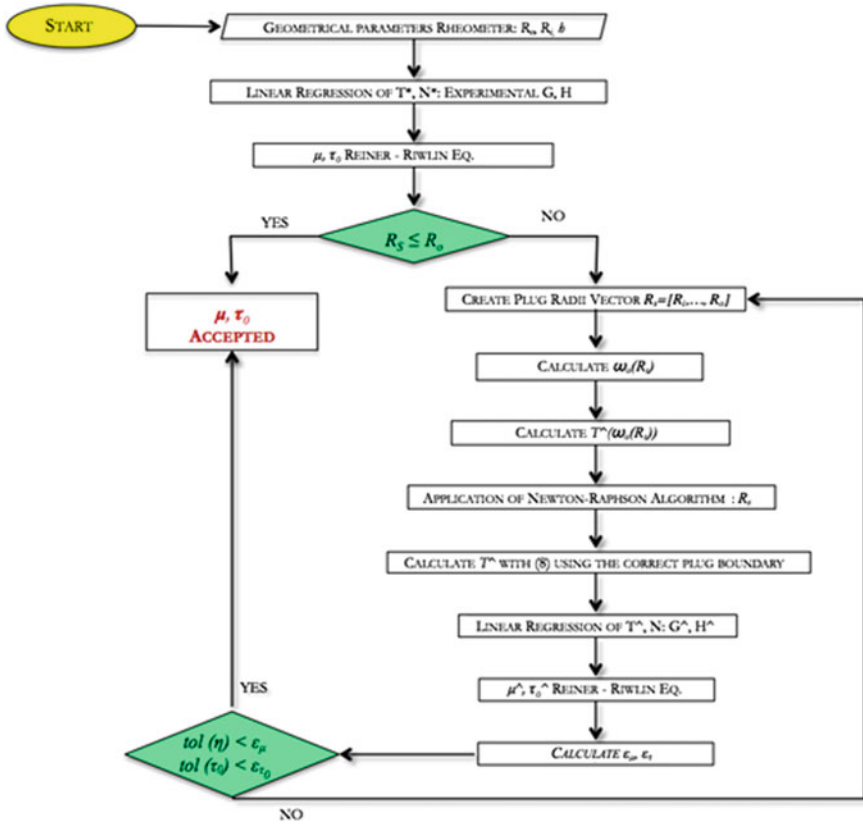


Fig. 3.10 Iterative procedure applied to extract Bingham rheology with plug state at plug flow boundary R_s (from [46])

$$\begin{cases} \epsilon_\mu = \frac{\hat{\mu} - \mu}{\mu} \\ \epsilon_{\tau_0} = \frac{\hat{\tau}_0 - \tau_0}{\tau_0} \end{cases} \quad (3.66)$$

Another concomitant problem may occur at high rotational velocity, especially in concrete batches with low fresh mortar content and high aggregate volume. Coarse aggregate suspended in the fresh mortar matrix may migrate from high shear rate regions to low ones, i.e. from the inner part of the rotating cylinder to the outer boundary, in a coaxial cylinders viscometer. This phenomenon has been extensively reported in the literature [45, 49], also when testing recycled aggregate concrete, especially when designed with the EMV method [46]. If this phenomenon occurs, the measured rheological parameters do not properly represent the tested mixes. However, the values can describe the remaining fat concrete, which does not rigidly move under shear rate gradient $-\nabla\dot{\gamma}$.

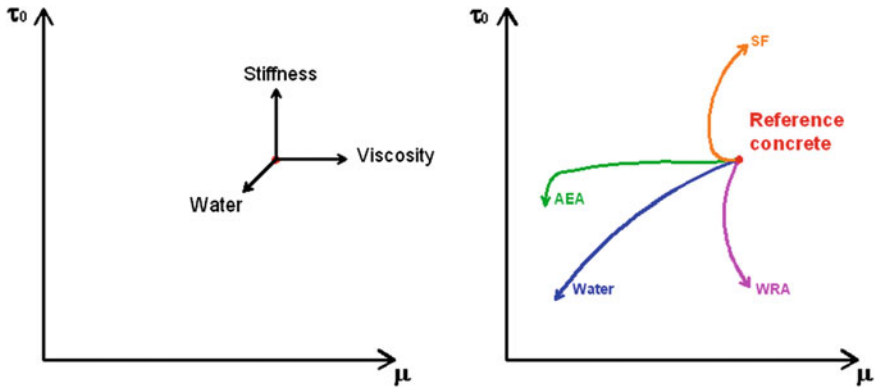


Fig. 3.11 The use of rheographs for highlighting the effect of adding water, water-reducing admixture (WRA), air-entrainer admixture (AEA) and silica fume (SF) on Bingham parameters (adapted from [50])

3.4.3 Rheographs

As mentioned in Sect. 3.2.1., most of fresh ordinary concretes can be satisfactorily considered to flow according to Bingham model, and hence rheological quantities can be obtained in terms of yield stress and plastic viscosity, which can be experimentally evaluated in coaxial cylinder viscometers. When these parameters have been obtained, they can be used to draw the so-called “rheographs”, which are useful to plot the relation between the yield stress τ_0 (the y-axis) and the plastic viscosity μ (the x-axis) as a function of material properties, time, additives, etc. A rheograph is able to reveal systematically the influence of e.g. a mixture component on the overall rheological behavior of the tested material. The first application of these diagrams is due to Wallevik in 1983 [39], who analyzed the influence of water, air-entrainer, water-reducing admixture content, and silica fume addition in fresh concrete batches. Figure 3.11 shows an example of a rheograph, where the arrows highlight the effects of adding some components on Bingham parameters of the reference mixture.

3.5 Mix Proportion Design of Coarse Recycled Aggregate Concrete and Its Effect on Workability

One of the most common solutions to improve sustainability in concrete production is given by the possibility to include recycled concrete aggregates in the place of virgin aggregates, at least in limited replacement ratio. This possibility is allowed by several International Codes and Recommendations, also for structural concrete applications, with the only prescriptions that recycled aggregate must comply with

some minimum requirements, mainly concerning chemical stability and physical–mechanical characteristics. Literature research has widely studied the problems linked to the mechanical and durability-related properties in recycled aggregate concretes, however limited information is reported about the properties of fresh recycled concretes, even though it has been often recognized that the introduction of recycled aggregate generally worsens workability. This problem arises significantly when recycled concrete is designed using a particular mix proportion method, called Equivalent Mortar Volume (EMV) [51], which produces stiffer concretes than the control ones. The parameters controlling fresh concrete properties should be carefully taken into account with this method, due to the reduced amount of fresh mortar in the mix in favor of increased coarse aggregate volume. Knaack and Kurama [52], studying the rheological and mechanical behavior of RAC designed according to various methods—direct weight replacement (DWR), direct volume replacement (DVR), EMV methods—concluded that, compared with conventionally designed RAC (DWR, DVR), the workability of concrete mixes designed with the EMV method is significantly worsened. It should be noted that rheological behavior was analyzed according to the “mini slump test”, a variation on the conventional test described by the same authors [53], based on a single-number result. For the above reasons, the rheological properties of various concrete mixes produced with differing mixture proportioning methods have been studied in [46], obtaining that, even though the addition of super-plasticizer can overcome significant workability losses, there is still a relevant difference between recycled concretes produced with the EMV method and DVR or DWR methods, in terms of rheological behavior.

3.5.1 DVR, DWR and EMV Proportioning Methods

Generally, when recycled concrete is designed, recycled aggregates are just take as the natural ones, replacing them or maintaining the same volume or weight proportion. The first method is called direct volume replacement (DVR), and the latter direct weight replacement (DWR). Both these methods typically cause losses against mechanical strength, due to the worse characteristics of recycled aggregates [54–56], when containing high amount of adhered mortar (Fig. 3.12).

The EMV method is based on the concept that the recycled aggregate concrete (RAC) mix should be proportioned to have the same total mortar volume as a reference concrete mix, made entirely with fresh natural aggregates (NAs). Accordingly the produced concrete will not suffer the above cited strength losses often experienced when using conventional proportioning methods. The total amount of mortar is defined by the new fresh mortar content plus the old adhered mortar onto the recycled concrete aggregates (RCAs). Hence, the proportioning method essentially involves the effective determination of the amounts of RCA and



Fig. 3.12 Recycled aggregates with high attached mortar content

the fresh mortar in RCA concrete, attached to the NAs. In addition, this method just takes into account recycled aggregate (RA) as coarse recycled aggregate (CRA), whereas the fine recycled part is not analyzed.

The procedure to design properly a concrete with the EMV method is herein reported, according to [51]. First of all, it is necessary to specify the properties of the RCA, both at the fresh and hardened state. Accordingly, a reference concrete is designed by means of conventional proportioning method: this is the NAC mix. The volume of natural aggregates inside this mix is defined as V_{NA}^{NAC} .

Then the RAC is designed. The first step is given by the definition of V_{NA}^{RAC} : it is the volume of natural aggregates inside the recycled mix. The NA content ratio is defined as R :

$$R = \frac{V_{NA}^{RAC}}{V_{NA}^{NAC}} \tag{3.67}$$

If $R = 0$: the coarse aggregate in the mix is 100 % RCA; if $R = 1$ the mix is made just by NA and no RCA is present. In order to have the same hardened concrete properties, the EMV method proposes that two conditions must be satisfied (Eq. 3.68 and 3.69): the volume of the total mortar in the two mixes must be the same, and the volume of the total natural aggregates in both the concretes should remain constant. This can be expressed as follow:

$$V_{TM}^{RAC} = V_M^{NAC} \tag{3.68}$$

$$V_{TNA}^{RAC} = V_{NA}^{NAC} \tag{3.69}$$

The total volume of mortar (TM) in RAC is given by two contributions: the residual mortar V_{RM}^{RAC} and the new fresh mortar V_{NM}^{RAC} :

$$V_{TM}^{RAC} = V_{RM}^{RAC} + V_{NM}^{RAC} \quad (3.70)$$

The total volume of natural aggregates (TNA) inside RAC is given by the sum of the volumes of new coarse NA (V_{NA}^{RAC}) and the original NA present in the RCA (V_{OVA}^{RAC}):

$$V_{TNA}^{RAC} = V_{NA}^{RAC} + V_{OVA}^{RAC} \quad (3.71)$$

It should be noted that some differences in the final hardened properties of the two mixes can be obtained according to the type of mortar and natural aggregates: it is possible that the quality of recycled aggregates is lower than NA (i.e. higher RM porosity with respect to the new fresh mortar), hence some slight variations in the mechanical properties can be expected. The word slight has in this case a strong meaning: in fact, it is expected that even if the RCA comes from highly deteriorated concrete, the attached mortar could not survive to the crushing processes; hence, the quality of the adhered mortar is not expected to be too worse than the new one.

According to the over-mentioned formula, the quantity of the old natural aggregates inside RAC (V_{OVA}^{RAC}) should be determined. It can be done knowing the residual mortar content (RM) and the bulk specific gravity of OVA in RAC. RM can be determined in a number of ways, e.g. through chemical or thermo-shock methods. The quantity of the old natural aggregates inside RAC (V_{OVA}^{RAC}) is:

$$V_{OVA}^{RAC} = V_{RCA}^{RAC} \cdot (1 - RM) \cdot \frac{SG_b^{RCA}}{SG_b^{OVA}} \quad (3.72)$$

where V_{RCA}^{RAC} is the quantity of RCA inside the RAC mix, SG_b^{RCA} and SG_b^{OVA} are respectively the bulk specific gravity of RCA and OVA . Lastly, the required volumes V (and oven-dried weights W) of RCA and new NA in the RCA concretes can be evaluated as:

$$V_{RCA}^{RAC} = \frac{V_{NA}^{RAC} \cdot (1 - R)}{(1 - RM) \cdot \frac{SG_b^{RCA}}{SG_b^{OVA}}} \quad (3.73)$$

$$V_{NA}^{RAC} = V_{NA}^{NAC} \cdot R \quad (3.74)$$

$$W_{OD-RCA}^{RAC} = V_{RCA}^{RAC} \cdot SG_b^{RCA} \cdot 1000 \quad (3.75)$$

$$W_{OD-NA}^{RAC} = V_{NA}^{RAC} \cdot SG_b^{NA} \cdot 1000 \quad (3.76)$$

When the quantity of aggregates necessary in the RAC mix are properly defined, water, cement and sand content should also be defined. The design starts from the definition of V_{RM}^{RAC} , which can be obtained as:

$$V_{RM}^{RAC} = V_{RCA}^{RAC} \cdot \left(1 - (1 - RMC) \cdot \frac{SG_b^{RCA}}{SG_b^{OVA}} \right) \quad (3.77)$$

Then the quantity of new fresh mortar inside RAC can be calculated (from Eq. 3.69, 3.70 and 3.77):

$$V_{NM}^{RAC} = V_M^{NAC} - V_{RM}^{RAC} \quad (3.78)$$

Now, the quantity of the other components can be obtained by multiplying the ratio of the quantities present in the NAC. The further quantities of water, cement and sand (fine aggregates—oven dried) are expressed in weight.

$$W_w^{RAC} = W_w^{NAC} \cdot \frac{V_{NM}^{RAC}}{V_M^{NAC}} \quad (3.79)$$

$$W_c^{RAC} = W_c^{NAC} \cdot \frac{V_{NM}^{RAC}}{V_M^{NAC}} \quad (3.80)$$

$$W_{OD-FA}^{RAC} = W_{OD-FA}^{NAC} \cdot \frac{V_{NM}^{RAC}}{V_M^{NAC}} \quad (3.81)$$

RCA can hence be designed with the same TM and total NA volumes of the reference mix. If different replacement ratios are used (increasing), it will not result in different (higher) mortar content in RCA concrete compared to the companion NA, on the contrary of what can result if conventional proportioning methods (DVR and DWR) are used.

However, a limit about the application of this method is given by the RMC : its effect determines a higher limit in replacement ratio (upper boundary). This limit is given by the R_{min} value:

$$R_{min} = 1 - \frac{(1 - RMC)}{V_{DR-NA}^{NAC}} \cdot \frac{SG_b^{RCA}}{SG_b^{NA}} \geq 0 \quad (3.82)$$

where V_{DR-NA}^{NAC} is the dry-rodded volume of NA in the NAC mix. Rearranging Eq. 3.82, it is also possible to define a maximum RMC value to design a RAC concrete with a fixed replacement ratio, i.e. fixing that $R = 100\%$, it is possible to determine a quality standard about the residual mortar content of the RCA. This can be obtained with:

$$RMC(\%) = \left[1 - V_{DR-NA}^{NAC} \cdot \frac{SG_b^{NA}}{SG_b^{RCA}} \right] \cdot 100 \quad (3.83)$$

3.5.2 Slump Test Results

Faleschini et al. [46] have studied the influence of the aggregates proportioning method on fresh recycled concrete properties. In terms of slump test, they have reported that the EMV method strongly affects the consistency of the fresh materials, when evaluated with this simple test method.

Several experimental mixes were analyzed varying the w/c ratio, water-reducing admixture (WRA) content, recycled aggregate proportioning method, and coarse aggregate replacement ratio. Concrete mixes were prepared with calcareous sand, limestone and, in the case of RAC, locally available RA in Catalunya (Spain). The RA was composed of 37 % clean aggregate, 59 % aggregate with attached mortar, and 4 % bituminous particles. Aggregates were all produced by crushing, but were not all from the same source. The cement chosen was of CEM I 52.5 R type, and the admixture was a polycarboxylate-based WRA. Table 3.2 lists the main physical properties of both natural and coarse recycled aggregate used.

Twenty mixes were produced and analyzed: 4 conventional concrete mixes, made entirely with natural aggregate; 8 RAC designed by simple replacement of a quantity of NA by RA through DVR method; and 8 RAC designed with the EMV method. The aggregate replacement ratios were 20 and 35 %. WRA content was chosen in order to reach at least an S4 slump class for all concrete samples. Table 3.3 shows the mix design: the first three letters indicate the type of concrete (natural, recycled with DVR, and recycled with EMV method), then the w/c ratio is reported, and lastly the percentage of the WRA on cement weight is reported. Figure 3.13 explains the reason of the increase of the WRA content in the EMV batches: if designed with the same WRA content of the RAC, the slump would result too low, and the fresh concrete could not be analyzed through viscometric measurements as a fluid according to the hypotheses stated in Sect. 3.1

The same casting and mixing procedure and environmental conditions were used for all the analyzed batches. Results in terms of slump, evaluated at 9 min after the first water addition in the batches, are reported in Table 3.4.

The increased WRA content in EMV batches seems to represent a valid solution to allow concretes reaching the same (or similar) slump values. However it has been experimentally recognized by the authors that concretes proportioned with the EMV methods are stiffer than the ones designed following conventional procedures. Accordingly, the authors have analyzed also the rheological behavior through the analysis of Bingham parameters.

Table 3.2 Main physical properties of aggregates used (from [46])

	Absorption (%)	OD specific gravity (kg/m ³)	DR density (kg/m ³)	Mortar content (%)	D _{max} (mm)
Sand	1.3	2677	–	–	4
NA	0.5	2682	1501	–	12.5
RCA	6.3	2292	1288	34.6	12.5

Table 3.3 Mix design of the concrete analyzed (from [46])

	ID	RCA (%)	w/c	Water (kg)	Cement (kg)	Sand (kg)	Gravel (kg)	RCA (kg)	WRA (kg)
BOLOMEY	NAC/0.4-1	0	0.4	182	455	835	1031	0	4.6
	NAC/0.4-1.2	0	0.4	182	455	835	1031	0	5.5
	NAC/0.5-1	0	0.5	182	364	880	1064	0	3.6
	NAC/0.5-1.2	0	0.5	182	364	880	1064	0	4.4
BOLOMEY RAC 20 %	RAC20/0.4-1	20	0.4	182	455	835	794	203	4.6
	RAC20/0.4-1.2	20	0.4	182	455	835	794	203	5.5
	RAC20/0.5-1	20	0.5	182	364	880	820	209	3.6
	RAC20/0.5-1.2	20	0.5	182	364	880	820	209	4.4
BOLOMEY EMV 20 %	EMV20/0.4-1.5	20	0.4	169	422	774	887	227	6.3
	EMV20/0.4-1.7	20	0.4	169	422	774	887	227	7.2
	EMV20/0.5-1	20	0.5	168	336	812	915	234	3.4
	EMV20/0.5-1.2	20	0.5	168	336	812	915	234	4.0
BOLOMEY RAC 35 %	RAC35/0.4-1	35	0.4	182	455	835	633	340	4.6
	RAC35/0.4-1.2	35	0.4	182	455	835	633	340	5.5
	RAC35/0.5-1	35	0.5	182	364	880	649	355	3.6
	RAC35/0.5-1.2	35	0.5	182	364	880	649	355	4.4
BOLOMEY EMV 35 %	EMV35/0.4-1.5	35	0.4	158	395	725	772	407	5.9
	EMV35/0.4-1.7	35	0.4	158	395	725	772	407	6.7
	EMV35/0.5-1.5	35	0.5	156	313	756	793	427	4.7
	EMV35/0.5-1.7	35	0.5	156	313	756	793	427	5.3

3.5.3 Viscometric Results

For evaluating Bingham parameters, about 17 L of fresh concrete were used in a coaxial cylinders viscometer [46], decreasing the rotation speed of the outer cylinder from max. $f_{max} = 0.44$ rps to min. $f_{min} = 0.09$ rps in 7 steps. For each velocity, 50 measures were taken in 3 s; after the 7th step, increased speed was



Fig. 3.13 Left RAC20/0.4-1 %WRA; Right EMV20/0.4-1 %WRA

Table 3.4 Results of slump test

#	Method	w/c	SP (%)	RAC (%)	Slump (mm)
1	NAC	0.4	1	0	210
2	NAC	0.4	1.2	0	210
3	NAC	0.5	1	0	215
4	NAC	0.5	1.2	0	230
5	DVR	0.4	1	20	200
6	DVR	0.4	1.2	20	220
7	DVR	0.4	1	35	206
8	DVR	0.4	1.2	35	210
9	DVR	0.5	1	20	220
10	DVR	0.5	1.2	20	230
11	DVR	0.5	1	35	215
12	DVR	0.5	1.2	35	225
13	EMV	0.4	1.5	20	200
14	EMV	0.4	1.7	20	210
15	EMV	0.4	1.5	35	195
16	EMV	0.4	1.7	35	220
17	EMV	0.5	1	20	200
18	EMV	0.5	1.2	20	215
19	EMV	0.5	1.5	35	190
20	EMV	0.5	1.7	35	190

applied to the outer cylinder, reaching $f_{seg} = 2/3f_{max}$. Between the 50 measures taken for each velocity step, the ten lowest were chosen and averaged to obtain a single value \hat{T} .

Measured torque values \hat{T} and angular velocity Ω were plotted to obtain relative viscosity H (Nm s) and flow resistance G (Nm), to be converted into Bingham

parameters. Linear correlation was evaluated for each test performed, obtaining high values of R^2 ($0.980 \leq R^2 \leq 0.999$), confirming the hypothesis that fresh recycled concrete can be modeled as a Bingham fluid. The results obtained by the authors confirm the observation obtained when performing the slump test: even though the EMV concrete has higher WRA content, it is stiffer than the one design with DVR method. The ability of WRA to reduce yield stress in the same manner for EMV and RAC batches was experimentally observed in all mixes at $w/c = 0.4$. Conversely, the EMV method caused a great increase in plastic viscosity: about this problem, Vázquez et al. (personal communication to the authors) obtained that the use of AEA can overcome this increase, leading to significant workability improvements of EMV batched.

Experimental results, represented in the following rheographs (Figs. 3.14 and 3.15), were expressed in terms of rheological parameters, i.e. Bingham parameters, calculated both neglecting and considering plug flow (see Sects. 3.4.1. and 3.4.2). When τ_0 was too high for full shearing in the gap between the cylinders of the apparatus, large differences were found in the rheological measures computed with the two methods. These discrepancies were generally less than 5 % for both estimated viscosity and yield stress. Instead, in a few cases, plug flow could not be neglected, as it lasted even at higher rotational speeds, i.e., at higher values of the τ_0/μ ratio. Recycled concrete samples produced with the two aggregate proportioning methods clustered into two separated groups, showing significantly different rheological behavior. Recycled samples proportioned with DVR method behaved similarly to traditional mixes; instead, the EMV method gave rise to less fluid concretes, as also confirmed by the slump results (Table 3.4). As expected, the increased WRA content reduced yield stress values in both cases; in particular, for $w/c = 0.4$, the increased WRA content with the EMV method gave equivalent

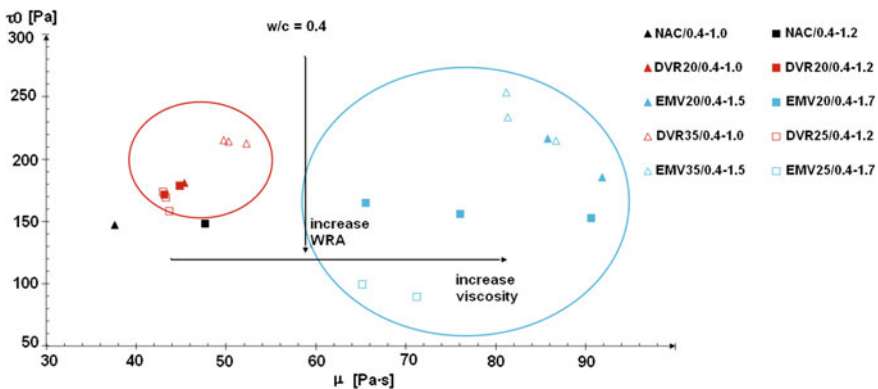


Fig. 3.14 Effect of WRA content, substitution ration and aggregates proportioning method ($w/c = 0.4$)

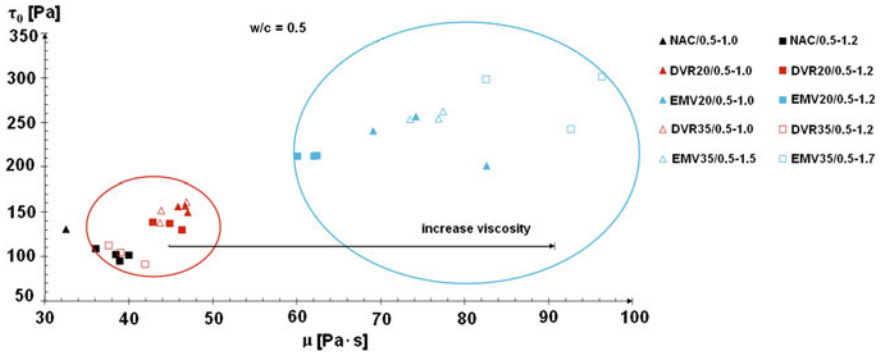


Fig. 3.15 Effect of WRA content, substitution ration and aggregates proportioning method ($w/c = 0.5$)

concretes in terms of yield stress. Comparison of Fig. 3.14 with Fig. 3.15 shows that the higher water content causes a general reduction in both viscosity and yield stress in all mixes.

Gravel migration has been experimentally observed by the authors, mainly in the EMV mixes, with low fresh mortar contents, and this may have partially affected the results. Visual inspections during testing showed that the layer of packed gravel particles close to the outer cylinder was in the range 0–1.5 cm, becoming more solid as the substitution ratio increased. In this case, its influence could not be determined accurately, although Wallevik reported that gravel migration may give rise to under-estimation of yield stress and a poorly defined effect on plastic viscosity estimates [48].

3.5.4 Slump—Yield Stress Relation

Slump value is the result of one of the most simple rheology test: as the Abrams cone is lifted up, the concrete sample flows down under gravity action. As fresh concrete is considered as a yield stress fluid (in this case, a Bingham fluid), it stops flowing downward just when the applied shear stress by the gravity force, becomes less than the yield stress τ_0 . Accordingly, it is expected that yield stress and the slump value are strictly correlated. Several authors attempted to determine a valid equation which relates those two measures. As a consequence a number of equations have been proposed, empirically based on a number of experiments, with the aim to relate the slump, which measurement is simple, to physically-based measures, which evaluation could be done at lab-scale through viscometric tests. Tanigawa et al. [57] proposed a graph which correlates the slump with the yield stress, whereas the relation with the plastic viscosity was less significant, in agreement with the physical interpretation of the phenomenon. Another formulation

was given by Murata and Kukawa [58], who proposed the following equation, where slump is expressed in (mm):

$$\tau_0 = 714 - 473 \cdot \log(S/10) \tag{3.84}$$

Then de Larrard [59] proposed to insert in the equation the specific weight of the concrete sample, arguing that the equation should be governed by the quantity $\tau_0/(g \cdot \rho_{sg})$, where g is gravity and ρ_{sg} is the specific gravity ρ/ρ_{ref} . The reference density is the density of a reference fluid which can be considered the water at 4 °C (hence, $\rho_{ref} = 1000 \text{ kg/m}^3$). Accordingly, in a NIST report, de Larrard with Ferraris

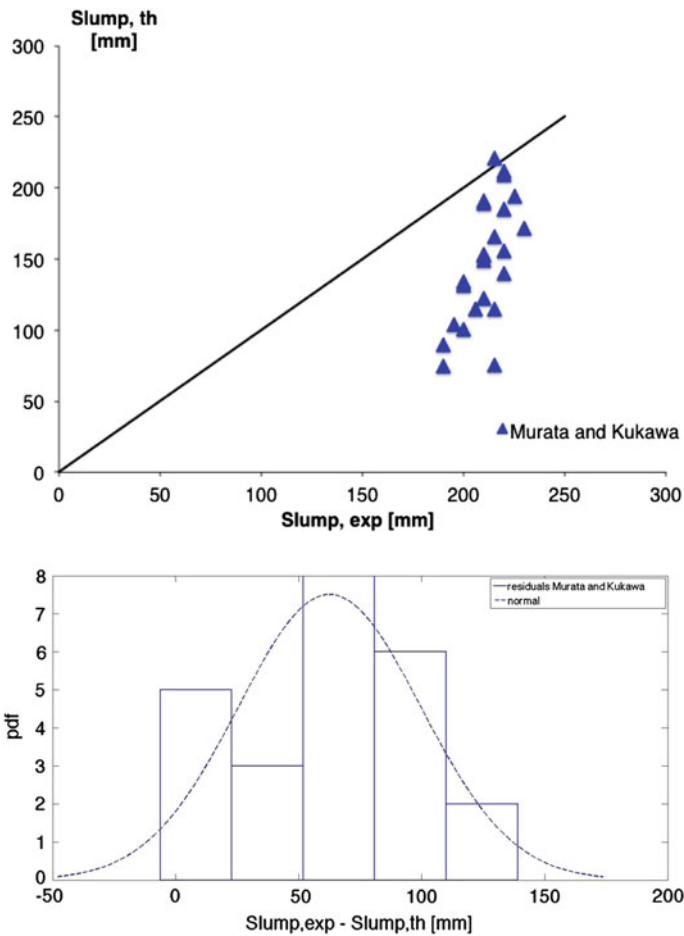


Fig. 3.16 Scatter plot and distribution of residuals of theoretical and experimental slump value according to Murata and Kukawa relation

[60] proposed the following equation, derived using a BTRHEOM viscometer, for ordinary concrete:

$$S = 300 - 0.347 \frac{(\tau_0 - 212)}{\rho_{sg}} \tag{3.85}$$

This equation can be slightly modified to be applied for measurements with a ConTec BML rheometer [60], and it is reported below:

$$S = 300 - 0.416 \frac{(\tau_0 - 394)}{\rho_{sg}} \tag{3.86}$$

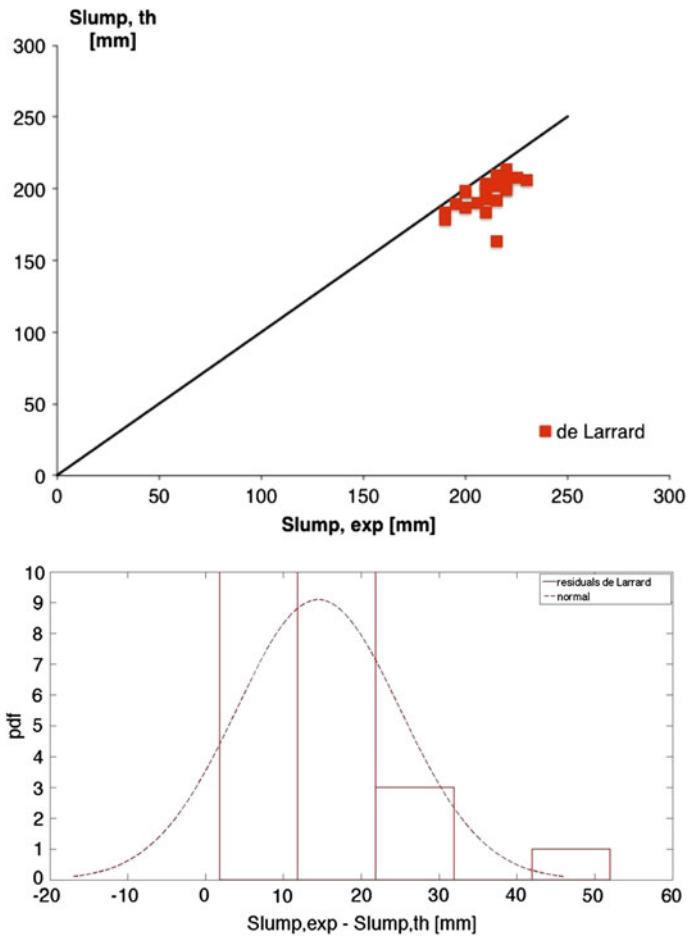


Fig. 3.17 Scatter plot and distribution of residuals of theoretical and experimental slump value according to de Larrard relation

The reason because those equation are different is that those two types of viscometer measure differently yield stress: BTRHEOM gives a higher value of τ_0 than the ConTec BML rheometer. However, the relation between those systems is well-known, and reported also in [47].

The above relations were derived empirically for ordinary concrete and SCC; on the contrary, validation for recycled concrete is still missing. Up to now, a dataset of experimental results is not available due to the scarcity of viscometric measurements of RAC in literature. However, with the available data of [46], and ones communicated by Vázquez (UPC), it was possible to estimate the accuracy of the predicting formulations on a set of recycled aggregates fresh concrete. The equation proposed by de Larrard seems to fit better the experimental results than Murata and Kukawa relation, however still a high dispersion of the results is present (Figs. 3.16 and 3.17).

3.6 Conclusions

Very few experimental results are currently available in literature about the influence of recycled aggregates use in fresh recycled concrete, particularly on fundamental physical parameters, i.e. on Bingham parameters. Fresh recycled concrete can indeed be considered as a Bingham fluid, when the slump value is higher than 80–100 mm. Accordingly, the two Bingham parameters, viscosity μ and yield stress τ_0 can properly describe its rheological behavior.

The aggregates proportioning method greatly affects rheological parameters. In particular, the EMV method strongly reduces slump and thus causes an increase in yield stress. The method also affects plastic viscosity. The increase in WRA content in EMV batches reduces concretes yield stress, but is not sufficient to allow rheological behavior similar to that of RAC, although the same slump values may be reached. In a personal communication, Vázquez has informed the authors that the use of AEA helped in reducing the high plastic viscosity displayed by the EMV concretes.

It should be noted that, when dealing with recycled aggregate concrete, other than with stiff fresh ordinary concretes, two concomitant phenomena may occur during a viscometric measurement, i.e. plug flow and gravel migration. The former may be treated by varying the boundary position when analytically solving the inverse Couette problem for a Bingham fluid. Plug flow generally caused errors of $\pm 5\%$ in both μ and τ_0 ; this error may increase for mixes with high yield stress. Gravel migration mainly occurs in batches characterized by low fresh mortar content, i.e. in fresh concretes proportioned with the EMV method. This phenomenon must be carefully taken into account when analyzing experimental results. In order to reduce the possibility of migration during viscometer measurements, reduced rotational speed applied to the outer cylinder of the apparatus can be applied. This solution may have beneficial effects in lowering the shear rate gradient inside the viscometer.

Concerning the relation between slump and yield stress, no validation has been done for recycled aggregate concretes, due to the scarcity of experimental results, which should be conducted all in the same operational conditions (casting, mixing procedure, humidity and temperature conditions).

Acknowledgments The authors would like to thank Prof. Enric Vázquez, Prof. Marilda Barra, Dr. Diego Aponte and Dr. Cristian Jimenez (UPC, Barcelona) for their collaboration and suggestions.

References

1. Ferraris CF, de Larrard F, Martys N (2001) Fresh concrete rheology: recent developments. In: Mindess S, Skalny J (eds) *Materials science of concrete VI*. The American Ceramic Society, 735 Ceramic Place, Westerville, OH 43081, pp 215–241
2. Feys D, Verhoeven R, De Schutter G (2009) Why is fresh self-compacting concrete shear thickening? *Cem Concr Res* 39:510–523
3. Banfill PFG (2003) The rheology of fresh cement and concrete—a review. In: 11th international cement chemistry congress, Durban, May 2003
4. Hackley V, Ferraris CF (2001) Guide to rheological nomenclature: measurements in ceramic particulate systems. National Institute of Standards and Technology Special Publication 946, 31 pages
5. Bingham EC (1916) An investigation of the laws of plastic flows. *U.S. Bur Stand Bull* 13:309–353
6. de Larrard F, Ferraris CF, Sedran T (1998) Fresh concrete: a Herschel-Bulkley material. *Mater Struct* 31(7):494–498
7. Feys D, Verhoeven R, De Schutter G (2007) Evaluation of time independent rheological models applicable to fresh self-compacting concrete. *Appl Rheol* 17(5):56244.1–56244.10
8. Papo A (1998) Rheological models of cement pastes. *Mater Struct* 21:41–46
9. vom Berg W (1979) Influence of specific surface and concentration of solids upon the flow behavior of cement pastes. *Mag Concr Res* 31:211–216
10. Tattersall GH (1976) *The workability of concrete*. A viewpoint Publication, PCA
11. Atzeni C, Massida L, Sanna U (1985) Comparison between rheological models for Portland cement pastes. *Cem Concr Res* 15:511–519
12. Atzeni C, Massida L, Sanna U (1983) New rheological model for Portland cement pastes, *Il Cemento* 80
13. Yahia A, Khayat KH (2001) Analytical models for estimating yield stress of high-performances pseudoplastic grout. *Cem Concr Res* 31(5):731–738
14. Roussel N, Gram A (eds) (2014) *Simulation of fresh concrete flow*. Springer, Netherlands
15. Krieger IM, Dougherty TJ (1959) A mechanism for Non-Newtonian flow in suspensions of rigid spheres. *Trans Soc Rheol* 31(1):137–152
16. Barnes HA (1997) Thixotropy—a review. *J Non-Newtonian Fluid Mech* 70(1–2):1–33
17. Mewis J (1979) Thixotropy—a general review. *J Non-Newtonian Fluid Mech* 6(1):1–20
18. Wallevik JE (2005) Thixotropic investigation on cement paste: experimental and numerical approach. *J Non-Newtonian Fluid Mech* 132(1–3):86–99
19. Lapasin R, Papo A, Rajgelj S (1983) The phenomenological description of the thixotropic behavior of fresh cement pastes. *Rheol Acta* 22:410–416
20. Bagnold RA (1954) Experiments on a gravity-free dispersion of large solid spheres in a Newtonian fluid under shear. *Proc Roy Soc* 225A:49–63
21. Comité Européen de Normalisation (2009) EN 12350-2:2009—testing fresh concrete. Slump-test, Brussels, Belgium

22. ASTM International (2015) ASTM C143/C143M-15—standard test method for slump of hydraulic-cement concrete. West Conshohocken, PA
23. ASTM International (1992) ASTM C360-92—test method for ball penetration in freshly mixed hydraulic cement concrete (Withdrawn 1999). West Conshohocken, PA
24. Comité Européen de Normalisation (2008) EN 196.3:2005+A1:2008—methods of testing cement. Determination of setting times and soundness. Bruxells, Belgium
25. ASTM International (2013) ASTM C191-13—standard test methods for time of setting of hydraulic cement by Vicat Needle. West Conshohocken, PA
26. ASTM International (2009) ASTM C1362—09—standard test method for flow of freshly mixed hydraulic cement concrete (withdrawn 2014). West Conshohocken, PA
27. Hopkins CJ, Cabrera JG (1985) The turning-tube viscometer: an instrument to measure the flow behavior of cement-pfa pastes. *Mag Concr Res* 37(131):101–106
28. Comité Européen de Normalisation (2009) EN 12350-3:2009—testing fresh concrete. Vebe test, Bruxells, Belgium
29. Comité Européen de Normalisation (2010) EN 12350-10:2010—testing fresh concrete. Self-compacting concrete. L box test. Bruxells, Belgium
30. Comité Européen de Normalisation (2010) EN 12350-12:2010—testing fresh concrete. Self-compacting concrete. J-ring test. Bruxells, Belgium
31. ASTM International (2014) ASTM C1621/C1621M-14, Standard test method for passing ability of self-consolidating concrete by J-Ring, West Conshohocken, PA
32. Comité Européen de Normalisation (2010) EN 12350-19:2010—testing fresh concrete. Self-compacting concrete. V-funnel test. Bruxells, Belgium
33. Ferraris CF, de Larrard F (1998) Modified slump test to measure rheological parameters of fresh concrete. *Cem Concr Aggregates* 20(2):241–247
34. Wallevik OH, Gjrv OE (1990) Development of a coaxial cylinder viscometer for fresh concrete. Chapman and Hall, Hanover, pp 213–224
35. de Larrard F, Hu C, Szitkar JC, Joly M, Claux F, Sedran T (1995) A new rheometer for soft-to-fluid fresh concrete. LCPC internal report
36. Powers TC, Wiler EM (1941) A device for studying the workability of concrete. In: *Proceeding of the ASTM 41, American Society for Testing and Materials, Philadelphia, US*, pp 1003–1015
37. Powers TC (1968) *The properties of fresh concrete*. Wiley, US
38. Tattersall GH, Banfill PFG (1983) *The rheology of fresh concrete*. Pitman Books Limited, Great Britain
39. Wallevik OH (1990) *The rheology of fresh concrete and its application on concrete with and without Silica Fume*. The Norwegian Institute of Technology, Dr. Ing. Thesis no. 1990:45, Trondheim, Norway
40. Wallevik JE (2008) Minimizing end-effects in the coaxial cylinders viscometer: viscoplastic flow inside the ConTec BML viscometer 3. *J Non-Newtonian Fluid Mech* 155:116–123
41. Yeow Y, Ko W, Tang P (2000) Solving the inverse problem of Couette viscometry by Tikhonov regularization. *J Rheol* 44(6):1335–1351
42. Ancey C (2005) Solving the Couette inverse problem using a wavelet-vaguelette decomposition. *J Rheol* 49(2):441–460
43. Reiner M (1949) *Deformation and flow. An elementary introduction to theoretical rheology*. H.K. Lewis & Co. Limited, Great Britain
44. Heirman G, Vandewalle L, Van Gemerta D, Wallevik O (2008) Integration approach of the Couette inverse problem of powder type self-compacting concrete in a wide-gap concentric cylinder rheometer. *J Non-Newtonian Fluid Mech* 150:93–103
45. Heirman G, Hendrickx R, Vandewalle L, Van Gemert D, Feys D, De Schutter G, Desmet B, Vantomme J (2009) Integration approach of the Couette inverse problem of powder type self-compacting concrete in a wide-gap concentric cylinder rheometer. Part II. Influence of mineral additions and chemical admixtures on the shear thickening flow behaviour. *Cem Concr Res* 39:171–181

46. Faleschini F, Jiménez C, Barra M, Aponte D, Vázquez E, Pellegrino C (2014) Rheology of fresh concretes with recycled aggregates. *Constr Build Mater* 73:407–416
47. Ferraris CF, Brower LE (2001) Comparison of concrete rheometers: international tests at LCPC (Nantes, France) in October, 2000. NISTIR 6819
48. Wallevik JE (2003) Rheology of particle suspensions, fresh concrete, Mortar and cement paste with various types of lignosulfonates. Department of Structural Engineering, The Norwegian University of Science and Technology, Ph.D. Thesis, Trondheim, Norway
49. Leighton D, Acrivos A (1987) The shear-induced migration of particles in concentrated suspensions. *J Fluid Mech* 181:415–439
50. Wallevik OH, Wallevik JE (2011) Rheology as a tool in concrete science: the use of rheographs and workability boxes. *Cem Concr Res* 41:1279–1288
51. Fathifazl G, Abbas A, Razaqpur AG, Isgor OB, Fournier B, Foo S (2009) New mixture proportioning method for concrete made with coarse recycled concrete aggregate. *J Mater Civil Eng*: 601–611
52. Knaac AM, Kurama YC (2012) Rheological and mechanical behavior of concrete mixtures with recycled concrete aggregates. In: Structures congress 2012. American Society of Civil Engineers, Chicago (US), pp 2257–2267
53. Knaack AM, Kurama YC (2011) Design of normal strength concrete mixtures with recycled concrete aggregates. In: Structures congress 2011. American Society of Civil Engineers, Las Vegas (US), pp 3068–3079
54. Marinković S, Radonjanin V, Malešev M, Ignjatović I (2010) Comparative environmental assessment of natural and recycled aggregate concrete. *Waste Manage* 30:2255–2264
55. Abbas A, Fathifazl G, Isgor OB, Razaqpur AG, Fournier B, Foo S (2009) Durability of recycled aggregate concrete designed with equivalent mortar volume method. *Cem Concr Res* 39:555–563
56. Jiménez C, Aponte D, Vázquez E, Barra M, Valls S (2013) Equivalent mortar volume (EMV) method for proportioning recycled aggregate concrete: validation under the Spanish context and its adaptation to Bolomey methodology for concrete proportioning. *Mater Construcc* 63(311):341–360
57. Tanigawa Y, Mori H (1989) Analytical study on deformation of fresh concrete. *J Eng Mech* 115(3):493–508
58. Murata J, Kukawa H (1992) Viscosity equation for fresh concrete. *ACI Mater J* 89(3):230–237
59. de Larrard F (1999) Concrete mixture proportioning. A scientific approach. F & FN Spon, New York
60. Ferraris CF, de Larrard F (1998) Testing and modelling of fresh concrete, NISTIR 6094. Gaithersburg, MD, US

Chapter 4

Electric Arc Furnace Slag Concrete

4.1 Introduction

A number of attempts have been made to enhance the re-use of by-products coming from the metallurgical industry in construction materials, with the aim to reduce the high environmental impacts due to the disposal of huge amounts of waste. In this context, the use of Electric Arc Furnace slag (EAF) from carbon steel has been explored from several years, in relation to various civil engineering applications, e.g. in bituminous mixtures [1–3] and as recycled aggregate in concrete [4–6]. As described in Chap. 2, slag properties are generally influenced by the steel production process, and by the quality of steel scraps melted into the furnace; however, some recurrent features in the European EAF slag can be found. EAF slag has a black-color stone appearance, it is very dense with respect to other natural aggregates, it has typically a rough texture and an angular shape (Fig. 4.1). Iron, calcium and silicon oxides are the main constituents of EAF slag, whereas other compounds (magnesium, aluminum, manganese) are present in minor concentrations. The percentages of its components may vary in relation to the steel productive process, thus also affecting some physical properties, e.g. slag density and porosity. Typically the iron oxides content varies between 27–42 % in weight, silicon 10–30 %, aluminum 4–8 %, manganese 2–5 % and magnesium 1.5–5 % [7–9]. Accordingly, specific gravity ranges between 3.3 and 4.0 t/m³ [7, 8, 10].

One of the main problems which may hinder EAF slag application in cement-based products at large scale is related to its possible dimensional instability: in some slag, especially when not pre-treated, high quantities of free lime (CaO) and periclase (MgO) can be present, which can hydrate and determine expansive phenomena. The presence of those compounds may be associated to some impurities in the furnace, which will affect the quality of the slag. A number of studies were focused on this issue, and some pre-treatment operations were demonstrated to be effective in limiting further instability, e.g. through slag weathering and wetting before the use [11].



Fig. 4.1 Electric arc furnace slag vs. siliceous aggregates

The growing interest in identifying sustainable materials for concrete production, the necessity of establishing a correct management of metallurgical slag and the lack of a thorough study on the influence of the substitution ratio between slag and natural aggregates on concrete properties, induce to study this theme in detail. Here the results of some recent experimental campaigns are reported, with the aim of comprehensively understand the effects of including EAF slag on mechanical and durability-related properties of structural concrete. Chemical and microstructural characterization of the materials are analyzed, as well as the evaluation of some concretes properties (both ordinary and high strength concretes), where EAF slag has been used both for replacing coarse and fine aggregates. Also the structural behavior of some reinforced concrete elements casted with EAF concrete is here analyzed.

4.2 EAF Slag Properties

Aggregates constitute more than 60 % in volume of a concrete mixture, and even though they are generally considered as inert filler, they influence the property of the produced concretes, particularly when recycled aggregates are used. Electric arc furnace can be used as both coarse and fine aggregates replacement, after some pre-treatment operations already described in Chap. 2. Here the main relevant properties of the slag are reported.

4.2.1 Physical Properties

Electric arc furnace slag appears as a very dense black stone, characterized by an angular shape, with a rough texture. Its physical properties are highly influenced by

the up-stream production process of steel. However, as reported in Chap. 2, some common features to the slag analyzed in literature, can be obtained: specific gravity ranges between 3.3 and 4.0 t/m³, Los Angeles value is less than 20 %, water absorption is less than 2 % [6–8].

Here the characteristics of the EAF slag supplied by a plant sited in Padova (Italy) are reported, and compared with the ones reported in various experimental campaign collected from literature.

EAF aggregates shape has been analyzed evaluating shape and flakiness indexes, as shown in Table 4.1. The importance of aggregate particles shape is well-recognized, due to its influence on the mechanical behavior, and in particular on the development of bond with cement matrix, and mostly on fresh concrete behavior. With this respect, it is worth noting that concrete is more workable when smooth and rounded aggregates are used. Roundish gravel and sand are generally excellent for providing workable mixtures. On the contrary, crushed stone products have higher surface-to-volume ratio, and they require more cement paste to produce a workable mixture. Differently from natural aggregates, which have generally roundish shape, EAF aggregates, obtained by crushing, screening and other mechanical processes, have a crushed shape, very irregular.

Concerning aggregates texture, it may be either smooth or rough: the former improves workability of the mixtures where they will be used; the latter promotes a better bond between the paste and the aggregates, enhancing the strength in the hardened state. In the case of EAF slag aggregates, the texture is rough.

The density of the aggregates is also another important property, necessary when dealing with the design of concrete. Bulk specific weight (or apparent specific weight) measures the volume that the graded aggregate will occupy in the mix, taking into account the solid aggregates plus the voids between them. For mixture design purposes, the oven dried conditions are generally used to proportion the quantity of aggregates to be used. In case of normal weight aggregates, their apparent specific weight is about 2.7 t/m³; EAF aggregates, on the contrary, can be considered heavyweight (3.3 and 4.0 t/m³).

The moisture content of aggregates is necessary when dealing with the definition of concrete w/c ratio. Accordingly, their absorption capacity should be evaluated, in order to exactly determine the available water content in the mixture. Generally low quality aggregates are characterized by high water absorption, which is higher in the fine fractions due to the increased surface specific area. Typically EAF slag have comparable water absorption with respect to natural aggregates.

Table 4.1 Shape of EAF aggregates (from [12])

Index	(%)
Shape index (4–8 mm)	2.2
Shape index (8–16 mm)	2.7
Shape index (16–22 mm)	1.5
Flakiness index (4–8 mm)	4.4
Flakiness index (8–16 mm)	6.1
Flakiness index (16–22 mm)	3.6

Table 4.2 shows the characterization of three EAF slag (coarse fraction), each being the result of at least three samples, all supplied by the same plant, but in three different years. The properties of the slag seem quite stable in time, hence highlighting that a proper management of the upstream process allows to obtain a quite homogeneous product, at least in terms of physical properties. It should be noted that the lower size of the EAF 3 slag may have influenced the results in terms of water absorption, which is slightly higher than in the other two samples.

Table 4.3 shows instead the physical properties of fine EAF slag, obtained from [13].

The grading (or size distribution) of the aggregates is also very important, as it influences the workability of the produced concrete: the higher is the void space between the particles, the greater amount of cement paste is required to obtain a workable mixture. If particles are well graded, this will improve not only workability but also mechanical strength. Hence, when dealing with a crushed product, as it occurs working with EAF slag, it is necessary to ensure that the aggregates are enough graded, and the processing techniques should be carefully analyzed. For assessing if the required grading is achieved, it is possible to evaluate if the limits of ASTM C33 [14] are respected.

4.2.2 Chemical Composition

The chemical composition of slag is highly influenced by the up-stream processes of steel production, and by the quality of the scrap melted in the electric arc furnace. Steel works influence indeed the quality of the EAF slag in every process step, starting with the selection of input materials, which have the major influence for the chemical slag composition, e.g. different types of scrap and slag formers. It is very important that lime and other slag formers are completely dissolved during melting, because an unbalanced kinetic may potentially lead to the appearance of further expansive compounds in the slag, i.e. free CaO and MgO. Cooling conditions are also very important, with respect not only to dimensional stability, but also with regard to potential leaching of toxic compounds.

Table 4.2 Physical properties of EAF slag (coarse fraction)

	EAF 1 (2009)	EAF 2 (2013)	EAF 3 (2015)
Size (m)	2–22.4	4–22.4	4–16
Apparent specific gravity (t/m^3)	3.64–3.97	3.88–3.90	3.76–3.85
Water absorption (%)	0.18–0.45	0.4–0.5	0.81–0.95
Los Angeles loss (%)	<20	<20	<20

Table 4.3 Physical properties of EAF slag (fine fraction) [13]

	EAF fine
Size (m)	0–4
Apparent specific gravity (t/m^3)	3.78
Water absorption (%)	1.613

The most abundant oxides typically evaluated in EAF slag correspond to Fe_2O_3 , CaO , SiO_2 and Al_2O_3 . A special attention should be paid when analyzing EAF slag composition, with respect to the detection of free lime and magnesia: those compounds are responsible for possible further expansive reactions, which will cause dimensional instability, hindering the use of the slag in construction materials. The above cited pre-treatment operations, consisting in a weathering of about 90 days and water spraying for a couple of days before the use, generally are considered suitable in limiting this risk. More details about this problem are discussed in Chap. 2.

EAF slag is basic, and mainly constituted of crystalline phases, even though less basic than ladle furnace slag (LDF) and basic oxygen furnace slag (BOF). It should be noted that the reactivity of free CaO increases with the basicity, and hence problems of expansion linked to EAF slag seem to be very limited. The crystalline nature of the slag can be also confirmed via the analysis of X-Ray Diffraction (XRD) patterns: wüstite, larnite and gehlenite are some of the main phases present in the slag [4]. The different phases can also be recognized analyzing slag cross-section via Scanning Electron Microscope images, taken in the Back-Scattered mode (SEM-BSE): lighter zones are rich in Fe, whereas the darker in Ca and Si. Figure 4.2 shows for instance in point 1 a solution of (Fe, Mn, Mg)O, structurally close to wüstite (FeO), in point 2 larnite, and point 3, enriched in Cr with Mn, Fe, Al and Mg, is related to magnesiochromite phase.

Concerning leaching potential of toxic compounds, minor components of slag, such as chromium and vanadium, may represent an environmental issue, and hence should be carefully taken into account. On this regard, the CEN/TC 351 is currently taking into considerations problems concerning leaching of granular materials used in civil engineering applications.

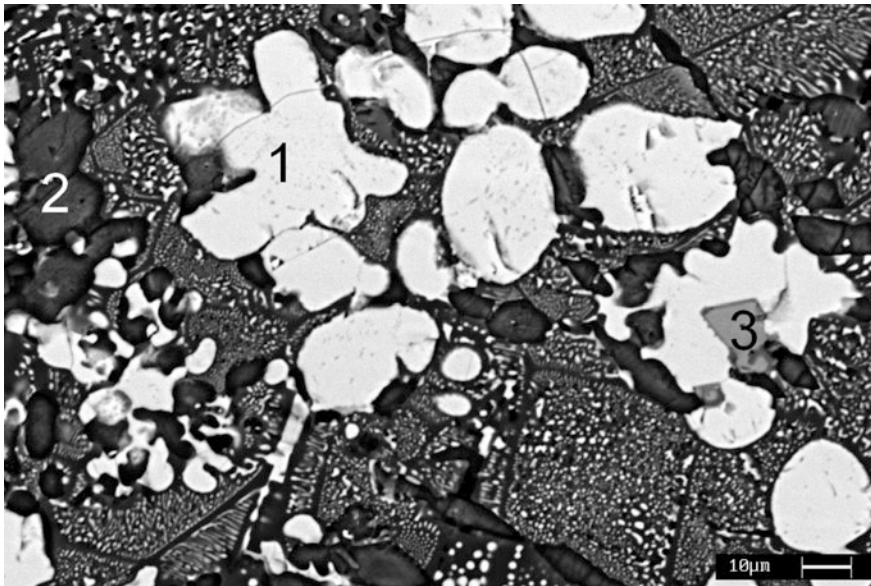


Fig. 4.2 SEM-BSE image of the cross section of the slag aggregate (from [4])

4.3 Ordinary Strength Concrete with EAF Aggregates

Many works reported in literature obtained satisfying results with the use of EAF slag as replacement of coarse natural aggregates. Mechanical properties seem positively affected by the replacement, particularly in terms of compressive and tensile strength. Also the elastic modulus increases. However, workability of EAF concrete suffers for the high water demand of recycled aggregates. Durability-related properties seem similar to the ones of the reference concrete, even in extreme environments, or when accelerate expansion tests are carried out. Some doubts still exist when dealing with the use of the fine fraction of the slag, although its use in limited replacement ratios seems not to affect negatively concrete properties. Here some results collected from literature are discussed, analyzing the effect of the replacement on fresh and hardened concrete properties.

4.3.1 Fresh Concretes Properties

As above cited, the use of slag as recycled aggregates typically affects negatively workability, resulting in concretes with lower slump values, and in some cases, segregation problems. Workability loss can be explained by the physical characteristics of the slag, which is rough and angular, thus increasing the water demand of the mixture. Additionally, if the slag is not well graded, this will affect also the fresh property of the concrete. Concerning instead the segregation phenomenon, this is due to the high specific weight of the slag, and the possible insufficient viscosity of the cement paste, which will participate in causing the migration of the two phases.

Consider now the two following concretes, a reference/control and one made with EAF slag as full replacement of coarse natural aggregates (NA), with aggregates properties listed in Table 4.4.

Table 4.5 shows the mixtures details (per m³): these two concretes are proportioned with the same aggregates grading curve, similar w/c and cement content, to achieve the same target, both in terms of compressive strength and workability. Particularly, the S4 consistency class was the fresh concrete property target. However, the EAF mixture slump was about 16.2 cm, whereas reference concrete slump was 21.2 cm, even though a slight increase in super-plasticizer was given in the former. To prevent this workability loss, the choice of the water-reducing

Table 4.4 Physical properties of aggregates (from [12])

	NA gravel	EAF slag	NA sand
Size (m)	4–31.5	4–22.4	0–4
Apparent specific gravity (t/m ³)	2.72–2.74	3.88–3.90	2.72
Water absorption (%)	0.8–1.16	0.4–0.5	0.8

admixture should be carefully taken into account, as well as the grading curve: EAF slag indeed have fewer fine particles content, and may be not properly graded. Hence, an increase in the fines should be given, through a slight addition of sand or filler.

Consider now the following concretes, a reference/control and five made with EAF slag as partial replacement of coarse and fine natural aggregates, with aggregates properties listed in Table 4.6. Mixture details (per m³) are shown in Table 4.7, whereas aggregates grading curves are shown in Fig. 4.3.

Water/cement ratio slightly varies in the produced mixes, due to the necessity of reaching the same consistency class (S4 slump class also in this case) for all the fresh concretes. A slightly increase in w/c ratio was given with the increase in the recycled fine aggregates content, to take into account the increased water absorption of the EAF fine aggregates than fine NA. Moreover w/c slightly increased in EAF conglomerates with respect to traditional ones also because traditional conglomerate has roundish aggregates whereas EAF slag is more angular and, as a consequence, this implies an expected reduction of workability for the related mixes. Fresh concrete properties, including fresh concrete density and slump, are listed in Table 4.8.

Workability of the produced mixtures is similar for all the mixtures, not experiencing high losses as in the previous example: this was possible due both to the increase in water content and in cement dosage, when using high EAF slag replacement ratio. During production of Mix 5 (containing only recycled aggregates) some difficulties were experienced, because the paste showed a high water demand. Moreover, the air-entrainer admixture (AEA) did not work well in this

Table 4.5 Mixture details (from [12])

	EAF concrete	Reference concrete
Cement (kg)	310	290
Water (kg)	164.3	159.5
w/c	0.53	0.55
EAF slag SSD ^a (kg)	2041	–
NA SSD ^a (kg)	617.24	2098.43
Super-plasticizer (kg)	1.24	1.16
Air entrainer (g)	49.6	46.4

^aSSD = saturated surface dry conditions

Table 4.6 Physical properties of aggregates (from [13])

	NA gravel	EAF slag gravel	NA sand	EAF slag gravel
Size (m)	4–22.4	4–22.4	0–4	0–4
Apparent specific gravity (t/m ³)	2.73	3.85	2.72	3.78
Water absorption (%)	0.75	0.53	0.8	1.613

Table 4.7 Mixture details (from [13])

	Traditional	Mix 1	Mix 2	Mix 3	Mix 4	Mix 5
NA gravel (%)	100	100	100	50	–	–
NA sand (%)	100	50	–	50	50	–
EAF medium/coarse (%)	–	–	–	50	100	100
EAF fine (%)	–	50	100	50	50	100
Cement (kg)	330	335	340	340	350	355
w/c	0.47	0.47	0.49	0.53	0.53	0.55
Total EAF SSD ^a fraction (kg)	–	514	1019	1278	1894	2508
Total NA SSD ^a fraction (kg)	1861	1480	1102	920	456	–
Plasticizer admixture (kg)	1.31	1.33	1.36	1.36	1.39	1.42
Air-entrainer (g)	56	56	56	56	56	56

^aSSD = saturated surface dry conditions

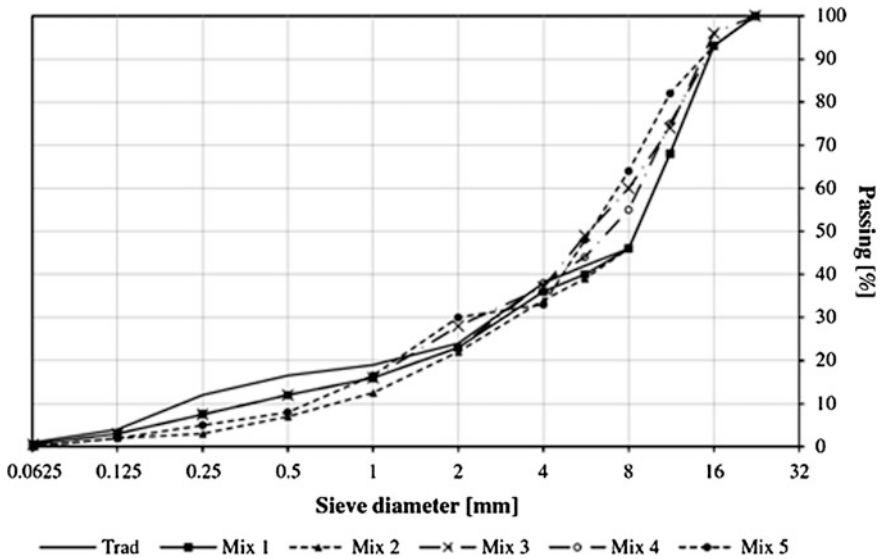


Fig. 4.3 Aggregates grading curves

case, causing the development of great diameter bubbles during concrete placement. It should be noted that, in literature, there are works showing the strong difficulty to produce conglomerates with EAF aggregates only.

Concerning the specific weight of fresh concretes, it is worth noting that in all the cases EAF slag use causes an increase of this parameter, being related to the high density of the slag. Concrete specific weight increases with the replacement ratio.

Table 4.8 Results of the slump test (from [13])

	Trad	Mix 1	Mix 2	Mix 3	Mix 4	Mix 5
Specific weight (kg/m ³)	2530	2660	2850	2830	3000	3190
Slump (cm)	20.0	19.0	20.0	19.5	19.5	18.0

4.3.2 Mechanical Properties

Most of the experimental campaigns conducted in literature agree in observing that the use of EAF slag is responsible for increasing concrete mechanical strength [5–8, 11–13, 15, 16]. This is due to very good physical and mechanical properties of the slag, and also due to the strong bond between the aggregate and the cement matrix which is developed when EAF slag is used.

When EAF slag is used as coarse recycled aggregate, compressive and tensile strength, and elastic modulus increase. Additionally, when performing cyclic loading tests, it is possible to observe an increase in the maximum stress until which the stress-strain curve remains linear, being this limit up to 70 % of f_c in some cases. Arribas et al. [16] have also observed that the quality of the interfacial transition zone (ITZ) is denser and less porous than in conventional concretes, characterized by a singular morphology, which may explain the better bond between aggregates and cement paste. Considering the two concrete mixtures of Table 4.5, the influence of the total replacement of coarse NA with EAF slag can be summarized in Table 4.9: here compressive strength of EAF concrete is almost double than in the natural aggregate concrete (NAC), this occurring already from the first days of hardening. A remarkable result refers also to tensile strength, evaluated with splitting test, due to the better bond between the mixture compounds.

The influence on mechanical properties due to the substitution of fine aggregates is instead more complex, as reported in Table 4.10. Referring to concrete mixtures shown in Table 4.7, mean compressive strengths obtained are similar for traditional and recycled concretes, and for some replacement ratios, they result greater than in the control mix. The failure mode is similar for specimens made with traditional and recycled aggregates, with exception of Mix 2 and, above all, Mix 5, which showed a more brittle behavior. With respect to the tensile strength, the influence of EAF slag also as substituting fine NA is more clear, resulting in higher strength than in reference concrete. Splitting surfaces (Fig. 4.4) in concrete containing EAF slag are less regular than in the traditional mix, in particular when the coarse aggregates are substituted. On the other hand, substitution of fine aggregates may cause a decrease of the mechanical strength, because cement paste becomes less cohesive.

Table 4.9 Mechanical properties of concretes (from [12])

Mix type	Specific weight after 28 days (kg/m ³)	$f_{c,cube}$ 7d (MPa)	$f_{c,cube}$ 28d (MPa)	$f_{ctm, exp}$ (MPa)	$E_{cm, exp}$ (GPa)
EAF slag	3006	48.80	58.30	4.38	40.05
Reference	2447	27.20	34.50	3.54	37.40

Table 4.10 Mechanical properties of concretes (from [13])

	Trad	Mix 1	Mix 2	Mix 3	Mix 4	Mix 5
7 days						
Specific weight (kg/m ³)	2380	2530	2710	2830	2900	3120
f _{cm,cube} (MPa)	37.80	35.30	33.10	37.50	36.00	33.90
28 days						
Specific weight (kg/m ³)	2490	2610	2780	2790	2940	3130
f _{cm,cube} (MPa)	44.63	45.42	44.00	45.23	45.10	41.40
f _{ctm} (MPa)	3.54	3.73	3.62	3.56	4.01	3.76
E _{cm} (GPa)	37.51	37.36	38.68	40.39	40.04	38.47

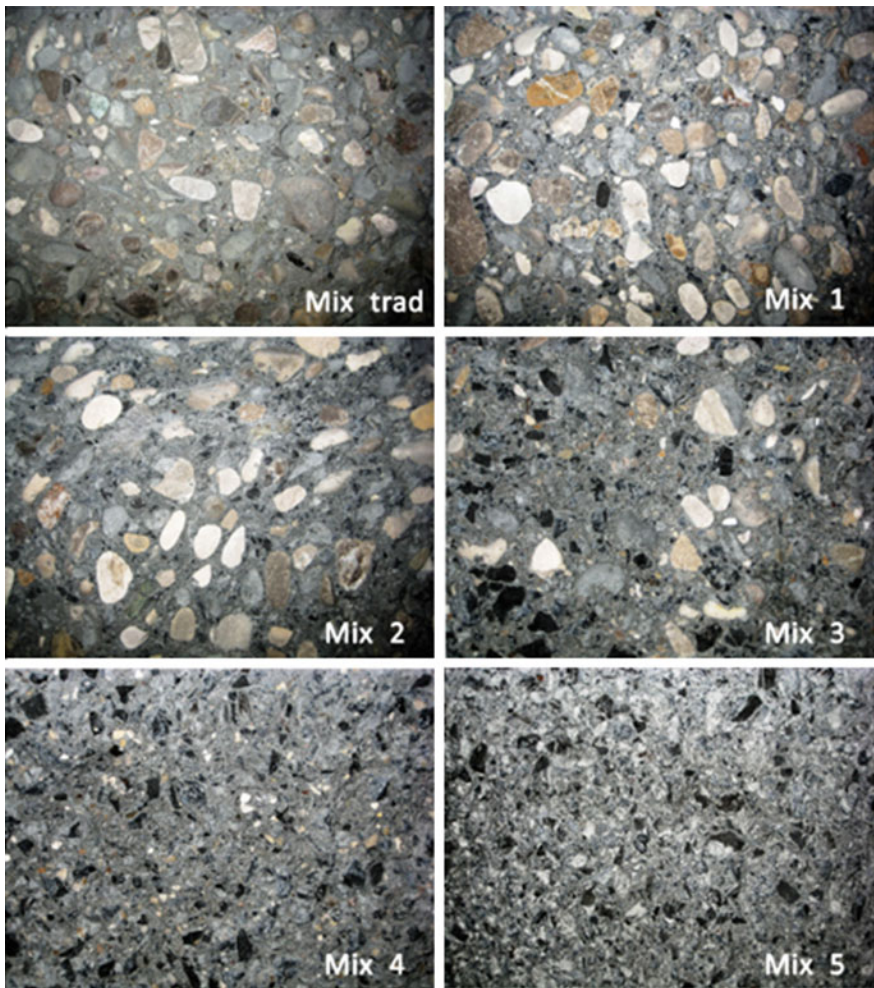


Fig. 4.4 Splitting surfaces of the concretes with EAF slag

Concerning Young modulus results, they are similar for all the concretes and, in most cases, EAF mixtures have greater modulus. The modulus is obtained from cyclic loading of specimens under compressive test, between $f_c/10$ and $f_c/3$. In this range, the stress–strain curve is linear for all the analyzed mixes. However, the fluctuation in experimental values is more evident for the mixes containing high percentage of EAF slag, in particular for the conglomerates with the whole fine part made by recycled aggregate, than for traditional concrete.

4.3.3 Durability-Related Properties

Durability of concretes can be evaluated through a number of test methods, aiming to assess for instance concrete porosity, water absorption, carbonation, etc. Concerning EAF slag, not many works have been carried out analyzing the evolution of their properties when exposed to detrimental agents. Most aspects about durability of this material are still not explored: none or very few works exist about chlorides exposure, carbonation, fire exposure [17, 18].

Here the effect of detrimental environmental conditions is analyzed, both on concretes including only EAF coarse aggregates, and both with coarse and fine recycled aggregates. The analyzed conditions are here reported.

After the 28-days standard maturation, durability tests were performed. Three specimens for each concrete have been subjected to three types of accelerated ageing for periods varying from 25 to 32 days.

The first durability test *D1* investigates the potential expansion of dense graded compacted aggregates, which could induce hydration of free lime (CaO) and periclase (MgO) generally contained in most slag used, leading to consequent volume increase. Wang et al. [19] have indeed reported that, in some cases, EAF slag can contain high levels of expansive compounds, which can hydrate and increase their volume. This problem, typically recognized for BOF slag, may occur when EAF slag are not pretreated. The test follows ASTM D-4792 standard [20]: specimens were completely dipped in a thermostatic tub containing 70 °C water and properly covered to limit evaporation for a total duration of 32 days. A further set of three specimens for each mix was subjected to the same treatment described above, and then exposed to outdoor weathering for 90 days under atmospheric conditions (*D1-2*), with direct sun and rain exposure.

The second accelerated ageing test (*D2*) concerns the investigation of durability of concrete with an alternation of freezing and thawing conditions. Three specimens for each mix were subjected to 25 daily cycles consisting in a first phase with a duration of 18 h in which specimens were frozen at the temperature of -17 °C and a second phase with a duration of 6 h in which they were dipped in 4 °C water.

The last durability test (*D3*) was done on three specimens for each mix; they were subjected to 30 wetting/drying daily cycles. Specimens were dipped for 16 h in potable water at room temperature, and then dried for 8 h in a electric oven at 110 °C. The main objective of these tests is to obtain some elements about the durability of the various mixes, comparing compressive strength after standard and

accelerated ageing, and individuating the conditions that mainly affect the mechanical characteristics of concrete containing such recycled aggregates in time.

Concerning the concretes including EAF slag as coarse only, and also the ones including slag both as fine and coarse aggregates, after the *DI* test, all the specimens, including the traditional ones, showed white powder outcrops. The formation of this type of efflorescence could be assigned to the cementitious matrix hydration, which leads to the formation of a calcium carbonate powder on specimen surfaces. Specific chemical and microstructural analyses were performed to understand the nature of this phenomenon, revealing a composition mainly consisting in calcium, silicon, magnesium, and aluminum oxides (Fig. 4.5). Iron presence was null,

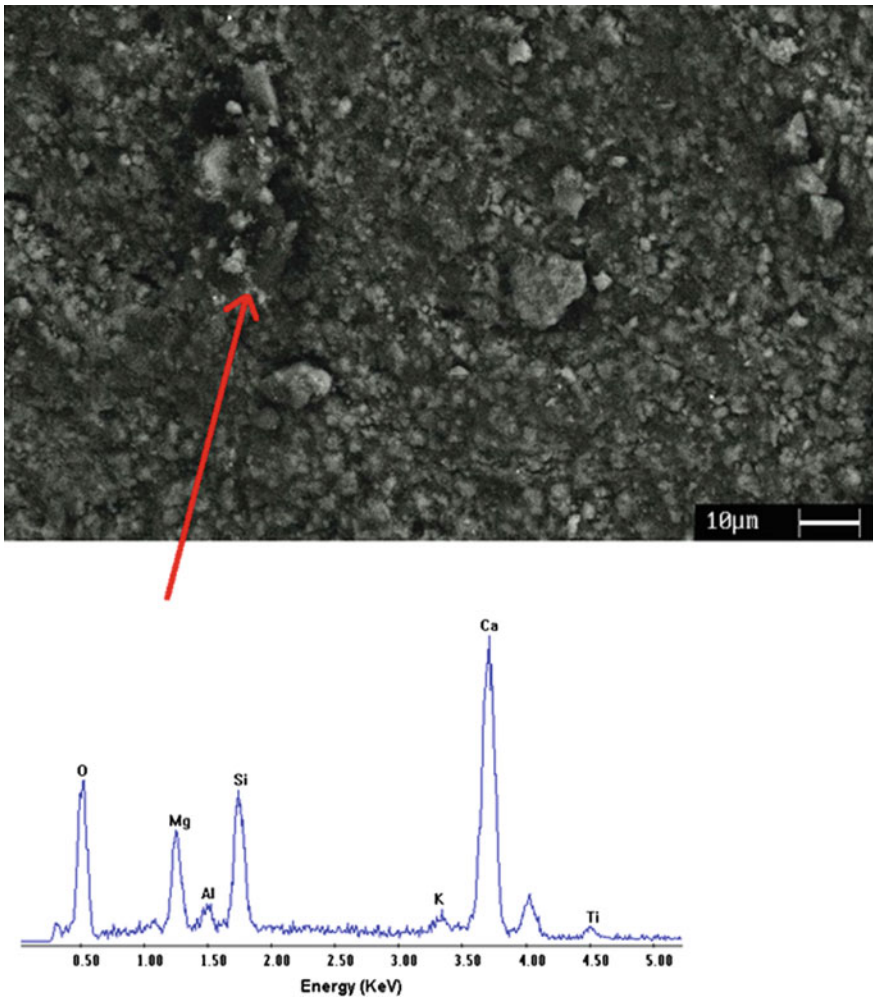


Fig. 4.5 SEM-BSE image of the efflorescence + EDS spectrum

indicating that this material is not connected with EAF slag use, but that it was composed by dissolved salts transported on specimen surface through water evaporation.

Table 4.11 shows the values of mean compressive strength measured after the above durability test for each mix of Table 4.7, compared to the strength after 28 days of natural ageing. All the specimens increased their mechanical strength, even if the treatment in hot water has a worse effect on conglomerates with high content of EAF slag, which were strongly subjected to free oxides hydration and subsequent inner differential micro-expansion. There are no significant differences in specific weight due to this durability test, since the absorption of oxides hydration water only slightly increased the weight of the specimens (the maximum variation is +2.3 %).

Concerning instead the effect of this treatment on concretes including EAF slag as coarse aggregate only, a slight decrease in compressive strength was observed by Pellegrino and Gaddo [8], of about -5 %, whereas the reference concrete displayed an increase of 9 % of strength in the same conditions. The strength loss may be associated to a micro-cracking phenomenon that may occurred as a consequence of a slight expansion of the slag. Both the concretes specific weight increased of about +2 %, as in the case of the former concretes.

A further set of three specimens for each mix produced was subjected to the durability test *D1-2*. Results of concrete mixtures reported in Table 4.7 are shown in Table 4.12: long outdoor weathering is predominant and mitigates the effects of the previous accelerated ageing, allowing a further increase in compressive strength, both in the traditional and experimental conglomerates. Concerning concretes made with only coarse EAF slag, a slight decrease in compressive strength was observed by Pellegrino and Gaddo [8], of about -2 %, whereas the reference concrete displayed an increase of 8 % of strength in the same conditions.

The second accelerated ageing test *D2* concerns the investigation of durability of concrete with an alternation of freezing and thawing conditions. All the specimens passed this test without showing significant surface deteriorations, both in the two types of EAF concretes. This suggests that the AEA admixture potentially contributes to form an air bubble system preventing that a great quantity of water penetrates in concrete pores, and limiting thermal expansion. However, in the case of concrete with only coarse EAF slag, Pellegrino and Gaddo [8] reported a loss of

Table 4.11 Compressive strength in specimens after accelerated ageing for 32 days (from [13])

	28 + 32 days (MPa)	28 days (MPa)	Δ (%)
Mix Trad	51.59	44.63	+13.49
Mix 1	47.02	45.42	+3.39
Mix 2	44.76	44.00	+1.70
Mix 3	50.79	45.23	+10.95
Mix 4	47.52	45.10	+5.10
Mix 5	42.36	41.40	+2.28

Table 4.12 Compressive strength in specimens after accelerated ageing for 32 days plus weathering for 90 days (from [13])

	28 + 32 + 90 days (MPa)	28 days (MPa)	Δ (%)
Mix Trad	54.50	44.63	+18.10
Mix 1	53.85	45.42	+15.65
Mix 2	51.08	44.00	+13.87
Mix 3	56.24	45.23	+19.58
Mix 4	53.19	45.10	+15.21
Mix 5	48.32	41.40	+14.33

about 7 % in compressive strength, whereas the reference mixture's strength was improved by 10 %.

Concerning instead concretes prepared with Table 4.7 dosages, after the freezing and thawing cycles, measured compressive strength values increased with respect to the corresponding before cycles both for traditional specimens and specimens with EAF slag (Table 4.13) probably due to further cement hydration occurred by direct contact with water pushed through the frozen saturated surface micro-porosity, and the natural ageing of the material. Mix 3 and Mix 4 showed a reduced increase in compressive strength with respect to Mix 1 and Mix 2, probably due to their higher water/cement ratio. On the other hand, Mix 5, the one containing recycled material only, showed a significant increase in strength after the cycles. All the specimens showed the same failure mode, with the exception of Mix 2 and Mix 5, showing a more brittle failure than the others (particularly for Mix 5).

The last durability test *D3* has the objective of simulating the behavior of concrete under critical environmental conditions, with intense moisture conditions alternated to drying ones. Mean compressive strength was evaluated at the end of the treatment, and the results are listed in Table 4.14. All the mixes (both traditional and recycled) showed a significant decrease in strength, due to the highly harmful conditions of the test combining both the alternating effect of expansion and contraction due to thermal variation plus that due to inner and surface humidity variation. Surface damages were not observed in any specimens. Nevertheless strength loss could be assigned to some expansion phenomena occurred and to micro-cracking induced by thermal pressure during the test. Moreover, the small

Table 4.13 Compressive strength in specimens after freezing/thawing cycles for 25 days (from [13])

	28 + 25 days (MPa)	28 days (MPa)	Δ (%)
Mix Trad	50.14	44.63	+10.98
Mix 1	51.74	45.42	+12.21
Mix 2	50.36	44.00	+12.63
Mix 3	49.63	45.23	+8.86
Mix 4	48.83	45.10	+7.64
Mix 5	50.50	41.40	+18.03

Table 4.14 Compressive strength in specimens wetting/drying cycles for 30 days (from [13])

	28 + 30 days (MPa)	28 days (MPa)	Δ (%)
Mix Trad	39.24	44.63	-13.74
Mix 1	42.80	45.42	-6.12
Mix 2	41.65	44.00	-6.42
Mix 3	37.86	45.23	-19.48
Mix 4	36.91	45.10	-22.17
Mix 5	37.35	41.40	-10.84

increase in specific weight in all the conglomerates with respect to that measured before the test, could be due to absorption of hydration water, which probably balances the concomitant expansion. Failure mode was similar for all the specimens tested, with the exception of Mix 2 and Mix 5, which showed a more brittle failure, revealing a less cohesive matrix.

The same occurred for concrete with EAF slag as coarse aggregate: the strength loss was about 25 %, whereas only 5 % reduction in compressive strength was observed in the reference concrete [8].

4.3.4 Structural Behavior of RC Beams with EAF Concrete

Very few experimental works have been done analyzing the behavior of real-scale reinforced concrete elements including EAF slag. Pellegrino and Faleschini [12] studied the flexural behavior of reinforced concrete beams casted with EAF concrete under four point bending test. Kim et al. [21] have investigated the structural performance of spirally confined concrete, obtaining that the confined EAF concrete was characterized by enhanced ductility when high confinement ratio was used. In both the cases only EAF coarse aggregates have been used; particularly, the properties of the concretes used to cast the above beams are reported in Table 4.9. Here a brief review of the results obtained in [12] is reported.

Twelve RC beams have been casted with the following dimensions: width $w = 185$ mm; height $h = 300$ mm; length $l = 2000$ mm; effective depth $d = 270$ mm; and shear span $a = 750$ mm. The beams have been designed for obtaining bending or shear failure and were divided in four typologies, according to their steel reinforcement configuration.

For each failure type, one specimen has been tested with traditional concrete, and two with concrete containing slag as aggregate. Geometrical characteristics of the cross sections of the beams are illustrated in Fig. 4.6. Reinforcement steel has a mean yield strength of 535 MPa, and a mean ultimate strength of 650 MPa. For type A beams, the detailed disposition of steel reinforcement is shown in Fig. 4.7.

Two different typologies of beams have been designed to obtain flexural failure: the first has a low steel reinforcement ratio (type A1: three bars with 10 mm

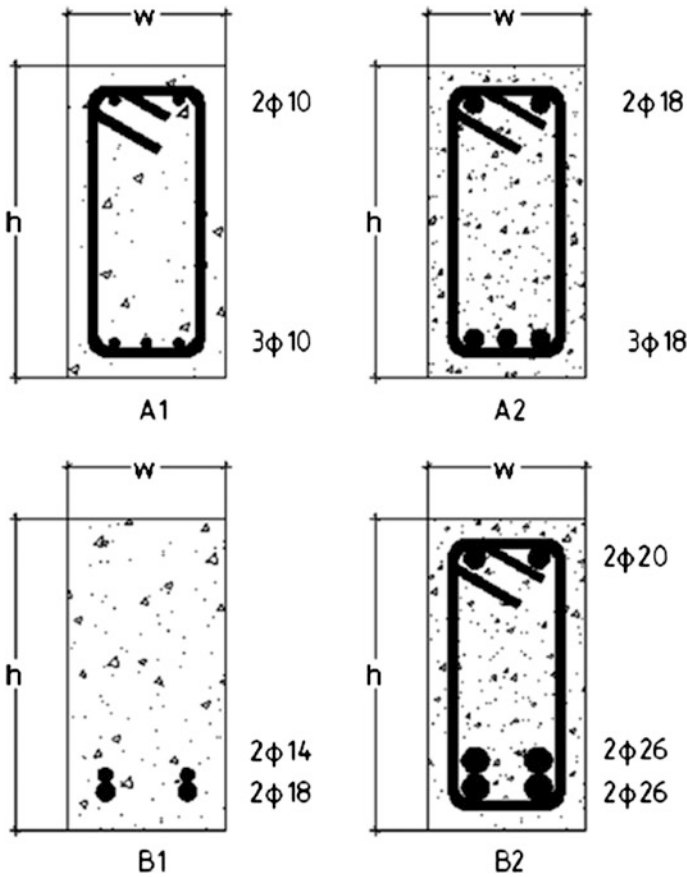


Fig. 4.6 Disposition of steel reinforcement in the cross-section of the beams (from [12])

diameter at the tensile side; steel reinforcement ratio $\rho = \frac{A_w}{bd} = 0.157\%$), whereas the second has a high reinforcement ratio (type A2: three bars with 18 mm diameter at the tensile side $\rho = \frac{A_w}{bd} = 1.527\%$). Two steel reinforcement ratios have been adopted to obtain flexural failures with different levels of ductility. Deflection has been measured at midspan by using ± 0.01 mm precision linear variable differential transducers (LVDTs). Cracks widths have been measured by using ± 0.001 mm precision deformation transducers.

Two different typologies of beams have been designed to obtain a shear failure: the first without shear reinforcement, and the second with stirrups. The first type has been designed with the aim of obtaining shear capacity due to concrete only. It was necessary to provide a very high longitudinal reinforcement ratio in both beams to prevent bending failure ratio $\rho = \frac{A_w}{bd} = 1.634\%$ in B1 beams; $\rho = \frac{A_w}{bd} = 3.62\%$ in B2 beams).

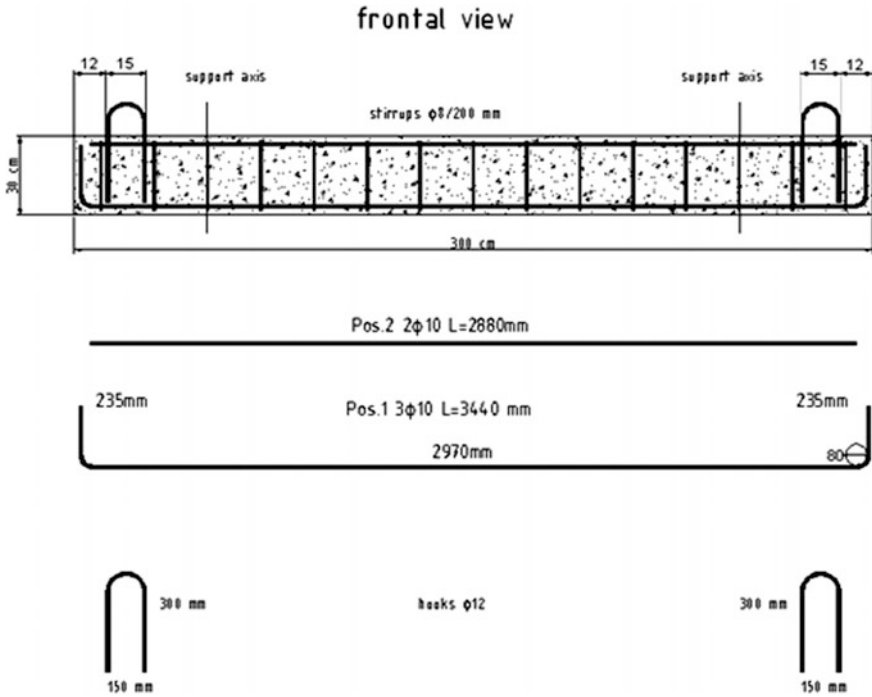


Fig. 4.7 Disposition of steel reinforcement in type A beams (from [12])

Table 4.15 shows the main experimental results for the beams failing in bending, namely the A1 and A2 types. Average mechanical properties and unit safety coefficients have been assumed to compare theoretical and experimental results in this work.

Load-versus-deflection diagrams are illustrated in Fig. 4.8 and load-versus-crack width diagrams are shown in Fig. 4.9. An increase of ultimate flexural capacity is observed for all the beams with EAF slag with respect to beams with traditional aggregates; furthermore, no significant difference in structural behavior in terms of cracking pattern and failure mode is noted. Ultimate capacity and first cracking moment are higher and crack widths are smaller for the beams with recycled

Table 4.15 Experimental and theoretical results in terms of ultimate load P_{ult} and deflection f_{ult} . (from [12])

Beam	Mix type	$P_{ult,th}$ (kN)	$P_{ult,exp}$ (kN)	f_{ult} (mm)
A1_1	Reference	85.25	82.37	36.7
A1_2	With EAF	88.66	89.85	26.17
A1_3	With EAF	88.66	82.88	33.57
A2_1	Reference	262.24	274.46	15.95
A2_2	With EAF	269.30	304.28	16.09
A2_3	With EAF	269.30	294.06	18.63

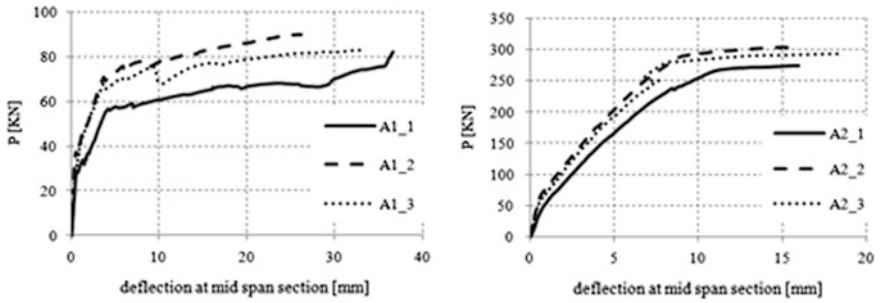


Fig. 4.8 Load versus deflection at midspan diagrams for type A beams (from [12])

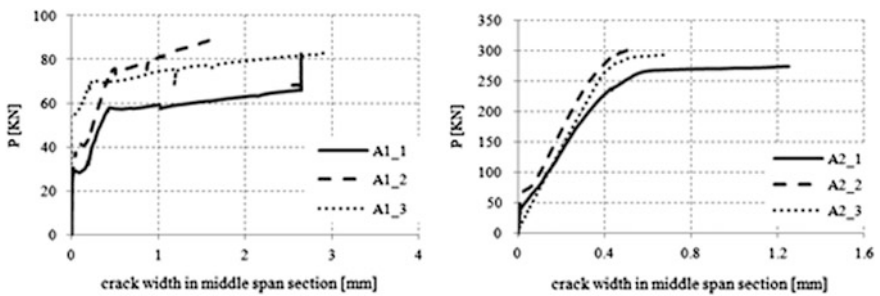


Fig. 4.9 Load versus crack width diagrams for type A beams (from [12])

concrete due to a combination of factors: slightly higher cement content; slightly lower w/c; higher tensile strength of EAF slag; and higher cohesion in the matrix in beams containing EAF slag with respect to those made with traditional concrete. As cited in Sect. 4.2.1, aggregates with angular sharp edges can improve the cohesion of concrete matrix because of the good abrasion properties due to rough surface and porosity. This phenomenon is observed both in RC beams with low and high reinforcement ratios. Cracks patterns were obtained for all the RC elements tested, and they are represented in Fig. 4.10, and shown in Figs. 4.11 and 4.12, where cracking and crushing can be seen.

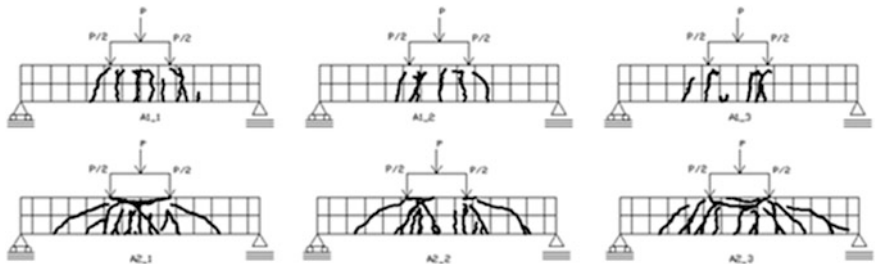


Fig. 4.10 Crack patterns in RC structural elements after bending failure (from [12])

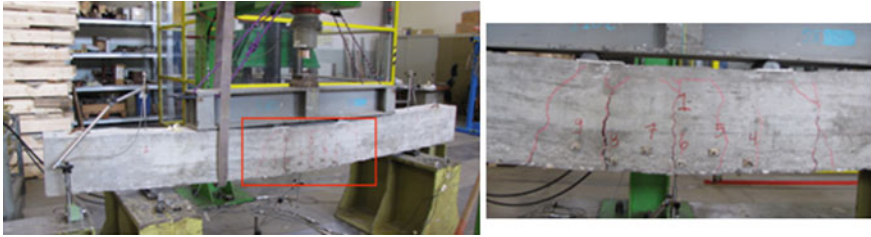


Fig. 4.11 Bending failure: concrete cracking in A1 beams



Fig. 4.12 Bending failure: concrete crushing in A2 beams

Table 4.16 shows the main experimental results for the beams failing in shear, namely the B1 and B2 types. Average mechanical properties and unit safety coefficients have been assumed to compare theoretical and experimental results in this work. Eurocode 2 formula was used to calculate theoretical values of ultimate load, both for elements with and without shear reinforcement. In the beams failing in shear, the typical failure with development of diagonal cracks was observed. Particularly for B1 elements (without shear reinforcement), the experimental ultimate load was significantly higher than the theoretical one, both for traditional and recycled concrete.

Load-versus-deflection diagrams are shown in Fig. 4.13 and load versus crack width diagrams in Fig. 4.14. The ultimate shear capacity was higher in members

Table 4.16 Experimental and theoretical (from [12])

Beam	Mix type	$P_{ult,th}$ (kN)	$P_{ult,exp}$ (kN)	f_{ult} (mm)
B1_1	Reference	108.04	180.44	8.65
B1_2	With EAF	135.22	205.90	5.27
B1_3	With EAF	135.22	198.06	7.23
B2_1	Reference	326.57	350.54	9.40
B2_2	With EAF	326.57	428.15	9.16
B2_3	With EAF	326.57	378.62	7.48

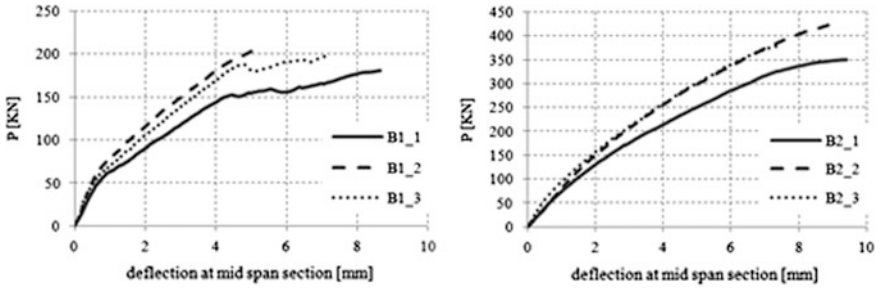


Fig. 4.13 Load versus deflection at midspan diagrams for type B beams (from [12])

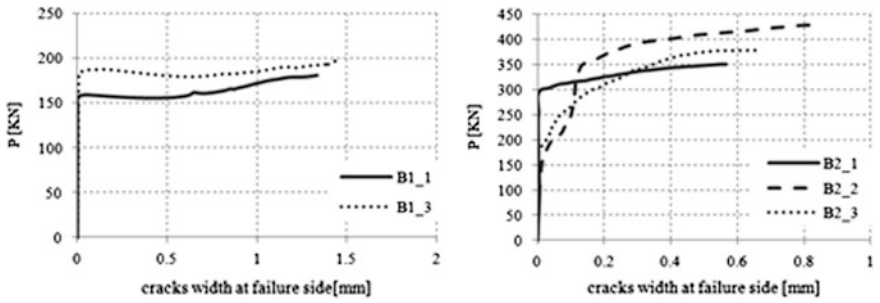


Fig. 4.14 Load versus crack width diagrams for type B beams (from [12])

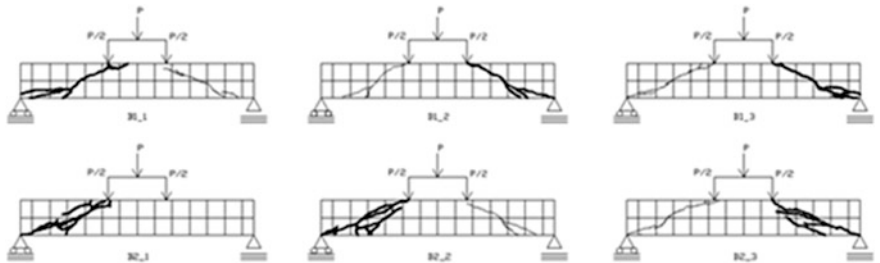


Fig. 4.15 Crack patterns in RC structural elements after shear failure (from [12])

containing slag with respect to those made with NAC, again probably due to the higher cohesion of matrix containing slag. In Fig. 4.15 crack patterns at failure are shown. In all the cases, including the specimens with EAF concrete, the main crack direction is that from the bearing axis to the point of application of the load (Fig. 4.16).



Fig. 4.16 Shear failure in B2 beams

4.4 High Strength Concrete with EAF Aggregates

The quality of the aggregates influences concrete properties, and their characteristics are particularly important when dealing with high-performance concrete (HPC), characterized by a significant improvement of many properties with respect to ordinary concrete (OC), i.e. higher mechanical strength, better workability and durability. In this case, the use of recycled old concrete aggregates (from C&DW) is mostly not recommended in HPC design, due to their high absorption capacity, unstable property and weak strength [22, 23]. Also the current Codes and regulations prevent their use in concretes with high strength class (see Chap. 2). However, the reuse of electric arc furnace (EAF) slag, may represent a key solution to achieve both the sustainability and mechanical/durability performances' goals.

The use of HPC in the construction of important civil engineering applications, e.g. high-rise buildings and long-span bridges, is regulated by several Codes and Guidelines [24, 25]. Generally HPC mixtures include high quantity of binders, a certain dosage of supplementary cementing materials, e.g. fly ash or silica fume, and are characterized by very low water/binder ratios, usually ranging between 0.2 and 0.4. This is due to the necessity of producing a very dense material, characterized by low permeability which enhances concrete strength and durability. High dosages of super-plasticizers are typically adopted in HPC mix, to achieve the required workability with the constraint of having low water content. Concerning the aggregates, they should be strong, typically with crushed shape, and durable: their stiffness and strength should be comparable to the paste.

Here some recent results about HPC concrete made with EAF slag are summarized: it is worth to be noted that, to the knowledge of the authors, only coarse aggregates have been used up to now, achieving this target. However, several research groups are working currently to increase the substitution ratio, with the aim to obtain a full replacement of the natural aggregates with slag, including fine fraction, for producing HPC. With this regard, an initiative between several European research groups, including University of Thessaloniki (GR), University of Burgos (ES), University of the Basque Country (ES) and University of Padova (IT), is currently active, with the aim of establishing new pre-normative standards

about use of EAF slag as aggregate for building materials. Particular attention is currently paid to quality assurance of slag pretreatment processes, durability-related aspects of EAF concrete, and development of HPC with enhanced properties in terms of workability (self-compacting concrete), strength (high strength concrete) and permeability (for radiation shielding).

4.4.1 Fresh and Hardened Concrete Properties

As previously said, HPC mixtures are characterized by reduced w/c ratio, high cement dosages, and possibly, by the use of mineral additions. The aggregates grading should also be studied, to allow concrete to be designed with a compact curve.

Here some tentative mixtures for HPC design including EAF concretes as coarse aggregates are reported (Table 4.17): HPC mixtures are the ones proportioned using w/c = 0.4, whereas for the others, the strength target lies in ordinary strength classes. Note that the w/c ratio used represents the upper boundary of the above limit (0.2–0.4) to produce HPC, and that no mineral additions are used. Concerning the cement dosage, a relatively low cement content is here used (400 and 350 kg/m³), with respect to typical HPC design. Cement type is Ordinary Portland cement CEM I 52.5 R, to achieve high strength. Natural aggregates are siliceous, whereas two sizes of EAF slag have been used to allow the concrete to have a proper grading. Conventional method for design concrete is used (Direct Volume Replacement method), and Bolomey grading curve was used. The inclusion of mineral additions, e.g. silica fume, fly ash or granulated blast furnace slag, results in significant strength improvement only when very low water/binder ratios are used, i.e. with w/b < 0.3.

In the following table (Table 4.18), the control mixtures are reported, to be compared with the EAF ones.

Concerning concretes fresh property, as occurs with ordinary strength concretes, also in case of HPC the water demand increases when EAF slag is used. In the cases

Table 4.17 Mix details for HPC and OPC design with EAF slag referring to 1 m³ of concrete (from [4])

	w/c	Water (kg)	Cement (kg)	NA Sand (kg)	EAF slag (kg)	SP ^a (%)
E400-0.4	0.4	160	400	1020	1190	1.45
E400-0.45	0.45	180	400	994	1148	1.2
E400-0.5	0.5	200	400	965	1115	1.0
E350-0.4	0.4	140	350	1067	1245	1.2
E350-0.45	0.45	157.5	350	1029	1200	1.0
E350-0.5	0.5	175	350	1014	1171	0.8

^aExpressed in cement weight percentage

Table 4.18 Mix details natural aggregates concrete referring to 1 m³ of concrete (from [4])

	w/c	Water (kg)	Cement (kg)	NA Sand (kg)	NA Gravel (kg)	SP ^a (%)
C400-0.4	0.4	160	400	836	1020	1.2
C400-0.45	0.45	180	400	812	992	1.0
C400-0.5	0.5	200	400	789	963	0.8

^aExpressed in cement weight percentage

when the w/c ratio is low, it is necessary to increase the content of the super-plasticizer admixture (note that about +0.2 % of SP was used in the concretes denoted with E400), but attention should be paid to prevent aggregates segregation problems. A slight increase in the fine particles content may be useful to allow the fresh concrete to be more workable (here a slight increase in the sand content was given in the EAF concretes to account for the difference in shape and texture of the slag; filler can alternatively be used). Results are listed in Table 4.19: for the concretes designed with the lower w/c ratio it was not possible to achieve the same slump of NAC, whereas when the w/c is higher, the control of the workability is easier. However, as analyzed in details in Chap. 3, two concretes having the same slump, do not have necessarily the same fresh concrete properties, but only the yield stress (Bingham parameter) should be similar. In this case, it is expected that EAF concrete is characterized by a high viscosity, because during casting it generally displays a stiffer behavior than natural concrete, especially when low w/c are used. Accordingly, also the choice of water-reducing agent and viscosity modifying admixtures may be useful to allow EAF concrete to reach the required workability.

Concerning concrete density, the use of EAF slag determines an increase in specific weight, which is more remarkable in the low w/c ratio mixtures.

A relevant improvement in the compressive and tensile strength, and in elastic modulus, is obtained when EAF slag replaces the coarse natural aggregates, as already obtained in ordinary strength concretes. It is worth noting that, with this mixture proportion, including limited quantity of cement content with respect to typical HPC dosages (generally higher than 500 kg/m³), without any mineral additions and high w/c ratio, the high-strength target can be achieved. The strength

Table 4.19 Fresh properties of HPC and OPC concretes with EAF slag (from [4])

	Density (kg/m ³)	Slump (cm)
C400-0.4	2447	21
C400-0.45	2388	18
C400-0.5	2394	21
E400-0.4	2835	17
E400-0.45	2795	21
E400-0.5	2751	21
E350-0.4	2846	17
E350-0.45	2758	18
E350-0.5	2751	21

target of C50/60 (considered as the limit between HPC and OPC) for the concretes designed with the lower w/c ratio has been achieved by almost all the EAF-concretes, including the ones with the higher w/c. This does not occur for conventional mixes with high w/c, being the strength affected by the water content and the poorer quality of the aggregates (Fig. 4.17).

Compressive failure occurs in all the cases in the cement paste and between the paste and the aggregates in the EAF mixtures; on the contrary, in conventional concretes, failure occurs in cement paste and interface in the high w/c mixtures, whereas in C400 mixture, with 400 kg/m^3 of cement, also some natural siliceous aggregates failed. Strength increase is ranging between +35 to +45 %, depending on the mixture; no significant differences are displayed between E400 and E350 mixes with the same w/c ratio, in terms of compressive strength and elastic modulus, even with a cement reduction of 50 kg/m^3 in the latter. Cement content reduction may be balanced with the increase of aggregate content and with the lower absolute water content per cubic meter of concrete inside the mixture (-12.5 %).

The increase in tensile strength is higher than in OPC, due to the more quantity of available paste that allows a very strong bond between aggregates and cement matrix (Fig. 4.18). With this regard, Fig. 4.19 shows the splitting failure of two HPC mixtures, C400-0.4 concrete ($f_{ct} = 3.75 \text{ MPa}$), and E350-0.4 ($f_{ct} = 4.91 \text{ MPa}$): it seems that, in the latter, there is a compenetration of the cement paste into the surface porosity of the EAF aggregate, thus enhancing the bond between them.

Also the secant modulus of elasticity is higher for the EAF concretes, due to the higher strength and density of the slag with respect to NA: particularly, the stress-strain curve under a uniaxial cyclic loading, remains linear up to the 70 % of the maximum load. Figure 4.20 shows the results in terms of elastic modulus.

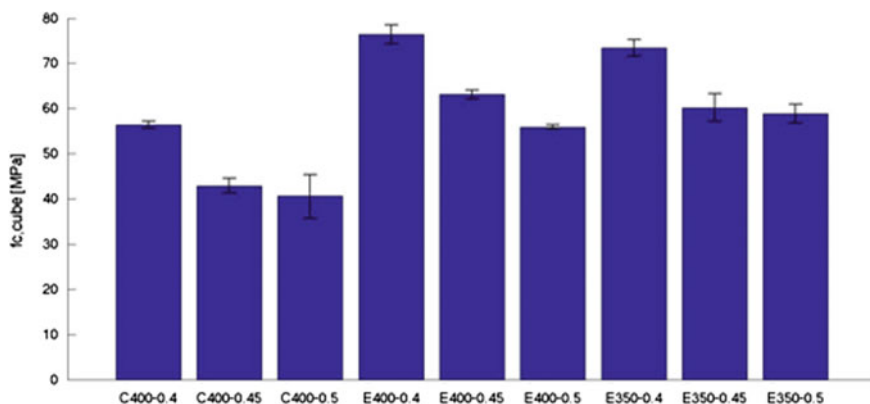


Fig. 4.17 Cubic compressive strength of the examined concretes

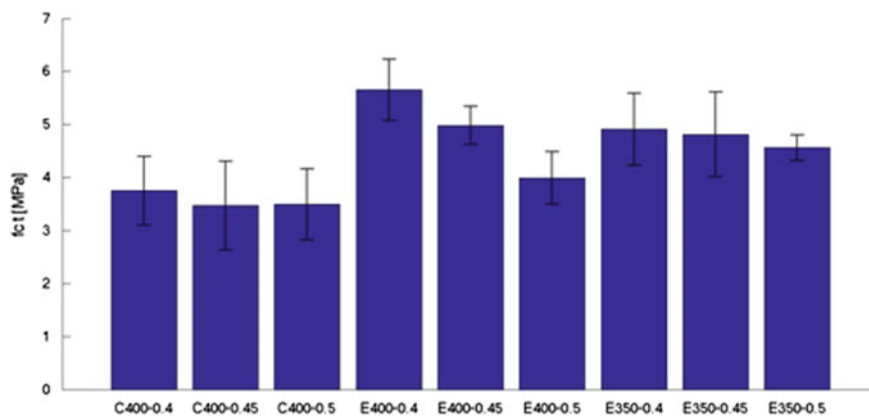


Fig. 4.18 Tensile strength of the examined concretes

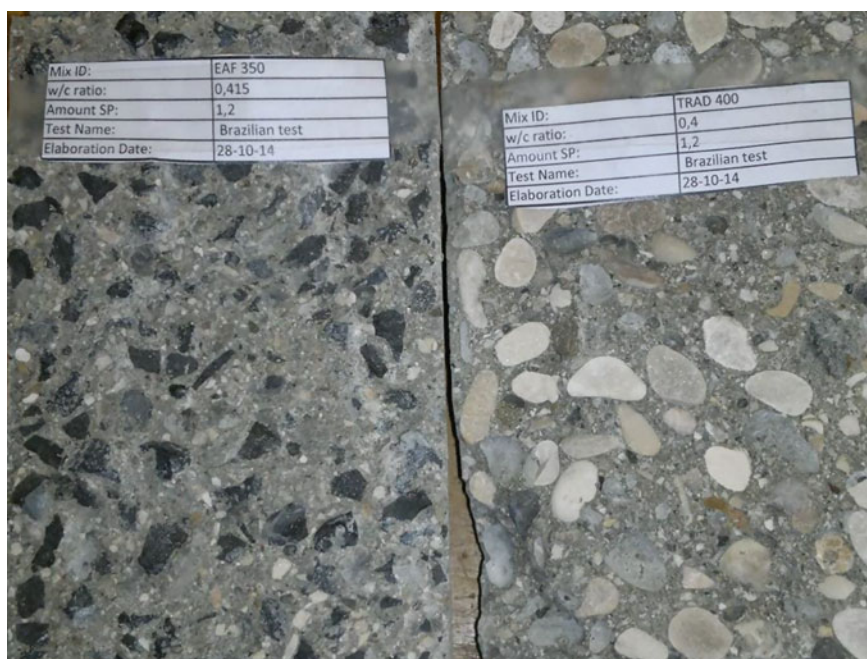


Fig. 4.19 Splitting failures of two HPC concretes

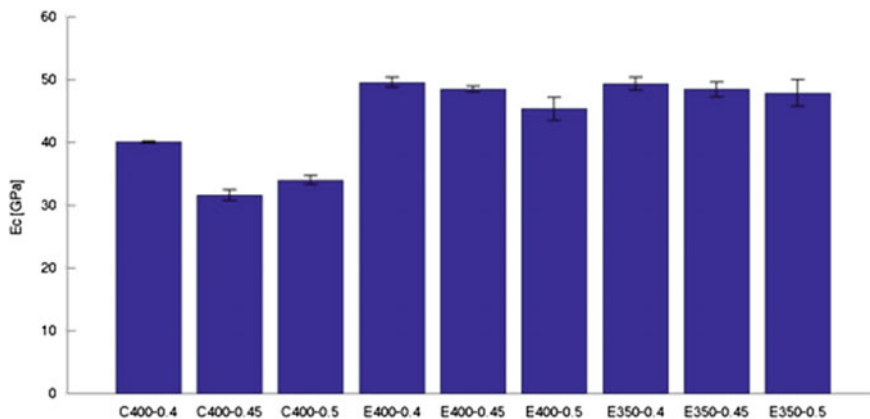


Fig. 4.20 Elastic modulus of the examined concretes (from [4])

4.4.2 Durability-Related Concrete Properties

Durability of EAF slag concrete has been not analyzed widely in literature, not only for ordinary strength concretes, but also for HPC. In this case no data are available about the exposure in detrimental environments, i.e. when HPC is exposed to wetting/drying, freezing/thawing conditions, or when accelerate ageing tests are conducted. The reduced permeability and enhanced strength may induce to think that durability properties are improved in these environment, but it should be carefully taken into account that long-term expansion, due e.g. to thermal pressure applied in cyclic drying/wetting conditions, may occur. Also the fire behavior of HPC with EAF slag should be analyzed, being typically HPC potentially subjected to spalling, and in case of slag, some compounds may change phases during heating, causing micro-cracking and altering the bond between slag and cement paste.

However, it should be recalled that HPC with EAF slag has a very low permeability, and this could improve the durability properties of the material when exposed to carbonation and/or chlorides environment. Also its water absorption should be very low. About this regard very few experimental data are available, however some recent results about resistance of HPC with EAF slag against chlorides penetration have been reported in literature [17].

The diffusion coefficient D is the key parameter generally used for describing concrete durability, often used to predict RC structures service life. The normative NT Build 443 [26] can be used to evaluate the determination of the chlorides profile inside a concrete specimen, after a standard maturation of 28 days and possibly other 90 days should be waited to reduce possible further hydration. After curing, the cylindrical specimens (with typical dimension used for compressive strength evaluation) can be cut in two halves perpendicularly to cylinder axis, obtaining final test specimens with $h = 100$ (or 150) mm approximately. Then specimens should be immersed in a saturated $\text{Ca}(\text{OH})_2$ solution at about 23° , to minimize leaching

during the diffusion test. Specimens' surfaces should be then coated with an impermeable layer, except for the freshly sawn surface that should be in contact with the NaCl solution. After saturation, the samples can be immersed in an aqueous NaCl solution, with the required concentration.

Typically at least two exposure times in the NaCl water tank should be done, varying between 28 and 365 days. After the exposure to the NaCl solution, samples should be splitted into two pieces, perpendicularly to the exposed surface. A sole 0.1 M AgNO₃ [27, 28] aqueous solution is typically used for colorimetric test to highlight the penetration depth of chlorides. It should be sprayed in the freshly split sections: the chloride-exposed zone reacts, assuming a lighter color (light-grey or white) with respect to the chloride-free zone, which remains darker (dark-grey or black). The colors observed can vary depending on the chloride content and the mix composition: the borderline between chloride-contaminated and chloride-free zones is clearly visible in approximately 15 min, and the average free chloride penetration depth x_d related to the time t can be obtained, through the measure of the distance between the exposed surface and the borderline. To avoid border effects, depth readings should not be taken in the zone within about 10 mm from specimen edges.

In the case of EAF slag concrete, for both conventional and EAF HPC concretes, the chloride-free zone turned into a dark brown color (darker for EAF concrete), whereas the chloride-affected zone in the EAF case turned into a bluish-grey color, compared with the purple of the conventional specimens, according to [17]. This can be seen in Fig. 4.21, whereas the apparent diffusion coefficients, evaluated through the fitting of the experimental results with Fick second law are show in Table 4.20. Typically values of D_{app} for OPC range between 66.2 and 293.3 mm²/year, and for

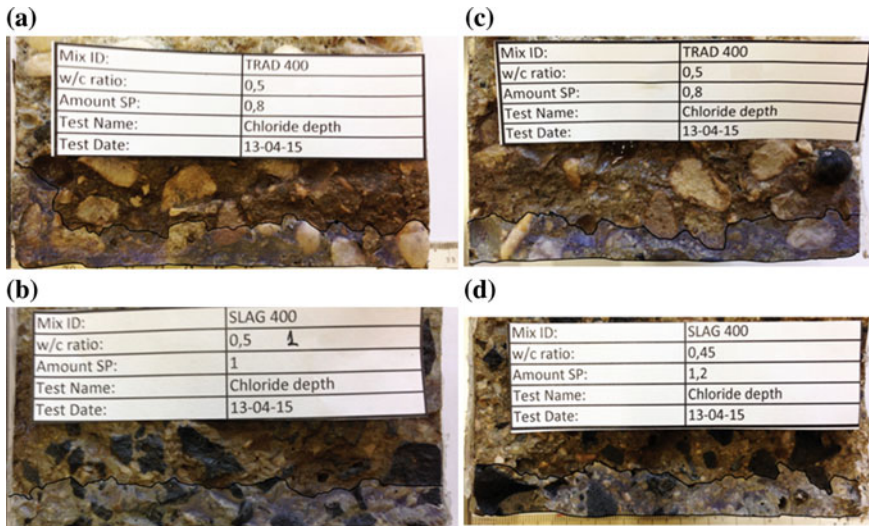


Fig. 4.21 Ordinary performance concrete: conventional (a) and EAF (b); High performance concrete: conventional (c) and EAF (d)

Table 4.20 Apparent diffusion coefficients for OPC and HPC with EAF slag (from [17])

	D_{app} (mm ² /year)
C400-0.45	45.0
C400-0.5	59.1
E400-0.45	40.4
E400-0.5	50.1

HPC between 13.6 and 63.1 mm²/year, all referred to free chlorides content. The values obtained in [17] for EAF concretes, are in agreement with the results obtained for EAF concrete, being its D_{app} within the range of HPC.

4.5 Conclusions

When dealing with the design of concrete including EAF slag as partial replacement of natural aggregates, the typical direct volume or weight replacement (DVR or DWR) proportioning methods can be used. However, the slag are characterized by different physical and chemical properties with respect to NA, and hence this should be taken into account for enhancing final concrete properties.

The most well-recognized difference between EAF slag and NA lies into the higher specific weight of the slag, which enables to produce heavy-weight concrete, useful in many applications, e.g. in geotechnical structures (retaining walls, foundations, etc.), and when radiation-shielding properties should be achieved. This property may have a negative impact instead on fresh concrete workability: if not taken into account, aggregates migration can occur under gravity, leading to segregation phenomena and final strength losses. The cement paste should be proportioned to support the aggregates and prevent this problem, mainly when high replacement ratios are used.

EAF slag shape and texture have also a negative influence on workability of fresh concretes. Also the grading of the particle may be not satisfy the requirements to allow a workable mix. Workability problems have also been experienced principally when EAF fine aggregates were used at high replacement ratio, due to their lack in fine fractions: it is thus recommended to use at least 50 % of fine natural aggregates, to prevent difficulties in mix preparations.

However, the above slag properties improves concrete strength, in terms of compressive, tensile strength and elastic modulus. Better bond of these aggregates with the cement-paste has been detected in literature. Total replacement of coarse aggregate with EAF slag has been found suitable to produce both ordinary strength and high performance concretes. In this regard, the production of HPC with EAF slag has been demonstrated to be possible, maintaining relatively high w/c ratios (higher than 0.4), and without using mineral additions, commonly used to achieve high strength.

The use of EAF slag improves concrete durability in chloride-exposed environment, leading to a reduction of the diffusion coefficient, which has been

evaluated through colorimetric tests. It is worth noting that the color of EAF-concrete, when sprayed with AgNO_3 , turns into a bluish-grey in the contaminated zone, differently from conventional concretes, which generally become purple.

The influence of detrimental environmental cycles on compressive strength of ordinary strength concrete including EAF slag (both as fine and as coarse aggregate) is generally similar for traditional and recycled concrete. This has not been already investigated instead for HPC. Lack of data exists indeed about durability-related properties of EAF concrete.

Lastly, concerning the expansion of some compounds present in the slag, i.e. free lime and periclase, it seems that this possibility is very low when dealing with EAF slag, due to its basic nature and to the well developed crystalline lattice that should improve its dimensional stability.

Acknowledgments The authors would like to acknowledge Zerocento Srl, Calcestruzzi Zillo SpA, Cementi Candeo SpA, for their economical support and for supplying the EAF slag and cement.

References

1. Pasetto M, Baldo N (2011) Mix design and performance analysis of asphalt concretes with electric arc furnace slag. *Constr Build Mater* 125(8):3458–3468
2. Wu S, Xue Y, Ye Q, Chen Y (2007) Utilization of steel slag as an aggregate for stone mastic asphalt (SMA) mixtures. *Build Environ* 42:2580–2585
3. Motz H, Geiser J (2001) Products of steel slags an opportunity to save natural resources. *Waste Manage* 21:285–293
4. Faleschini F, Brunelli K, Zanini MA, Dabalà M, Pellegrino C (2015) Electric arc furnace slag as coarse recycled aggregate for concrete production. *J Sustain Metall*. doi:10.1007/s40831-015-0029-1
5. Polanco JA, Manso JM, Setién J, González JJ (2011) Strength and durability of concrete made with electric steelmaking slag. *ACI Mater J* 108:196–203
6. Papayianni I, Anastasiou E (2010) Production of high-strength concrete using high volume of industrial by-products. *Constr Build Mater* 24:1412–1417
7. Manso JM, Polanco JA, Losanez M, Gonzalez JJ (2006) Durability of concrete made with EAF slag as aggregate. *Cem Concr Comp* 28:528–534
8. Pellegrino C, Gaddo V (2009) Mechanical and durability characteristics of concrete containing EAF slag as aggregate. *Cem Concr Comp* 31:663–671
9. Tossavainen M, Engstrom F, Yang Q, Menad N, Larsson ML, Bjorkman B (2007) Characteristics of steel slag under different cooling conditions. *Waste Manage* 27(7):1335–1344
10. Maslehuddin M, Sharif AM, Shameem M, Ibrahim M, Barry MS (2003) Comparison of properties of steel slag and crushed limestone aggregate concretes. *Constr Build Mater* 17:105–112
11. Manso JM, Gonzalez JJ, Polanco JA (2004) Electric arc furnace slag in concrete. *J Mater Civ Eng* 16:639–645
12. Pellegrino C, Faleschini F (2013) Experimental behavior of reinforced concrete beams with electric arc furnace slag as recycled. *ACI Mater J* 110(2):197–206

13. Pellegrino C, Cavagnis P, Faleschini F, Brunelli K (2013) Properties of concretes with black/oxidizing electric arc furnace slag aggregate. *Cem Concr Compos* 37:232–240
14. ASTM International (2013) ASTM C33/C33M. Standard Specification for Concrete Aggregates, West Conshohocken
15. Manso JM, Hernández D, Losáñez MM, González JJ (2011) Design and elaboration of concrete mixtures using steelmaking slags. *ACI Mater J* 108(6):673–681
16. Arribas I, Santamaría A, Ruiz E, Ortega-López V, Manso JM (2015) Electric arc furnace slag and its use in hydraulic concrete. *Constr Build Mater* 90:68–79
17. Faleschini F, Fernández-Ruiz MA, Zanini MA, Brunelli K, Pellegrino C, Hernández-Montes E (2015) High performance concrete with electric arc furnace slag as aggregate: mechanical and durability properties. *Constr Build Mater* 101:113–121
18. Adegoloye G, Beaucour A-L, Ortola S, Noumowé A (2015) Concretes made of EAF slag and AOD slag aggregates from stainless steel process: mechanical properties and durability. *Constr Build Mater* 76:313–321
19. Wang G, Wang Y, Gao Z (2010) Use of steel slag as a granular material: volume expansion prediction and usability criteria. *J Hazard Mater* 184:555–560
20. ASTM International (2006) ASTM 4792-00. Standard test method for potential expansion of aggregates from hydration reactions; ASTM Committee D04 on Road and Paving Materials, West Conshohocken, PA
21. Kim S-W, Kim Y-S, Lee J-M, Kim K-H (2013) Structural performance of spirally confined concrete with EAF oxidizing slag aggregate. *Eur J Environ Civ Engin* 17(8):654–674
22. Limbachiya MC, Leelawat T, Dhir RK (2000) Use of recycled concrete aggregate in high-strength concrete. *Mater Struct* 33:574–580
23. Ajdukiewicz A, Kliszczewicz A (2002) Influence of recycled aggregates on mechanical properties of HS/HPC. *Cem Concr Compos* 24:269–279
24. American Concrete Institute (2014) ACI Committee 318. Building code requirements for structural concrete (ACI 318-4)
25. International Federation for Structural Concrete (2008) *fib* Bulletin 42. Constitutive modelling of high strength/high performance concrete
26. Nordtest Method (1995) NT Build 443. Concrete hardened: accelerated chloride penetration
27. He F, Shi C, Yuan Q, Chen C, Zheng K (2012) AgNO₃-based colorimetric methods for measurement of chloride penetration in concrete. *Constr Build Mater* 26:1–8
28. Baroghel-Bouny V, Belin P, Maultzsch M, Henry D (2007) AgNO₃ spray tests: advantages, weaknesses, and various applications to quantify chloride ingress into concrete. Part 1: Non-steady-state diffusion tests and exposure to natural conditions. *Mater Struct* 40:759–781

Chapter 5

Sustainability of Recycled Concretes Through Life Cycle Assessment

5.1 Introduction

In the recent years a number of strategies have been introduced to allow the construction industry to reduce its high environmental impacts. This industrial sector has an essential and priority role in the development of competitiveness and prosperity of European general economy. Concrete is one of the most widely used building materials in roads, buildings, bridges and other infrastructures. On average, approximately 1 ton of concrete is produced each year for every human being in the world [1]. As an indicative data, in Italy, which is the first manufacturer of cement in Europe and the thirteenth in the world, and its cement and concrete manufacturing sector represents the 14 % of EU-27 production [2], about 36 million tons of cement have been produced in 2009, equivalent to about 601 kg for every human [3]. Because of this global extensive use, it is imperative to evaluate the environmental impact of this material correctly, that should be equated, among the others, with its effect on greenhouse gas emissions and climate change. In 2007, a research report indicated that from 5 until 7 % of the all anthropogenic CO₂ emissions were at the expense of the cement industry [4]. The answer to this growing interest in producing building materials with reduced environmental impacts is the growth of several types of recycled concrete. Recycled components have been studied to replace, at least partially, the main constituents of concrete, i.e. cement [5, 6] and virgin aggregates [7, 8]. This strategy aims to improve the environmental sustainability of construction industry. But what do we mean with the word “sustainability”? According to the World Commission of Environment and Development of the United Nations, “sustainability” can be defined by “*meeting the needs of the present without compromising the ability of the future generations to meet their own needs*” [9]. This concept is often associated with the aim to do not increase, and even reduce, the emissions in atmosphere of greenhouse gases (GHGs), and in particular of CO₂. Another significant aspect necessary to promote sustainability in concrete industry is related to the consumption of raw materials, and in particular of

limestone, which availability is limited, especially in some geographical regions [10, 11].

However very few proofs of the real embodied energy of the product, and of the environmental gains due to the use of recycled components, are reported when dealing with a novel concrete. This rarely happens also for the evaluation of the environmental impacts associated to the production of the material, for a properly defined functional unit, according to the LCA protocols [12, 13]. Some examples of an attempt of quantifying sustainability of recycled concretes or of their components are shown in [1, 14, 15]. Concretes designed with a sustainable target should not only use recycled materials, but also have low energy costs, high durability, and display at least equivalent mechanical properties then their reference. A recent work developed by Marinkovic et al. [16] showed that often mechanical and durability-related properties of recycled aggregate concrete (RAC) with coarse recycled aggregates are lower than the properties of the reference natural aggregate concrete (NAC), due to the often-observed worse properties of recycled concrete aggregate (RCA). This results in a limit on the utilization of RCA in structural concrete at high replacement ratio, if no pre-treatment operations are performed to improve the quality of the recycled aggregates. Hence, to obtain the same strength class, which is necessary for a proper comparison of a reference functional unit of the products, an increase in cement content was necessary for RAC mixtures, resulting in that RAC was not sustainable as expected. In fact, 1 m³ was responsible of about +11 % of CO₂ with respect to the reference NAC, and about +22 % of energy used for its production. However, for non-structural applications, or when alternative aggregates proportioning methods are used [17–19], RCA use becomes competitive both from an economical and environmental point of view, as no further cement addition is required.

In this context, the proper evaluation of the emissions due to the production of the aggregates to be used in the concrete industry represents a fundamental starting point to assess the effective sustainability of a building material. Therefore in this section some tools used to assess the environmental impacts of these products are described, and applied to evaluate the impacts of natural and recycled aggregates. Particularly Life Cycle Assessment (LCA) and the Abiotic Depletion Indicator (ADP) have been satisfactorily applied in literature, being those indicators able to quantitatively estimate the environment impacts due to the production of aggregates and concretes, i.e. in terms of CO₂ emissions, or consumption of non-renewable resources.

The same procedure used here to evaluate the environmental impacts of the analyzed natural and EAF aggregates can be used to assess the impacts of other recycled components. Then some examples about the estimation of environmental impacts of some recycled concretes is shown, highlighting the effects of substituting NA with recycled aggregates (in this case, EAF slag).

5.2 Recycled Aggregates and Potential Environmental Issues

Construction industry is one of the main consumers of raw materials, and it causes also great streams of waste, particularly of construction and demolition waste (C&DW). This material accounts for about 25–30 % in mass of the whole waste produced in the EU [20]. It typically comprises large quantities of inert mineral materials, with smaller amounts of other components, depending on the source and separation techniques. Despite the high potential for recycling of C&DW in the aggregate market, a large fraction ends up in C&D landfills, and barriers to materials recovery still exist. As a consequence, a great amount of land is currently dedicated to the disposal of those materials, leading to the increase of the ecological footprint of the construction industry.

Recycled aggregates (RA) are valuable resources which could be used in a number of applications, depending on their quality, i.e. for environmental filling and rehabilitation of depleted quarries and landfills, in road works as sub-base, base or unbound material, as granular bedding or filter material for drainage layers, and in concrete production as paving block, pedestrian paving slab, curbs, roads meridians, anti-crash barriers, railway platform, mass concrete applications e.g. bridge abutments, seawall blocks, shore protection works, and high grade applications e.g. precast elements.

However environmental concerns should also be taken into account, related to the release of dangerous substances to outdoor and indoor air, soil, surface water and groundwater, particularly with respect to leaching potential [21]. Currently these problems are under consideration by the Technical Committee CEN/TC 351. Some researchers have also reported the possibility that more energy is spent due to the recycling chain with respect to waste disposal, and that transportation-related environmental loads may heavily contribute to the aggregates' impacts, especially where the geographical coverage of market demand is not enough for RA [16, 22].

Concerning leaching concerns, other than RA from C&DW, also aggregates from industrial waste may undergo potential environmental issues. Leaching should be carefully analyzed e.g. when dealing with aggregates coming from metallurgical industry. Some researchers have indeed reported that some minor constituents of EAF slag may hinder its further application in civil engineering works, due to their potential leaching. EAF slag is an oxide system, liquid at temperatures typical of the steel process, which begins to solidify at temperatures below 1500 °C. The solidified slag is a multiphase system, very influenced by the composition of the slag and the cooling practices. Here the behavior of these minor compounds, e.g. chromium or vanadium [23], is influenced by these phases, which could be stable or not, and hence causing their leaching.

5.3 Sustainability Indicators

The word “indicator” identifies the instrument allowing the policy makers to take better decisions and more effective actions, by means of simplifying, clarifying and making aggregate information available. They also can help in incorporating physical and social science knowledge into decision-making, and they can help measure and calibrate progress toward sustainable development goals. Accordingly, they have been introduced by the United Nations Conference on Environment and Development in 1992 to help Countries to make informed decisions concerning sustainable development [24]. Chapter 40 of Agenda 21 [25], which is the action plan adopted in 1992 at the United Nations Conference on Environment and Development in Rio de Janeiro, has in fact called on countries, as well as international, governmental and non-governmental organizations, to develop indicators of sustainable development that can provide a solid basis for decision-making at all levels. The first draft results in a set of 134 indicators, divided into various themes, which was later modified several times, until arriving to the newly revised Commission on Sustainable Development (CSD) indicators. They are divided in a core of 50 indicators, plus other 46, which enable countries to do a more comprehensive and differentiated assessment of sustainable development. Between these, just a limited number refer to environmental sustainability, whereas a great number of them concerns to social, economical and institutional themes. Between the environmental indicators, some of the core ones are reported below:

carbon dioxide emissions: this indicator measures the emissions of carbon dioxide, which is known to be the most important, or at least the most well-known anthropogenic greenhouse gas (GHG), in terms of impact on global warming;

consume of ozone depleting substances: this indicator depicts the progress towards the phase out of ozone depleting substances (ODSs) by the countries which have ratified the Montreal Protocol on Substances that Deplete the Ozone Layer and its Amendments;

ambient concentration of air pollutants in urban areas: this indicator provides a measure of the state of the environment in terms of air quality and of particulate matter (PM₁₀, PM₂₅) and is an indirect measure of population exposure to air pollution of health concern in urban areas;

arable and permanent crop land: this indicator shows the amount of land available for agricultural production and, inter alia, the cropland area available for food production;

proportion of total water resources used: it shows the degree to which total renewable water resources are being exploited to meet the country’s water demands and is thus a measure of water scarcity.

Between the non-core indicators, some relevant ones are herein listed:

emission of greenhouse gases: this indicator measures the main six greenhouse gases (GHGs) emissions, carbon dioxide (CO₂), methane (CH₄), nitrous oxide (N₂O), hydrofluorocarbons (HFCs), perfluorocarbons (PFCs), sulphur hexafluoride

(SF₆). Emissions are then converted into equivalent CO₂ through the so-called global warming potentials (GWPs) provided in assessments of the Intergovernmental Panel on Climate Change (IPCC);

land degradation: this indicator measures the extent of land degradation, which is an impediment to sustainable development in general, and to sustainable agriculture in particular. Degradation refers to land affected by soil erosion, deterioration of the physical, chemical and biological or economic properties of soil and/or long-term loss of natural vegetation;

fertilizer use efficiency: this indicator shows the potential environmental pressure from inappropriate fertilizer application. Data on the quantities of fertilizers used are converted into the three basic nutrient components (nitrogen N, phosphorous P₂O₅ and potassium K₂O) and aggregated.

Hence, if we want to determine how an activity or a production process participates into the sustainable development of a country, from the environmental point of view, at least some of these indicators should be evaluated. One common way to assess environmental sustainability is through Life Cycle Analysis (LCA), which is a systems-based approach for quantifying the impacts on human health and environment associated with a product's life, from "cradle-to-grave", or from "cradle-to-cradle". A well-established set of methods is already applied into LCA tools, which enable a direct comparison of alternatives associated with the analyzed product or technology. Despite being a mature tool with well-established data, including extensive data quality procedures, some limitations occur: LCA usually models "average" systems, and may not capture the impacts of policies that cause indirect changes or significant (non-marginal) changes in the market. In addition, gaps in the availability of inventory data may represent a barrier to LCA practice. Near to LCA, also other alternatives are available, such as environmental footprint analysis (EFA), cumulative energy demand (CED) or some indexes referring to a particular environmental problem, such as the abiotic depletion indicator (ADP). EFA is an accounting tool which measures human demand on ecosystem services required to support a certain level and type of consumption by an individual, product, or population. CED is a screening impact indicator to provide information on potential product environmental impacts and estimation of energy resource depletion by capturing direct and indirect energy use/demand during the complete life cycle of a product. Lastly, ADP is an indicator which assesses the depletion of non-renewable abiotic natural resources.

5.3.1 Life Cycle Assessment

Life-cycle assessment is a systems-based approach allowing the quantification of the impacts (both on human health and environment) associated with a product's entire life, generally from "cradle-to-grave", or from "cradle-to-cradle". Hence, a full LCA addresses all the stages of the product life-cycle, and it should take into

account alternative uses as well as associated waste streams, raw material extraction, material transport and processing, product manufacturing, distribution and use, repair and maintenance, and wastes or emissions associated with a product, process, or service as well as end-of-life disposal, reuse, or recycling. LCA considers multiple environmental indicators, i.e. emission of greenhouse gases, consume of ozone depleting substances and water quality. According to the ISO standards [12, 13], it consists of four phases, as shown in Fig. 5.1: (a) the goal and scope definition; (b) the compilation of the life-cycle inventory (LCI); (c) the life-cycle impact assessment (LCIA); and (d) the interpretation of the results.

The definition of the LCA goals should be chosen according to the specific product or process, and scope includes definition of “system boundaries” for the analysis, e.g. whether an analysis considers end-of-life management for a product or if transportation scenarios should be included or not in the analysis. Goal and scope in a sustainability context should be defined through stakeholder engagement and collaboration and identify which products and technologies should be evaluated. Additionally in this phase the functional unit (*FU*) should be defined, in order to properly describe the analyzed product. *FU* is the product, service or function on which to base the analysis and comparison with possible alternative uses. So it allows to normalize all data input and output so as to compare the results of the LCA. The functional unit is an arbitrary standardization parameter to describe all the final results and can be either a product that a service. Hence it is a necessary reference to ensure the comparability of LCA results. It is useful when different systems are evaluated and when the comparison must be made on a common basis.

The analysis of inventory includes the compilation and quantification of relevant input and output elements of a product during its life cycle. It develops in three phases: data collection, calculation procedure allowing to quantify the I/O elements

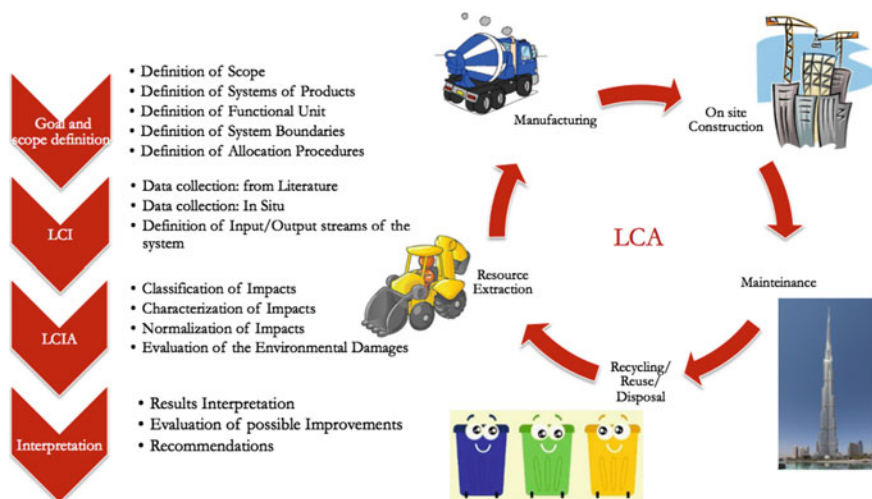


Fig. 5.1 Life Cycle Assessment phases

of a relevant product system, and their allocation. Significance can be determined by threshold for mass (e.g. more than 1 % of inputs), energy and environmental significance (potential for harm). The collected data allow to define the input and output elements of the system, and in particular they can be classified into broad categories including:

energy inputs, raw material inputs, ancillary inputs, other physical inputs;
products, co-products and waste;
emissions to air, discharges to water and soil;
other environmental aspects.

All collected data must include the details of their collection, which are constituted by the period in which the data were collected and all the information on data quality indicators. The description of each stage unit must be made. It includes tracking of the flow charts that describe all unit processes included in the model, the detailed description of each process unit (specifying the factors that influence the inputs and output), a list of streams, the list of the units used, the description of the data collection and calculation techniques, and all the other issues associated with the data provided/included. The calculation procedures are used to produce the results of inventory system defined, for each process unit and to define the functional unit of the system analyzed. The following operating steps must be done:

validation of the data collected: during data collection there is the necessity to validate data, to confirm and provide evidences that the requirements of data quality for the intended application have been met. Among the available systems, mass and energy balances can be used;
correlation of the data to the unit processes: quantitative input and output data of the process unit must be calculated in relation to an appropriate flow. All streams of unit processes must be connected to the reference flow;
correlation of the flow of data to the reference functional unit: the result of the calculations should lead to report all system input and output data to functional unit;
refining the system boundary: the data to be included must be chosen on the bases of a sensitivity analysis, and their significance must be evaluated. The initial system boundary shall be revised in accordance with the cut-off criteria established in the definition of the scope.

Allocation procedures are important to take into account multiple products and recycling systems: all input and output are allocated according to the different products. They should be defined and justified. The allocation procedure shall identify the processes shared with other product systems and it deals with them according to the stepwise procedure presented below:

Step 1: Wherever possible, allocation should be avoided by: dividing the unit process to be allocated into two or more sub-processes and collecting the input and output data related to these sub-processes, or expanding the product system to include the additional functions related to the co-products;

- Step 2: Where allocation cannot be avoided, the inputs and outputs of the system should be partitioned between different products or functions in a way that reflects the underlying physical relationships between them; i.e. they should reflect the way in which the inputs and outputs are changed by quantitative changes in the products or functions delivered by the system;
- Step 3: Where physical relationship alone cannot be established or used as the basis for allocation, the inputs should be allocated between the products and functions in a way that reflects other relationships between them. For example, input and output data might be allocated between co-products in proportion to the economic value of the products.

In general the procedures of allocation for recycling and reuse of materials should use in order [12, 13]: (a) physical properties (e.g. mass); (b) economic value (e.g. market value of the scrap material or recycled material in relation to market value of primary material); (c) the number of subsequent uses of the recycled material (explained in ISO/TR 14049).

Life-cycle impact assessment of the product/technology/process is performed using the LCI data and one or more assessment methods that translate emissions into one or more impact categories, such as global warming potential (based on GHG emissions), water quality impacts, human health impacts, or many others. LCIA must be in accordance with the purpose and with the scope of the study and thus the data quality and results of the LCI have to verify this. The LCI output must be controlled so as to calculate the results of the indicators for the LCIA. The functional unit, the LCI, the aggregation and allocation methods should be suitably chosen to reduce the environmental relevance of the LCIA results. Three mandatory phases should be done during LCIA:

selection of impact categories, category indicators and characterization models;
assignment of LCI results to the selected impact categories;
calculation of category indicator results.

Optional elements can be performed, depending on the objective and scope of the LCA. They are:

normalization: calculating the magnitude of category indicator results relative to reference information;
grouping: sorting and possibly ranking of the impact categories;
weighting: converting and possibly aggregating indicator results across impact categories using numerical factors based on value-choices. Data prior to weighting should remain available;
data quality analysis: better understanding the reliability of the collection of indicator results, the LCIA profile.

As above cited, in this phase the methodology and impact categories should be chosen. Mid-point indicators may be very useful to provide information not affected by uncertain end-point results, which modeling is more complex and time-consuming.

Accordingly it is possible to use a problem-oriented methodology [26] for the impact assessment: this approach involves environmental impacts associated with climate change, eutrophication, acidification, human toxicity, eco-toxicity, etc. The evaluation procedure can hence be based on the basic categories of CML 2002 Method [27]: hence, the chosen mid-point indicators are Global Warming Potential (kg CO₂ eq.), Acidification (kg SO₂ eq.), Eutrophication (kg PO₄ eq.), Photochemical Oxidation (kg C₂H₄ eq.), Human Toxicity (kg 1,4-DCB eq.), Eco-Toxicity (kg 1,4-DCB eq.) and Ozone Layer Depletion (kg R11 eq.). Other methods are of course available, including different impact categories. The most well-known are: Ecopoint 97 [28], EcoIndicator 99 [29], Impact 2002+ [30].

Concerning climate change, there is not a direct proof (even if the great part of the scientific world supports this cause-effect relationship) that links green-house gases (GHG) emissions to global climate change, but following the principle of prevention, several measures have been taken at the international level. Between these, the most famous one is the Kyoto Protocol, that states internationally the necessity to reduce GHG emissions. Recently the IPCC report of November 2014 on the GHG emissions stated the necessity to reduce the emissions from the current level until a value reduced by the 40–70 % before the 2050. Emissions responsible for this problem are mainly nitric oxide, carbon dioxide and methane. The increase of these gases are indeed responsible for the greenhouse effect that is the atmosphere capacity to hold more or less heat.

Eutrophication is caused by the emission of ammonia, nitrates, nitrogen oxides, phosphorus and nitrogen (nutrients). Nutrients are essential to life in ecosystems, but at the same time, when nutrient intakes increased disproportionately in relation to the ability to metabolize by the aquatic environment, an environmental problem occurs. For example, when the amount of nutrients in a lake is excessive, they cause the uncontrolled algae growth in the surface layers, because algae are able to assimilate the nutrients very quickly. When the algae will die, they will be the carbon source for the aerobic bacteria that will begin the processes of decomposition using the dissolved oxygen. The birth of an anaerobic layer will lead to the gradual disappearance of the fauna and progressive wetland.

Acidification is due to the emission of ammonia, nitrogen oxides and sulfur dioxide. In particular, sulfur dioxide (SO₂) is due to the combustion of coal and oil, instead of nitrogen oxides (NO_x) which are produced by all motor vehicles that work inside a plant and by other combustion processes that may be present. Acidifying compounds may fall to the ground with rain or snow (acid rain) as wet deposition, or in the form of particles or gases as dry deposition. Acid rain is caused by the interaction of these three substances with water, which are transformed into sulfuric acid (H₂SO₄) and nitric acid (HNO₃).

Concerning photo-oxidant formation, benzene, 1,3-butadiene, sulphur dioxide, carbon monoxide, methane and non-methane volatile organic compounds (NMVOC), emitted to the atmosphere from many natural or anthropogenic processes, undergo a complex system of photochemical reactions induced by light present in the ultraviolet sun rays, all leading to the formation of ozone (O₃), peroxyacetyl nitrate (PAN), peroxybenzoyl nitrate (PBN), aldehyde and hundreds of

other substances. These substances are reactive (especially ozone) and they are harmful to human and ecosystems health. This problem is also referred to as “summer smog”, easily identified by its color ranging from yellow-orange to brown and more common when solar radiation is more intense and therefore the ozone legal limits are exceeded.

The industrial activities are responsible for the release of substances hazardous to human health (human toxicity). Substances become dangerous to health when they enter into the body, they are absorbed and are metabolized, through processes such as ingestion, inhalation or through the skin. A substance is toxic when its concentration in the body is greater than a threshold value. Of course, the threshold value varies from the individual susceptibility and from substance to substance: the substance potential toxicity depends on its characteristic structure (small structural differences may correspond to large differences in toxic effects induced). Concerning the construction industry, for instance the emissions from aggregates extraction and recycled aggregates treatment plants which may be toxic are benzene, 1,3-butadiene, PM₁₀, nitrogen oxides, sulphur dioxide and non-methane volatile organic compounds (NMVOC).

The pollutant toxicity on the ecosystem depends on the biological effects it causes and by its concentration. Emissions of benzene, 1,3-butadiene and non-methane volatile organic compounds (NMVOC) may cause the problem appointed as ecotoxicity, which may be aquatic or terrestrial. The substances responsible for ecotoxicity can damage the structure and the organization of an ecosystem exerting toxic effects on organisms that inhabit it, until their death. The presence of persistent substances (those substance characterized by low biodegradability and which remain in the environment for long periods without undergoing any type of change) is responsible for toxic effects that occur for a long time (chronic toxicity). Therefore, this type of ecotoxicity is linked to the intrinsic substance toxicity, to its biodegradability and its ability to accumulate in tissues.

Concerning the ozone layer depletion, stratospheric ozone represents a natural shield for the Earth, and it is able to filter the dangerous ultraviolet (UV) radiation that can be harmful to humans and other organisms. This layer can be damaged by industrial processes; in particular, it can be related to the energy sources used (electricity and diesel) in a productive process. The damage of this layer, known as the “ozone hole”, causes excessive human skin exposure to UV radiation, accelerates the cataract onset and interferes with photosynthesis putting at risk the plants growth.

The last phase of LCA is the interpretation of the results: this discussion should transparently communicate the limitations and uncertainties associated with the LCA results, including uncertainties associated with data limitations, and with analytical (scenario and scope) assumptions.

Several commercially available software can be used to perform a life cycle analysis, based on existing commercial databases.

5.3.2 Abiotic Depletion and Exhaustion Time Indicators

The depletion of natural resources is one of the main category indicator of life cycle analysis. Although, the available methods generally focus on the depletion of biotic resources and, when referring to abiotic ones, they concern minerals and energy resources, such as coal or oil. Resources can be divided into biotic such as biodiversity, sylvicultural products (wood, fish, etc.) and abiotic (that gathers all non biotic resources). Within abiotic resources, there are mineral resources, e.g. metals, and bulk materials, e.g. sand, gravel or lime, and energy resources, e.g. fossil fuels. Bulk materials are often excluded by the main Impact Assessment methods, i.e. CML [27], Ecopoint 97 [28], EcoIndicator 99 [29], Impact 2002+ [30], because the natural resources for those materials are considered infinitely available. However quarrying activity, for instance, is generally responsible for high impacts, both direct and indirect, mainly at the local and regional scales, for which indicators and impact models have received less consensus with respect to the ones applied to global level [31]. Recent studies [10, 11] have highlighted how the hypothesis of infinite stock of abiotic bulk resources is incorrect, especially at local scale. Hence, an abiotic indicator was introduced in [10]:

$$DP_i = \frac{DMC - PR}{(R + PR)^2} \times \frac{(RS_b)^2}{DRS_b} \quad (5.1)$$

where DMC is the Domestic Material Consumption in (ton/year), PR refers to the Recycling in (ton/year); I refers to the Imports (ton/year); RS_b is the reserve of a reference material, assumed as antimony (ton); DRS_b is the extraction rate of antimony in (ton/year); R refers to the potential reserve in (ton) and it is calculated in the time interval between t_O and the exhaustion time t_R , as following:

$$R = \int_{t_0}^{t_R} DMC(t) \cdot \left(1 - \frac{I}{DMC}(t)\right) dt \quad (5.2)$$

The exhaustion time of the resource is then evaluated according to the extraction rate and trend in time. If a constant rate is assumed, it is rapidly obtained by Eq. 5.3 and it expressed in years:

$$t_R = \frac{R}{DMC - PR - I} \quad (5.3)$$

Concerning the exhaustion time, this indicator can be applied directly for analyzing e.g. the impacts of a quarrying activity. In this case, t_R of the quarry can be used as a further environmental indicator. The resource stock R represents the

remaining authorized volume to be excavated, which can be evaluated as the integral of the extraction rate ER until the quarry closure:

$$R = \int_{t_0}^{t_R} ER(t)dt \tag{5.4}$$

Through the estimation of the extraction rate in time it is possible to evaluate the estimated exhaustion time of the analyzed facility.

5.3.3 Land Use

When dealing with the evaluation of environmental emissions of construction materials, non-renewable bulk materials are involved. The depletion of this resource can be analyzed through the above indicators, or also via the land use.

Indicators for land use are rarely applied in LCA, because they typically require a site-specific approach, whereas LCA was developed as a methodology for time- and space-independent impact assessment. The use of land for a specific productive process makes it unavailable for other activities, causing possible variation in land quality, during both the transformation and occupation phases (Fig. 5.2). When dealing with the evaluation of natural aggregates impacts, the extraction activity is responsible for significant visual impacts, degradation problems related to soil depletion, and lastly topography alteration. Additionally, erosion/geotechnical problems may arise locally, due to vegetation removal and lack of available soil on

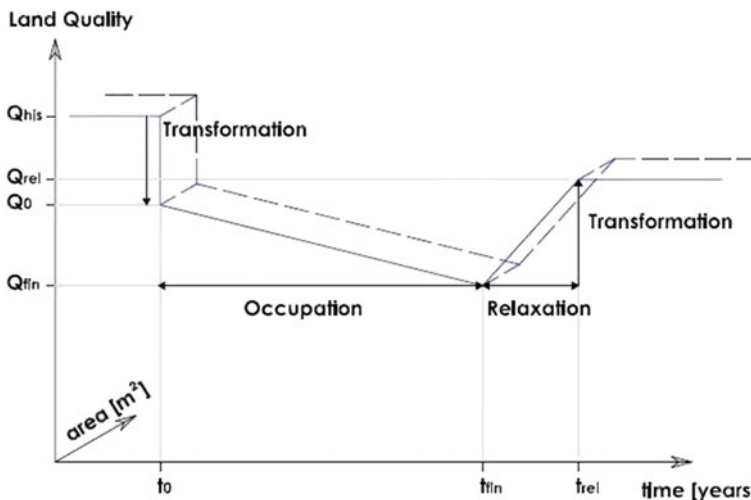


Fig. 5.2 Land quality evolution: transformation and occupation effects (adapted from [32])

quarry steep slopes. However, most of the available LCIA methods fail to consistently address all the main impacts related to land occupation and transformation processes [33].

5.4 LCA of Natural and Recycled Aggregates

LCA framework is generally accepted as a reliable assessment tool and allows comparing the environmental impact of a strength and durability/service life related functional unit (*FU*) of reference over its entire life cycle, within determined system boundaries. This tool is growing to be also applied to evaluate building materials sustainability, and hence it can be applied also to evaluate the environmental impacts associated to the production of the aggregates to be used in concrete or in other civil engineering applications. A fundamental step concerns the collection of Life Cycle Inventory (LCI) data, which can be obtained on site, by means of experiments and compilation of a questionnaire by the operators of the facility, or when this is not possible, collected from literature or available databases. Collected data must be computed through an allocation procedure, and then the I/O flows should be translated into indicators associated with different pressures, such as climate change, acidification, or toxicity to plants, animals and people, according to the chosen method in the LCIA phase (in this case, mid-point indicators have been listed). All emissions contributing to each environmental problem have to be converted into common units (e.g., kg CO₂-equivalent for climate change, or kg SO₂-eq. for acidification) using conversion factors known as “characterization factors” (e.g., for a climate change over a 100-year time frame, 1 kg of methane is equivalent to 25 kg of CO₂). In this section some productive processes for natural and recycled aggregates are analyzed as case-studies: here just high quality aggregates are considered, i.e. their characteristics should be comparable and comply with the minimum requirements for structural concrete applications (e.g. they should meet EN12620 [34] requirements).

5.4.1 Natural Aggregates

The goal of this analysis is to assess the environmental emissions due to natural aggregates productive chain, to be compared with the ones of other aggregates’ productive processes. The production system is considered from the extraction and processing of raw materials (“cradle”) to actual production and assembly of the product (“gate”) at the company that places it on the market, taking into account all the production and transport fluxes inside the system. The chosen functional unit *FU* is 1ton of aggregate. The analysis of inventory includes the quantification of the relevant input and output elements of the product during its life cycle. The allocation procedure for the environmental loads is based on physical/chemical

causation per unit mass of aggregate produced. It should be remembered that the capital required for the system installation and in general the costs incurred are not part of the parameters considered in the model (mass allocation procedure).

Figure 5.3 shows the considered production system of natural aggregates (NA), which has a daily production of about 400 ton/d. The characteristics of the facility analyzed here are typical of many quarries located in Italy, and they have been taken from [35]. For each step in the productive chain, the average amount of I/O material, energy and diesel consumption are used to calculate emissions. Releases are divided between direct and indirect: in particular, last ones refer to dust (PM_{10} release in atmosphere) and combustion gases due to energetic consumption (TSP, PM_{10} , CO, benzene, 1,3-butadiene, CO_2 and NO_x).

Typically experimental data can be used, for instance using chemical analyses on water (I/O from inner wastewater plant of the facility), or leaching tests results. When no experimental data are available, it is possible to use data collected from commercially available databases, or, in case of the emission to air body, they can be analytically computed according to [36–38]. These relations are here reported.

The general formula for estimating air pollutant emissions according to [36] is:

$$E = A \cdot EF \cdot (1 - ER/100) \quad (5.5)$$

where E represents the emission, A is the activity rate expressed, in this case, as (ton_{material}/year), EF is the emission factor expressed as (kg/ton_{material}) and ER is the overall emission reduction, expressed in (%). The emission reduction mainly depends by the potential use of devices and control methods for improving efficiency, applied to limit the releases. An example is the use of water sprays to limit dust releases during quarrying operations. Emissions factors can be evaluated according to [37, 38] respectively for direct and indirect releases. Specific default EF values can be instead used for some of the process operations, such as grinding, drying and crushing, according to [38].

Concerning direct emissions, the following formulas can be used to estimate the particulate matters emissions for PM_{10} . The EF due to the use of excavators, shovels, front-end loaders, expressed in (kg/ton), is:

$$PM_{10} = 0.35 \cdot 0.0016 \cdot (v_w/2.2)^{1.3} \cdot (w/2)^{-1.4} \quad (5.6)$$

where v_w is the mean wind velocity expressed in (m/s) and w is the mean moisture content expressed in (%).

The EF for dust generation due to transport on unpaved roads, expressed in (kg/ton), is:

$$PM_{10} = 0.733 \cdot (s/12)^{0.8} \cdot [(g_v/3)^{0.4}]/[(w/0.2)^{0.3}] \quad (5.7)$$

where s is the mean silt content expressed in (%), g_v is the vehicle gross mass expressed in (ton).

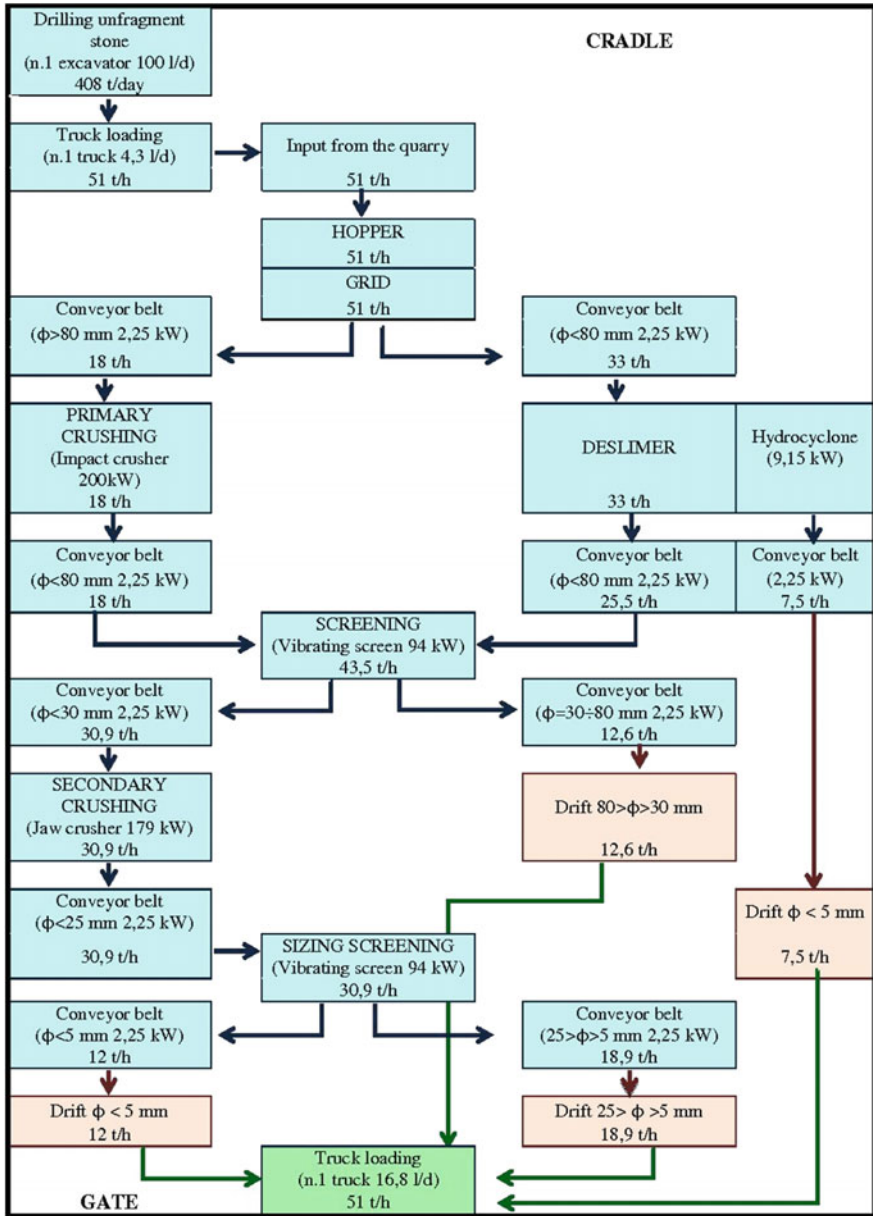


Fig. 5.3 Block diagram of the activities in the analyzed quarry (from [39])

The *EF* due to the use of scrapers, expressed in (kg/ton), is:

$$PM_{10} = 1.32 \times 10^{-5} \cdot s^{1.4} \cdot g_v^{2.5} \quad (5.8)$$

where s is the mean silt content expressed in (%), g_v is the vehicle gross mass expressed in (ton).

The *EF* due to the use of bulldozers, expressed in (kg/h), is:

$$PM_{10} = 0.34 \cdot v_b^{1.5} \cdot w^{-1.4} \quad (5.9)$$

where v_b is the mean vehicle speed expressed in (km/h) and w is the mean moisture content expressed in (%).

Concerning direct emissions, the following formula can be used to estimate the particulate matters emissions for $PM_{2.5}$. The *EF* due to the use of excavators, shovels, front-end loaders, expressed in (kg/ton), is:

$$PM_{2.5} = 0.11 \cdot 0.0016 \cdot (v_w/2.2)^{1.3} \cdot (w/2)^{-1.4} \quad (5.10)$$

where v_w is the mean wind velocity expressed in (m/s) and w is the mean moisture content expressed in (%).

Concerning direct emissions, the following formulas can be used to estimate the particulate matters emissions for *TSP*. The *EF* due to the use of excavators, shovels, front-end loaders, expressed in (kg/ton), is:

$$TSP = 0.74 \cdot 0.0016 \cdot (v_w/2.2)^{1.3} \cdot (w/2)^{-1.4} \quad (5.11)$$

where v_w is the mean wind velocity expressed in (m/s) and w is the mean moisture content expressed in (%).

The *EF* for dust generation due to transport on unpaved roads, expressed in (kg/ton), is:

$$TSP = 2.82 \cdot (s/12)^{0.8} \cdot [(g_v/3)^{0.5}]/[(w/0.2)^{0.4}] \quad (5.12)$$

The *EF* due to the use of scrapers, expressed in (kg/ton), is:

$$TSP = 7.6 \times 10^{-6} \times s^{1.3} \cdot g_v^{2.4} \quad (5.13)$$

Concerning indirect emissions, the general formula to estimate vehicle emissions factors as NO_x , PM_{10} , CO, HC (VOCs, including methane), benzene, 1,3-butadiene and CO_2 , expressed as (g/km) is the following:

$$EF = (a + b \cdot v + c \cdot v^2 + d \cdot v^e + f \cdot \ln(v) + g \cdot v^3 + h/v + i/v^2 + j/v^3) \cdot x \quad (5.14)$$

where $a, b, c, d, e, f, g, h, i$ and j are NAEI vehicle emission factors coefficients, depending on the vehicle typology, on the used fuel and on the substance considered.

The emission (kg/d) is then calculated as:

$$E = EF \times 10^{-3} \cdot f / 100 \cdot n_h \cdot n_s \cdot n_v \quad (5.15)$$

where f is the use frequency expressed as (%), n_h is the number of hours per shift, n_s is the number of shift per day and n_v is the number of the vehicles of the same type used in each process phase. Indirect emission due to electricity consumption and to diesel consumption refers to default emission factors, and they are reported to the daily releases through the specific daily consumption of each device considered within system boundaries.

In case of emissions acting on water body and industrial soil compartment, it is possible to use experimental data collected from the chemical analyses on water (I/O from inner wastewater plant) and leaching tests. These results will allow to experimentally obtain for each substance the emission factor, expressed as EF (mg/l). Then, the emission, expressed as (kg/ton), can be analytically evaluated through:

$$E = EF \times 10^{-6} \cdot W / \rho_w \cdot n_d \quad (5.16)$$

where W is the monthly volume of water discharged expressed as (m^3), ρ_w is water density expressed as (kg/m^3) and n_d is the number of days per month of discharging.

After the computation of the environmental emissions, the impact assessment phase should be performed. As stated before, there are various approaches which can be used. Problem-oriented methodology can be satisfactorily applied, analyzing the environmental impacts associated with climate change, eutrophication, acidification, human toxicity, eco-toxicity, etc. Mid-point indicators may be very useful to provide information not affected by uncertain end-point results, even though end-point indicators can be more easily understood by decision-makers and society. The choice of the indicators is hence very important, and should be related to the expected impacts of the productive chain under consideration.

Here mid-point indicators are chosen, as reported in Table 5.1, which shows the results obtained using this approach for the chosen functional unit, in the considered system boundary.

Results can be also normalized, dividing them to a reference figure, which can be the total production of the defined unit measure within an area (e.g. Europe). Further details about this result are reported in [39].

Table 5.1 Environmental emissions for natural aggregates ($FU = 1$ ton)

Category	Direct emissions	Indirect emissions	Total emissions	U.M.
Climate change	4.65E-01	8.01E+00	8.47E+00	kg CO ₂ eq.
Eutrophication	7.46E-04	2.18E-03	2.92E-03	kg PO ₄ eq.
Acidification	2.87E-03	4.42E-02	4.71E-02	kg SO ₂ eq.
Photo-oxidant formation	1.32E-04	2.64E-03	2.77E-03	kg ethylene eq.
Human toxicity	2.14E-01	5.61E-01	7.75E-01	kg 1.4-DCB eq
Eco-toxicity	5.08E-09	4.12E+02	4.12E+02	kg 1.4-DCB eq
Ozone layer depletion	–	1.48E-05	1.48E-05	kg R11 eq.

5.4.2 Electric Arc Furnace Slag Aggregates

The goal of this analysis is to assess the environmental emissions due to EAF aggregates productive chain, to be compared with the ones of NA. The production system is considered from the delivering of raw materials (“cradle”) to the actual production and assembly of the product (“gate”) at the company that places it on the market. Also in this case all the production and transport fluxes inside the system are considered. The chosen functional unit FU is *1ton* of aggregate, as in the previous case. The analysis of inventory includes the quantification of the relevant input and output elements of the product during its life cycle. The allocation procedure for the environmental loads is based on physical/chemical causation per unit mass of aggregate produced. Also here a mass allocation procedure is chosen: the analysis methodology performed for analyzing EAF slag is the same as for NA. It is recalled that here EAF slag are analyzed using the so-called the “zero burden assumption” [40], meaning that, in this case, slag does not carry any of the upstream burdens into the waste-management system.

Figure 5.4 shows the considered production system of Electric Arc Furnace slag (EAF), which has a daily production of about 400 ton/d. This plant is very similar in terms of productivity to the one considered in the previous analysis, allowing the comparison between the two productive systems. EAF slag treatment plant data were collected in situ from a real plant, sited in Padova (Italy). For each step in the productive chain, the average amount of I/O material, energy and diesel consumption are used to calculate emissions. Releases are divided between direct and indirect, as done in the previous case. Experimentally available data have been used and collected from the existing plant: for more details, look at [39].

Emissions can be evaluated according to the equations listed in Sect. 5.4.1, and then used to compute the environmental impacts through the same methods applied for NA. Table 5.2 shows the emission values resulting from the processing chain of

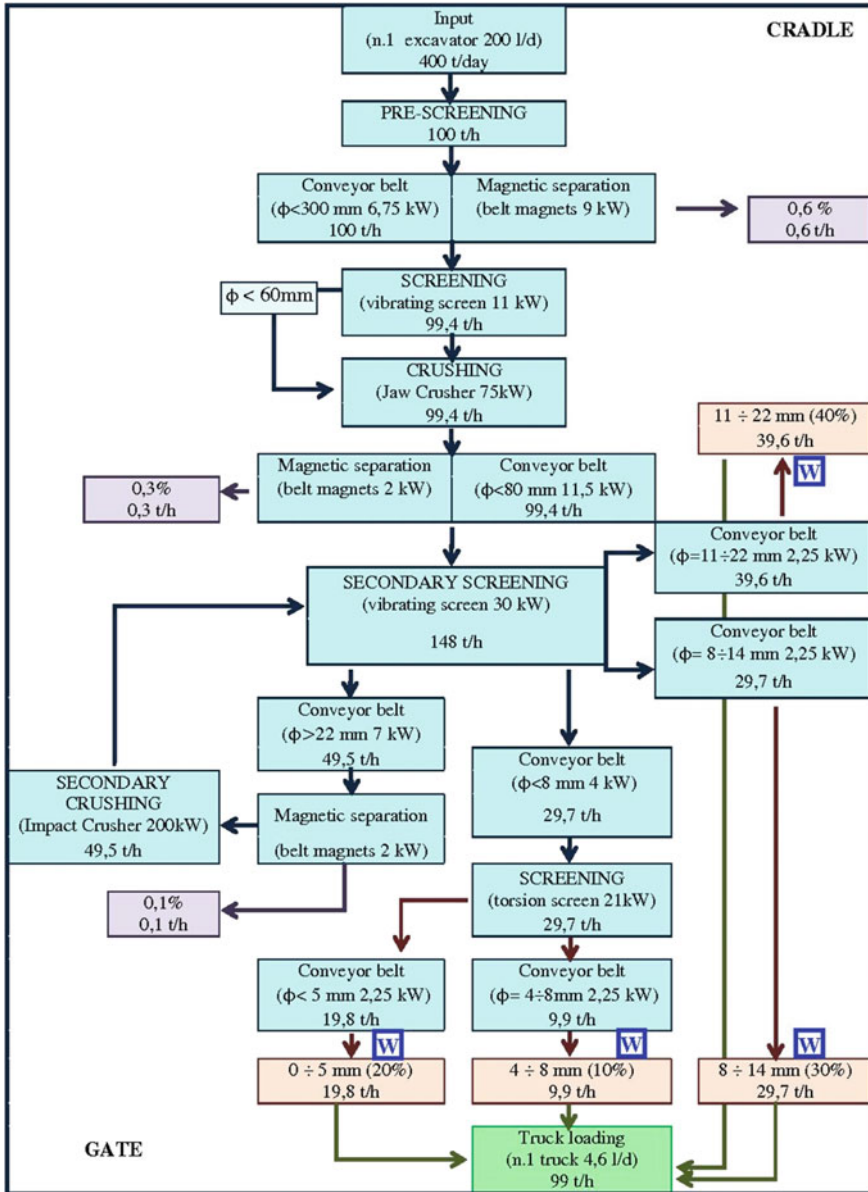


Fig. 5.4 Block diagram of the activities in the treatment plant of EAF aggregates (from [39])

EAF aggregates: EAF slag emissions are significantly lower than emissions calculated for NA, especially regarding the indirect impacts related to the energy demand. The higher simplicity of the EAF processing system (i.e. the reduced number of unit processes during aggregates processing, and the avoidance of the

Table 5.2 Environmental emissions for EAF aggregates ($FU = 1$ ton)

Category	Direct emissions	Indirect emissions	Total emissions	U.M.
Climate Change	3.30E-01	2.76E+00	3.09E+00	kg CO ₂ eq.
Eutrophication	8.66E-04	7.68E-04	1.69E-03	kg PO ₄ eq.
Acidification	3.13E-03	1.53E-02	1.86E-02	kg SO ₂ eq.
Photo-oxidant formation	1.73E-04	9.73E-04	1.15E-03	kg ethylene eq.
Human Toxicity	2.77E-01	1.97E-01	4.74E-01	kg 1.4-DCB eq
Eco-toxicity	2.24E-09	1.54E+02	1.54E+02	kg 1.4-DCB eq
Ozone layer depletion	–	3.82E-07	3.82E-07	kg R11 eq.

overburden removal and excavation phases) promotes a more sustainable use of fossil resources and energy consumptions, hence reducing significantly greenhouse gases (GHG) releases.

5.5 LCA of Concretes with Recycled Aggregates

The goal of this analysis is to provide a useful tool to compare the environmental impacts related to the production of two different concretes, produced with different components, e.g. natural aggregates and EAF slag. The functional unit FU is 1 m^3 of concrete: it is recalled that functional unit should allow a full comparison of two products, i.e. it should describe a unit of reference in terms of product performances. Hence it should be influenced by mechanical properties, physical-chemical characteristics, durability and of course, it is related to the unit of mass of the product.

In this section, three case-studies of the application of the LCA framework will be presented, analyzing the environmental emissions related to the production of some concretes, including recycled aggregates coming from metallurgical industry. The environmental emissions will be compared with reference/control concrete mixtures.

The first example aims to analyze two concretes produced with the same mix-design, but the former includes only natural aggregates, and the latter is with EAF aggregates. Constant parameters are: total aggregates volume and grading curve, water/cement ratio, and almost the cement content.

In the second example, two concretes are compared, the former with only natural aggregates, and the latter with EAF aggregates. However, in this case, the two concretes are designed with two different mix designs, with the aim to reach similar mechanical strength, taking into account the differences of the aggregates in terms

of physical and mechanical properties (see Chap. 4). This example is remarkable to highlight the influence of the cement content inside a concrete mix on the environmental emissions.

The last case aims to analyze the effects of different specific weight of the two analyzed concretes, on transportation costs and related impacts: the system boundaries have been expanded, and some insights about the influence of the choice of FU are given.

5.5.1 Concrete with EAF Slag

Once recycled and natural aggregate emissions estimation has been performed, the assessment of the environmental impacts of two experimental concrete mixes can be completed (scope of the LCA analysis). In this case only impacts related to materials production are considered, thus neglecting both transportation and manufacturing of concrete. This choice can be justified by the necessity of comparing only the influence of the main compounds of the mixes that affect environmental emissions, once the chosen FU allows comparing two concretes with similar strength and durability/service life.

The concretes analyzed here were designed with the same mixture proportions (Table 5.3), with almost constant w/c ratio, cement type and content, and aggregates volume and grading curve. However they do not have the same mechanical strength (Table 5.4), but better EAF slag performances are assumed to mitigate the effects of the higher density of EAF concrete on the results. Compressive strength improves of about +68 %, whereas specific weight increases of about +23 % when using EAF slag as coarse aggregate.

Cement data are taken from [41], and they are reported in Table 5.5, referring to 1 kg of Cement Portland type II as functional unit. These values are then multiplied by the quantity of cement inside each mixes, and then summed to the emissions due to respective quantities of NA and EAF slag in each concrete. It is noticeable that cement determines huge environmental emissions with respect to the ones deriving

Table 5.3 Mix details of the two analyzed concretes

	EAF slag concrete	Control concrete
D_{\max} (mm)	22.4	31.5
$V_{\text{aggregates}}$ (l)	762.7	746.34
Cement content (kg/m^3)	310	290
Water (kg)	164.3	159.5
w/c	0.53	0.55
Total EAF slag SSD ^a (kg/m^3)	2041	–
Total NA SSD ^a (kg/m^3)	617.24	2098.43
Super-plasticizer agent (kg/m^3)	1.24	1.16
Air-entrainer admixture (g/m^3)	49.6	46.4

^aSSD = saturated surface dry

Table 5.4 Mechanical properties of the two analyzed concretes

Mix type	Specific weight after	Slump	$f_{c,cube\ 7d}$	$f_{c,cube\ 28d}$	$f_{ctm,\ exp}$	$E_{cm,\ exp}$
	28 days (kg/m^3)	(cm)	(MPa)	(MPa)	(MPa)	(GPa)
EAF slag concrete	3006	16.8	48.80	58.30	4.38	40.05
Control concrete	2447	21.2	27.20	34.50	3.54	37.40

Table 5.5 Environmental emission related to global and regional scale categories—cement ($FU = 1\ kg$)

Category	Total emissions	U.M.
Climate Change	5.86E-01	kg CO ₂ eq.
Eutrophication	2.04E-04	kg PO ₄ eq.
Acidification	1.22E-03	kg SO ₂ eq.

from the productive chain of aggregates (both natural and slag): a nominal dosage of 300 kg/m^3 of cement CEM II in a concrete mix produces about 175 kg of CO₂, according to data reported in Table 5.6, whereas NA in the traditional mix (about 2 ton/ m^3) is responsible of only about 17.8 kg of CO₂.

The amount of cement required to produce the control concrete described in this section is 290 kg/m^3 , whereas 310 kg/m^3 are used for EAF mixture. As a consequence, the two concretes are generally comparable from the environmental point of view since cement quantities are similar (slightly increased for concrete with EAF slag), nevertheless the use of EAF aggregates is responsible for lower impacts than NA. Table 5.6 lists the results derived from the environmental assessment of the concrete mixes considered in this analysis, involving Climate Change, Acidification, Eutrophication categories only (other data are not available for cement). Concrete with EAF slag, containing 20 kg/m^3 more cement than the traditional one, showed a maximum increase in emissions on the Eutrophication category (+4.71 %), whereas it presents less impacts on Acidification problem (-1.62 %).

Table 5.6 Total environmental emission related to global and regional scale categories—NA concrete and EAF slag concrete ($FU = 1\ m^3$)

Category	Emissions for control concrete	Emissions for EAF slag concrete	U.M.	Δ Emissions (%)
Climate change	1.88E+02	1.93E+02	kg CO ₂ eq.	+2.92
Eutrophication	6.53E-02	6.84E-02	kg PO ₄ eq.	+4.71
Acidification	4.53E-01	4.45E-01	kg SO ₂ eq.	-1.62

5.5.2 *The Influence of Cement Content on Concrete Emissions*

The second application of the comparative LCA procedure analyzes two concretes, designed to have similar mechanical performances, and hence being comparable from the technical point of view in terms of strength, durability and service life. However, to reach the same performances, two different mixes were designed, with different cement content, w/c ratio, plasticizer type and content. Mix details are reported in Table 5.7: the difference, in terms of cement content is relevant. The reference mix contains 90 kg/m³ (22.50 %) cement more than the EAF concrete. The main mechanical properties are listed in Table 5.8.

It should be re-called that this example aims to show the influence of the cement content on concretes' emissions (scope of the LCA analysis).

The analyzed concretes have similar compressive strength at 7 and 28 days, and also elastic modulus. Tensile strength is slightly different, because the mechanical strength of the cementitious matrix is higher in the reference concrete (with 22.5 % more cement) than in the EAF concrete. Concerning workability, the two mixes belong to the same consistency class (S4), and hence they can be considered comparable. On the other hand, it is worth noting that also in this case the specific weight of the two concretes is different, and this may determine higher emissions when concretes will be transported into the market. This item will be analyzed in the further example (currently transportation from the production site to the market is not included in the system boundaries).

Cement emission were taken from [41], as in the previous example, and then they are summed with the ones deriving by the production of the aggregates. Then the impacts related to the production of the concrete mixtures could be obtained. In this example the influence of the cement for the emissions evaluation is remarkable: the amount of 90 kg/m³ less in the EAF slag mixture determines a carbon saving of

Table 5.7 Mix details of the two analyzed concretes

	EAF slag concrete	Control concrete
D _{max} (mm)	22.4	22.4
V _{aggregates} (l)	762.7	706.6
Cement content (kg/m ³)	310	400
Water (kg)	164.3	160
w/c	0.53	0.4
Total EAF slag SSD ^a (kg/m ³)	2041	–
Total natural aggregate SSD ^a (kg/m ³)	617.24	1839.00
Super-plasticizer agent 1 (kg/m ³)	1.24	–
Super-plasticizer agent 2 (kg/m ³)	–	5.8
Air-entrainer admixture (g/m ³)	49.6	–

^aSSD = saturated surface dry

Table 5.8 Mechanical properties of the two analyzed concretes

Mix type	Specific weight after 28 days (kg/m ³)	Slump (cm)	$f_{c,cube\ 7d}$ (MPa)	$f_{c,cube\ 28d}$ (MPa)	$f_{ctm,\ exp}$ (MPa)	$E_{cm,\ exp}$ (GPa)
EAF slag concrete	3006	16.8	48.80	58.30	4.38	40.05
Control concrete	2466	18.5	44.00	56.25	5.40	39.10

Table 5.9 Total environmental emission related to global and regional scale categories—NA concrete and EAF slag concrete ($FU = 1\ m^3$)

Category	Emissions for NA concrete	Emissions for EAF slag concrete	U.M.	Δ Emissions	U. M.
Climate Change	2.49E+02	1.93E+02	kg CO ₂ eq.	-22.71	%
Eutrophication	8.69E-02	6.84E-02	kg PO ₄ eq.	-21.40	%
Acidification	5.74E-01	4.45E-01	kg SO ₂ eq.	-22.51	%

about 23 %. From this example it is possible to highlight the great influence that the cement content has with respect to the environmental emissions related to concrete production (Table 5.9).

5.5.3 *The Influence of Aggregates Specific Weight on Concrete Emissions: System Boundary Expansion*

This example aims to analyze the influence of the different specific weight of the EAF concrete with respect to the control mix on the environmental emissions. In general, it is possible to say that the use of EAF slag in a concrete mix determines an increase of specific weight, which varies in relation to the replacement amount (Tables 5.4 and 5.8). This difference may have a significant impact on transportation costs: accordingly, it is necessary to expand the system boundaries to take into account its effect. The system should include also the transportation from the production site to the product placement on the market.

The assessment of the transportation impacts in terms of carbon emissions can be used as a significant indicator, and can be quantified both for the product aggregates, and for concretes. Considering the transportation emissions related to aggregates placement into the market, they generally have the same magnitude order than the emissions due to aggregates productive chain (Fig. 5.5). As an indicative data, a Euro II type fully loaded truck can be considered: it consumes about 1 L of diesel per 3 km [37], and hence indirect emissions alone are

responsible for about 900 g CO₂/km. In addition, direct emissions increase this number depending on type and mass of the vehicle. They can be evaluated according to Eq. 5.7, converting PM₁₀ emissions to CO₂. Globally, CO₂ emissions due to transport can be estimated around 40 g CO₂/km ton_{aggregate}, being then relevant with respect to the one evaluate considering the system boundaries shown in Figs. 5.3 and 5.4.

Figure 5.5 shows the environmental emission in terms of carbon production when the system boundaries have been expanded: the y-axis interception shows the “km-0” emissions, i.e. it represents the current emission estimated considering the system boundaries shown in Figs. 5.3 and 5.4, respectively for NA and EAF slag. As long as the distance increases, also the impacts increase, due to the transportation emissions from the production site to the market placement. The upper

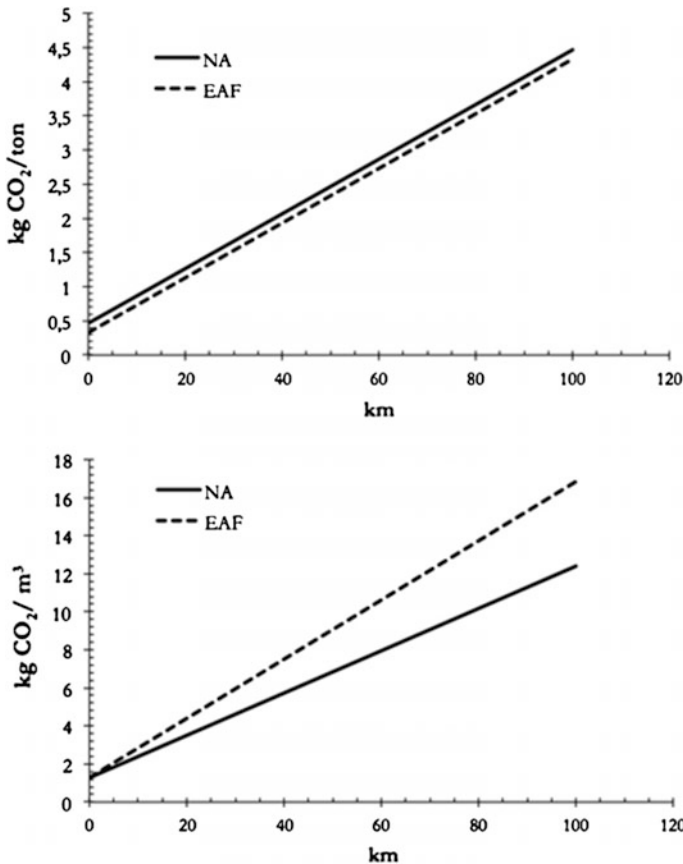


Fig. 5.5 The effect of system boundaries expansion on carbon emissions for aggregates productive chains. Upper: transportation emission per unit mass; transportation per unit volume

graph represents the emissions in terms of carbon emission per unit mass, whereas the lower in terms of carbon emission per unit volume. The graphical interpretation of the results expressed with the two functional unit (mass and volume unit) can be very different when high differences in terms of specific weight are present, as occurs in this case. As a matter of fact, the higher specific weight of the slag determines that, for the same maximum truck load, a reduced quantity (in volume) of material can be transported.

Conversely, when expanding the system boundaries for including transportation during the LCA of concrete production, it is possible to observe that transportation does not contribute significantly on the overall emissions. Concrete impacts are highly affected by cement manufacturing processes, which are responsible for great environmental emissions. Results shown in Fig. 5.6 refer to the two mixtures described in Table 5.7, and they are expressed in carbon emission per unit volume of concrete.

5.5.4 The Choice of the Functional Unit

When comparing two different concretes, and more in general, two products, the choice of a proper functional unit is fundamental. Functional unit is the reference unit of the system for which the environmental impacts will be calculated. It is the product, service or function on which to base the analysis and possible further comparisons with alternatives. It allows to normalize all data input and output so as

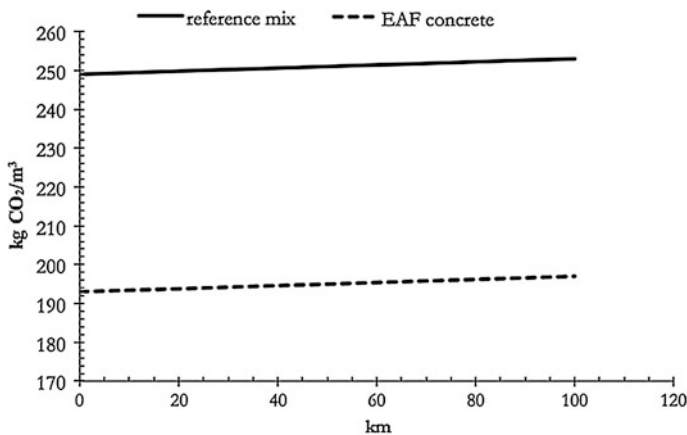


Fig. 5.6 The effect of system boundaries expansion on carbon emissions for concrete production. Transportation emissions are expressed per unit volume of concrete

to compare the results of the LCA. The functional unit is an arbitrary standardization parameter able to describe all the final results and can be either a product that a service. Hence it is a necessary reference to ensure the comparability of LCA results. It is useful when different systems are evaluated and when the comparison must be made on a common basis.

The functional unit for a concrete should be influenced by the mechanical properties, by physical and chemical characteristics, by the durability and of course, it is related to the unit of mass. However it is often difficult to define a proper *FU* when comparing so different types of concrete. Looking at the two concretes described in Tables 5.4 and 5.5, EAF slag concrete compressive strength was almost the double of the control mix strength: however, at the present case, there are no indications for proper accounting this difference. Better mechanical properties can be achieved when using EAF slag with respect to traditional aggregates, and this could involve less concrete volume (and hence less impacts) to obtain the same performance. In the first example the higher compressive strength of EAF concrete was assumed to balance the significant difference in specific weight between the two mixtures, without other indications.

In the second example, two concretes comparable from the mechanical and workability point of view have been analyzed. Here the cement content influence on the environmental emission of the mixtures has been highlighted: results show that cement is the major responsible of environmental emissions during concrete life cycle. This outcome is also confirmed by the results of the last example, where transportation costs are slightly relevant with respect to the emissions carried into the process by the use of cement.

5.6 Natural Aggregates Depletion at Local Scale

The depletion of natural bulk resources can be a relevant problem at regional or local scale. These materials, whose stock can be considered infinite at global scale, can be considered non-renewable at local scale, due to their limited availability in some regions. An example of this statement is conducted here.

Consider here a small region, located in northeast Italy: the quarrying activity is regulated by a regional plan [42], which has a duration of 10 years, and it authorizes a volume of extraction of about 36 millions of m^3 for natural gravel and sand during its validity. In the regional territory, there were 88 existing quarries in 2008, with an estimated volume of 106,431,675 m^3 of available aggregates representing the potential reserve of the bulk natural resources. This volume is subdivided into three main districts. The mining activity from 1990 until 2008, with the imports of natural aggregates, are illustrated in Fig. 5.7: the trend is overall decreasing, even though some fluctuations occurred in the first years of 1990s. Additionally, the

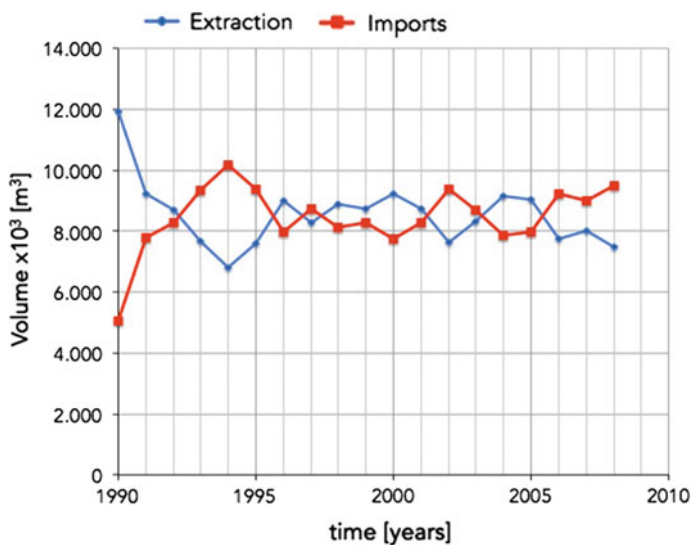


Fig. 5.7 Extraction and imports rate of natural aggregate in the analyzed territory [43]

extracted volume of gravel and sand in 2011, which is the last official available data [42], is about $5,850,835 \text{ m}^3$, highlighting a decreasing trend from 2008 to 2011, due to the economic crisis after 2009.

On the contrary, the imports have been increased during the last 20 years, and in particular the I/DMC ratio, where I represents the imports and DMC is the domestic consumption, has been raised from 0.298 in 1990 until 0.560 in 2008. According to [11], the temporal evolution of this parameter should be used as the base to assess the potential stock of bulk resources available for concrete industry since it well describes the potentially accessible stock of resources, considering all the constraints from the anthroposystem (e.g. the social constraints due to noise and dust, or the environmental ones due to new quarries opening), and not only the geological availability in one site. In the analyzed case, Fig. 5.7 shows the temporal evolution of I/DMC ratio in the analyzed territory: the housing demand, which was very high during the first years of 1990, was predominantly satisfied by the local extraction activity. Nowadays the consumption has been reduced due to the economic crisis, however, as many of other commodities, the imports have been increased, reflecting a potential depletion state at local scale, highly affected by social constraints.

However, the recycling of waste materials and their processing into added-values products such as recycled aggregate can lead to relevant environmental savings also in terms of non-renewable resources, thus limiting the scarcity problems of bulk non-renewable resources that may arise at local scale (Fig. 5.8).

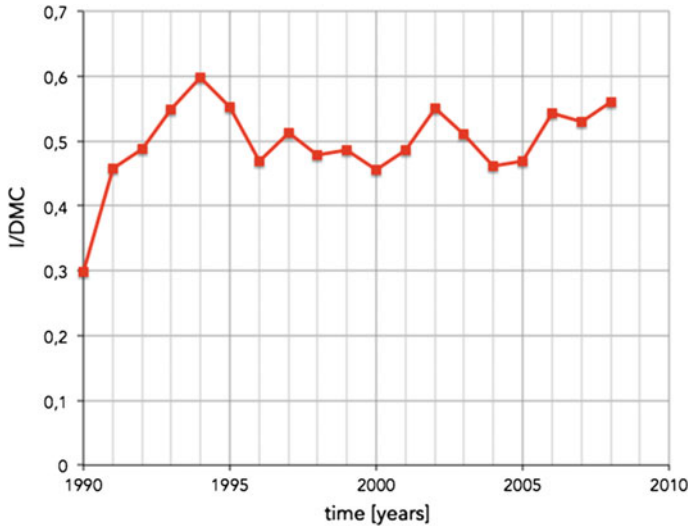


Fig. 5.8 Temporal evolution of *I/DMC* in the analyzed territory [43]

5.7 Land Use Preservation

When dealing with recycled aggregates, a fundamental issue that should be also analyzed relates to their alternative end-of-life, which is represented, in most of the cases, by their landfill. For instance, if C&DW are not treated and processed into recycled aggregates for bound or unbound materials application, or as aggregate for concrete production, they may be also disposed into landfills for inert material. This practice occurs in many cases where recycling is not enough developed. Inert landfill can accept different materials depending on national regulations: for instance, in Italy, construction and demolition waste, e.g. concrete, masonry, ceramics, soils (with some restrictions), and other wastes are accepted. The materials should comply with some limits prescribed in [43], mainly in terms of concentration of metals and other compounds in the leachate.

In the same analyzed territory described in the previous section, there are 38 authorized landfills for inert wastes, according to [44]. In 2010 about 510,000 ton of inert wastes have been disposed, of which about 335,000 ton constituted by marble sludge and the remaining 175,000 ton coming from construction and demolition operations. The estimated available volume for disposal in the region is about 6,000,000 m³ (official available data from 2010): accordingly, the average service life of the existing landfills is about 15 years.

The improve of recycling rates can extend the exhaustion time of the existing landfills, leading to relevant environmental savings, i.e. landfill avoidance of inert

waste, and partial displacement of environmental impacts of quarrying activities. The achievement of these objectives will result in savings in terms of use of land (a scarce resource in countries such as Italy), which has been dedicated to C&DW disposal during the last years [45].

Concerning the land use indicator, Table 5.10 shows inventory data for land use obtained in a small-size integrated plant sited in Northeastern Italy, where both quarrying, recycling of C&DW and inert waste landfill take place. Here site-specific data have been used, and hence they may be just representative for highlighting the influence of landfilling with respect to the other two activities. It is worth noting that, according to Fig. 5.2, disposal of C&DW has relevant impacts not only during the occupation time (during dumping), but also transformation both to industrial area before the starting of the operations and after the site closure, may significantly affect the overall land use indicator.

For this integrated facility, the exhaustion time of the quarrying activity has been also calculated. The current available resources of natural aggregates should be calculated with Eq. 5.4, and in this case $R_{2014} = 64.000.000 \text{ m}^3$. Then the rate of extraction should be estimated on the base of the available statistics of the previous years productivity: here a constant rate of extraction, equal to $6,000,000 \text{ m}^3/\text{year}$, has been obtained. Accordingly it is expected that the resources will be exhausted in $t_R = 11$ years.

The reduction of the extraction rate value ER can be achieved if the recycling activity is improved. Here a constraint about the maximum improvement of the C&DW management plant productivity is fixed. This will allow, as expected, an improvement of the service life of the quarrying plant (Fig. 5.9), leading to a preservation of until $10,000 \text{ m}^3/\text{year}$ of virgin aggregates. Additionally, as the exhaustion time t_R of the quarry increases, also the environmental impacts due to the quarry operation and maintenance (related to permanent infrastructure and road networks) are reduced, within the avoided impacts of creating a new mining facility.

Table 5.10 Example of inventory data for land use

C&DW landfill		
Transformation, from vegetation to industrial area	0.068	m^2/ton
Occupation, dump site	$0.068 * 15$	$\text{m}^2/\text{ton} * \text{year}$
Transformation, from industrial to vegetation area	0.068	m^2/ton
Quarry		
Transformation, from vegetation to industrial area	0.033	m^2/ton
Occupation, mineral extraction	$0.033 * 40$	$\text{m}^2/\text{ton} * \text{year}$
Transformation, from industrial to vegetation area	0.033	m^2/ton
C&DW recycling		
Occupation, industrial area	$0.15 * 15$	$\text{m}^2/\text{ton} * \text{year}$

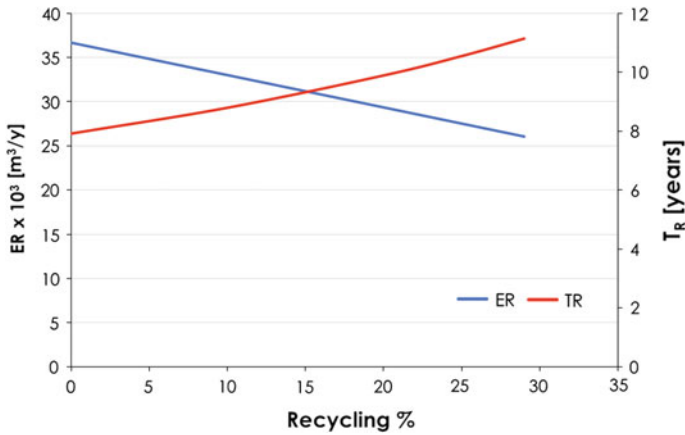


Fig. 5.9 Quarry exhaustion time: *ER* stands for extraction rate, *t_R* is the exhaustion time

5.8 Conclusions

The use of recycled aggregates for producing structural concrete allows reducing environmental emissions of concrete productive chain. However, this should be quantified and estimated through solid indicators, which should be easily understood and quantified.

A well-established set of methods is already applied into LCA tools, which enable a direct comparison of alternative products. Other indicators can be also used, to capture specific problems, e.g. land use and exhaustion time of a reserve of bulk natural materials. Those two indicators are particularly relevant when dealing with aggregates productive chains, because this activity causes high environmental emissions, in a confined region, hence involving local scale impacts. Land use and preservation of natural resources are however difficult to be accounted directly in LCA framework, because they are highly site-specific.

When dealing with LCA analysis of recycled aggregates concrete, huge lack of data is present in literature and in commercially available software. The first problem relates to the allocation of the upstream emissions due, e.g. in case of EAF slag, to the steel production. The “zero burden assumption” can be use if the recycled aggregates come from waste material, but not if the original material is considered as a by-product. In this case the up-stream emissions should be accounted through an allocation procedure (mass or economical allocation).

Recycled aggregates, coming from different origin (C&DW, steel slags, etc.) can play an important role to achieve the sustainability goals asked by the European Commission to the construction industry. Their use allows preserving existing natural resources and land use.

Transportation emissions should be carefully taken into account, because they can influence the environmental footprint of the aggregates. This has been observed

analyzing two aggregates having different specific weight. Additionally, attention should be paid in relation to the coverage of the market for recycled aggregates supply facilities, which may be not as available as for natural aggregates.

Concerning the emissions evaluation, when the scope of the analysis relates the influence of the use of a recycled component, emissions due to concrete manufacturing can be neglected, if no special mixing processes are required. It is worth to be recalled that cement is the main responsible for the huge emissions of concrete, and in this case transportation emission are significantly less relevant with respect to the case of aggregates analysis.

Acknowledgments The authors would like to thank EGAP Srl and ZeroCento Srl for their economical support and availability in supplying materials and data.

References

1. Van den Heede P, De Belie N (2012) Environmental impact and life cycle assessment (LCA) of traditional and 'green' concretes: literature review and theoretical calculations. *Cem Concr Compos* 34(4):431–442
2. European Commission, Eurostat (2009) Cement and concrete production statistics 2009. NACE Rev. 1.1
3. Ministero dello Sviluppo Economico (2009) Statistiche – Andamento della produzione di cemento anno 2009. Italy (in Italian), Rome
4. Metz B, Davidson OR, Bosch PR, Dave R, Meyer LA (2007) Climate change 2007: mitigation. Contribution of working group III to the fourth assessment report of the IPCC
5. Papayianni I (1987) Investigation of the pozzolanicity and hydraulic reactivity of a high-lime fly ash. *Mag Concr Res* 39(138):231–235
6. Langley WS, Carette GS, Malhotra VM (1989) Structural concrete incorporating high volumes of ASTM Class F fly ash. *ACI Mater J* 86(5):507–514
7. Evangelista L, de Brito J (2007) Mechanical behaviour of concrete made with fine recycled concrete aggregates. *Cem Concr Comp* 29:397–401
8. Manso JM, Polanco JA, Losañez M, González JJ (2006) Durability of concrete made with EAF slag as aggregate. *Cem Concr Comp* 28:528–534
9. UNFCCC COP9 Report (2004) Delivering the Kyoto baby. *Refocus*, international renewable energy magazine, pp 52–53
10. Naik TR (2008) Sustainability of concrete constructions. *Practice periodical on structural design and construction*, ASCE, pp 98–103
11. Habert G, Bouzidi Y, Chen C, Jullien A (2010) Development of a depletion indicator for natural resources used in concrete. *Res Conserv Recycl* 54:364–376
12. European Committee for Standardization (2006) ISO 14044:2006—Environmental management—Life cycle assessment—Requirements and guidelines. Technical Committee ISO/TC 207
13. European Committee for Standardization (2006)—ISO 14040:2006—Environmental management—Life cycle assessment—Principles and framework. Technical Committee ISO/TC 207
14. Zabalza Bribián I, Valero Capilla A, Aranda Usón A (2011) Life cycle assessment of building materials: comparative analysis of energy and environmental impacts and evaluation of the eco-efficiency improvement potential. *Build Environ* 46(5):1133–1140

15. Habert G, D'Espinose De Lacaillerie JB, Roussel N (2011) An environmental evaluation of geopolymer based concrete production: reviewing current research trends. *J Clean Prod* 19 (11):1229–1238
16. Marinkovic' S, Radonjanin V, Malešev M, Ignjatovic' I (2010) Comparative environmental assessment of natural and recycled aggregate concrete. *Waste Manage* 30:2255–2264
17. Fathifazl G, Abbas A, Razaqpur AG, Isgor OB, Fournier B, Foo S (2009) New mixture proportioning method for concrete made with coarse recycled concrete aggregate. *J Mater Civ Eng* 601–611
18. Pepe M, Toledo Filho RD, Koenders EAB, Martinelli E (2014) Alternative processing procedures for recycled aggregates in structural concrete. *Constr Build Mater* 69(124):132
19. Ferreira L, de Brito J, Barra M (2012) Influence of the pre-saturation of recycled coarse concrete aggregates on concrete properties. *Mag Concr Res* 63(8):617–627
20. European Commission Joint Research Centre JRC-IES (2011) Institute for Environment and Sustainability Supporting Environmentally Sound Decisions for Construction and Demolition (C&D) Waste Management, Luxembourg
21. Hjelmar O, van der Sloot HA, Comans RNJ, Wahlström M (2013) EoW criteria for waste-derived aggregates. *Waste Biomass Valoriz* 4(4):809–819
22. Blengini GA, Garbarino E (2010) Resources and waste management in Turin (Italy): the role of recycled aggregates in the sustainable supply mix. *J Clean Prod* 18:1021–1030
23. Cirilli F, Di Donato A, Di Sante L, Martini U, Miceli P (2015) V leaching in EAF slags. *Euroslag 2015 Conf Proceed*, Linz
24. United Nations Publication (2007) Indicators of sustainable development: guidelines and methodologies. United Nations, New York (US)
25. Agenda 21 (1992) Programme of Action for Sustainable Development, adopted at the United Nations Conference on Environment and Development, Rio de Janeiro (Brazil)
26. Bare JC, Hofstetter P, Pennington DW, Udo de Haes HA (2000) Midpoints versus endpoints: the sacrifices and benefits. *Int J Life Cycle Assess* 5(6):319–326
27. Guinée JB, Gorée M, Heijungs R, Huppes G, Kleijn R, de Koning A, van Oers L, Wegener Sleswijk A, Suh S, Udo de Haes HA, de Bruijn H, van Duin R, Huijbregts MAJ (2002) Handbook on life cycle assessment. Operational guide to the ISO standards. Iia: Guide. Iib: operational annex. Kluwer Academic Publishers, Dordrecht, p 692
28. Braunschweig A, Bär P, Rentsch C, Schmidt L, Wüest G (1997) *Bewerung in Ökobilanzen mit der Methode der ökologischen Knappheit, Ökofaktoren 1997, Methodik für Ökobilanzen*. Buwal Schriftenreihe Umwelt, 297. 100 pp (in German)
29. Goedkoop M, Spriensma R (2001) The Eco-indicator 99, a damage oriented method for Life Cycle Impact Assessment, methodology report. PRé Consultants, B.V. 132 pp. <http://www.pre.nl>
30. Jolliet O, Margni M, Charles R, Humbert S, Payet J, Rebitzer G, Rosenbaum R (2003) IMPACT 2002+: a new life cycle impact assessment methodology. *Int J Life Cycle Asses* 10:324–330
31. Blengini GA, Garbarino E, Solar S, Shields DJ, Hámor T, Vinai R, Agioutantis Z (2012) Life Cycle Assessment guidelines for the sustainable production and recycling of aggregates: the Sustainable Aggregates Resources Management project (SARMA). *J Clean Prod* 27:177–181
32. Lindeijer E, Müller-Wenk R, Steen B (2002) Impact assessment of resources and land use. In: Udo de Haes HA, Finnveden G, Goedkoop M, Hauschild M, Hertwich EG, Hofstetter P, Jolliet O, Olsen SI, Pennington DW, Potting J, Steen B (eds) *Life cycle assessment: striving towards best practice*. SETAC, Pensacola, USA, pp 11–64
33. Milà i, Canals L, Bauer C, Depestele J, Dubreuil A, Knuchen RF, Gaillard G, Michelsen O, Müller-Wenk R, Rydgren B (2007) Key elements in a framework for land use impact assessment within LCA. *Int J LCA* 12(1):5–15
34. Comité Européen de Normalisation (2008) EN 12620: 2008. Aggregates for concrete. Brussels, Belgium
35. Barbaro A, Giovannini F, Maltagliati S (2009) Linee guida per la valutazione delle emissioni di polveri provenienti da attività di produzione, manipolazione, trasporto, carico o stoccaggio

- di materiali polverulenti. AFR Modeling Forecasting - Province of Florence and ARPAT - Regional Agency for Environmental Protection of Tuscany (in Italian)
36. U.S. Environmental Protection Agency (1995) US-EPA. AP-42 Compilation of Air Pollutant Emission Factors
 37. National Atmospheric Emissions Inventory (2003) Vehicle speed emission factors. NAEI, UK
 38. National Pollutant Inventory (2000) Emission estimation technique manual for mining and processing of non-metallic minerals. Version 2.0. NPI, Australia
 39. Faleschini F, De Marzi P, Pellegrino C (2014) Recycled concrete containing EAF slag: Environmental assessment through LCA. *Euro J Environ Civil Eng* 18(9):1009–1024
 40. Ekvall T, Assefa G, Björklund A, Eriksson O, Finnveden G (2007) What life-cycle does and does not do in assessments of waste management. *Waste Manage* 27:989–996
 41. Josa A, Aguado A, Cardim A, Byars E (2007) Comparative analysis of the life cycle impact assessment of available cement inventories in the EU. *Cem Concr Res* 37(5):781–788
 42. Regione del Veneto (2013) PRAC 2013. Piano Regionale Attività di Cava. Delibera n. 2015, 4/11/2013, Venezia, Italy (in Italian)
 43. DM 27/09/2010 e ss.mm.ii (2010). Definizione dei criteri di ammissibilità dei rifiuti in discarica (in Italian)
 44. Agenzia Regionale per la Prevenzione e Protezione Ambientale del Veneto (2010) Osservatorio Regionale dei Rifiuti, ARPAV (in Italian)
 45. Faleschini F, Zanini MA, Pellegrino C, Pasinato S (2016) Sustainable management and supply of natural and recycled aggregates in a medium-size integrated plant. *Waste Manage* 49:146–155

Chapter 6

Experimental Database of EAF Slag Use in Concrete

6.1 Introduction

The existing literature about the use of EAF slag for civil engineering is not wide as for recycled aggregates from construction and demolition waste. Many aspects have not analyzed yet in details, mainly related to durability properties and long-term behavior. In the last years however many experimental works have been conducted, improving the number of works on this theme.

The database collects the results published in 46 papers [1–46], including works about slag characterization, and uses in cement-based materials and asphalt concrete. Between these, very few works deal with the use of stainless steel slag (EAF-S) [16], whereas the most deals with carbon steel slag (EAF-C). Table 6.1 summarizes the field of application of EAF slag in the collected works: 24 papers deals with concrete, 9 with asphalt and 11 with other applications (cement, mortars, composites, civil engineering works in general).

6.2 Physical Properties

Physical properties analyzed in this database are: apparent specific weight, water absorption, aggregates size, porosity, los angeles loss, flakiness and shape index. Table 6.2 summarizes the properties of the slag considered in the database: more than 50 types of slag are here listed, with their respective properties, both considering fine and coarse aggregate fractions. Almost all the experimental results gathered here characterize the slag as a heavy-weight material; a great variability is obtained in terms of absorption and porosity values. Few results are present in terms of geometrical characteristics of the material (flakiness and shape index), as well as about resistance against crushing and abrasion. With respect to those properties, which are commonly used to evaluate the hardness of the aggregates, the

Table 6.1 Field of applications of the collected works

References	Year	Field of application	Country
[1]	2004	Concrete/Mortars	Spain
[2]	2006	Cement	Canada
[3]	2007	General	Sweden
[4]	2014	Ceramics	Malaysia
[5]	2009	Asphalt	Sweden
[6]	2012	Concrete	Arab Emirates
[7]	2010	Asphalt	Italy
[8]	2011	Cement	Greece
[9]	2012	Asphalt	Italy
[10]	2007	Cement	Italy
[11]	2010	Concrete	Spain
[12]	2011	Asphalt	Italy
[13]	2013	Asphalt	Iran
[14]	2014	Concrete	Spain
[15]	2014	Asphalt	Iran
[16]	2015	Concrete	France
[17]	2015	Concrete	Taiwan
[18]	2006	Concrete	Spain
[19]	2013	Concrete	Italy
[20]	1011	Concrete	China
[21]	2013	Concrete	South Korea
[22]	2003	Concrete	Iran
[23]	2012	Asphalt	Croatia
[24]	2013	Concrete	Italy
[25]	2014	Soil	Nigeria
[26]	2009	Concrete	Italy
[27]	2014	Concrete	Greece
[28]	2014	Concrete	Italy
[29]	2015	Concrete	Italy
[30]	2015	Concrete	Italy
[31]	2009	Concrete	Jordan
[32]	2000	General	Spain
[33]	2011	Concrete	Greece
[34]	2015	Asphalt	Italy
[35]	2015	Concrete	Spain
[36]	2011	Asphalt	Italy
[37]	2004	General	Spain
[38]	2015	Concrete	USA
[39]	2015	General	Taiwan
[40]	2015	Polymer Matrix Composites	Italy

(continued)

Table 6.1 (continued)

References	Year	Field of application	Country
[41]	2011	Concrete	Spain
[42]	2009	Cement	India
[43]	2001	Concrete	Spain
[44]	2003	Concrete	Saudi Arabia
[45]	2014	Concrete	Jordan
[46]	2013	Cement	Belgium

experimental results obtained in literature agree in characterizing the slag as a very resistant material.

6.3 Chemical Composition

Chemical composition of EAF slag may vary highly depending on the production process and on the quality and origin of the steel scraps to be melted in the furnace. Table 6.3 shows the typical components of the slag: generally it is made by iron, calcium, silicon, aluminum oxides, and a minor content of other oxides, e.g. magnesium and manganese oxides. In almost all the analyzed works the most abundant oxides are iron ones: in some particular cases they can reach more than 90 % of the total [31], even though in some cases [16, 39] its content is very low. The average content of global iron oxides (both FeO and Fe₂O₃) is about 31.5 %. Then EAF slag are generally rich in calcium and silicon oxides (average content 28 and 16 % respectively). The average composition of the analyzed slag of the minor compounds is 8.2 % of aluminum oxides, 4.4 % of magnesium oxides and 4.3 % of manganese oxides. Concerning free lime content, few experimental results are present in literature [1, 9, 16, 18]: typically its value ranges between 0 and 10 % in mass.

6.4 Mineralogy

Concerning mineralogical phases, the most abundant phases in EAF slag are typically wüstite, magnetite and hematite (iron oxides), merwinite, larnite, gehlenite, bredigite (silicate oxides) and calcite, portlandite and eventually calcium silicates. Table 6.4 summarizes the main phases that can be detected through XRD analysis in EAF slag, and reported in the database. Other mineralogical phases that can be found are: dicalcium silicate [1, 3, 15, 16, 19, 24], tricalcium silicate [1, 19, 24], dicalcium ferrite [1, 19, 24], quartz [15], calcium hydroxide [2, 43], akermanite [15, 16], and other solid solutions e.g. of spinel or wüstite-type. Mineralogical phases

Table 6.2 Physical properties of EAF slag—database

References	Type	Apparent specific weight (t/m^3)	Absorption (%)	Size (mm)	Porosity (%)	Los Angeles loss (%)	Flakiness index (%)	Shape index (%)
[1]	Coarse EAF slag	3.35	3.29	4.76–25	10.5	20	–	–
[1]	Fine EAF slag	3.7	2.84	0–4.76	–	–	–	–
[3]	Type 1	3.25	–	–	–	–	–	–
[3]	Type 2	3.59	–	–	–	–	–	–
[6]	EAF	3.68	–	–	–	–	–	–
[7]	Type 1	3.86	–	0–10	4.66	24	1.4–2.8	1.5–2.5
[7]	Type 2	3.91	–	0–10	4.09	15.5–21.5	3.7–10.3	3.7–20.3
[9]	Type 1	3.91	1.5–1.7	0–32	–	22–23	4.0–6.0	3.0–4.0
[9]	Type 2	3.9	2.0–2.2	0–32	–	23	1.0–3.0	1.0–3.0
[11]	EAF	3.32	1.73	–	–	–	–	–
[12]	Type 1	3.86	–	0–10	4.66	24	1.4–2.8	1.5–2.5
[12]	Type 2	3.91	–	0–10	4.09	15.5–21.5	3.7–10.3	3.7–20.3
[13]	Fine EAF slag	3.06	–	–	–	–	–	–
[13]	Coarse EAF slag	3.01	–	–	–	14.2	–	–
[14]	Fine EAF slag	3.31	2.47	0–4	–	–	–	–
[14]	Coarse EAF slag 1	3.57	0.81	4.0–10	–	–	–	–
[14]	Coarse EAF slag 2	3.53	1.18	10–20.0	–	20	–	–
[15]	Filler EAF	–	–	–	–	–	–	–
[15]	Fine EAF slag	2.95	1.8	–	–	–	–	–
[15]	Coarse EAF slag 1	3.05	2.1	–	–	13.4	–	–

(continued)

Table 6.2 (continued)

References	Type	Apparent specific weight (t/m^3)	Absorption (%)	Size (mm)	Porosity (%)	Los Angeles loss (%)	Flakiness index (%)	Shape index (%)
[17]	Type 1	3.44	3	4.8-2.4	40.75	-	-	-
[17]	Type 2	3.44	3	9.5-4.8	42.96	-	-	-
[18]	Coarse EAF slag	3.35	10.5	4.0-20	-	-	-	-
[18]	Fine EAF slag	3.7	-	0-4	-	<20	-	-
[19]	Fine EAF slag	3.78	1.613	0-4	-	-	-	-
[19]	Coarse EAF slag	3.85	0.53	4.0-22	-	<20	-	-
[20]	Fine EAF slag	3.59	1.2	0-5	-	-	-	-
[20]	Coarse EAF slag	3.28	0.96	5.0-25	-	-	-	-
[21]	Coarse EAF slag	3.78	2	-	-	-	-	-
[21]	Fine EAF slag	3.77	2	-	-	-	-	-
[22]	Coarse EAF slag	3-3.7	0.2-2	-	-	20-25	-	-
[24]	EAF slag	3.88-3.9	0.4-0.5	-	-	-	-	-
[26]	EAF slag	3.64-3.97	0.18-0.45	2-22.4	-	-	3.6-6.1	1.5-2.7
[27]	Coarse EAF slag	3.3	3.16	4.0-12	-	-	-	-
[27]	Fine EAF slag	-	3.73	0-4	-	-	-	-
[28]	EAF slag	3.876-3.9	0.4-0.5	4-22.4	-	<20	8	-
[29]	EAF slag	3.854	0.95	4.16.00	-	<20	-	-
[30]	EAF slag	3.854	0.95	4-16.0	-	-	-	-

(continued)

Table 6.2 (continued)

References	Type	Apparent specific weight (t/m^3)	Absorption (%)	Size (mm)	Porosity (%)	Los Angeles loss (%)	Flakiness index (%)	Shape index (%)
[31]	Fine EAF slag	3.25	0.8	0-10	-	-	-	-
[31]	Coarse EAF slag	-	1.65	2-37.5	-	-	-	-
[32]	Type 1	3.37	1.56	-	-	-	-	-
[32]	Type 2	3.13	4.21	-	-	-	-	-
[33]	Coarse EAF slag	3.33	2.5	4-31.5	-	-	8	-
[33]	Fine EAF slag	-	3.16	0-4	-	-	-	-
[34]	EAF slag	-	-	-	-	28	12	-
[35]	Type 1	3.01	7.37	-	14.4	-	-	-
[35]	Type 2	3.32	3.35	-	7.8	-	-	-
[36]	Type 1	3.86	-	-	4.66	24	1.4-2.8	1.5-2.5
[36]	Type 2	3.91	-	-	4.09	15.5-21.5	3.7-10.3	3.7-20.3
[38]	EAF slag	3.89	1.75	0-25	-	-	-	-
[39]	Fine EAF slag	-	1.2-1.8	-	-	-	-	-
[39]	Coarse EAF slag	-	1.8-5.4	-	-	-	-	-
[41]	Coarse EAF slag	3.35	-	2-19.0	-	18	-	-
[41]	Fine EAF slag	3.7	-	0-2	-	14	-	-
[43]	Fine EAF slag	3.35	3.385	-	-	-	-	-

(continued)

Table 6.2 (continued)

References	Type	Apparent specific weight (t/m^3)	Absorption (%)	Size (mm)	Porosity (%)	Los Angeles loss (%)	Flakiness index (%)	Shape index (%)
[43]	Coarse EAF slag 1	3.75	1.41	-	-	-	-	-
[43]	Coarse EAF slag 2	3.67	1.13	-	-	-	-	-
[44]	EAF slag	3.51	0.12	2-19.0	-	11.6	-	-
[45]	EAF slag	-	0.8	-	-	-	-	-

Table 6.3 Chemical composition of EAF slag—database

References		FeO/Fe ₂ O ₃	Cr ₂ O ₃	CaO	TiO ₂	SiO ₂	Al ₂ O ₃	MgO	MnO	P ₂ O ₅	SO ₃
[1]	EAF	50		25		11	5	5	4		
[2]	EAF	24.9		36.5		12.9	5.9	9.5			0.28
[3]	EAF	25.9		38.8		14.1	6.7	3.9	5		
[4]	EAF	31.7– 32.52		29– 29.45		19.73– 20.5	8.83– 8.58	2.6– 3.13	3.94– 3.95		
[6]	EAF	24.2		39.62		17.23	4.08	9.23	0.7		
[7]	Type 1	32.84	4.03	29.6	0.25	13.02	9.3	3.65	5.09		
[7]	Type 2	33.12	4.07	29.33	0.36	12.95	9.28	3.62	5.15		
[8]	EAF	26.3	1.38	32.5	0.47	18.1	13.3	2.53	3.94	0.48	0.44
[9]	Type 1	25.38		20.375		15.05	5.835	2.16			
[9]	Type 2	36.21		17.37		18.845	5.82	2.26			
[10]	EAF	2.1		53.09		28.48	5.86	2.1			1.08
[11]	EAF	37.6	1.83	21.77	0.64	18.28	8.32	6.14	4.43	0.21	0.23
[12]	Type 1	32.84	4.03	29.6	0.35	13.02	9.3	3.65	5.09		
[12]	Type 2	33.12	4.07	29.33	0.36	12.95	9.28	3.62	5.15		
[13]	EAF	35.16		25.58	1.595	18.72	2.75	7.5	0.304		
[14]	EAF	25.8	1.6	30.2	1	19	12.7	4.6	4.8		
[15]	EAF	25.75		38.86	2.11	17.47	4.03	5.01	2.32	1.5	0.48
[16]	EAF	0.5	3.5	41.7	2.2	34.7	6.3	9.1	2.1		
[17]	EAF	18.87		23.4		21.38	6.09	8.32			0.03
[18]	EAF	18.87		23.9		15.3	7.4	5.1	4.5		0.1
[19]	EAF	33.75	2.17	27.79		16.61	10.99	4.02	4.67		
[20]	EAF	18		34.09		28.92	3.72	4.15	2.23		0.13
[21]	EAF	21.2		26.7		17.7	12.2	5.3	7.9		
[22]	EAF	15–30		40–52		10.0– 19	1–3.0	5– 10.0	5–8.0	0.5– 1	
[24]	EAF	33.75	2.17	27.79		16.61	10.99	4.02	4.67		
[26]	EAF	37.72– 44.8	2.5– 4.1	24.2– 29.5		10.1– 14.7	5.2– 7.2	1.9– 4.6	5.1– 5.7		
[28]	EAF	33.75	2.17	27.79		16.61	10.99	4.02	4.67		
[30]	EAF	33.28	2.67	30.3		14.56	10.2	2.97	4.34		
[31]	EAF	97.05		0.4	0.01	0.8		0.4	1.07		
[32]	Type 1	27.41	0.7	29.11	0.54	6.04	14.07	3.35	15.58	1.24	
[32]	Type 2	34.36	0.99	24.4	0.56	15.35	12.21	2.91	5.57	1.19	
[33]	EAF			20.6		22.8	8.5	3.63			
[35]	EAF	30.8		32.52	0.59	17.17	7.96	4.56	3.8	0.58	0.25
[35]	EAF	27.54		25.72	0.71	17.88	11.62	3.82	4.15	0.46	0.01
[36]	Type 1	32.84	4.03	29.6	0.35	13.02	9.3	3.65	5.09		

(continued)

Table 6.3 (continued)

References		FeO/Fe ₂ O ₃	Cr ₂ O ₃	CaO	TiO ₂	SiO ₂	Al ₂ O ₃	MgO	MnO	P ₂ O ₅	SO ₃
[36]	Type 2	33.12	4.07	29.33	0.36	12.95	9.28	3.62	5.15		
[38]	EAF	23.9		18.8	0.5	9.6	3.9	8.5	3.5		
[39]	EAF	0.59	4.85	44.67	1.69	33.64	3.75	6.16	3.05		0.48
[40]	EAF	37.53	2.77	27.92		9.71	8.21	2.17	4.68	0.34	
[41]	EAF	42		24		15.5	7.5	5			0.5
[42]	EAF	20–30		25–35		8–18.0	3–10.0	3–9.0			<0.5
[43]	EAF	32–46	1–2.5	25–35		10–16.0	5–10.0	3.3–6.4	2–6.5		
[44]	EAF	89		10		1					
[45]	EAF	37		29.7		15.5	4.7	6.5	2.9	0.4	0.3
[46]	EAF	26.3	1.38	32.5	0.47	18.1	13.3	2.53	3.94	0.48	0.44

can vary before and after the pre-treating operations used for dimensionally stabilize the slag, particularly due to cooling operations. The additions used in the furnace influence the mineralogy of the material too. According to the XRD analysis results here reported, it is possible to state that generally EAF slag present abundant crystalline material.

6.5 Leaching

Concerning the leaching of potentially toxic compounds into water body, leaching tests have been collected into the database. Tests are conducted according to the standard method described in EN 12457-2, using a solid-to-volume ratio equal to 2 and water as liquid. Table 6.5 summarizes the collected results, where *SL* states for sulfates, *FL* for fluorides, *Cr* is the total chromium, *CL* are chlorides, *NI* the nitrates, and *CY* the cyanides. Results are expressed in (mg/l). Other than the evaluation of potential leaching of toxic compounds, also the leaching of other main slag compounds have been analyzed in [3], where Ca, Mg, Fe, Si, Al, Mo and V have been also detected. According to the collected results, it is significant to note that chromium and vanadium compounds are the objective of major concern in the environmental perspective. However it should be recalled that the present standard about leaching experimental method is currently under revision by CEN/TC 351 group.

Table 6.4 Chemical composition of EAF slag—database

References		Wustite	Merwinite	Lamite	Gehlenite	Magnetite	Bredigite	Calcite	Hematite	MgO
[1]	EAF	x								
[2]	EAF	x						x		
[3]	EAF	x	x							
[4]	EAF	x		x	x					
[6]	EAF	x		x		x	x			
[15]	EAF	x						x		
[16]	EAF		x			x				
[19]	EAF	x							x	x
[24]	EAF	x							x	x
[30]	EAF	x		x	x	x				
[32]	EAF				x	x	x			x
[37]	EAF-1			x	x		x			
[37]	EAF-2	x		x	x		x			
[38]	EAF	x				x	x	x		
[42]	EAF		x	x	x	x				
[43]	EAF	x	x	x	x	x	x	x	x	x
[46]	EAF	x	x	x	x	x				

Table 6.5 Leaching potential of EAF slag—database

	1	3	4	7	9	12	19	24	26	28	34	36	40
SL	93.7				5.5		<200	<200	15-50	<200			
FL	6.6				0.301	<1.5	<1.5	<1.5	<1.5				
Cr	0.02	0.73	0.005	<0.05	0.0148	<0.05	<0.002	<0.002	<0.05	<0.002	<0.04	<0.05	0.131
V		0.3		<0.01	0.116	<0.01	0.103	0.103	<0.25	0.103		<0.25	
Cd			0	<0.005	<0.001	<0.005	<0.003	<0.003	<0.005	<0.003	<0.001	<0.005	<0.001
Cu			0.005	<0.05	0.0085	<0.05	<0.001	<0.001	<0.005	<0.001	0.01	<0.05	<0.005
Mn			0										
Pb			0.041	<0.05		<0.05	<0.04	<0.04	<0.05	<0.04	<0.02	<0.05	<0.005
Zn			0.04	<3	0.07	<3	<0.03	<0.03	<0.059	<0.03	<0.01	<3	0.011
Hg				<0.001	<0.001	<0.001	<0.001	<0.001	<0.001	<0.001	<0.001	<0.001	<0.005
Se				<0.01	0.001	<0.01	<0.01	<0.01	<0.01	<0.01	<0.005	<0.01	<0.002
As				<0.25	<0.005	<0.25	<0.02	<0.02	<0.05	<0.02	<0.005	<0.05	<0.005
Be				<0.01		<0.01	<0.005	<0.005	<0.01	<0.005		<0.01	
Tl				<0.003		<0.0026						<0.0026	
Co				<0.25		<0.25	<0.01	<0.01	<0.25	<0.01		<0.25	
Sb				0.01		0.01						0.01	
Sn				<0.002		<0.002						<0.002	
Ba					0.263	0.0125	0.0125	<0.14	0.0125	<0.5		0.776	
CL					2.1		<75	<75	5.0-75	<75			
NI					2.3		<40	<40	<50	<40			
CY							<0.03	<0.03	<50	<0.03			

6.6 Application in Concrete as Recycled Aggregate

The database collects the results of 17 works about the use of EAF slag for producing structural concrete. Table 6.6 summarizes the mixture details of the concretes produced in 17 works among the whole 24 ones analyzed in this chapter, for which it was possible to gather the full composition and the hardened properties of the conglomerates. Parameters such as water and cement dosage and type, water-to-binder ratio, substitution ratio, aggregates dosage and type, use of supplementary cementing material (e.g. fly ashes, silica fume, etc.), water reducing admixture and air entrainer dosage are here included in the description of the mixtures. All the components are expressed in (kg/m^3): water, cement dosage, NA (natural aggregate) sand, NA gravel, EAF sand, EAF gravel, WRA (water-reducing admixture), SCM (supplementary cementing material) and lastly AEA (air-entrainer admixture). An ID has been assigned to each mixture, according to the nomenclature given by the authors in the original papers. Cement type has been reported, as well as the water-to-binder ratio (w/b). R states for the replacement ratio, where the ratio between EAF over natural aggregates is shown, divided both for the fine (S) and the coarse fraction (G). The type of the natural aggregates has been reported: L states for limestone, DS for dune sand, CS for crushed sand, Si for siliceous aggregates, B for baritic aggregates, $Si-C$ for siliceous-calcareous aggregates, C for calcareous aggregates, D for dolomitic aggregates, FSi for siliceous filler, Fl for limestone filler, S for sand (0–4 mm), G for gravel (>4 mm) and lastly RCA states for recycled aggregates from construction and demolition waste. Between the SCM, fly ashes (FA type F and C) have been used in the works included in the database, as well as silica fume (SF), ladle-furnace slag (LFS) and ground-granulated blast furnace slag ($GGBF$). Hence, in many case, ternary concretes including more source of recycled components have been already investigated, with the aim to address the effects of the substitution on the overall property of the material.

Fresh concrete properties are also shown in Table 6.6: fresh concrete density (expressed in kg/m^3) and slump value (mm), evaluated just after concrete mixing are reported. Hardened concrete properties analyzed in the database are: compressive strength f_{cm} at 7, 28 and 90 days of standard maturation, tensile strength f_{ctm} (evaluated through splitting test), secant elastic modulus E_{cm} and flexural strength f_{cfm} (evaluated through bending test). Compressive strength (expressed in MPa) refers to cylindrical strength (related to cylindrical specimens with diameter and length respectively of 100 and 200 mm). When secant modulus (expressed in GPa) was not present in the original papers, the dynamic modulus has been used in the database. Durability-related properties analyzed in the existing literature are very different one from the other: many authors have investigated the potential expansion of the slag in concrete through ASTM D-4792 test, which aims to analyze the specific weight and compressive strength losses after curing the specimens in hot water (typically around 70 °C) for a prolonged period [1, 18, 19, 41]. Many other works focus also on alternation of severe deteriorating conditions, e.g.

Table 6.6 Concrete mixtures details including EAF slag

References	Mix ID	Water (kg/m ³)	Cement (kg/m ³)	Cement type	w/b	R (%)	NA type	NA S (kg/m ³)
[1]	M-1	186	310	OPC type I	0.60	0	L	930
[1]	M-2	186	310	OPC type I	0.60	100	–	–
[1]	M-3	186	310	OPC type I	0.60	0S-100G	L	960
[1]	M-4	186	310	OPC type I	0.60	50S-100G	L	480 (FI)
[1]	M-5	186	310	OPC type I	0.60	50S-100G	L	480 (FI)
[1]	M-6	186	310	OPC type I	0.60	66S-100G	L	330 (FI)
[6]	30	172	330	OPC type I	0.52	0S-70G	L + DS + CS	830
[6]	50	152	400	OPC type I	0.38	0S-70G	L + DS + CS	825
[6]	70	133	460	OPC type I	0.29	0S-70G	L + DS + CS	830
[6]	50FA	144	280	OPC type I	0.36	0S-70G	L + DS + CS	825
[6]	70SF	133	433	OPC type I	0.29	0S-70G	L + DS + CS	830
[11]	TRAD	165	300	CEM I 52.5R	0.65	0	L	879
[11]	EAF25	165	300	CEM I 52.5R	0.65	0S- 30G	L	878
[11]	EAF50	165	300	CEM I 52.5R	0.66	0S-50G	L	878
[11]	EAF100	165	300	CEM I 52.5R	0.67	0S- 100G	L	851
[11]	TRAD-2	175	350	CEM I 52.5R	0.57	0	L	766
[11]	EAF25-2	175	350	CEM I 52.5R	0.58	0S- 30G	L	764.7
[11]	EAF50-2	175	350	CEM I 52.5R	0.59	0S-50G	L	764.7
[11]	EAF100-2	175	350	CEM I 52.5R	0.60	0S- 100G	L	750.8
[14]	TRAD A	145	275	CEM II/A-L 42.5R	0.53	0	L	1003
[14]	TRAD B	155	275	CEM II/A-L 42.5R	0.56	0	L	1003
[14]	EAF-1 A	152.7	275	CEM II/A-L 42.5R	0.56	0S-100G	Si	295 (FSi)
[14]	EAF-1 B	152.7	275	CEM II/A-L 42.5R	0.56	0S-100G	Si	295 (FSi)
[14]	EAF-2 A	143.2	275	CEM II/A-L 42.5R	0.52	0S-100G	Si	295 (FSi)
[14]	EAF-2 B	149.5	275	CEM II/A-L 42.5R	0.54	0S-100G	Si	295 (FSi)
[14]	EAF-3 A	140	275	CEM II/A-L 42.5R	0.51	0S-100G	L	300 (FI)
[14]	EAF-3 B	133	275	CEM II/A-L 42.5R	0.48	0S-100G	L	300 (FI)

(continued)

Table 6.6 (continued)

References	Mix ID	Water (kg/m ³)	Cement (kg/m ³)	Cement type	w/b	R (%)	NA type	NA S (kg/m ³)
[14]	EAF-4 A	140	275	CEM II/A-L 42.5R	0.51	0S-100G	L	300 (Fl)
[14]	EAF-4 B	146.4	275	CEM II/A-L 42.5R	0.53	0S-100G	L	300 (Fl)
[14]	BAR A	140	275	CEM II/A-L 42.5R	0.51	0	B	1003
[14]	BAR B	123	275	CEM II/A-L 42.5R	0.45	0	B	1003
References	Mix ID	NA G (kg/m ³)	EAF S (kg/m ³)	EAF G (kg/m ³)	WRA (kg/m ³)	SCM (kg/m ³)	AEA (kg/m ³)	Density (kg/m ³)
[1]	M-1	935	–	–	–	–	–	2340
[1]	M-2	–	950	945	–	–	–	2390
[1]	M-3	–	–	895	–	–	–	2380
[1]	M-4	–	480	895	–	–	–	2500
[1]	M-5	–	480	620	–	–	–	2560
[1]	M-6	–	630	620	–	–	–	2590
[6]	30	390	–	880	6.50	–	–	2790
[6]	50	390	–	875	8.50	–	–	2750
[6]	70	390	–	875	7.00	–	–	2790
[6]	50FA	395	–	880	10.00	120 (FA– F)	–	2810
[6]	70SF	390	–	875	7.00	27 (SF)	–	2790
[11]	TRAD	1137	–	–	1.50	–	–	2410
[11]	EAF25	853	–	358	1.65	–	–	2490
[11]	EAF50	568	–	716.5	2.10	–	–	2580
[11]	EAF100	–	–	1467.6	2.85	–	–	2730
[11]	TRAD-2	1182	–	–	0.00	–	–	–
[11]	EAF25-2	886.1	–	372.4	2.28	–	–	–
[11]	EAF50-2	590.8	–	744.8	2.98	–	–	–
[11]	EAF100-2	–	–	1507.6	5.60	–	–	–
[14]	TRAD A	938	–	–	2.76	–	–	2364
[14]	TRAD B	938	–	–	2.76	–	–	2374
[14]	EAF-1 A	–	1130	967	2.76	–	–	2822
[14]	EAF-1 B	–	1130	967	3.58	–	–	2823
[14]	EAF-2 A	–	1130	967	2.76	–	–	2813
[14]	EAF-2 B	–	1130	967	3.58	–	–	2820
[14]	EAF-3 A	–	1130	967	2.76	–	–	2815
[14]	EAF-3 B	–	1130	967	3.58	–	–	2809
[14]	EAF-4 A	–	1130	0	2.76	–	–	2815

(continued)

Table 6.6 (continued)

References	Mix ID	Water (kg/m ³)	Cement (kg/m ³)	Cement type	w/b	R (%)	NA type	NA S (kg/m ³)		
[14]	EAF-4 B	–	1130	0	3.58	–	–	2822		
[14]	BAR A	2201	–	–	2.76	–	–	3622		
[14]	BAR B	2201	–	–	2.76	–	–	3605		
References	Mix ID	Slump (mm)	fcm 7 (MPa)	fcm 28 (MPa)	fctm (MPa)	Ecm (GPa)	fcm (MPa)	fcm 90 (MPa)	WA (%)	Porosity (%)
[1]	M-1	70	29.4	36.3	–	–	–	41.30	5.5	13
[1]	M-2	Collapsed	12.8	20.6	–	–	–	22.40	12.7	30.4
[1]	M-3	50	26.3	32.3	–	–	–	38.70	6.8	16.2
[1]	M-4	70	28.9	34.8	–	–	–	42.20	6.5	16.1
[1]	M-5	120	22.8	29.8	–	–	–	39.50	6.9	17.6
[1]	M-6	70	25.6	31.9	–	–	–	40.40	7.6	19.6
[6]	30	190	45.7	49.8	2.87	–	–	–	2.6	–
[6]	50	220	55.6	66.4	3.53	–	–	–	1.9	–
[6]	70	230	70.6	83.0	4.37	–	–	–	1.03	–
[6]	50FA	210	62.3	74.7	3.13	–	–	–	1.6	–
[6]	70SF	220	78.9	103.8	2.87	–	–	–	0.8	–
[11]	TRAD	90	–	22.0	2.40	30.14	–	–	–	–
[11]	EAF25	70	–	24.1	2.50	30.26	–	–	–	–
[11]	EAF50	70	–	22.1	2.20	26.31	–	–	–	–
[11]	EAF100	90	–	20.3	1.80	23.55	–	–	–	–
[11]	TRAD-2	75	–	39.3	3.60	36.37	–	–	–	–
[11]	EAF25-2	95	–	47.1	3.30	35.58	–	–	–	–
[11]	EAF50-2	90	–	46.3	3.30	36.22	–	–	–	–
[11]	EAF100-2	55	–	54.1	3.30	36.20	–	–	–	–
[14]	TRAD A	30	42.7	50.5	–	40.95	–	60.7	–	–
[14]	TRAD B	70	36.6	50.4	–	38.16	–	53.2	–	–
[14]	EAF-1 A	20	37.1	49.8	–	43.11	–	55.4	–	–
[14]	EAF-1 B	20	40.4	50.7	–	46.12	–	59.1	–	–
[14]	EAF-2 A	20	39.0	51.2	–	43.72	–	57.0	–	–
[14]	EAF-2 B	10	39.9	50.8	–	45.23	–	57.5	–	–
[14]	EAF-3 A	5	43.9	56.1	–	48.30	–	63.4	–	–
[14]	EAF-3 B	50	33.2	41.7	–	43.06	–	51.2	–	–
[14]	EAF-4 A	60	32.8	45.3	–	43.22	–	50.7	–	–
[14]	EAF-4 B	40	35.5	46.4	–	44.86	–	54.0	–	–
[14]	BAR A	90	28.3	37.2	–	26.04	–	39.1	–	–
[14]	BAR B	90	31.1	39.1	–	27.58	–	42.2	–	–
References	Mix ID	WD (mm)	Durability test 1	Delta	Durability test 2					
[1]	M-1	32	ASTM D-4792	–0.26 %w; +2.86 % MPa	Soundness					
[1]	M-2	Total	ASTM D-4792	–1.88 %w; +10.4 % MPa	Soundness					
[1]	M-3	45	ASTM D-4792	–0.7 %w; +6.9 % MPa	Soundness					
[1]	M-4	5	ASTM D-4792	–0.9 %w; +9.13 % MPa	Soundness					
[1]	M-5	5	ASTM D-4792	–0.8 %w; +8.59 % MPa	Soundness					

(continued)

Table 6.6 (continued)

References	Mix ID	WD (mm)	Durability test 1	Delta	Durability test 2	
[1]	M-6	25	ASTM D-4792	-0.6 %w; +9.97 % MPa	Soundness	
[6]	30	NIL	ASTM C1202	NN	-	
[6]	50	NIL	ASTM C1203	NN	-	
[6]	70	NIL	ASTM C1204	NN	-	
[6]	50FA	NIL	ASTM C1205	NN	-	
[6]	70SF	NIL	ASTM C1206	NN	-	
[11]	TRAD	-	-	-	-	
[11]	EAF25	-	-	-	-	
[11]	EAF50	-	-	-	-	
[11]	EAF100	-	-	-	-	
[11]	TRAD-2	-	4H @800 °C	-62 % MPa	Sorptivity	
[11]	EAF25-2	-	4H @800 °C	-48 % MPa	Sorptivity	
[11]	EAF50-2	-	4H @800 °C	-49 % MPa	Sorptivity	
[11]	EAF100-2	-	4H @800 °C	-56 % MPa	Sorptivity	
[14]	TRAD A	-	-	-	Attenuation coeff	
[14]	TRAD B	-	-	-	Attenuation coeff	
[14]	EAF-1 A	-	-	-	Attenuation coeff	
[14]	EAF-1 B	-	-	-	Attenuation coeff	
[14]	EAF-2 A	-	-	-	Attenuation coeff	
[14]	EAF-2 B	-	-	-	Attenuation coeff	
[14]	EAF-3 A	-	-	-	Attenuation coeff	
[14]	EAF-3 B	-	-	-	Attenuation coeff	
[14]	EAF-4 A	-	-	-	Attenuation coeff	
[14]	EAF-4 B	-	-	-	Attenuation coeff	
[14]	BAR A	-	-	-	Attenuation coeff	
[14]	BAR B	-	-	-	Attenuation coeff	
References	Mix ID	Delta	Durability test 3	Delta	Durability test 4	Delta
[1]	M-1	-	-	-	-	-
[1]	M-2	-	-	-	-	-
[1]	M-3	-	-	-	-	-
[1]	M-4	-	-	-	-	-
[1]	M-5	-	-	-	-	-
[1]	M-6	-	-	-	-	-
[6]	30	-	-	-	-	-
[6]	50	-	-	-	-	-
[6]	70	-	-	-	-	-
[6]	50FA	-	-	-	-	-
[6]	70SF	-	-	-	-	-
[11]	TRAD	-	-	-	-	-
[11]	EAF25	-	-	-	-	-
[11]	EAF50	-	-	-	-	-
[11]	EAF100	-	-	-	-	-
[11]	TRAD-2	-	Length variation	-	-	-

(continued)

Table 6.6 (continued)

References	Mix ID	Delta	Durability test 3	Delta	Durability test 4	Delta		
[11]	EAF25-2	–	Length variation	–	–	–		
[11]	EAF50-2	–	Length variation	–	–	–		
[11]	EAF100-2	–	Length variation	–	–	–		
[14]	TRAD A	–	–	–	–	–		
[14]	TRAD B	–	–	–	–	–		
[14]	EAF-1 A	–	–	–	–	–		
[14]	EAF-1 B	–	–	–	–	–		
[14]	EAF-2 A	–	–	–	–	–		
[14]	EAF-2 B	–	–	–	–	–		
[14]	EAF-3 A	–	–	–	–	–		
[14]	EAF-3 B	–	–	–	–	–		
[14]	EAF-4 A	–	–	–	–	–		
[14]	EAF-4 B	–	–	–	–	–		
[14]	BAR A	–	–	–	–	–		
[14]	BAR B	–	–	–	–	–		
References	Mix ID	Water (kg/m ³)	Cement (kg/m ³)	Cement type	w/b	R (%)	NA type	NA S (kg/m ³)
[16]	TRAD	150	500	CEM I 52.5R	0.30	0	Si-C	649
[16]	EAF50	150	500	CEM I 52.5R	0.30	0S-50G	Si-C	649
[16]	EAF100	150	500	CEM I 52.5R	0.30	0S-100G	Si-C	649
[17]	35A70	158	451	OPC type I	0.35	100S	–	–
[17]	35A80	180	515	OPC type I	0.35	100S	–	–
[17]	35A90	203	579	OPC type I	0.35	100S	–	–
[17]	35A70+	158	451	OPC type I	0.35	100S	–	–
[17]	35A80+	180	515	OPC type I	0.35	100S	–	–
[17]	35A90+	203	579	OPC type I	0.35	100S	–	–
[17]	45A70+	176	392	OPC type I	0.45	100S	–	–
[17]	45A80+	202	448	OPC type I	0.45	100S	–	–
[17]	45A90+	227	504	OPC type I	0.45	100G	–	–
[17]	35B70	150	427	OPC type I	0.35	100G	–	–
[17]	35B80	171	488	OPC type I	0.35	100G	–	–
[17]	35B90	192	549	OPC type I	0.35	100G	–	–
[17]	35B70+	150	427	OPC type I	0.35	100G	–	–
[17]	35B80+	171	488	OPC type I	0.35	100G	–	–
[17]	35B90+	192	549	OPC type I	0.35	100G	–	–
[17]	45B70+	167	372	OPC type I	0.45	100G	–	–
[17]	45B80+	191	425	OPC type I	0.45	100G	–	–
[17]	45B90+	215	478	OPC type I	0.45	100G	–	–
[17]	35C70	138	393	OPC type I	0.35	0	–	1684
[17]	35C80	157	449	OPC type I	0.35	0	–	1684

(continued)

Table 6.6 (continued)

References	Mix ID	Water (kg/m ³)	Cement (kg/m ³)	Cement type	w/b	R (%)	NA type	NA S (kg/m ³)		
[17]	35C90	177	505	OPC type I	0.35	0	–	1684		
[17]	35C70+	138	393	OPC type I	0.35	0	–	1684		
[17]	35C80+	157	449	OPC type I	0.35	0	–	1684		
[17]	35C90+	177	505	OPC type I	0.35	0	–	1684		
[17]	45C70+	154	342	OPC type I	0.45	0	–	1684		
[17]	45C80+	176	391	OPC type I	0.45	0	–	1684		
[17]	45C90+	198	440	OPC type I	0.45	0	–	1684		
[18]	M-1	186	310	CEM I 42.5 R	0.60	0	L	930		
References	Mix ID	NA G (kg/m ³)	EAF S (kg/m ³)	EAF G (kg/m ³)	WRA (kg/m ³)	SCM (kg/m ³)	AEA (kg/m ³)	Density (kg/m ³)		
[16]	TRAD	1052	–	0	3.30	–	–	2420		
[16]	EAF50	526	–	592	3.60	–	–	2600		
[16]	EAF100	–	–	1183	3.80	–	–	2640		
[17]	35A70	–	1960	–	–	–	–	2288		
[17]	35A80	–	1960	–	–	–	–	2361		
[17]	35A90	–	1960	–	–	–	–	2410		
[17]	35A70+	–	1960	–	0.45	–	–	2348		
[17]	35A80+	–	1960	–	0.52	–	–	2397		
[17]	35A90+	–	1960	–	0.58	–	–	2452		
[17]	45A70+	–	1960	–	0.39	–	–	2275		
[17]	45A80+	–	1960	–	0.45	–	–	2347		
[17]	45A90+	–	1960	–	0.50	–	–	2391		
[17]	35B70	–	–	1850	–	–	–	2042		
[17]	35B80	–	–	1850	–	–	–	2205		
[17]	35B90	–	–	1850	–	–	–	2263		
[17]	35B70+	–	–	1850	0.43	–	–	2085		
[17]	35B80+	–	–	1850	0.49	–	–	2232		
[17]	35B90+	–	–	1850	0.55	–	–	2274		
[17]	45B70+	–	–	1850	0.37	–	–	1999		
[17]	45B80+	–	–	1850	0.43	–	–	2044		
[17]	45B90+	–	–	1850	0.48	–	–	2061		
[17]	35C70	–	–	–	–	–	–	1990		
[17]	35C80	–	–	–	–	–	–	2011		
[17]	35C90	–	–	–	–	–	–	2078		
[17]	35C70+	–	–	–	0.39	–	–	2027		
[17]	35C80+	–	–	–	0.45	–	–	2076		
[17]	35C90+	–	–	–	0.51	–	–	2111		
[17]	45C70+	–	–	–	0.34	–	–	1976		
[17]	45C80+	–	–	–	0.39	–	–	1991		
[17]	45C90+	–	–	–	0.44	–	–	2062		
[18]	M-1	935	–	–	–	–	–	2340		
References	Mix ID	Slump (mm)	fcm 7 (MPa)	fcm 28 (MPa)	fctm (MPa)	Ecm (GPa)	fcm (MPa)	fcm 90 (MPa)	WA (%)	Porosity (%)
[16]	TRAD	190	–	67.0	6.10	46.00	–	–	–	9.9

(continued)

Table 6.6 (continued)

References	Mix ID	Slump (mm)	fcm 7 (MPa)	fcm 28 (MPa)	fctm (MPa)	Ecm (GPa)	fcfm (MPa)	fcm 90 (MPa)	WA (%)	Porosity (%)
[16]	EAF50	180	–	71.0	6.20	50.00	–	–	–	10.9
[16]	EAF100	160	–	72.0	6.20	53.00	–	–	–	12.4
[17]	35A70	–	–	19.0	2.75	–	3.60	–	–	–
[17]	35A80	–	–	22.0	2.90	–	3.80	–	–	–
[17]	35A90	–	–	28.0	3.00	–	4.00	–	–	–
[17]	35A70+	–	–	16.5	2.50	–	3.25	–	–	–
[17]	35A80+	–	–	20.0	2.85	–	3.50	–	–	–
[17]	35A90+	–	–	27.0	2.95	–	3.90	–	–	–
[17]	45A70+	–	–	15.0	2.40	–	3.10	–	–	–
[17]	45A80+	–	–	16.0	2.60	–	3.35	–	–	–
[17]	45A90+	–	–	18.5	2.70	–	3.65	–	–	–
[17]	35B70	–	–	10.5	1.75	–	2.90	–	–	–
[17]	35B80	–	–	14.0	1.85	–	3.30	–	–	–
[17]	35B90	–	–	15.0	2.00	–	3.40	–	–	–
[17]	35B70+	–	–	9.0	1.60	–	2.75	–	–	–
[17]	35B80+	–	–	12.0	1.70	–	3.00	–	–	–
[17]	35B90+	–	–	14.0	1.80	–	3.15	–	–	–
[17]	45B70+	–	–	8.0	1.50	–	2.65	–	–	–
[17]	45B80+	–	–	11.0	1.60	–	2.95	–	–	–
[17]	45B90+	–	–	13.0	1.75	–	3.05	–	–	–
[17]	35C70	–	–	18.0	2.60	–	3.50	–	–	–
[17]	35C80	–	–	19.5	2.80	–	3.60	–	–	–
[17]	35C90	–	–	27.0	2.90	–	3.65	–	–	–
[17]	35C70+	–	–	15.5	2.00	–	3.10	–	–	–
[17]	35C80+	–	–	19.5	2.60	–	3.35	–	–	–
[17]	35C90+	–	–	20.0	2.75	–	3.60	–	–	–
[17]	45C70+	–	–	12.0	1.85	–	3.00	–	–	–
[17]	45C80+	–	–	14.0	2.20	–	3.10	–	–	–
[17]	45C90+	–	–	14.5	2.40	–	3.40	–	–	–
[18]	M-1	70	26.2	32.0	–	–	–	41.9	5.5	13
References	Mix ID	WD (mm)	Durability test 1		Delta			Durability test 2		
[16]	TRAD	–	Permeability		–			Soundness		
[16]	EAF50	–	Permeability		–			Soundness		
[16]	EAF100	–	Permeability		–			Soundness		
[17]	35A70	–	Permeability		–			Soundness		
[17]	35A80	–	Permeability		–			Soundness		
[17]	35A90	–	Permeability		–			Soundness		
[17]	35A70+	–	Permeability		–			Soundness		
[17]	35A80+	–	Permeability		–			Soundness		
[17]	35A90+	–	Permeability		–			soundness		
[17]	45A70+	–	Permeability		–			Soundness		
[17]	45A80+	–	Permeability		–			Soundness		
[17]	45A90+	–	Permeability		–			Soundness		

(continued)

Table 6.6 (continued)

References	Mix ID	WD (mm)	Durability test 1	Delta	Durability test 2
[17]	35B70	–	Permeability	–	Soundness
[17]	35B80	–	Permeability	–	Soundness
[17]	35B90	–	Permeability	–	Soundness
[17]	35B70+	–	Permeability	–	Soundness
[17]	35B80+	–	Permeability	–	Soundness
[17]	35B90+	–	Permeability	–	Soundness
[17]	45B70+	–	Permeability	–	Soundness
[17]	45B80+	–	Permeability	–	Soundness
[17]	45B90+	–	Permeability	–	Soundness
[17]	35C70	–	Permeability	–	Soundness
[17]	35C80	–	Permeability	–	Soundness
[17]	35C90	–	Permeability	–	Soundness
[17]	35C70+	–	Permeability	–	Soundness
[17]	35C80+	–	Permeability	–	Soundness
[17]	35C90+	–	Permeability	–	Soundness
[17]	45C70+	–	Permeability	–	Soundness
[17]	45C80+	–	Permeability	–	Soundness
[17]	45C90+	–	Permeability	–	Soundness
[18]	M-1	32	ASTM D-4792	-0.26 %w; +2.86 % MPa	Freezing/thawing
References	Mix ID	Delta	Durability test 3	Delta	
[16]	TRAD	–	Length variation	–	
[16]	EAF50	–	Length variation	–	
[16]	EAF100	–	Length variation	–	
[17]	35A70	–	Length variation	–	
[17]	35A80	–	Length variation	–	
[17]	35A90	–	Length variation	–	
[17]	35A70+	–	Length variation	–	
[17]	35A80+	–	Length variation	–	
[17]	35A90+	–	Length variation	–	
[17]	45A70+	–	Length variation	–	
[17]	45A80+	–	Length variation	–	
[17]	45A90+	–	Length variation	–	
[17]	35B70	–	Length variation	–	
[17]	35B80	–	Length variation	–	
[17]	35B90	–	Length variation	–	
[17]	35B70+	–	Length variation	–	
[17]	35B80+	–	Length variation	–	
[17]	35B90+	–	Length variation	–	
[17]	45B70+	–	Length variation	–	
[17]	45B80+	–	Length variation	–	
[17]	45B90+	–	Length variation	–	
[17]	35C70	–	Length variation	–	
[17]	35C80	–	Length variation	–	

(continued)

Table 6.6 (continued)

References	Mix ID	Delta	Durability test 3	Delta				
[17]	35C90	–	Length variation	–				
[17]	35C70+	–	Length variation	–				
[17]	35C80+	–	Length variation	–				
[17]	35C90+	–	Length variation	–				
[17]	45C70+	–	Length variation	–				
[17]	45C80+	–	Length variation	–				
[17]	45C90+	–	Length variation	–				
[18]	M-1	–0.14 %w; –15 % MPa	Wetting/drying	–0.08 %w; –29 % MPa				
References	Mix ID	Durability test 4		Delta				
[16]	TRAD	–	–	–				
[16]	EAF50	–	–	–				
[16]	EAF100	–	–	–				
[17]	35A70	–	–	–				
[17]	35A80	–	–	–				
[17]	35A90	–	–	–				
[17]	35A70+	–	–	–				
[17]	35A80+	–	–	–				
[17]	35A90+	–	–	–				
[17]	45A70+	–	–	–				
[17]	45A80+	–	–	–				
[17]	45A90+	–	–	–				
[17]	35B70	–	–	–				
[17]	35B80	–	–	–				
[17]	35B90	–	–	–				
[17]	35B70+	–	–	–				
[17]	35B80+	–	–	–				
[17]	35B90+	–	–	–				
[17]	45B70+	–	–	–				
[17]	45B80+	–	–	–				
[17]	45B90+	–	–	–				
[17]	35C70	–	–	–				
[17]	35C80	–	–	–				
[17]	35C90	–	–	–				
[17]	35C70+	–	–	–				
[17]	35C80+	–	–	–				
[17]	35C90+	–	–	–				
[17]	45C70+	–	–	–				
[17]	45C80+	–	–	–				
[17]	45C90+	–	–	–				
[18]	M-1	Autoclave test		–0.48 %w; –52 % MPa				
References	Mix ID	Water (kg/m ³)	Cement (kg/m ³)	Cement type	w/b	R (%)	NA type	NA S (kg/m ³)
[18]	M-2	186	310	CEM I 42.5 R	0.60	100	–	–
[18]	M-3	186	310	CEM I 42.5 R	0.60	0S-100G	L	960

(continued)

Table 6.6 (continued)

References	Mix ID	Water (kg/m ³)	Cement (kg/m ³)	Cement type	w/b	R (%)	NA type	NA S (kg/m ³)
[18]	M-4	186	310	CEM I 42.5 R	0.60	50S-100G	L	480 (Fl)
[18]	M-5	186	310	CEM I 42.5 R	0.60	50S-100G	L	480 (Fl)
[18]	M-6	186	310	CEM I 42.5 R	0.60	66S-100G	L	330 (Fl)
[19]	TRAD	155	330	CEM II/A-L 42.5R	0.47	0	C	759
[19]	M-1	158	335	CEM II/A-L 42.5R	0.47	50S-0G	C	378
[19]	M-2	167	340	CEM II/A-L 42.5R	0.49	100S-0G	C	–
[19]	M-3	180	340	CEM II/A-L 42.5R	0.53	50S-50G	C	369
[19]	M-4	185	350	CEM II/A-L 42.5R	0.53	50S-100G	C	456
[19]	M-5	195	355	CEM II/A-L 42.5R	0.55	100	–	–
[24]	EAF	164.3	310	CEM II/A-L 42.5R	0.53	100G	C	617.24
[24]	TRAD	159.5	290	CEM II/A-L 42.5R	0.55	0	C	2098.43
[26]	EAF	165	317	CEM II/A-L 42.5R	0.52	100G	C	361
[26]	TRAD	150	288	CEM II/A-L 42.5R	0.52	0	C	1888
[27]	K1	140	400	CEM I 42.5 N	0.35	0	L	1046
[27]	K2	140	400	CEM I 42.5 N	0.35	0S-100G	L	1202
[27]	K3	140	400	CEM I 42.5 N	0.35	50S-100G	L	639
[27]	K4	140	280	CEM I 42.5 N	0.35	0S-100G	L	1182
[27]	K5	140	200	CEM I 42.5 N	0.35	0S-100G	L	1176
[27]	K6	140	200	CEM I 42.5 N	0.35	50S-100G	L	624
[29]	C400-0.4	160	400	CEM I 52.5R	0.40	0	Si	836
[29]	C400-0.45	180	400	CEM I 52.5R	0.45	0	Si	812
[29]	C400-0.5	200	400	CEM I 52.5R	0.50	0	Si	789
[29]	E400-0.4	160	400	CEM I 52.5R	0.40	100G	Si	1020
[29]	E400-0.45	180	400	CEM I 52.5R	0.45	100G	Si	994
[29]	E400-0.5	200	400	CEM I 52.5R	0.50	100G	Si	965
[29]	E350-0.4	140	350	CEM I 52.5R	0.40	100G	Si	1067
[29]	E350-0.45	157.5	350	CEM I 52.5R	0.45	100G	Si	1029
[29]	E350-0.5	175	350	CEM I 52.5R	0.50	100G	Si	1014
[30]	C	160	400	CEM I 52.5R	0.40	0	Si	832
References	Mix ID	NA G (kg/m ³)	EAF S (kg/m ³)	EAF G (kg/m ³)	WRA (kg/m ³)	SCM (kg/m ³)	AEA (kg/m ³)	Density (kg/m ³)
[18]	M-2	–	950	945	–	–	–	2390
[18]	M-3	–	–	895	–	–	–	2380
[18]	M-4	–	480	895	–	–	–	2500
[18]	M-5	–	480	620	–	–	–	2560

(continued)

Table 6.6 (continued)

References	Mix ID	NA G (kg/m ³)	EAF S (kg/m ³)	EAF G (kg/m ³)	WRA (kg/m ³)	SCM (kg/m ³)	AEA (kg/m ³)	Density (kg/m ³)		
[18]	M-6	–	630	620	–	–	–	2590		
[19]	TRAD	1102	–	–	1.31	–	0.056	2530		
[19]	M-1	1102	514	–	1.33	–	0.056	2660		
[19]	M-2	1102	1019	–	1.36	–	0.056	2850		
[19]	M-3	551	588	690	1.36	–	0.056	2830		
[19]	M-4	369	514	1380	1.39	–	0.056	3000		
[19]	M-5	–	1128	1380	1.42	–	0.056	3190		
[24]	EAF	–	–	2041	1.24	–	0.049	–		
[24]	TRAD	–	–	–	1.16	–	0.046	–		
[26]	EAF	–	–	2111	1.27	–	0.049	2365		
[26]	TRAD	–	–	–	1.15	–	0.046	2951		
[27]	K1	892	–	–	4	–	–	2295		
[27]	K2	–	–	945	7	–	–	2629		
[27]	K3	–	639	1005	5.6	–	–	2750		
[27]	K4	–	–	929	6	120 (LFS)	–	2713		
[27]	K5	–	–	924	8	200 (FA C)	–	2574		
[27]	K6	–	624	981	9	200 (FA C)	–	2635		
[29]	C400-0.4	1020	–	–	4.8	–	–	2447		
[29]	C400-0.45	992	–	–	4	–	–	2388		
[29]	C400-0.5	963	–	–	3.2	–	–	2394		
[29]	E400-0.4	–	–	1190	5.8	–	–	2835		
[29]	E400-0.45	–	–	1148	4.8	–	–	2795		
[29]	E400-0.5	–	–	1115	4	–	–	2751		
[29]	E350-0.4	–	–	1245	4.2	–	–	2846		
[29]	E350-0.45	–	–	1200	3.5	–	–	2758		
[29]	E350-0.5	–	–	1171	2.8	–	–	2751		
[30]	C	1008	–	–	4.8	–	–	2477		
References	Mix ID	Slump (mm)	fcm 7 (MPa)	fcm 28 (MPa)	fctm (MPa)	Ecm (GPa)	fcfm (MPa)	fcm 90 (MPa)	WA (%)	Porosity (%)
[18]	M-2	Collapsed	10.6	17.1	–	–	–	22.4	12.7	30.4
[18]	M-3	50	22.7	28.0	–	–	–	39.2	6.8	16.2
[18]	M-4	70	23.3	29.3	–	–	–	43.8	6.5	16
[18]	M-5	120	19.8	25.1	–	–	–	38.3	6.9	17.6
[18]	M-6	70	20.8	25.5	–	–	–	38.1	7.6	19.6
[19]	TRAD	200	31.4	37.0	3.54	37.51	–	–	–	–
[19]	M-1	190	29.3	37.7	3.73	37.36	–	–	–	–
[19]	M-2	205	27.5	36.5	3.62	38.68	–	–	–	–
[19]	M-3	195	31.1	37.5	3.56	40.39	–	–	–	–
[19]	M-4	195	29.9	37.4	4.01	40.04	–	–	–	–
[19]	M-5	180	28.1	34.4	3.76	38.47	–	–	–	–
[24]	EAF	168	40.5	48.4	4.38	40.05	–	–	–	–
[24]	TRAD	212	22.6	28.6	3.54	37.40	–	–	–	–

(continued)

Table 6.6 (continued)

References	Mix ID	Slump (mm)	fcm 7 (MPa)	fcm 28 (MPa)	fctm (MPa)	Ecm (GPa)	fcfm (MPa)	fcm 90 (MPa)	WA (%)	Porosity (%)
[26]	EAF	150	30.9	35.1	2.12	24.06	–	–	–	–
[26]	TRAD	150	21.0	27.0	2.21	30.69	–	–	–	–
[27]	K1	–	43.6	53.3	5.20	–	8.30	–	5.0	–
[27]	K2	–	53.8	58.3	5.52	–	9.13	–	4.3	–
[27]	K3	–	58.8	64.7	5.89	–	9.86	–	4.5	–
[27]	K4	–	47.5	53.4	5.17	–	8.29	–	4.4	–
[27]	K5	–	44.0	60.7	5.78	–	8.53	–	4.9	–
[27]	K6	–	47.1	59.2	5.40	–	8.78	–	4.9	–
[29]	C400-0.4	210	–	46.8	3.75	40.01	–	–	–	–
[29]	C400-0.45	180	–	35.6	3.47	31.55	–	–	–	–
[29]	C400-0.5	210	–	33.7	3.49	33.95	–	–	–	–
[29]	E400-0.4	170	–	63.4	5.65	49.50	–	–	–	–
[29]	E400-0.45	210	–	52.3	4.98	48.42	–	–	–	–
[29]	E400-0.5	210	–	46.4	3.99	45.31	–	–	–	–
[29]	E350-0.4	170	–	61.0	4.91	49.29	–	–	–	–
[29]	E350-0.45	180	–	49.9	4.81	48.42	–	–	–	–
[29]	E350-0.5	210	–	48.7	4.56	47.81	–	–	–	–
[30]	C	210	37.9	46.8	4.50	38.50	–	–	–	–
References	Mix ID	WD (mm)	Durability test 1		Delta		Durability test 2			
[18]	M-2	Total	ASTM D-4792		NN		Freezing/thawing			
[18]	M-3	45	ASTM D-4792		–1.88 %w; +6.13 % MPa		Freezing/thawing			
[18]	M-4	5	ASTM D-4792		–0.7 %w; +10.4 % MPa		Freezing/thawing			
[18]	M-5	5	ASTM D-4792		–0.9 %w; +9.85 % MPa		Freezing/thawing			
[18]	M-6	25	ASTM D-4792		–0.8 %w; +9.97 % MPa		Freezing/thawing			
[19]	TRAD	–	ASTM D-4792		–0.07 %w; +13.49 % MPa		Freezing/thawing			
[19]	M-1	–	ASTM D-4792		–0.19 %w; +3.39 % MPa		Freezing/thawing			
[19]	M-2	–	ASTM D-4792		+0.68 %w; +1.70 % MPa		Freezing/thawing			
[19]	M-3	–	ASTM D-4792		+2.29 %w; +10.95 % MPa		Freezing/thawing			
[19]	M-4	–	ASTM D-4792		+0.38 %w; +5.10 % MPa		Freezing/thawing			
[19]	M-5	–	ASTM D-4792		–0.29 %w; +2.28 % MPa		Freezing/thawing			
[24]	EAF	–	–	–	–	–	–	–	–	–
[24]	TRAD	–	–	–	–	–	–	–	–	–
[26]	EAF	–	–	ASTM D-4792	–	+2.08 %w; –5.65 % MPa	–	–	–	Freezing/thawing
[26]	TRAD	–	–	ASTM D-4792	–	+2.63 %w; +9.07 % MPa	–	–	–	Freezing/thawing
[27]	K1	15	–	Abrasion (mm)	–	3.103	–	–	–	F/T (deicing salt)
[27]	K2	15	–	Abrasion (mm)	–	0.806	–	–	–	F/T (deicing salt)
[27]	K3	10	–	Abrasion (mm)	–	0.701	–	–	–	F/T (deicing salt)
[27]	K4	30	–	Abrasion (mm)	–	NN	–	–	–	F/T (deicing salt)
[27]	K5	10	–	Abrasion (mm)	–	NN	–	–	–	F/T (deicing salt)
[27]	K6	15	–	Abrasion (mm)	–	NN	–	–	–	F/T (deicing salt)
[29]	C400-0.4	–	–	–	–	–	–	–	–	–
[29]	C400-0.45	–	–	Cl [–] diffusion (mm ² /y)	–	45	–	–	–	–
[29]	C400-0.5	–	–	Cl [–] diffusion (mm ² /y)	–	59.1	–	–	–	–
[29]	E400-0.4	–	–	–	–	–	–	–	–	–

(continued)

Table 6.6 (continued)

References	Mix ID	WD (mm)	Durability test 1	Delta	Durability test 2
[29]	E400-0.45	–	Cl ⁻ diffusion (mm ² /y)	40.4	–
[29]	E400-0.5	–	Cl ⁻ diffusion (mm ² /y)	50.1	–
[29]	E350-0.4	–	–	–	–
[29]	E350-0.45	–	–	–	–
[29]	E350-0.5	–	–	–	–
[30]	C	–	–	–	–
References	Mix ID	Delta	Durability test 3	Delta	
[18]	M-2	NN	Wetting/drying	NN	
[18]	M-3	-1.02 %w; -39 % MPa	Wetting/drying	-0.12 %w; -41 % MPa	
[18]	M-4	-0.27 %w; -23 % MPa	Wetting/drying	-0.15 %w; -30 % MPa	
[18]	M-5	-0.94 %w; -44 % MPa	Wetting/drying	-0.16 %w; -45 % MPa	
[18]	M-6	-1.18 %w; -48 % MPa	Wetting/drying	-0.28 %w; -49 % MPa	
[19]	TRAD	+0.22 %w; +10.98 % MPa	Wetting/drying	+0.33 %w; -13.74 % MPa	
[19]	M-1	-0.32 %w; +12.21 % MPa	Wetting/drying	+0.00 %w; -6.12 % MPa	
[19]	M-2	+0.70 %w; +12.63 % MPa	Wetting/drying	+1.66 %w; -6.42 % MPa	
[19]	M-3	+1.14 %w; +8.86 % MPa	Wetting/drying	+2.06 %w; -19.48 % MPa	
[19]	M-4	+0.51 %w; +7.64 % MPa	Wetting/drying	+2.23 %w; -22.17 % MPa	
[19]	M-5	+0.05 %w; +18.03 % MPa	Wetting/drying	+1.65 %w; -10.84 % MPa	
[24]	EAF	–	–	–	
[24]	TRAD	–	–	–	
[26]	EAF	+1.37 %w; -7.28 % MPa	Wetting/drying	+0.79 %w; -5.68 % MPa	
[26]	TRAD	+2.15 %w; +11.53 % MPa	Wetting/drying	+2.85 %w; -26.52 % MPa	
[27]	K1	-0.05 %w	–	–	
[27]	K2	-0.08 %w	–	–	
[27]	K3	-0.05 %w	–	–	
[27]	K4	-0.0 %w	–	–	
[27]	K5	-2.20 %w	–	–	
[27]	K6	-1.75 %w	–	–	
[29]	C400-0.4	–	–	–	
[29]	C400-0.45	–	–	–	
[29]	C400-0.5	–	–	–	
[29]	E400-0.4	–	–	–	
[29]	E400-0.45	–	–	–	
[29]	E400-0.5	–	–	–	
[29]	E350-0.4	–	–	–	
[29]	E350-0.45	–	–	–	
[29]	E350-0.5	–	–	–	
[30]	C	–	–	–	
References	Mix ID	Durability test 4	Delta		
[18]	M-2	Autoclave test	NN		
[18]	M-3	Autoclave test	-0.15 %w; -38 % MPa		
[18]	M-4	Autoclave test	-0.28 %w; -33 % MPa		
[18]	M-5	–	–		

(continued)

Table 6.6 (continued)

References	Mix ID	Durability test 4		Delta				
[18]	M-6	-		-				
[19]	TRAD	ASTM D-4792 + weathering		-0.17 %w; +18.10 % MPa				
[19]	M-1	ASTM D-4792 + weathering		-1.56 %w; +15.65 % MPa				
[19]	M-2	ASTM D-4792 + weathering		+0.13 %w; +13.87 % MPa				
[19]	M-3	ASTM D-4792 + weathering		+0.97 %w; +19.58 % MPa				
[19]	M-4	ASTM D-4792 + weathering		-0.29 %w; +15.21 % MPa				
[19]	M-5	ASTM D-4792 + weathering		-0.50 %w; +14.33 % MPa				
[24]	EAF	-		-				
[24]	TRAD	-		-				
[26]	EAF	ASTM D-4792 + weathering		+0.26 %w; -2.371 % MPa				
[26]	TRAD	ASTM D-4792 + weathering		+0.41 %w; +8.35 % MPa				
[27]	K1	-		-				
[27]	K2	-		-				
[27]	K3	-		-				
[27]	K4	-		-				
[27]	K5	-		-				
[27]	K6	-		-				
[29]	C400-0.4	-		-				
[29]	C400-0.45	-		-				
[29]	C400-0.5	-		-				
[29]	E400-0.4	-		-				
[29]	E400-0.45	-		-				
[29]	E400-0.5	-		-				
[29]	E350-0.4	-		-				
[29]	E350-0.45	-		-				
[29]	E350-0.5	-		-				
[30]	C	-		-				
References	Mix ID	Water (kg/m ³)	Cement (kg/m ³)	Cement type	w/b	R (%)	NA type	NA S (kg/m ³)
[30]	E1	160	400	CEM I 52.5R	0.40	100G	Si	832
[30]	E2	140	350	CEM I 52.5R	0.40	100G	Si	872
[30]	E-SF	184	400	CEM I 52.5R	0.40	100G	Si	810
[31]	1	205	330	-	0.62	15S-0G	L	512
[31]	2	205	427	-	0.48	15S-0G	L	510
[31]	3	205	536	-	0.38	15S-0G	L	510
[31]	4	205	330	-	0.62	30S-0G	L	422
[31]	5	205	427	-	0.48	30S-0G	L	420
[31]	6	205	536	-	0.38	30S-0G	L	420
[31]	7	205	330	-	0.62	50S-0G	L	302
[31]	8	205	427	-	0.48	50S-0G	L	300
[31]	9	205	536	-	0.38	50S-0G	L	300
[33]	A	136	270		0.50	0	L	614

(continued)

Table 6.6 (continued)

References	Mix ID	Water (kg/m ³)	Cement (kg/m ³)	Cement type	w/b	R (%)	NA type	NA S (kg/m ³)
				CEM I 42.5 N				
[33]	B	136	108	CEM I 42.5 N	0.50	0	L	656
[33]	C	136	108	CEM I 42.5 N	0.50	100G	L	840
[33]	D	136	108	CEM I 42.5 N	0.50	50S-100G	L	442.3
[38]	NA	137	242.9	OPC type I	0.37	0	D	692.8
[38]	EAF	137	242.9	OPC type I	0.37	100G	D	692.8
[41]	D1	215	360	CEM I 42.5 R	0.60	50S-100G	L	540
[41]	D2	250	355	CEM I 42.5 R	0.70	75S-100G	L	265
[41]	D3	240	370	CEM I 42.5 R	0.65	100	L	–
[41]	D4	270	340	CEM I 42.5 R	0.80	100	L	–
[41]	D5	215	305	CEM I 42.5 R	0.70	100	L	–
[45]	1	197	303	OPC type I	0.65	0	L	775
[45]	2	197	303	OPC type I	0.65	0S-25G	L + RCA	775
[45]	3	197	303	OPC type I	0.65	0S-50G	L + RCA	775
[45]	4	197	303	OPC type I	0.65	0S-75G	L + RCA	775
[45]	5	197	303	OPC type I	0.65	0S-100G	L + RCA	775
[45]	6	197	358	OPC type I	0.55	0	L	740
[45]	7	197	358	OPC type I	0.55	0S-25G	L + RCA	740
[45]	8	197	358	OPC type I	0.55	0S-50G	L + RCA	740
References	Mix ID	NA G (kg/m ³)	EAF S (kg/m ³)	EAF G (kg/m ³)	WRA (kg/m ³)	SCM (kg/m ³)	AEA (kg/m ³)	Density (kg/m ³)
[30]	E1	–	–	1408	4.8	–	–	2935
[30]	E2	–	–	1476	4.2	–	–	3008
[30]	E-SF	–	–	1370	4.8	60 (SF)	–	2777
[31]	1	1131	90.5	–	–	–	–	–
[31]	2	1057	90	–	–	–	–	–
[31]	3	967	90	–	–	–	–	–
[31]	4	1131	181	–	–	–	–	–
[31]	5	1057	180	–	–	–	–	–
[31]	6	967	180	–	–	–	–	–
[31]	7	1131	302	–	–	–	–	–
[31]	8	1057	300	–	–	–	–	–
[31]	9	967	300	–	–	–	–	–
[33]	A	1434	–	–	1.35	0	–	2463
[33]	B	1373	–	–	1.35	162 (FA C)	–	2358
[33]	C	–	–	1414	1.35	162 (FA C)	–	2670

(continued)

Table 6.6 (continued)

References	Mix ID	NA G (kg/m ³)	EAF S (kg/m ³)	EAF G (kg/m ³)	WRA (kg/m ³)	SCM (kg/m ³)	AEA (kg/m ³)	Density (kg/m ³)		
[33]	D	–	357.7	1628	1.35	162 (FA C)	–	2782		
[38]	NA	1124	–	–	1.3	37.4 (FA C) + 93.4GGBF	0.3	2243		
[38]	EAF	–	–	1531	1.3	37.4 (FA C) + 93.4GGBF	0.3	2528		
[41]	D1	–	540	1080	–	–	–	2735		
[41]	D2	–	530	1060	–	265 (LFS)	–	2725		
[41]	D3	–	830	1110	–	280 (LFS)	–	2830		
[41]	D4	–	515	1030	–	515 (LFS)	–	2670		
[41]	D5	–	860	1150	–	860 (LFS)	–	2815		
[45]	1	985	–	0	–	–	–	–		
[45]	2	740 + 218R	–	305	–	–	–	–		
[45]	3	495 + 436R	–	610	–	–	–	–		
[45]	4	245 + 654R	–	915	–	–	–	–		
[45]	5	873R	–	1221	–	–	–	–		
[45]	6	985	–	0	–	–	–	–		
[45]	7	740 + 218R	–	305	–	–	–	–		
[45]	8	495 + 436R	–	610	–	–	–	–		
References	Mix ID	Slump (mm)	fcm 7 (MPa)	fcm 28 (MPa)	fctm (MPa)	ecm (GPa)	fcm (MPa)	fcm 90 (MPa)	WA (%)	Porosity (%)
[30]	E1	170	57.3	63.4	5.65	49.50	–	–	–	–
[30]	E2	160	50.3	61.3	5.37	49.20	–	–	–	–
[30]	E-SF	210	45.3	54.0	4.65	45.50	–	–	–	–
[31]	1	110	21.6	28.2	–	–	4.05	30.7	–	–
[31]	2	110	31.1	32.8	–	–	4.95	36.5	–	–
[31]	3	110	34.9	38.6	–	–	4.95	42.7	–	–
[31]	4	100	19.9	25.7	–	–	4.50	28.2	–	–
[31]	5	100	21.6	29.1	–	–	5.50	32.4	–	–
[31]	6	100	36.5	39.4	–	–	6.15	44.0	–	–
[31]	7	90	29.9	24.1	–	–	4.50	36.5	–	–
[31]	8	90	29.9	31.5	–	–	5.95	34.9	–	–
[31]	9	90	32.4	34.4	–	–	6.50	38.2	–	–
[33]	A	–	–	33.8	3.47	35.80	6.92	–	–	–
[33]	B	–	–	30.7	3.07	35.70	6.62	–	–	–
[33]	C	–	–	41.1	4.67	39.10	7.11	–	–	–
[33]	D	–	–	33.7	3.68	39.30	6.69	–	–	–
[38]	NA	83	–	46.0	6.20	–	–	–	–	–
[38]	EAF	76	–	48.0	4.50	–	–	–	–	–
[41]	D1	20	29.4	38.7	–	–	–	43.3	–	14.3
[41]	D2	35	33.0	43.9	–	–	–	48.4	–	16.3
[41]	D3	5	45.9	50.1	–	–	–	52.2	–	15.1
[41]	D4	45	20.7	26.1	–	–	–	29.1	–	18.5
[41]	D5	5	28.3	39.5	–	–	–	42.5	–	14.8

(continued)

Table 6.6 (continued)

References	Mix ID	Slump (mm)	fcm 7 (MPa)	fcm 28 (MPa)	fctm (MPa)	ecm (GPa)	fcfm (MPa)	fcm 90 (MPa)	WA (%)	Porosity (%)
[45]	1	100–120	–	34.2	6.32	32.51	–	–	–	–
[45]	2	100–120	–	30.8	6.76	31.53	–	–	–	–
[45]	3	100–120	–	32.5	6.95	31.21	–	–	–	–
[45]	4	100–120	–	34.2	7.27	30.56	–	–	–	–
[45]	5	100–120	–	34.2	7.43	29.91	–	–	–	–
[45]	6	100–120	–	29.6	5.83	4.81	–	–	–	–
[45]	7	100–120	–	–	–	–	–	–	–	–
[45]	8	100–120	–	–	–	–	–	–	–	–
References	Mix ID	WD (mm)	Durability test 1	Delta	Durability test 2					
[30]	E1	–	–	–	–					
[30]	E2	–	–	–	–					
[30]	E-SF	–	–	–	–					
[31]	1	–	–	–	–					
[31]	2	–	–	–	–					
[31]	3	–	–	–	–					
[31]	4	–	–	–	–					
[31]	5	–	–	–	–					
[31]	6	–	–	–	–					
[31]	7	–	–	–	–					
[31]	8	–	–	–	–					
[31]	9	–	–	–	–					
[33]	A	–	–	–	–					
[33]	B	–	–	–	–					
[33]	C	–	–	–	–					
[33]	D	–	–	–	–					
[38]	NA	–	Shrinkage	–	–					
[38]	EAF	–	Shrinkage	–	F/T (deicing salt)					
[41]	D1	36	ASTM D-4792	–0.28 %w; –1.1 % MPa	Freezing/thawing					
[41]	D2	44	ASTM D-4792	+1.05 %w; –8.7 % MPa	Freezing/thawing					
[41]	D3	39	ASTM D-4792	+1.53 %w; –3.1 % MPa	Freezing/thawing					
[41]	D4	68	ASTM D-4792	+2.40 %w; +6.0 % MPa	Freezing/thawing					
[41]	D5	57	ASTM D-4792	+1.80 %w; –3.2 % MPa	Freezing/thawing					
[45]	1	–	–	–	–					
[45]	2	–	–	–	–					
[45]	3	–	–	–	–					
[45]	4	–	–	–	–					
[45]	5	–	–	–	–					
[45]	6	–	–	–	–					
[45]	7	–	–	–	45					
[45]	8	–	–	–	45					
References	Mix ID	Delta	Durability test 3	Delta						
[30]	E1	–	–	–						
[30]	E2	–	–	–						

(continued)

Table 6.6 (continued)

References	Mix ID	Delta	Durability test 3	Delta
[30]	E-SF	-	-	-
[31]	1	-	-	-
[31]	2	-	-	-
[31]	3	-	-	-
[31]	4	-	-	-
[31]	5	-	-	-
[31]	6	-	-	-
[31]	7	-	-	-
[31]	8	-	-	-
[31]	9	-	-	-
[33]	A	-	-	-
[33]	B	-	-	-
[33]	C	-	-	-
[33]	D	-	-	-
[38]	NA	-	-	-
[38]	EAF	-1.2 %w	-	-
[41]	D1	+0.43 %w; -7.5 % MPa	Wetting/drying	+0.07 %w; +6.9 % MPa
[41]	D2	+0.66 %w; -38.8 % MPa	Wetting/drying	-0.39 %w; -19.8 % MPa
[41]	D3	+0.62 %w; -36.4 % MPa	Wetting/drying	-0.15 %w; -6.1 % MPa
[41]	D4	+2.78 %w; -78.4 % MPa	Wetting/drying	+0.06 %w; -26.7 % MPa
[41]	D5	+0.11 %w; +10.4 % MPa	Wetting/drying	-0.41 %w; -19.1 % MPa
[45]	1	-	-	-
[45]	2	-	-	-
[45]	3	-	-	-
[45]	4	-	-	-
[45]	5	-	-	-
[45]	6	-	-	-
[45]	7	-	-	-
[45]	8	-	-	-
References	Mix ID	Durability test 4		Delta
[30]	E1	-		-
[30]	E2	-		-
[30]	E-SF	-		-
[31]	1	-		-
[31]	2	-		-
[31]	3	-		-
[31]	4	-		-
[31]	5	-		-
[31]	6	-		-
[31]	7	-		-
[31]	8	-		-
[31]	9	-		-
[33]	A	-		-

(continued)

Table 6.6 (continued)

References	Mix ID	Durability test 4		Delta						
[33]	B	-		-						
[33]	C	-		-						
[33]	D	-		-						
[38]	NA	-		-						
[38]	EAF	-		-						
[41]	D1	Wet chamber/expansion		+0.60 %w; -0.9 %w						
[41]	D2	Wet chamber/expansion		+0.22 %w; -1.21 %w						
[41]	D3	Wet chamber/expansion		+0.42 %w; -0.84 %w						
[41]	D4	Wet chamber/expansion		+0.93 %w; +0.96 %w						
[41]	D5	Wet chamber/expansion		+1.50 %w; +0.94 %w						
[45]	1	-		-						
[45]	2	-		-						
[45]	3	-		-						
[45]	4	-		-						
[45]	5	-		-						
[45]	6	-		-						
[45]	7	-		-						
[45]	8	-		-						
References	Mix ID	Water (kg/m ³)	Cement (kg/m ³)	Cement type	w/b	R (%)	NA type	NA S (kg/m ³)		
[45]	9	197	358	OPC type I	0.55	0S-75G	L + RCA	740		
[45]	10	197	358	OPC type I	0.55	0S-100G	L + RCA	740		
[45]	11	197	438	OPC type I	0.45	0	L	675		
[45]	12	197	438	OPC type I	0.45	0S-25G	L + RCA	675		
[45]	13	197	438	OPC type I	0.45	0S-50G	L + RCA	675		
[45]	14	197	438	OPC type I	0.45	0S-75G	L + RCA	675		
[45]	15	197	438	OPC type I	0.45	0S-100G	L + RCA	675		
References	Mix ID	NA G (kg/m ³)	EAF S (kg/m ³)	EAF G (kg/m ³)	WRA (kg/m ³)	SCM (kg/m ³)	AEA (kg/m ³)	Density (kg/m ³)		
[45]	9	245 + 654R	-	915	-	-	-	-		
[45]	10	873 R	-	1221	-	-	-	-		
[45]	11	985	-	0	-	-	-	-		
[45]	12	740 + 218R	-	305	-	-	-	-		
[45]	13	495 + 436R	-	610	-	-	-	-		
[45]	14	245 + 654R	-	915	-	-	-	-		
[45]	15	873 R	-	1221	-	-	-	-		
References	Mix ID	Slump (mm)	fcm 7 (MPa)	fcm 28 (MPa)	fctm (MPa)	Ecm (GPa)	fcfm (MPa)	fcm 90 (MPa)	WA (%)	Porosity (%)
[45]	9	100-120	-	-	-	-	-	-	-	-
[45]	10	100-120	-	-	-	-	-	-	-	-
[45]	11	100-120	-	21.9	4.81	25.35	-	-	-	-
[45]	12	100-120	-	24.0	4.67	24.84	-	-	-	-

(continued)

Table 6.6 (continued)

References	Mix ID	Slump (mm)	fcm 7 (MPa)	fcm 28 (MPa)	fctm (MPa)	Ecm (GPa)	fcm (MPa)	fcm 90 (MPa)	WA (%)	Porosity (%)
[45]	13	100–120	–	26.2	4.88	23.58	–	–	–	–
[45]	14	100–120	–	25.1	4.95	23.83	–	–	–	–
[45]	15	100–120	–	27.3	5.05	23.32	–	–	–	–
References	Mix ID	WD (mm)	Durability test 1	Delta	Durability test 2	Delta	Durability test 3	Delta		
[45]	9	–	–	–	–	–	–	–		
[45]	10	–	–	–	–	–	–	–		
[45]	11	–	–	–	–	–	–	–		
[45]	12	–	–	–	–	–	–	–		
[45]	13	–	–	–	–	–	–	–		
[45]	14	–	–	–	–	–	–	–		
[45]	15	–	–	–	–	–	–	–		
References	Mix ID	Durability test 4	Delta							
[45]	9	–	–							
[45]	10	–	–							
[45]	11	–	–							
[45]	12	–	–							
[45]	13	–	–							
[45]	14	–	–							
[45]	15	–	–							

freezing/thawing and wetting/drying cycles [18, 19, 26, 27, 41]. Additionally, some physical properties are also reported, e.g. concrete water absorption (WA %), porosity (%), and water penetration depth (WD mm) [1, 6, 16, 18, 27, 41]. The results of the experimental tests about the investigation of these properties are included in the database. Results about expansion and autoclave tests [18], chlorides diffusion coefficient [29], abrasion [27] and exposure to high temperature [11] are also included in the database. For some other specific properties, e.g. concrete soundness [1, 16, 17], radiation attenuation coefficient [14], sorptivity [11], permeability [16, 17], length variation in time [11, 16, 17] and shrinkage [38], a reference to the tests is only present, due to the scarcity of results among the dataset.

6.7 Conclusion

Many scientific works deal with the characterization and use of Electric Arc Furnace slag in civil engineering applications. Here, experimental results of 46 works have been collected into an experimental database, aiming to give a comprehensive view of the state-of-the-art of EAF slag applications. Physical properties, chemical composition, mineralogical phases and leaching potential have been included as relevant data. Concerning slag application, 24 works deal with the use of slag for structural concrete production, and among these, for 17 of them it was

possible to collect also mixtures' details, and the mechanical and durability-related properties of the produced conglomerates. Results of more than 130 experimental mixes have been collected, where replacement ratio, water-to-binder ratio, slag type, cement dosage, aggregates proportion, and admixtures use are the varying parameter. Fresh concrete properties, i.e. apparent specific weight and slump, and mechanical strength, i.e. compressive, tensile and flexural strength and elastic modulus have been analyzed for the majority of the mixes. For many of them also durability-related properties, e.g. exposure in detrimental environment, chloride penetration, water penetration and absorption have also been included. This database can represent an important state-of-the-art about the potential application of EAF slag as recycled aggregate for structural purposes.

References

1. Manso JM, Gonzalez JJ, Polanco JA (2004) Electric arc furnace slag in concrete. *J Mater Civ Eng* 16:639–645
2. Monkman S, Shao Y (2006) Assessing the carbonation behavior of cementitious materials. *J Mater Civ Eng* 18(6):768–776
3. Tossavainen M, Engstrom F, Yang Q, Menad N, Larsson ML, Bjorkman B (2007) Characteristics of steel slag under different cooling conditions. *Waste Manage* 27(7):1335–1344
4. Teo P-T, Seman AA, Basu P, Sharif NM (2014) Recycling of Malaysia's electric arc furnace (EAF) slag waste into heavy-duty green ceramic tile. *Waste Manage* 34(12):2697–2708
5. Suer P, Lindqvist J-E, Arm M, Frogner P-F (2009) Reproducing ten years of road ageing—accelerated carbonation and leaching of EAF steel slag. *Sci Total Environ* 407(18):5110–5116
6. Abu-Eishah SI, El-Dieb AS, Bedir MS (2012) Performance of concrete mixtures made with electric arc furnace (EAF) steelslag aggregate produced in the Arabian Gulf region. *Constr Build Mater* 34:249–256
7. Pasetto M, Baldo N (2010) Experimental evaluation of high performance base course and road base asphalt concrete with electric arc furnace steel slags. *J Hazard Mater* 181(1):938–948
8. Iacobescu R, Koumpouri D, Pontikes Y, Şaban R, Angelopoulos G (2011) Utilization of EAF metallurgical slag in “green” belite cement. *U.P.B. Sci Bull, Series B* 73 (1)
9. Sorlini S, Sanzeni, A Rondi L (2012) Reuse of steel slag in bituminous paving mixtures. *J Hazard Mater* 209–210:84–91
10. Bernardo G, Marroccoli M, Nobili M, Telesca A, Valenti GL (2007) The use of oil well-derived drilling waste and electric arc furnace slag as alternative raw materials in clinker production. *Res Conserv Recyc* 52(1–52):95–102
11. Etxeberria M, Pacheco C, Meneses JM, Berridi I (2010) Properties of concrete using metallurgical industrial by-products as aggregates. *Constr Build Mater* 24(9):1594–1600
12. Pasetto M, Baldo N (2011) Mix design and performance analysis of asphalt concretes with electric arc furnace slag. *Constr Build Mater* 25(8):3458–3468
13. Ameri M, Hesami S, Goli H (2013) Laboratory evaluation of warm mix asphalt mixtures containing electric arc furnace (EAF) steel slag. *Constr Build Mater* 49:611–617
14. González-Ortega MA, Segura I, Cavalaro SPH, Toralles-Carbonari B, Aguado A, Andrello AC (2014) Radiological protection and mechanical properties of concretes with EAF steel slags. *Constr Build Mater* 51:432–438
15. Kavussi A, Qazizadeh MJ (2014) Fatigue characterization of asphalt mixes containing electric arc furnace (EAF) steel slag subjected to long term aging. *Constr Build Mater* 72:158–166

16. Adegoloye G, Beaucour A-L, Ortola S, Noumowé A (2015) Concretes made of EAF slag and AOD slag aggregates from stainless steel process: Mechanical properties and durability. *Constr Build Mater* 76:313–321
17. Yeih W, Fu TC, Chang JJ, Huang R (2015) Properties of pervious concrete made with air-cooling electric arc furnace slag as aggregates. *Constr Build Mater* 93:737–745
18. Manso JM, Polanco JA, Losanez M, Gonzalez JJ (2006) Durability of concrete made with EAF slag as aggregate. *Cem Concr Comp* 28:528–534
19. Pellegrino C, Cavagnis P, Faleschini F, Brunelli K (2013) Properties of concretes with Black/Oxidizing Electric Arc Furnace slag aggregate. *Cem Concr Comp* 37:232–240
20. Chunlin L, Kumpeng Z, Depeng C (2011) Possibility of concrete prepared with steel slag as fine and coarse aggregates: a preliminary study. *Proc Eng* 24:412–416
21. Kim S-W, Kim Y-S, Lee J-M, Kim K-H (2013) Structural performance of spirally confined concrete with EAF oxidizing slag aggregate. *Eur J Environ Civ Engin* 17(8):654–674
22. Alizadeh M, Chini P, Ghods MH, Montazer S, Shekarchi M (2003) Utilization of electric arc furnace slag as aggregates in concrete—environmental issues. In: 6th CANMET/ACI international conference on recent advances in concrete technology, vol 1. Bucharest, Romania, pp 451–464
23. Sofilić T, Sofilić U, Brnardić I (2012) The significance of iron and steel slag as by-product for utilization in road construction. In: 12th international foundry men conference sustainable development in foundry materials and technologies, Opatija, Croatia
24. Pellegrino C, Faleschini F (2013) Experimental behavior of reinforced concrete beams with electric arc furnace slag as recycled aggregate. *ACI Mater J* 110:197–206
25. Akinwumi I (2014) Soil modification by the application of steel slag. *Period Polytech Civil Eng* 58(4):371–377
26. Pellegrino C, Gaddo V (2009) Mechanical and durability characteristics of concrete containing EAF slag as aggregate. *Cem Concr Comp* 31:663–671
27. Papayianni I, Anastasiou E (2010) Production of high-strength concrete using high volume of industrial by-products. *Constr Build Mater* 24:1412–1417
28. Faleschini F, De Marzi P, Pellegrino C (2014) Recycled concrete containing EAF slag: Environmental assessment through LCA. *Euro J Environ Civil Engineer* 18(9):1009–1024
29. Faleschini F, Fernández-Ruiz MA, Zanini MA, Brunelli K, Pellegrino C, Hernández-Montes E (2015) High performance concrete with electric arc furnace slag as aggregate: mechanical and durability properties. *Constr Build Mater* 101:113–121
30. Faleschini F, Brunelli K, Zanini MA, Dabalà M, Pellegrino C (2015) Electric arc furnace slag as coarse recycled aggregate for concrete production. *J Sustain Metall*. doi:10.1007/s40831-015-0029-1
31. Qasrawi H, Shalabi F, Asi I (2009) Use of low CaO unprocessed steel slag in concrete as fine aggregate. *Constr Build Mater* 23(2):1118–1125
32. Luxán MP, Sotolongo R, Dorrego F, Herrero E (2000) Characteristics of the slag produced in the fusion of scrap steel by electric arc furnace. *Cem Concr Res* 30(4):517–519
33. Papayianni I, Anastasiou (2011) Concrete incorporating high-calcium fly ash and EAF aggregates. *Mag Concr Res* 63(8):597–604
34. Pasetto M, Baldo N (2015) Experimental analysis of hydraulically bound mixtures made with waste foundry sand and steel slag. *Mater Struct* 48:2489–2503
35. Arribas I, Santamaría A, Ruiz E, Ortega-López V, Manso JM (2015) Electric arc furnace slag and its use in hydraulic concrete. *Constr Build Mater* 90:68–79
36. Pasetto M, Baldo N (2011) Performance comparative analysis of stone mastic asphalts with electric arc furnace steel slag: a laboratory evaluation. *Mater Struct* 45:411–424
37. Rojas MF, De Rojas MIS (2004) Chemical assessment of the electric arc furnace slag as construction material: expansive compounds. *Cem Concr Res* 34(10):1881–1888
38. Brand AS, Roesler JR (2015) Steel furnace slag aggregate expansion and hardened concrete properties. *Cem Concr Comp* 60:1–9

39. Kuo W-T, Shu C-Y (2015) Effect of particle size and curing temperature on expansion reaction in electric arc furnace oxidizing slag aggregate concrete. *Constr Build Mater* 94:488–493
40. Cornacchia G, Agnelli S, Gelfi M, Ramorino G, Roberti R (2015) Reuse of EAF slag as reinforcing filler for polypropylene matrix composites. *JOM* 67(6):1370–1378
41. Polanco JA, Manso JM, Setien J, Gonzalez JJ (2011) Strength and durability of concrete made with electric steelmaking slag. *ACI Mater J* 108(2):196–203
42. Muhmood L, Vitta S, Venkateswaran D (2009) Cementitious and pozzolanic behavior of electric arc furnace steel slags. *Cem Concr Res* 39(2):102–109
43. Vázquez Ramonich E, Barra M (2001) Reactivity and expansion of electric arc furnace slag in their application in construction. *Mater Construcc* 51:137–148
44. Maslehuddin M, Sharif AM, Shameem M, Ibrahim M, Barry MS (2003) Comparison of properties of steel slag and crushed limestone aggregate concretes. *Constr Build Mater* 17(2):105–112
45. Qasrawi I (2014) The use of steel slag aggregate to enhance the mechanical properties of recycled aggregate concrete and retain the environment. *Constr Build Mater* 54:298–304
46. Iacobescu RI, Pontikes Y, Koumpouri D, Angelopoulos GN (2013) Synthesis, characterization and properties of calcium ferroaluminate belite cements produced with electric arc furnace steel. *Cem Concr Comp* 44:1–8